

Dissertation zur Erlangung des Doktorgrades  
der Fakultät für Chemie und Pharmazie  
der Ludwig-Maximilians-Universität München

Twin-screw extruded lipid implants for controlled  
protein drug delivery

**Gerhard Ludwig Sax**

aus

Straubing

2012



### Erklärung

Diese Dissertation wurde im Sinne von § 7 der Promotionsordnung vom 28. November 2011 von Herrn Prof. Dr. Gerhard Winter betreut.

### Eidesstattliche Versicherung

Diese Dissertation wurde eigenständig und ohne unerlaubte Hilfe erarbeitet.

München, 17.04.2012

.....  
Gerhard Sax

Dissertation eingereicht am:	17.04.2012
1. Gutachter:	Prof. Dr. Gerhard Winter
2. Gutachter:	Prof. Dr. Wolfgang Frieß
Mündliche Prüfung am:	08.05.2012



## ACKNOWLEDGEMENTS

Foremost, I wish to express my thanks to Prof. Dr. Gerhard Winter for the possibility to join his research group, his professional guidance, his scientific support and the trust he put into me. He always encouraged and confirmed me in my work and allowed me to be part in several different projects.

My thanks go to Dr. Sandra Schulze who was my supervisor during my first 18 months of my studies. She introduced me into the field of lipid based implants and helped me starting my thesis.

I would like to thank Florian Feil, Dr. Christophe Jung and Prof. Dr. Christoph Bräuchle (Department of Chemistry and Center for Nanoscience (CeNS), LMU Munich) for our good collaboration and the conduction of the single-molecule diffusion measurements.

My thanks go to Dr. Kessler and Prof. Dr. Eckhard Wolf (Department of Veterinary Medicine, Chair for Molecular Animal Breeding and Biotechnology) for the performance of the *in-vivo* biodegradation study in rabbits. I would also like to thank Dr. Stefan Bauersachs (Department of Veterinary Medicine, Chair for Molecular Animal Breeding and Biotechnology) for our collaboration and the nice paper he generated.

Christian Minke from the Department of Chemistry and Biochemistry, LMU Munich is acknowledge for conducting the scanning electron microscopy measurements.

Veronika Fischbacher is acknowledge for her effort during her Bachelor and Master thesis conducting many release studies and helping me whilst I needed crutches.

I would like to thank Dr. Martin Schwab for introducing me into the *in-vitro* lipase assay.

I would like to thank Roche Diagnostics, GmbH, Penzberg for the donation of rh-interferon  $\alpha 2a$  as well as Sasol GmbH, Wittern, Germany for the design of the triglyceride 'H12'.

Many thanks go to all colleagues from the research groups of Prof. Dr. Winter and Prof. Dr. Frieß. My special thanks go to Angelika Freitag, Thomas Bosch, Sebastian Hertel, Julia Myschik, Markus Hofer and Elsa Kis for all the support and every assistance.

My special thanks go to Tim Serno who joined the lab with me.

Julia Myschik is acknowledged for proof-reading of this thesis.

Thanks are extended to Prof. Dr. W. Frieß, Prof. Dr. S. Zahler, Prof. Dr. C. Wahl, Dr. M. Ogris and Prof. F. Bracher for serving as members of my thesis advisor committee.

Finally, I would like to thank my parents Christa and Xaver and my wife Tanja.

# TABLE OF CONTENT

TABLE OF CONTENT .....	I
I. General introduction .....	1
1. Controlled release systems for pharmaceutical peptides and proteins .....	5
1.1. Definition of 'controlled release' .....	5
1.2. Currently marketed peptide and protein depot formulations .....	6
2. Matrix materials for the preparation of protein containing sustained release devices ..	9
3. Lipids as matrix materials for the preparation of protein containing sustained release devices .....	13
3.1. Lipid based drug delivery systems .....	13
4. Mechanism of release from implant matrices .....	31
4.1. Mechanism of release from triglyceride based implants .....	33
4.2. Mechanism of release from compressed and tsc-extruded implants .....	34
II. Aim of the thesis .....	37
III. Twin-screw extrudates for the sustained release of a therapeutic antibody .....	39
1. Introduction .....	39
2. Materials and methods .....	41
2.1. Materials .....	41
2.2. Quantification of mabB .....	41
2.3. Precipitation and re-dissolution studies .....	41
2.4. Antibody solubility studies in the presence of PEG 6000 .....	42
2.5. Sodium dodecyl sulfate polyacrylamide gel electrophoresis (SDS-PAGE) .....	42
2.6. Lyophilization of mabB .....	43
2.7. Lyophilization of PEG 6000 .....	44

2.8.	Coulometric Karl-Fischer headspace titration.....	44
2.9.	Preparation of lipid implants by tsc-extrusion .....	44
2.10.	Antibody release tests from tsc-extrudates.....	45
2.11.	Scanning electron microscopy.....	46
3.	Results and discussion .....	47
3.1.	Preliminary precipitation studies .....	47
3.2.	Antibody solubility studies in the presence of various amounts of PEG 6000.....	47
3.3.	MabB precipitation and re-dissolution after long-term incubation .....	49
3.4.	Production of lyophilized of mabB powder .....	52
3.5.	MabB release studies from tsc-extruded lipid implants.....	56
4.	Conclusion.....	63
IV.	Influence of the manufacturing strategy on protein release kinetics from lipid based implants.....	65
1.	Introduction.....	65
2.	Materials and methods.....	67
2.1.	Materials .....	67
2.2.	Methods.....	68
3.	Results .....	73
3.1.	Lysozyme release from lipid based implants.....	73
3.2.	Assessment of implant pore structure .....	75
3.3.	X-ray diffraction measurements .....	77
3.4.	DSC-measurements .....	80
4.	Summary .....	85
V.	Mechanistic studies on the release of lysozyme from twin-screw extruded lipid implants	
(I) –	influence of pore-former and lipid composition .....	87
1.	Introduction.....	87

1.1.	Material.....	87
1.2.	Methods.....	87
2.	Results of the influence of the pore-forming agent on lysozyme release .....	89
2.1.	Influence of PEG 4000 particle size on lysozyme release .....	89
2.2.	Influence of viscosity within the implant pores.....	92
2.3.	Influence of the dissolution rate of PEG .....	94
3.	Influence of lipid matrix composition .....	97
3.1.	Influence of the ratio between low and high melting lipid.....	97
3.2.	Influence of the high melting lipid.....	99
3.3.	Influence of the type of low-melting lipid .....	100
4.	Summary and outlook .....	105
VI.	Mechanistic studies on the release of lysozyme from twin-screw extruded lipid implants (II) – influence of implant melting.....	107
1.	Introduction.....	107
2.	Materials and methods.....	109
2.1.	Materials .....	109
2.2.	Preparation of lipid twin-screw extrudates (tsc-extrudates) .....	109
2.3.	Differential scanning calorimetry (DSC) .....	111
2.4.	Wide-angle X-ray scattering (WAXS).....	111
2.5.	<i>In-vitro</i> release tests .....	111
2.6.	Protein extraction from lipid implants .....	112
2.7.	Assessment of implant weight and weight loss .....	112
2.8.	Scanning electron microscopy (SEM) .....	112
3.	Results .....	113
3.1.	Preparation of lipid twin-screw extrudates.....	113

3.2.	Lysozyme release at various temperatures.....	113
3.3.	Lysozyme release from lipid implants comprising various low melting lipids .....	114
3.4.	Lysozyme release with various amounts of pore forming agent .....	115
3.5.	Scanning electron microscopy of tsc-extrudates after <i>in-vitro</i> release .....	117
3.6.	Result of DSC measurements.....	117
3.7.	Results of X-ray measurements.....	120
3.8.	Assessment of implant weight.....	122
4.	Discussion .....	123
4.1.	Lysozyme release at various temperatures.....	123
4.2.	Lysozyme release from implants comprising various low melting lipids.....	124
4.3.	Lysozyme release from implants comprising various amounts of pore forming agent	124
4.4.	X-ray diffraction measurements .....	127
5.	Conclusion.....	129
VII.	<i>In-vivo</i> biodegradability of lipid twin-screw extruded implants in rabbits .....	131
1.	Introduction.....	131
2.	Materials and Methods.....	133
2.1.	Materials .....	133
2.2.	Preparation of lipid implants.....	133
2.3.	Preliminary testing .....	135
2.4.	Differential scanning calorimetry (DSC) .....	136
2.5.	Scanning electron microscopy (SEM) .....	136
2.6.	Selection of test animals .....	136
2.7.	Animal treatment and <i>in-vivo</i> degradation study.....	136
2.8.	Recovery of implants and assessment of implant weights after <i>in-vivo</i> study ....	137

2.9.	<i>In-vitro</i> degradation study .....	138
3.	Results and discussion .....	139
3.1.	Preliminary studies .....	139
3.2.	Animal treatment and recovery of implants .....	140
3.1.	<i>In-vitro</i> degradation study of lipid implants .....	141
3.2.	<i>In-vivo</i> degradation of formulation A.....	145
3.3.	Influence of the amount of pore-former on the degradability of lipid tsc-extrudates 151	
3.4.	Influence of the type of low-melting lipid .....	153
4.	Conclusion.....	155
VIII.	Lipase induced <i>in-vitro</i> degradation study with tsc-extrudates.....	157
1.	Introduction.....	157
2.	Materials and methods.....	159
2.1.	Materials .....	159
2.2.	Methods.....	159
3.	Results .....	165
3.1.	Implant degradation after embedding of lipase .....	165
3.2.	Simultaneous release of lipase and lysozyme from lipid tsc-extrudates .....	168
4.	Conclusion.....	175
IX.	Single molecule fluorescence microscopy studies and release pathways of protein drug molecules from triglyceride based implants .....	177
1.	Introduction.....	177
2.	Materials and methods.....	179
2.1.	Materials .....	179
2.2.	Fluorescence labeling of IFN $\alpha$ .....	179

2.3.	Protein analysis .....	180
2.4.	Preparation of IFN $\alpha$ lyophilisates .....	180
2.1.	Preparation of lipid twin-screw extrudates and protein-lipid dispersions for wide-field fluorescence spectroscopy.....	180
2.2.	Preparation of PEG samples for fluorescence microscopy.....	182
2.3.	Scanning electron microscopy (SEM) .....	182
2.4.	Wide-field fluorescence microscopy.....	182
2.5.	Tracking of the proteins, visualization of the random walk and calculation of diffusion coefficients .....	182
2.6.	Protein release studies .....	183
3.	Results and discussion .....	185
3.1.	Scanning electron microscopy .....	185
3.2.	Quantification of fluo-IFN $\alpha$ .....	185
3.3.	IFN $\alpha$ release studies from tsc-extrudates.....	187
3.4.	IFN $\alpha$ release from protein-lipid dispersions.....	188
3.5.	Wide-field fluorescence microscopy of tsc-extrudates.....	189
3.6.	Diffusion pathways of fluo-IFN $\alpha$ molecules in tsc-extrudates .....	192
3.7.	Random walk of IFN $\alpha$ molecules .....	195
4.	Conclusion.....	199
X.	Final Summary .....	201
	REFERENCES.....	i

## I. General introduction

Protein drugs are an integral part of today's spectrum of active pharmaceutical ingredients and take up a market size of several billion dollars in total each year [1, 2]. Protein drugs are highly active drugs that selectively target the site of action by the inherent key-lock principle and specific interactions. Proteins are built from a sequence of amino acids (primary structure) and arrange themselves in a specific three-dimensional order forming, for example, so-called  $\beta$ -sheet or  $\alpha$ -helical structures (secondary structure). These structures again form a tertiary structure which is defined by the relative arrangement of secondary structure components. Compared to small molecular drugs, the highly ordered three-dimensional structure of proteins is prone to degradation upon inappropriate handling [3, 4]. A variety of chemical and physical degradation pathways have been investigated, and pharmaceutical companies screen for the best possible formulations for protein drug products to prevent aggregation and denaturation of the active during manufacturing, shipping, long-term storage and/or application to the patient [5-8].

In general, protein drugs need to be administered parenterally as the oral route is restricted by harsh pH conditions in the stomach, and a plethora of enzymes and surface active substances in the gastrointestinal tract which are detrimental to proteins [9-11]. Additionally, absorption of proteins from the gastrointestinal tract is per se limited due to their high molecular mass and the ionic structure of some amino acids. Buccal or dermal delivery of protein drugs generally fails due to the large amount of protein needed for systemic administration. In addition, the short plasma half-lives of proteins results in frequent applications of high doses which is hardly feasible for these delivery routes [11]. Pulmonary application of proteins was possible for inhalative insulin (Exubera<sup>®</sup>) which was marketed in 2006 but withdrawn in 2007 due to economic inefficiency. In addition, increased rates of anti-insulin antibody formation and a greater decline in pulmonary function under Exubera<sup>®</sup> treatment were reported [2, 12], which was a major drawback for the development of inhalative protein drug products. Thus until today parenteral application of protein drugs by injection or infusion is still the conventional route of administration.

Sustained delivery of protein drugs was investigated with the interest to reduce application frequency and systemic burden for the patients. As poly-lactic acid (PLA) and poly-lactic-co-glycolic acid (PLGA) implants and microparticles had already been approved by regulatory agencies, PLA/PLGA became first choice for the development of sustained release protein drug devices. Peptides like leuproreline and goserelin were successfully loaded onto and delivered from such systems [13-15], however, today no protein drug formulated in an implant or microparticulate device is on the market.

Besides other materials like hydroxyethylmethacrylate, ethylene-vinyl-acetate copolymer or polyvinyl alcohol [16, 17], using lipidic substances as matrix materials has attracted the interest of researchers for more than twenty years [18-20].

Lipids are natural substances that exhibit excellent biocompatibility and are in general biodegradable by lipases or body fluids [18, 21, 22]. Besides other lipid based sustained release formulations compressed triglyceride based implants have attracted much attention due to the easy preparation process and long term release of (protein) drugs from these devices [23-27]. Additionally, it has been reported that the fragile structure of a lyophilized protein, recombinant human interferon $\alpha$ -2a (IFN $\alpha$ ), was conserved during long-term storage and release [27, 28], when incorporated into triglyceride matrices.

Recently, Herrmann *et al.* demonstrated that the addition of PEG to the triglyceride implant matrix can be used to control the rate of IFN $\alpha$  release from compressed triglyceride implants by *in-situ* precipitation of the protein (IFN $\alpha$ ) [24, 29, 30]. *In-vivo* delivery of IFN $\alpha$  in rabbits was also successful and no adverse tissue reaction with respect to the lipid formulation was observed [31].

A change of the manufacturing strategy from compression to twin-screw extrusion (tsc-extrusion) allowed the production of rod-shaped and thus easily applicable implants. Moreover, the tsc-extrusion process seemed to affect the release profile of the implant and caused a more sustained protein drug release [32]. *In-vitro* degradation studies also showed that twin-screw extrudates were more prone to lipase induced degradation than compressed implants [33]. The sum of all features of twin-screw extrudates makes them a very promising

delivery platform for protein drugs. However, little is known about the underlying mechanism of sustained protein drug release from tsc-extrudates and the degradation properties of this type of implant and this will form the basis for this thesis.



## **1. Controlled release systems for pharmaceutical peptides and proteins**

### **1.1. Definition of ‘controlled release’**

‘Controlled drug delivery systems’ have been described in literature since the 1970th when Alejandro Zaffaroni founded ALZA Corporation. ALZA’s inventions and patents include many so called ‘therapeutic systems’ that allow to control the rate of drug release over time periods ranging from days to years [34]. Controlled release systems include systems for localized drug delivery (e.g. in the eye: Ocusert<sup>®</sup> [35]), sustained drug release (e.g. sustained release tablets: OROS<sup>®</sup> [34]) or transdermal drug delivery (e.g. therapeutic patches, transdermal therapeutic systems (TTS) [34, 36]). Today ‘controlled release’ is a major factor in developing and marketing of new drug products as well as for the extension of patents of already marketed active pharmaceutical ingredients.

Controlled drug delivery systems can be designed for local as well as for systemic drug administration, and various routes of application including oral, dermal, transdermal, vaginal, buccal, nasal, parenteral and pulmonary administration have been investigated [10, 37]. Sustained drug delivery devices can be divided in three major groups according to their control mechanism for the rate of drug release: matrix based systems, membrane based systems and chemically controlled systems [38].

In matrix based systems the drug is dissolved or dispersed in a matrix and released from the matrix either by diffusion through pores of the matrix (dispersed drug) or by diffusion within the matrix material itself (dissolved drug) [39, 40]. Membrane based systems control the drug release rate by an inert membrane which acts as a diffusional barrier [34]. Chemically controlled systems control the release rate either by matrix erosion (e.g. cleavage of ester bonds), by matrix swelling or cleavage of chemical bonds between the drug and a carrier system [36-38, 41, 42]. Release mechanisms will be discussed in detail later (see chapter I - 0).

Drug products for parenteral release include microspheres [43], implants [13], liposomes [44], gels [45], suspensions [46, 47], *in-situ* forming implants [48, 49], lipophilic solutions [50,

51] and solid lipid nanoparticles [52-54] and have been extensively reviewed by various authors [10, 37, 55].

## **1.2. Currently marketed peptide and protein depot formulations**

Usually the oral route is the easiest way to administer drugs in form of liquids, tablets or capsules. However, some active pharmaceutical ingredients like proteins or peptides cannot easily be administered orally due their instability in the gastrointestinal tract and/or bioavailability limitations. In order to circumvent these problems, parenteral application of protein drugs which includes subcutaneous injection and intravenous infusion is necessary. As already mentioned, most protein drugs possess only short half lives and thus frequent dosing is required, leading to poor patients' compliance and high therapy costs. Therefore, therapeutic systems have been developed for parenteral application which should minimize dosing frequencies (e.g. one injection/application lasts for months/years), resulting in better patients' compliance.

One of the first therapeutic systems on the market containing a peptide drug was Zoladex<sup>®</sup> (1990). It is available as a one-month or three-months depot formulation and its biodegradable matrix consists of poly-lactic-co-glycolic acid (PLGA) and poly-lactic acid PLA (1:1). It comprises Goserelin acetate – a gonadotropin releasing hormone (GnRH) super agonist – and is indicated for the treatment of prostate cancer and breast cancer [15]. Lupron-Depot<sup>®</sup> was released in 1993 and is composed of a microparticulate system (PLA and leuprorelin acetate) that is indicated for the treatment of prostate cancer [13, 14]. Profact Depot<sup>®</sup> also contains a peptide drug (buserelin acetate – LHRH analog – prostate cancer) and is formulated in PLA-PLGA 1:3. An *in-situ* forming implant system against prostate cancer is Eligard<sup>®</sup> which contains leuprorelin acetate as active ingredient and is formulated in PLGA and N-methyl-2-pyrrolidone (NMP). The only marketed depot device that contained a protein drug was Nutropin Depot<sup>®</sup>, which was an injectable suspension of PLGA microparticles loaded with recombinant human growth hormone (rhGH - somatropin) as the active ingredient. Nutropin Depot<sup>®</sup> was designed to release somatropin over a period of one

month and was marketed in 1998, but withdrawn in 2004 which was explained by 'significant resources required by both companies (Alkmers Inc. and Genentech Inc.) to continue manufacturing and commercializing the product` [56].



## **2. Matrix materials for the preparation of protein containing sustained release devices**

Protein drugs are usually administered by subcutaneous injection or intravenous infusion because of their inherent instability in the gastrointestinal tract [10, 14, 57, 58]. However, the exploration of alternative delivery routes like parenteral, nasal or buccal delivery led to an increased interest in matrix materials which are able to maintain peptide/protein stability during manufacturing and allow 'controlled' protein release [9, 10, 59]. Since Langer *et al.* studied the release of proteins from polymers [16], a broad variety of substances has been under investigation for their suitability as matrix material for sustained protein drug release [57, 59, 60].

In the 1980ies inert matrix materials studied by Langer and Siegel included hydroxyethylmethacrylate (HEMA), ethylene-vinyl-acetate copolymer (EVAc) and polyvinyl alcohol (PVA) [16, 17]. Model proteins (soybean trypsin inhibitor, lysozyme, alkaline phosphates, catalase and bovine serum albumin) were embedded into the matrix by a solvent evaporation method. The matrix materials were simply dissolved in an appropriate organic solvent or water, mixed with the protein and cast into moulds. After evaporation of the solvent under mild vacuum, the implants were additionally coated with identical matrix material by dipping and drying. *In-vitro* release from these polymer based implants lasted up to 100 days. However, these matrix materials were not bio-degradable and did not show any sign of erosion *in-vitro* and *in-vivo*. Thus the search for alternative carrier materials started.

Poly-lactic acid (PLA) and poly-lactic-co-glycolic acid (PLGA) had already been successfully used to prepare biodegradable systems (microparticles, implants) for small molecular drugs and had been approved by regulatory agencies. Thus, a plethora of researchers used PLA/PLGA as matrix materials for protein and peptide loaded microparticles and/or implants [43, 61-66]. The preparation of PLA/PLGA implants was performed by emulsion, suspension or dissolution methods where the matrix material was dissolved in organic solvent and the protein was emulsified, suspended or dissolved in the organic phase. Unfortunately, the use of organic solvent was shown to be problematic with respect to protein stability as proteins

tend to unfold and aggregate in hydrophobic environments and at interfaces [3, 67, 68]. Additionally, after protein loading and preparation of microparticles or implants the organic solvent had to be removed from the system by a drying step. Interestingly, drying was not reported to induce significant protein degradation in PLGA matrices [64]. However, implant erosion during release was reported to have a detrimental effect on protein stability. Degradation of PLA and/or PLGA resulted in lactic and glycolic acids and induced a pH drop in the core of the delivery systems [64, 69, 70]. This pH shift was reported to start and to accelerate protein aggregation, deamidation [64], and acylation [71]. Additionally, an increase in osmotic pressure was detected inside biodegradable microspheres as a consequence of matrix erosion [69]. In order to overcome these shortcomings various approaches to prevent protein degradation were conducted. Protein aggregation during preparation was limited if interface-active excipients like PEG, gelatin, human serum albumin [72], HP- $\beta$ -CD [73] or phosphatidylcholine [74] were used or anhydrous preparation methods were applied (solid-in-oil-in-oil dispersion) [75]. Preparation by suspension methods was generally more gentle for protein drugs as unfolding and aggregation processes were hindered. The conformation of the dry and solid protein was kinetically trapped in organic solvents [76]. Protein stability during release was increased by the addition of basic salts (e.g.  $Zn^{2+}$ ) which neutralize the acid degradation products of PLGA [62, 77, 78]. Alternatively, high protein loadings acted as buffer solutions and counteracted a pH drop [79]. The addition of surface active substances like Pluronic™ or BSA increased the rate of release and prevented aggregation of proteins probably by adsorption of surfactant molecules or BSA to the hydrophobic PLGA matrix [77]. Many therapeutic proteins have been embedded into PLGA based systems including recombinant human growth hormone [80], insulin [77], human epidermal growth factor [81], interferon  $\alpha$  [82-85], interferon  $\gamma$  [86], interleukin-1 $\alpha$  [74] and basic fibroblast growth factor [78]. Despite all these attempts, no protein drug containing product using PLA/PLGA is currently on the market.

As an alternative to PLA/PLGA, other material were studied as matrix material for protein drugs. Polyanhydrides consist of dimers of fatty acids and/or sebacic acid and offer better

control over polymer properties and erosion behavior than PLGA. Additionally, degradation products of polyanhydrides have a neutral pH and no acidic primary hydrolysis products are produced. Polyanhydrides have been used to successfully deliver a LHRH analogue over time periods of one month [87].

Biomaterials like chitosan have been used to prepare protein loaded nanoparticles or microparticles [88, 89]. Chitosan is a mucopolysaccharide which is generated by the deacetylation of chitin, the major compound of the exoskeletons in crustaceans. Various methods for nano- or microparticle preparation have been described in literature [88, 89]. Insulin [90], xylanase, lipase and protease [91] as well as an anti-TNF $\alpha$  antibody [92] have been incorporated in chitosan based delivery systems. However, chitosan is not approved by regulatory agencies for parenteral applications.

Collagen has been used for the delivery of recombinant human bone morphogenetic protein (rhBMP-2) from absorbable collagen sponges for bone regeneration [93, 94]. RhBMP-2 was loaded onto the sponges by simple soaking of the sponges with an rhBMP-2 containing solution. Additionally, collagen sponges were loaded with growth factors for e.g. dermal wound healing by dispersion and drying of protein containing solutions onto the matrices [95]. Collagen films were loaded with human growth hormone and growth factors [94]. Cylindrical collagen implants were used to deliver interferon *in-vitro* and *in-vivo* in a mouse model [96]. Collagen minipellets were loaded with interleukin-2 and pharmacokinetic studies in mice revealed that a single subcutaneous injection of a minipellet could prolong IL-2 retention. Recently, Chan *et al.* produced nano-fibrous collagen microspheres loaded with various proteins including nerve growth factor (NGF) by an emulsification process [97].

Besides these substances, alginate [98], hyaluronic acids [99, 100], starch, tricalcium phosphate, and synthetic polymers (polyester, polyiminocarbonates, polycaprolactones and polyphosphazenes) were investigated for controlled protein and peptide drug delivery [9, 57].

Alternatively, *in-situ* forming implants were extensively studied [45, 49, 101, 102]. They consist of biodegradable polymers dissolved in a biocompatible carrier. Upon contact with body fluids or at body temperature the polymer solidifies and forms solid implants. For

example, Jin *et al.* produced injectable, thermoreversible gels, comprised of chondroitin-6-sulfate, gelatin type A, methylcellulose and ammonium sulfate. The thermoreversible gels were formed from methylcellulose in the presence of the salting out agent ammonium sulfate. A complex coazervate of oppositely charged chondroitin-6-sulfate and positively charged high-molecular weight gelatin type A was embedded into the pre-formulated gel. FITC-BSA, which was simply admixed to the pre-formulated gel, was released over a period of 25 days *in-vitro* [45]. Thermoreversible hydrogels have also been described by Zentner *et al.* [103]. PLGA-PEG-PLGA triblock polymers (ReGel<sup>®</sup>) were used in this study and Zn-insulin, porcine growth hormone, G-CSF or recombinant hepatitis B surface antigen were incorporated into the gels. *In-vitro* and *in-vivo* studies indicated sustained release of the macromolecules after single-injections over a period 7-14 days and analysis showed equal biological effects compared to daily injections. Singh *et al.* demonstrated release of lysozyme from thermoreversible triblock copolymer implants over two to eight weeks [104]. Kang *et al.* utilized the Atrigel<sup>®</sup> system with incorporated insulin and found sustained protein release over up to 15 days [105]. The Atrigel<sup>®</sup> system consists of PLGA and lactic/caprolactone copolymers which are dissolved in an organic solvent (e.g. N-methyl-2-pyrrolidone (NMP), dimethyl sulfoxide (DMSO) or tetraglycol). Upon injection, the organic solvent dissipates and a phase separation step forms a depot at the site of injection [102].

Lipidic substances (lipids) have also been investigated as parenteral, sustained release dosage form and will be discussed in the next chapter.

### **3. Lipids as matrix materials for the preparation of protein containing sustained release devices**

#### **3.1. Lipid based drug delivery systems**

Lipids have been defined as 'biological substances that are generally hydrophobic in nature and in many cases soluble in organic solvents' [106] or as 'chemically heterogeneous group of substances, having in common the property of insolubility in water, but solubility in non-polar solvents' [107]. Thus, lipids are generally defined by their hydrophobic nature but not by a special chemical structure. Fahy *et al.* divided 'lipids' into eight categories according to their chemical composition: fatty acyls, glycerolipids, glycerophospholipids, sphingolipids, sterol lipids, prenol lipids, saccharolipids and polyketides [106].

In order to enhance the oral bioavailability of small molecular drugs, they are often formulated in 'lipid' formulations [108]. This became more and more important during the last decades as novel high throughput screening methods resulted in an increased number of sparingly soluble lipophilic drug candidates which have a generally lower bioavailability after oral application compared to more hydrophilic drugs due to dissolution problems [109]. Thus numerous attempts for the development of 'lipid' based drug delivery devices are described in literature for small molecular drugs including self-micro-emulsifying drug delivery systems (SMEDDSs) [110], self-nano-emulsifying drug delivery systems (SNEDDSs), solid or waxy lipid powders, granules or pellets and colloidal drug carrier systems like liposomes and solid lipid nanoparticles (SLN) [108, 111]. Preparation methods for lipid based drug delivery systems are e.g. spray-cooling, spray-drying, melt-granulation, melt-extrusion, supercritical-fluid based methods and high pressure homogenization [107, 109]. Most of these formulations aim for the improvement of the oral bioavailability of lipophilic drugs.

As already stated above, oral application of protein drugs is in most cases not feasible due to the inherent instability of proteins in the gastrointestinal tract. Therefore researchers aim for parenteral, transdermal or pulmonary application routes [10] and a broad variety of lipids were used to create such delivery systems for proteinaceous drugs [21, 112].

### 3.1.1. Lipid microparticles

Protein loaded lipid microparticles can be prepared by a variety of methods including spray-drying, spray-cooling, coazervation, w/o/w double emulsion techniques and supercritical fluid based techniques [113-115].

In 1988 Steber *et al.* patented a method for the preparation of bovine growth hormone loaded microspheres for subcutaneous (s.c.) injection. The microparticles consisted of glycerol tristearate and glycerol distearate and were prepared by spray-cooling [116].

Reithmeier *et al.* prepared thymocartin [117], insulin [117] and somatostatin [118] loaded microparticles by a modified solvent evaporation method as well as by a melt-dispersion method and used glycerol tripalmitate as matrix material. *In-vivo* studies showed that the microparticles were well tolerated by NMRI-mice and comparable to PLGA microparticles. Drug loading efficacy and release kinetics were dependent on the type of incorporated drug and the preparation method. Release from the microparticles lasted for up to 10 days, however, only incomplete release of the incorporated drug was achieved. Furthermore the melt dispersion technique resulted in the formation of the unstable  $\alpha$ -modification of the triglyceride crystals which led to a in decreased storage stability as a consequence of polymorphic transformations.

Del Curto *et al.* [119] prepared gonadotropin release hormone antagonist (Antide<sup>®</sup>) loaded lipid microparticles for subcutaneous administration based on monoglycerides (glycerol monobehenate and glycerol monostearate) by a cryogenic micronization process. Before cryo-milling within the flux of liquid nitrogen, the peptide was loaded onto the lipid matrix material by co-melting or solvent evaporation at 80-95 °C. Results from *in-vitro* release tests correlated well with *in-vivo* (rats) studies and Antide<sup>®</sup> plasma levels were present for 30 days after dosing in the animals. However, high temperatures were necessary to load the matrix which might be detrimental for the stability of protein drugs.

A supercritical fluid based process was used to coat bovine serum albumin (BSA) particles with glycerol trimyristate and Gelucire<sup>®</sup> 50/02 [120, 121]. The method operated with supercritical carbon dioxide (CO<sub>2</sub>) in which the lipids were dissolved. Subsequently the solid

protein powder was dispersed into the supercritical fluid and by adjustment of the process parameters (pressure/temperature) the solubility of the lipid in the supercritical fluid was decreased and the lipid accumulated on the surface of the protein particles. Solubility studies including a variety of lipids (waxes, triglycerides and mixtures of glycerides and fatty acid esters) indicated that the process was strongly influenced by the solubility of the lipid components in supercritical CO<sub>2</sub> [122]. *In-vitro* release tests indicated rapid BSA release from glycerol trimyristate microparticles but a sustained release over 24 hours from Gelucire<sup>®</sup> 50/02 microparticles. This was explained by the varying porosity values of the microparticles. The supercritical fluid based process was found to be a gentle preparation method without the use of organic solvents or elevated process temperatures (13 °C - 52 °C) and no BSA degradation was detected after processing. However, the release lasted for only 24 hours, which is too short for most applications.

Spray drying was used to prepare human IgG loaded PulmoSpheres<sup>™</sup> (hollow porous microspheres) for pulmonary delivery. Therefore an emulsion of phosphatidylcholine and perflubron in water was mixed with a solution comprising an human IgG antibody and hydroxyethylstarch and immediately spray dried with a standard spray dryer. The microparticles consisted mainly of phosphatidylcholine and antibody loading was approximately 20%. The microparticles were administered into the lung of BALB/c mice by instillation of a stable suspension in perflubron and the IgG antibody reached systemic circulation. Antibody bioavailability was only 27% after intratracheal instillation of PulmoSpheres<sup>™</sup> but reached up to 40% after instillation of IgG solution in saline. The advantage of the administration of IgG in PulmoSpheres<sup>™</sup> was a strongly increased immune response to the human antibody, which was explained by the incorporation of the antibody into the drug carrier (PulmoSpheres<sup>™</sup>). The microparticles showed an increased cellular uptake by macrophages and a sustained release of the antibody [123]. A similar formulation comprising an inactivated form of influenza virus and a Fc receptor ligand was used to induce an immune response in BALB/c mice by receptor mediated targeting of phagocytes [124]. However, only short release periods were achieved (80% release within 6 hours).

Nevertheless, the feasibility of lipids for the preparation of a controlled release device by spray drying was shown.

Spray congealing was used to prepare insulin loaded microparticles based on glycerol tripalmitate. Crystalline insulin was suspended in molten lipid at 70 °C with an ultraturrax and atomized at 70 °C and 4-6 bar spraying pressure. The atomized lipid particles were rapidly cooled in a stream of cold air (- 20 °C) and subsequently freeze dried to remove adherent water. Yields of encapsulation of 78-95% were reached and the protein was not affected by the spray congealing process. However, upon incubation deamidated insulin species as well as protein aggregates were detected within the matrix of the microparticles. *In-vitro* cell culture tests revealed that the protein was still biologically active and was only slowly released from the microparticles. After preparation the lipid crystallized in the unstable  $\alpha$ -modification, and this was found to influence the release kinetics. The authors recommended an additional tempering step at elevated temperatures to transform the lipids into the stable  $\beta$ -modification [125]. Protein release (fluorescence labeled BSA) from Softisan<sup>®</sup> 154 microparticles prepared by the same spray congealing method was found to be controlled by water intrusion velocity into the microparticles [126] and the size and shape of the incorporated protein particles. Smaller protein particles with a more uniform distribution throughout the microparticles and less direct contact to each other resulted in a more sustained protein release. Spray congealing was also used by Richard *et al.* to prepare human growth hormone loaded microparticles for subcutaneous or intramuscular injection. In a first step, human growth hormone was spray dried with in a bulking agent (e.g. sucrose) and surfactant (Poloxamer 188), and the resulting particles were then dispersed into a lipid melt consisting of fatty acids, mono-, di- or triglycerides or phospholipids and mixtures thereof. Microparticles were prepared by spray-congealing of the lipid dispersion and the diameters of the particles were less than 100  $\mu\text{m}$  [127].

Special types of lipid microparticles are lipospheres. They consist of a solid hydrophobic fat core stabilized by a monolayer of phospholipids and were firstly described by Domb *et al.* [128, 129]. The drug is usually dissolved or dispersed within the lipid core, which consists of

triglycerides or fatty acids. BSA (as an antigen) [128], somatostatin [118] and thymocartin [117] have been incorporated into such systems and their release behavior has been characterized [130].

### 3.1.2. **Solid lipid nanoparticles (SLNs) for peptide and protein delivery**

Since the beginning of the 1990s solid lipid nanoparticles (SLN) have been investigated as drug delivery devices for topical, oral, pulmonary and parental applications [53]. The preparation of SLNs can be performed by *(I)* high pressure homogenization, by *(II)* a microemulsion technique from a 'critical solution' or by *(III)* a precipitation technique. *(I)* Hot temperature high pressure homogenization is performed with emulsion of triglycerides in water stabilized with lecithin or surfactants and polymers. The lipid is molten and the drug is dissolved in the hydrophobic phase. This pre-emulsion is homogenized and cooled down whereupon the lipid re-crystallizes and forms SLNs. Cold homogenization can be applied to protect temperature sensitive drugs or hydrophilic drugs, which would dissolve in water. The drug containing lipid melt is ground and microparticles are prepared and dispersed in a pre-suspension comprising water, lipid and surfactants. Homogenization and preparation of SLNs is performed within water or a liquid with low solubility for the drug (e.g. PEG 600 or oils) and at temperatures well below the melting point of the lipid (10-20 K). The microemulsion technique *(II)* works with 'critical solutions' which are prepared from molten lipids in aqueous solutions containing surfactants and at temperatures above the melting point of the lipids (fatty acids and/or glycerides). This 'critical solution' is then dispersed into a cold aqueous medium wherein the lipid crystallizes and form nanoparticles. The precipitation technique *(III)* uses organic solvents in which the drug and the lipid are dissolved and emulsified in water. After preparation of a very fine emulsion the organic solvent is removed leaving back SLNs. However, the application of organic solvents renders this preparation method unsuitable for many applications [52, 53, 131, 132].

Protein and peptide loaded SLNs have been described by various authors [132]. For example Li *et al.* loaded yak interferon alpha by a double emulsion solvent evaporation method (w/o/w) into SLN [133]. *In-vitro* release tests showed antiviral activity of the preparation by a Madin-Darby bovine kidney (MDBK) cell assay for 16 days. Insulin and thymopentin release for gel-core SLNs was reported by Yang *et al.* [134, 135], who also used double emulsion solvent evaporation method. Release lasted for only 24 hours; however, oral bioavailability of insulin was reported in a rat model. Lysozyme [136], BSA [137], human recombinant epidermal growth factor [138] were embedded into SLN. Almeida *et al.* reported the incorporation of peptides like cyclosporine A, insulin and calcitonin into SLNs [139].

### 3.1.3. Liposomes

Since the introduction of liposomes as drug delivery devices by Bangham *et al.* [140] many groups prepared and described liposomal based drug delivery devices and in 2003 more than 2000 papers and 150 reviews have been published on this topic [141]. Liposomes are described as "spherical, self-closed structures formed by one or several concentric lipid bilayers with an aqueous phase inside and between the lipid bilayers" [141]. They show enhanced circulation times in the blood stream, can be used to passively (enhanced permeability and retention effect - EPR effect) or actively (immunoliposomes) target cells or organs and are well tolerated by the human body. PEGylated liposomes are described as "stealth" liposomes which are protected from opsonisation and clearance by the flexible PEG chains. Liposomes can be further divided into multilamellar vesicles (MLV), small unilamellar vesicles (SUV) and large unilamellar vesicles (LUV). Furthermore liposomes can be surface-modified by chemical conjugation of proteins, peptides, polymers or other molecules. A common approach is antibody-mediated liposome targeting of cancer cells e.g. anti-HER2 liposomes for the targeting of HER2 over expressing tumors [142]. In addition, liposomes were also prepared as carriers for protein and peptide drugs which were incorporated into the aqueous liposome core.

Liposomes were prepared to increase the circulation times of e.g. vasopressin [143] or interleukin-2 [144]. Locoregional treatment of head and neck tumors was possible by sustained release of interleukin-2 from liposomes at the site of action which reduced negative side effects [145]. Liposomal insulin was shown to effectively lower blood glucose levels over increased periods of time in diabetic rats [146] and even oral bioavailability of liposomal insulin in rats was described [147]. Recombinant human epidermal growth factor [148], human tumor necrosis factor [149] and other proteins or peptides were also successfully incorporated into liposomal formulations for the treatment of various diseases [132].

#### 3.1.4. DepoFoam™ formulations

Special forms of liposomes are so called multivesicular liposomes (MVLs, tradename: DepoFoam™) which are not designed for intra-vascular but parenteral application. MVLs are composed of one neutral lipid (e.g. triglyceride) and at least one membrane forming lipid (e.g. phospholipids) which form non-concentric multiple lipid layers. As a consequence the drug is only released from the outermost membranes of the MVLs but redistributes after release from internal vesicles. Therefore, the drug is released very slowly. A second advantage of this system is the high volume to lipid ratio which allows the encapsulation of high drug loadings. The preparation of DepoFoam™ formulations is performed in a two-step emulsification process. At first, a water-in-oil emulsion is prepared under the input of mechanical energy. The drug is dissolved in the aqueous phase which is subsequently emulsified in an organic solvent in which the lipids were dissolved. By the addition of an immiscible aqueous component, a second emulsion is prepared and the solvent spherules are dispersed in the aqueous component. The organic solvent is evaporated under reduced pressure and the solvent is completely removed leaving behind MVLs [150].

Marketed products like DepoCyt™ (cytarabine) and DepoDur™ (morphine) comprise small molecular drugs but also protein and peptide drugs have been incorporated into DepoFoam™ formulations. Qiu *et al.* prepared interferon  $\alpha$ -2b containing MVLs which slowly released the protein after subcutaneous injection into mice. *In-vitro* release lasted for up to 7

days and increased serum half-lives were detected by ELISA assays compared to subcutaneous injection of unencapsulated interferon  $\alpha$ -2b [151]. DepoFoam™ technology was used to prepare insulin-like growth factor loaded MVL which released the protein over a period of 7 days *in-vitro* and *in-vivo*. The protein was stable during the manufacturing process and biological activity was conserved [152]. Leridistim (chimeric growth factor containing interleukin-3 (IL-3) and granulocyte colony stimulating factor (G-CSF)) showed a sustained release from a DepoFoam™ formulation *in-vivo* in rats which resulted in elevated neutrophil counts for ten days in contrast to only two days for unencapsulated Leridistim [153]. Additionally, recombinant human insulin and peptides such as leuprolide, enkephalin and octreotide have been formulated into MVLs [154].

### 3.1.5. Vesicular phospholipid gels (VPGs)

Recent developments in lipid based drug delivery are so called vesicular phospholipid gels (VPG) in which lipophilic, amphiphilic or hydrophilic drugs can be incorporated. VPG consist of 30-60% phospholipids which form a viscous gel-like structure by numerous densely packed vesicles [155, 156]. VPGs can be dispersed in water and form small unilamellar liposomes and can therefore be prepared as storage-stable intermediates for liposomes. For the preparation of VPG two manufacturing strategies are described in literature: high pressure homogenization and dual asymmetric centrifugation.

High pressure homogenization is a one-step preparation method without the use of an organic solvent. At first, the phospholipids are mixed with water and drug and are allowed to swell for a certain period of time. Afterwards, the dispersion is processed by a high-pressure homogenizer for several times resulting in a uniform size distribution of the phospholipid vesicles.

Dual asymmetric centrifugation is a technique by which the sample is rotated around a central axis and also around a second axis in the centre of the sample container [157] (Figure 1). As a consequence, shear forces are generated which allow the mixing of highly viscous substances and lead to the formation of VPGs. The method is very easy and straight

forward and can be applied without further preparation steps by simple mixing of drugs and excipients. In contrast to high pressure homogenization, the method is more gentle (lower temperatures and less shear forces) and can therefore be used for the preparation of peptide and protein loaded VPGs. Tian *et al.* successfully loaded granulocyte colony stimulating factor (G-CSF), recombinant human erythropoietin (rhEPO) and an IgG<sub>1</sub> antibody into VPGs and described the sustained release of these macromolecules in *in-vitro* studies [158, 159]. EPO was released over 17 days, and no additional aggregated or fragmented protein species was detected after manufacturing or release. G-CSF was also linearly released from VPG over several days; however a protein loss was detected which was explained by the inherent instability of G-CSF in the release buffer. Release of IgG<sub>1</sub> antibody from VPGs lasted up to 40 days and showed close to zero-order release kinetics. For all experiments VPG erosion was found to be the major driving factor for protein drug release [160].

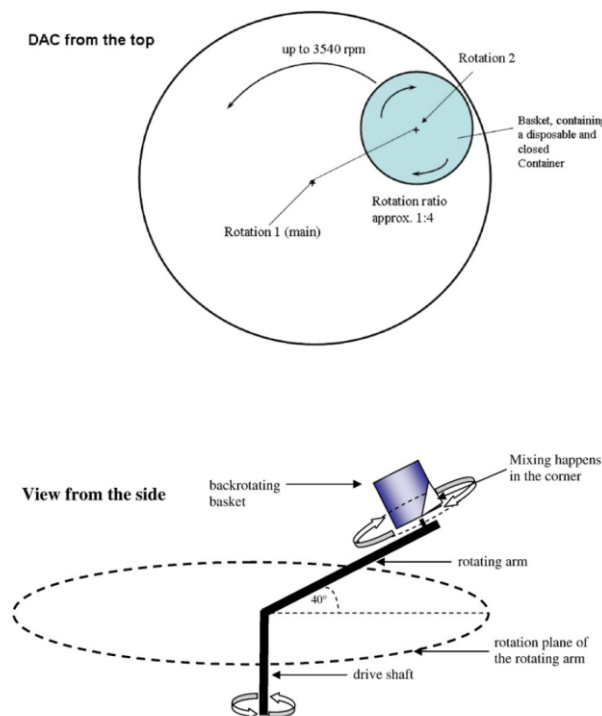


**Figure 1: Schematic drawing of the principal of asymmetric dual centrifugation. Taken from Massing *et al.* [157].**

### 3.1.6. Cubic phase gels as protein delivery systems

Cubic phase gels spontaneously form as liquid crystalline phases if polar amphiphilic lipids (like glyceryl monooleate) are placed in an aqueous environment. They consist of 'curved bicontinuous lipid bilayer(s) in three dimensions, separating two congruent networks of water channels' [161] (see Figure 2). Lipidic substances for the preparation of cubic phase gels include glyceryl monooleate, monoelaidin, phosphatidylethanolamine, phospholipids and PEGylated phospholipids. Successful incorporation into cubic phase gels and sustained release of proteins from cubic phase gels was described by Leslie *et al.* (hemoglobin) [162], Ericson *et al.* (lysozyme) [163] and Sadhale *et al.* (insulin) [164, 165]. The biological activity and the secondary and tertiary structure of the proteins were preserved in the lipid systems and insulin was even protected from agitation induced aggregation [164]. *In-vitro* protein release lasted for up to 1 week and *in-situ* forming placebo implant were well tolerated in *in-vivo* studies after intravaginal or periodontal application. Cubic phase gels can be dispersed into surfactant containing low-viscosity solutions whilst retaining their internal nanostructure. These dispersions contain so called 'cubosomes' (USPTO registered trademark of GS Development AB Corp., Sweden) which are discrete, sub-micron, nano-structured particles of bicontinuous cubic liquid crystalline phase [166]. Cubosomes were prepared for the delivery of protein vaccines (ovalbumin) by Rizwan *et al.* [167, 168] and exhibited high entrapment rates and slow release profiles.

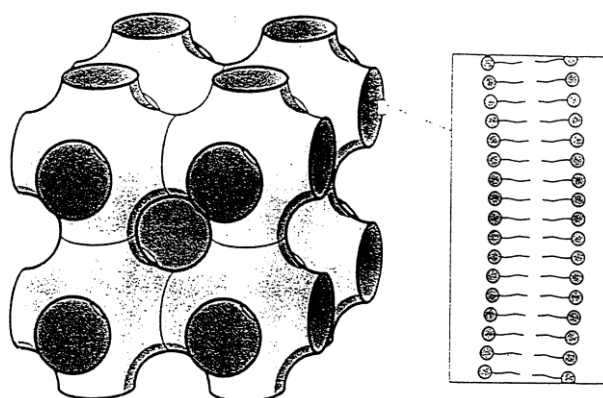
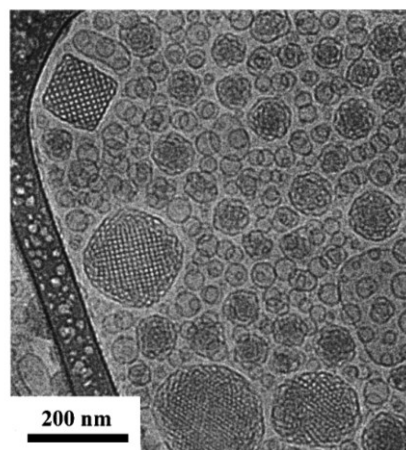


Figure 2: Structure of glyceryl monooleate-water cubic phase gel in three dimension. Taken from Shah *et al.* [161].



**Figure 3: Cryo-transmission electron micrograph of dispersed particles of cubic phase gels or 'cubosomes'. The cubosomes are approximately 150 nm in diameter. Taken from Spicer *et al.* [166].**

### 3.1.7. Compressed lipid implants for peptide or protein drug delivery

Compression has always been the first choice for the preparation of lipid based implant systems. The manufacturing by compression is very easy, cheap and can be performed without organic solvents and at low temperatures. A broad variety of solid lipids were used to prepare compressed implants and several authors used this technique to embed proteins or peptides into lipid matrixes [19, 27, 31, 169-172].

Already in 1984 Kent *et al.* embedded bovine growth hormone and insulin into cholesterol matrixes together with a binder and a lubrication agent. The patent claimed that macromolecules like growth hormones would show diffusion controlled release from the inert matrix and the rate of release could be adjusted by controlling the porosity of the implant [20].

Wang *et al.* released insulin from matrices consisting of cholesterol [173], various fatty acids, anhydrides of fatty acids and triglycerides [19]. The implants were prepared by simple admixture of the lipids and bovine insulin (Zn-salt) and compressed using a hydraulic press. Blood glucose level of diabetic Wistar rats could be controlled over 1 month after subcutaneous injection of lipid implants. Additionally implants consisting of palmitic acid were shown to start erosion during *in-vivo* release [171].

Compression was used by Khan *et al.* for the preparation of BSA loaded biodegradable lipid pellets. Cholesterol was used as matrix materials either alone or after a co-precipitation step and in a mixture with lecithin. BSA powder was mixed to the sieved lipid powders and compressed to 30 mg pellets. Subcutaneous implantation in mice resulted in measurable formation of anti-BSA antibodies after 40 days [174] and 10 months [175]. Increasing amount of lecithin resulted in an increased erosion rate and release rate. However, release lasted for only 10 days and no data about biocompatibility of such devices *in-vivo* were shown. Walduck *et al.* [22] used the same method and materials for the manufacturing of antigen loaded implants and successfully immunized sheep in a single immunization step.

In 2006, Guse *et al.* published data about the 'Biocompatibility and erosion of implants made of triglycerides and blends with cholesterol and phospholipids' [23]. They found that the matrix materials glycerol tripalmitate and cholesterol showed good biocompatibility after subcutaneous implantation on NMRI-mice. Increasing amounts of lecithin, however, resulted in increased inflammatory reactions at the site of administration. The erosion of the implants was higher if mixtures of lecithin and glycerol tripalmitate were used (implants comprising 50% lecithin collapsed at day 6) compared to pure glycerol tripalmitate or mixtures of cholesterol with glycerol tripalmitate. The latter implants stayed intact for up to 35 days and no sign of erosion or swelling was observed.

Release of tetramethylrhodamine (TAMRA) labeled bovine serum albumin (TAMRA-BSA) and hyaluronidase from compressed glycerol trimyristate matrices was investigated by Vogelhuber *et al.* [172]. High burst release during the first day of incubation and incomplete protein release was detected after *in-vitro* release tests. Incomplete release was explained by insufficient amounts of pore-forming agents. However, protein integrity was maintained during manufacturing and storage in the triglyceride matrix. Subcutaneous implantation into NMRI mice and subsequent recovery of the matrices revealed that the implant did not show any sign of erosion during 15 days of incubation.

Compressed implants consisting of glycerol tripalmitate were loaded with insulin and used for *in-vitro* cartilage engineering [169]. It was shown that insulin was released in a sustained

manner in its biologically active form from the triglyceride matrices and led to a weight increase in cartilaginous cell-polymer constructs. Implant manufacturing was performed by a wetting-compression method. In a first step, insulin was dissolved in water and appropriate amounts of the solution were added to mortars filled with the triglyceride powder. The mixtures were freeze-dried, manually homogenized in the mortar and subsequently compressed to cylindrical matrices. No aggregation or loss of activity was encountered during manufacturing or extraction from the matrices by chloroform. Matrices were loaded with 0.2%, 1.0% and 2.0% insulin and released 100%, 90% and 67% of the incorporated drug [169].

Compression was also used to prepare interleukin-18 (IL-18) loaded glycerol tripalmitate based implants. These implants were prepared to deliver IL-18 into rat-brains. The manufacturing process consisted of two steps. At first a modified co-lyophilization process by which the protein was lyophilized together with PEG 6000 [176] was applied. The lyophilized powder was dispersed into tetrahydrofuran (THF) and PEG was selectively dissolved leaving back fine protein microparticles. This dispersion was mixed with dissolved glycerol tripalmitate by ultrasonication and frozen in liquid nitrogen. The organic solvent was completely removed by application of vacuum and the remaining powder formulation was subsequently ground and compressed. The authors claimed that a very homogeneous protein distribution was achieved by this procedure. Additionally, PEG acted as a cryoprotectant during freezing and as pore-forming agent and protein stabilizer during *in-vitro* release. Incomplete release (< 35%) of IL-18 from the matrices was explained by insufficient amounts of pore-forming agents and the very fine distribution of the drug within the lipid matrix [25].

A comparison between four different manufacturing strategies for protein loaded compressed lipid implants was published by Könning *et al.* [177]. In a first attempt, lyophilized lysozyme was directly mixed with lipid powder and compressed to implant matrices. As an alternative, a solid-in-oil dispersion of lyophilized lysozyme in THF was mixed with a solution of the triglyceride. Thirdly, a water-in-oil (w/o) emulsion was prepared wherein the protein was

dissolved in the aqueous phase and the lipid in dichloromethane. At last, the protein was co-lyophilized with PEG 6000 and processed as already described above. Implants which were prepared from the pure powder mixture released the protein very rapidly (70%, 1 day) whereas manufacturing from the solid-in-oil dispersion led to incomplete drug release (25% total release). The w/o emulsion technique as well as the co-lyophilization technique released the protein more slowly over a period of 60 days. However, the w/o emulsion technique induced higher levels of aggregated protein species. Therefore the co-lyophilization technique was found to be the most appropriate technique for the preparation of slow releasing triglyceride implants. In continuative studies brain derived neurotropic factor (BDNF) was embedded into triglyceride matrices by this technique and *in-vitro* release studies were performed. The protein was continuously released for more than one month and the manufacturing process did not induce the formation of aggregated protein species.

Mohl *et al.* prepared recombinant human IFN $\alpha$  2a (IFN $\alpha$ ) loaded compressed implants from glycerol tristearin, PEG 6000 and lyophilized IFN $\alpha$  powder (lyophilized with HP- $\beta$ -CD or trehalose in a protein-excipient ratio of 1:3). More than 90% of the incorporated protein was released over a period of one month and the release rate was controlled by the amount of PEG 6000 which acted as porogen [27]. Long-term storage studies (6 months) revealed that the lyophilized protein was stable in the lipid matrix if lyophilized with HP- $\beta$ -CD as excipient. The use of trehalose as excipient resulted in increased levels of aggregated and oxidized IFN $\alpha$  species after storage and release [28].

Further investigation were performed by Herrmann *et al.* and Mohl *et al.* and revealed that PEG 6000 did not only act as porogen but was able to precipitated IFN $\alpha$  from solution and thereby modulate the release behavior [24, 27, 29]. Protein precipitation by PEG 6000 did not affect the stability of IFN $\alpha$  during release.

*In-vivo* IFN $\alpha$  release studies from compressed implants in rabbits were performed by Schwab *et al.* [31]. Sustained protein release was monitored by ELISA assays for nine days. Afterwards anti-drug antibodies were produced and eliminated IFN $\alpha$  from the rabbits`

bloodstream and thus IFN release could not be measured anymore. However, after 28 days of *in-vivo* incubation no adverse body reaction on the implant besides a minimal fibrous encapsulation was detected.

### 3.1.8. Twin-screw extruded lipid implants

Recently, twin-screw extrusion (tsc-extrusion) was introduced as a new manufacturing technique for the preparation of triglyceride based lipid implants by the group of Prof. Winter: [32, 33, 178]. Hereby, implants are prepared from powder mixtures comprising a protein drug powder, a release modifier, a high-melting and a low-melting lipid. A Haake MiniLab<sup>®</sup> Micro Rheology Compounder (Figure 4) is used for implant manufacturing which allows for the extrusion of low volumes.

The lipid composition facilitates twin-screw extrusion of the powders at gentle temperatures which are set slightly above the melting point of the low melting lipid. Due to lipid melting in the extruder barrel, the powder mixture softens and can be pressed through the extruder outlet die resulting in rod-shaped lipid implants. Advantages of the implant preparation by twin-screw extrusion are obvious:

- Implants can be prepared in a continuous mode with changing batch sizes without changing the extruder setup.
- Up-scaling of the process is easily possible.
- Resulting implant are rod-shaped and thus subcutaneous administration via a trochar is easy (Figure 6).
- Implant diameters can be easily varied (1.9 mm, 1.5 mm, 1.0 mm, 0.5 mm) by fixing different mouthpieces in front of the extruder outlet die (Figure 5 + Figure 6).
- Thorough mixing within the extruder barrel is provided by the rotating screws which leads to a very homogeneous distribution of drug within the matrix material.

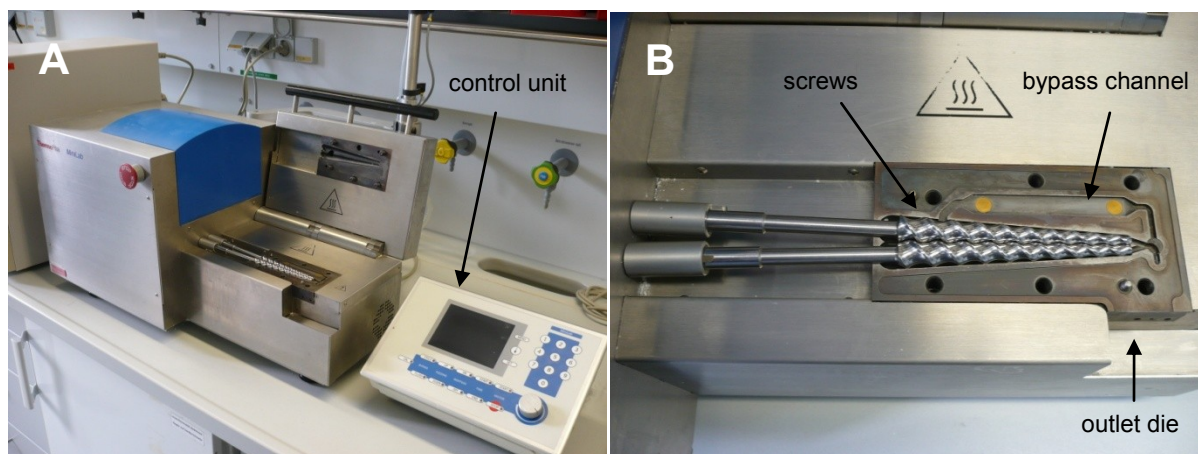


Figure 4: Haake MiniLab® Micro Rheology Compounder, Thermo Haake, Germany. A – twin-screw extruder and control unit. B – Close-up of the extruder barrel with screws and closed by-pass channel.

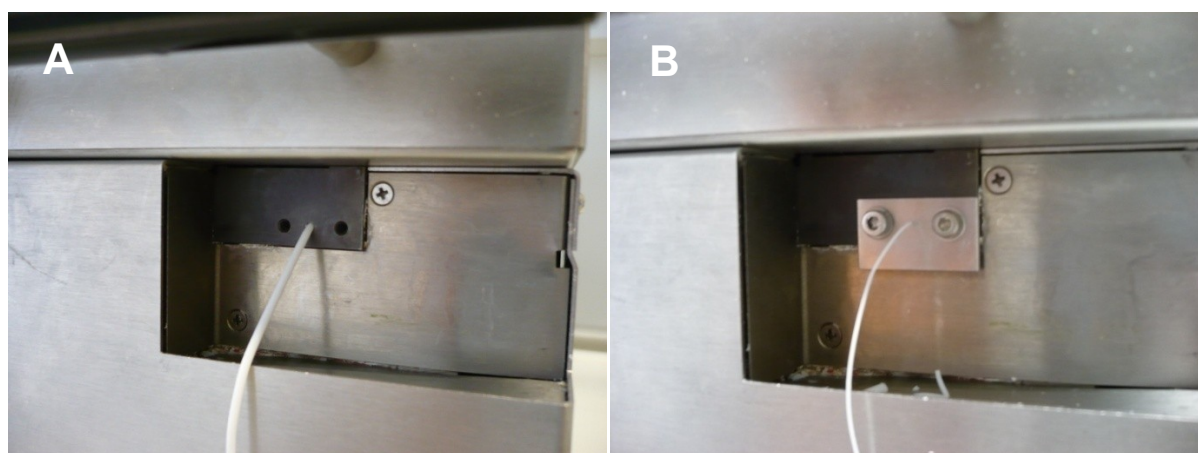
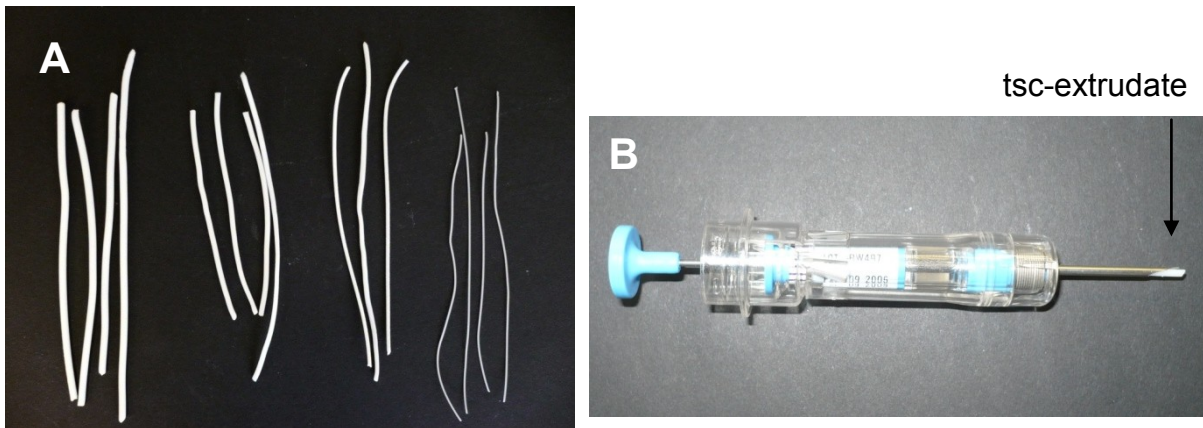


Figure 5: Extruder outlet die. A – standard outlet die ( $\varnothing = 1.9$  mm); B – outlet die with fixed mouthpiece ( $\varnothing = 1.0$  mm).

Schulze *et al.* prepared tsc-extrudates comprising IFN $\alpha$  and found sustained protein drug release which lasted for up to 40 days. Integrity of IFN $\alpha$  was not affected by the preparation process as shown by FTIR and SDS-PAGE studies [32]. Additionally, twin-screw extrusion was shown to result in a very homogenous distribution of a hydrophilic model compound methylene blue [179].

Schwab *et al.* performed an lipase based *in-vitro* degradation assay and found that tsc-extrudates were better degradable compared to compressed implants [33].



**Figure 6: (A) Rod shaped tsc-extrudates. Diameters from left to right: 1.9 mm, 1.5 mm, 1.0 mm and 0.5 mm. (B) Model device for the application (trochar) of tsc-extrudates by subcutaneous injection.**



#### 4. Mechanism of release from implant matrices

Mechanism of drug release from implant systems can be divided into 3 major groups:

- diffusion controlled systems,
- solvent activated systems (swelling controlled, osmotically driven) and
- erosion controlled release [42, 180].

Diffusion controlled systems can be further divided into matrix and membrane systems where diffusion occurs either within the implant matrix material or through a membrane. Diffusion represents the rate limiting step for drug release. A concentration gradient of the drug between the implant core and the implant surface allows drug release which follows Fick's second law of diffusion (Equation 1) which describes the dependency of the diffusion rate with respect to position and time of the diffusion borderline [181].

**Equation 1**                      
$$\frac{\partial C}{\partial t} = D \times \frac{\partial^2 C}{\partial^2 x}$$

For membrane or matrix systems zero-order release can be achieved as long as a constant diffusion gradient is established. This is the case if perfect sink conditions are prevailing and the concentration of the available drug is constant all the time. Membrane systems fulfill these requirements as long as the concentration of the drug in the core is much higher than the concentration which is able to diffuse through the membrane. As a consequence, the membrane is always saturated with the drug and constant amounts are released at the outer side of the membrane. Hereby, the solubility of the drug in the membrane is the rate limiting step for release and is controlling the rate of release. In the case of matrix systems, drug concentrations in the core are 'constant' if the system allows a dissolution of dispersed or precipitated drug, which is embedded into the matrix. Hereby, the released amount of the drug is compensated for by dissolution of formerly non-available drug material. This creates a constant starting concentration for release. It is important to note that the dissolution

velocity of the embedded drug is the rate limiting step for release. If dissolution is too fast, release will not be governed by the dissolution velocity but by drug diffusion according to the Higuchi equation (Equation 2). In matrix systems, the drug can be either dissolved in the matrix material (monolithic system) or is dispersed in the matrix and is dissolved upon contact in the release medium. In the former case, the drug diffuses through the matrix material and in the latter case, the drug is released through a porous network embedded into the matrix material and created upon dissolution of pore forming agent and/or drug (porous systems).

The most prominent way to describe drug release from inert systems is, as already mentioned, the Higuchi equation (Equation 2) where  $Q$  is the amount of drug released at time  $t$  per unit area,  $D$  is the diffusion coefficient and  $C_0$  and  $C_S$  are initial drug concentration and solubility of the drug, respectively :

$$\text{Equation 2} \quad Q = \sqrt{D \cdot (2C_0 - C_S) \cdot C_S \cdot t}, \quad \text{for } C_0 \gg C_S$$

The Higuchi equation is assuming that diffusion is only one dimensional,  $D$  is constant throughout the experiment, perfect sink conditions are present and  $C_0 \gg C_S$ . For this case, drug release is proportional to square root of time [39, 40].

Solvent activated systems can be swelling controlled as in the case of hydrogels [182] or osmotically driven as in the case of the Duros™ system [183]. In both cases, the permeation of the release medium into the implant device allows release of the active [184]. In swelling controlled systems a reordering of the implant polymer structures is responsible for drug release, whereas in osmotically driven systems the increased osmotic pressure releases the drug from the device.

The last class of drug release system is the erosion driven system. Implant erosion is mainly a chemical process where for example ester bonds between lactic acid and glycolic acids are cleaved. Thereby, the chain lengths of the polymers decrease finally leading to the formation

of small and water soluble molecules and a matrix breakdown. Implant erosion can be divided into bulk erosion and surface erosion, which can however not be strictly separated [185]. Surface erosion leads to degradation of the implant starting from the implants surface and a more or less constant implant weight loss can be measured. On the contrary, bulk erosion leads to a chemical degradation of the implant over the complete implant matrix and ends in a rapid breakdown of the implant matrix after a certain lag time. Factors like water penetration velocity, chemical stability of the matrix material and (auto-)catalysis of degradation strongly influence the degradation rate of such systems and tailor made polymers (mostly PLGA) have been produced to exactly control the rate of implant degradation [61, 69, 185]. Drug release from eroding implant is difficult to describe by mathematical models due to the large number of influencing factors such as water entry velocity, degradation rate, osmotic pressure, pH within the implant, size of the implant and so on. Calculation of drug release utilizes Monte Carlo models to simulate the influence of polymer cleavage rate and diffusion models based on the Higuchi equation [186].

In general, an exact assignment to which system a drug delivery device belongs is often difficult as all mentioned processes can occur simultaneously.

#### **4.1. Mechanism of release from triglyceride based implants**

For triglyceride based implants diffusion controlled release from inert matrices has been shown and protein release was explained by drug diffusion in water filled implant pores within the implant matrix. Mathematical models were successfully used to describe protein release from such systems [24, 29, 30, 179]. Factors like the wettability of the triglyceride matrix [170], drug particle size [187] or implant homogeneity [177] were shown to strongly influence drug release from triglyceride based systems.

## 4.2. Mechanism of release from compressed and tsc-extruded implants

Protein release from compressed implants was shown to be dominated by diffusion and sustained protein release from compressed devices was observed [27, 170, 188]. More sustained protein release from compressed triglyceride based implants was achieved by Herrmann *et. al* by an *in-situ* protein precipitation and re-dissolution process of the incorporated protein drug IFN $\alpha$  [24, 29]. In this system the drug (IFN $\alpha$ ) and the pore-forming agent (PEG 6000) dissolved in the incubation medium and created a highly concentrated solution of both substances within the implant pores. Due to the high PEG concentration, the protein drug precipitates within in implant pores and was not immediately released. After an initial burst release of IFN $\alpha$ , a phase of sustained protein release started which was explained by the rate limiting re-dissolution of precipitated IFN $\alpha$ . This release mechanism was proven by mathematical modeling [30] and it was shown that excipients (HP- $\beta$ -CD) and the precipitating agent (PEG 6000) were released faster than IFN $\alpha$  which was released linearly over 14 days (Figure 7).

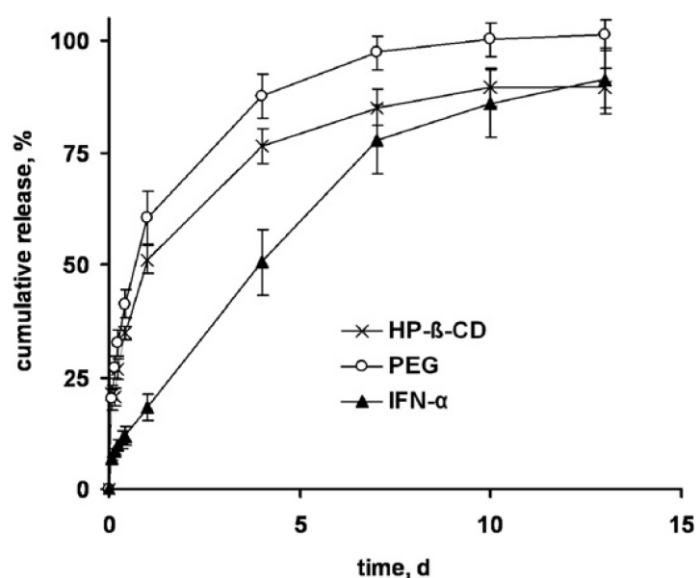


Figure 7: IFN $\alpha$  release from compressed lipid implants consisting of 10% IFN $\alpha$  lyophilisate, 10% PEG 6000 and glycerol tristearin in PBS buffer pH 7.4. Taken from [29].

Interestingly, by changing the preparation method from compression to tsc-extrusion an even more sustained release of IFN $\alpha$  was achieved. Compared to compressed implants, the matrix of tsc-extrudates only differed in the triglyceride composition but tsc-extrudates also comprised 10% PEG 6000 and 10% IFN $\alpha$  lyophilisate. Furthermore a higher surface to volume ratio was found for tsc-extrudates which usually facilitates faster drug release. In addition to the more sustained IFN $\alpha$  release from tsc-extrudates, the release profile changed and a triphasic release was observed. After a burst release, a lag-phase was observed which lasted for up to day 20 and merged into a linear release phase (Figure 8). Protein integrity was neither disturbed during precipitation and re-dissolution nor by tsc-extrusion [32]. The striking difference between compressed implants and tsc-extrudates needs to be further investigated as the manufacturing process itself obviously resulted in a more sustained release of IFN $\alpha$ .

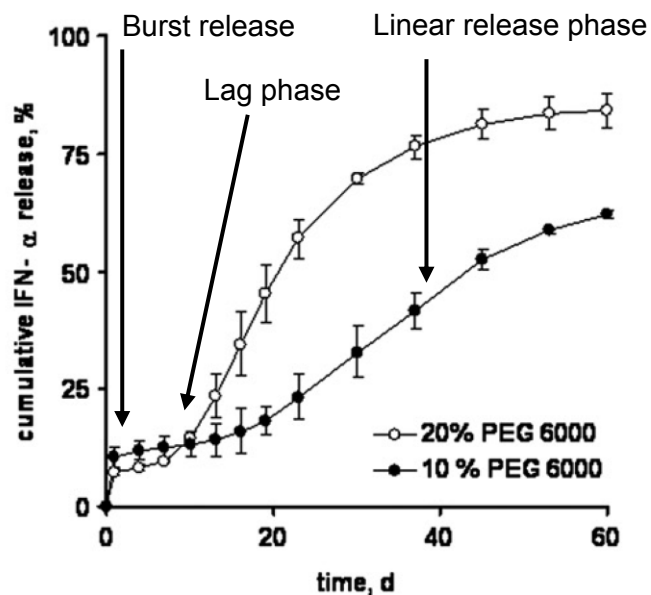


Figure 8: Release of IFN $\alpha$  from tsc-extrudates comprising 20% (open circles) and 10% (closed circles) PEG 6000 and 10% lyophilized IFN $\alpha$ . Taken from [32].



## II. Aim of the thesis

Extensive studies about the suitability of lipids as matrix materials for implants were performed during the last decades. With the emergence of protein pharmaceuticals and the concerns about protein stability in the currently used PLA/PLGA materials, lipids got back into the focus of researchers as material for long term delivery of drugs.

In previous work, it was shown that triglycerides – besides other lipidic materials – were able to maintain the stability of embedded lyophilized proteins during storage and release [24, 27, 28, 32]. Furthermore, triglyceride based implants proved to facilitate sustained release and allowed easy production of implants by simple compression [18, 24-26, 28, 172, 179, 189]. In continuative work it was even possible to tailor protein release e.g. by choice of implant geometry [32] or by admixing of protein precipitating agents (PEG) [24, 29].

Recently, a novel method for the preparation of lipid based (triglyceride based) implants was described: twin-screw extrusion (tsc-extrusion) [178]. Hereby a low-melting and a high-melting lipid were admixed and extruded with a commercially available twin-screw extruder. Similar to other triglyceride based implant systems, tsc-extrudates exhibited a sustained release profile [32, 179] and were shown to be degradable by *in-vitro* incubation with lipase [33]. However, compared to compressed implants, tsc-extrudates allowed slower release profiles and were much better degradable by lipases.

The exact reason for the beneficial release properties and the improved *in-vitro* degradability of tsc-extrudates was not yet fully understood. In this thesis mechanistic studies were conducted to explain the sustained protein release from tsc-extrudates. Besides long-term release experiments, protein release was also investigated on a molecular level by microscopic single-molecule tracking experiments. The superior *in-vitro* degradability of tsc-extrudates in the lipase degradation assay [33] was the starting point for further *in-vitro* studies and formed the platform for an *in-vivo* degradation study in rabbits. Further work included the tailoring of protein release by the application of a protein precipitation and re-dissolution mechanism already described by Herrmann et al. [24, 29]. We attempted to

transferred the mechanism from recombinant human interferon  $\alpha$  to other molecules to prove the general applicability of the described system.

Consequently the goal of the current thesis was to further develop and describe the properties of tsc-extrudates in order to facilitate the manufacturing of protein loaded triglyceride based implants for *in-vivo* application.

A summary of the goals of this thesis is given here:

- The general applicability of the precipitation and re-dissolution mechanism described for recombinant human interferon  $\alpha$ 2a to other proteinaceous molecules was studied.
- The mechanism for sustained protein release from tsc-extrudates was investigated with special interest on the influence of the manufacturing strategy and the implant matrix composition.
- The release mechanism of proteins from tsc-extrudates was analyzed on a molecular level by a microscopic approach. Our aim was to track single protein molecules inside triglyceride based implants by fluorescence microscopy and to elucidate the pathways via which the molecules were released from the implants.
- Finally, investigations about the *in-vitro* and *in-vivo* degradability of tsc-extrudates were carried out. Therefore the effects of lipase addition to the implant matrix for the enhancement of implant degradation were studied and an animal study in rabbit was conducted.

### III. Twin-screw extrudates for the sustained release of a therapeutic antibody

#### 1. Introduction

Antibodies are usually administered intravenously and large doses are required (up to 1 g / 70 kg patient) for systemic distribution. Multiple dosing is necessary as antibodies are cleared from the plasma after intravenous infusion in first-order kinetics exhibiting half-lives of a few days [190]. Additionally, due to painfully application procedures by injection, patients' compliance is often poor. From the point of view of a pharmaceutical company, systemic administration of an antibody is comparatively costly due to the high amounts of the protein drug required. Thus, a local sustained delivery system for antibodies would have the advantageous of direct delivery of the drug to the site of action, a reduction of systemic exposure and potential toxicity [191]. Furthermore, multiple injections could be avoided, if a delivery system released the antibody in a sustained (at best zero-order) way over prolonged time periods.

The local delivery of pooled human polyclonal antibodies was reported in mice for the prophylactic treatment of gram-positive and gram-negative abdominal infections [192]. Hereby, the antibody was loaded into a carboxymethylcellulose gel and antibody serum levels were detectable over a longer period of time compared to intravenous injection. The administration of the antibody showed a synergistic effect with antibiotics, and the mortality of the mice was drastically reduced. Similar results were reported by Felts *et al.* in two studies investigating burn wound models in mice [193, 194]. Parkhurst *et al.* reported antibody release from poly(ethylene-co-vinyl acetate) (PEVac) disc devices to neutralize leukocyte adhesion molecules. These devices were inserted into the vaginal canals of mice as prophylaxis against sexually transmitted diseases [195]. Other groups investigated the local delivery of an antibody by Pluronic™ based gels [196] or by the application of antibody comprising PLGA based microspheres [197].

Besides that, the topical application to mucosal surfaces, the cornea or the skin as well as pulmonary and respiratory antibody delivery has been reported [190]. For example antibody containing lipid-based hollow-porous microparticles (PulmoSpheres™) were produced by spray-drying of dipalmitoylphosphatidylcholine (DPPC) and were investigated for the ability to trigger or modulate immune responses in BALB/c mice after inhalation [124].

Of course implantable devices of various geometries (slabs, films, gels, cylinders) have also been under investigation [27, 32, 190, 192] to fit to the needs for local delivery.

A wide range of matrix materials was successfully used for the preparation of antibody releasing drug devices. Materials used were e.g. PLGA, PEVAc [198], tricalcium phosphate, carboxymethylcellulose [190], chitosan [92], hyaluronic acid [100], SiO<sub>2</sub> [199] and silk [200].

Thus, we identified a need for a controlled local delivery system for antibodies and triglyceride based twin-screw extrudates may exhibit an excellent delivery platform therefore. Zero-order release of a protein from triglyceride based implants was already achieved for IFN $\alpha$  by *in-situ* precipitation of drug in the presence of PEG 6000 [24, 29, 32].

Antibodies are also described to show reversible precipitation in the presence of PEG [201-203]. As reported in the literature, protein precipitation by PEGs can be used to gain highly concentrated protein solutions or to purify proteins [201, 204-207]. Additionally, subcutaneous delivery of crystalline monoclonal antibodies was performed after precipitation of antibodies with PEG. Hereby highly concentrated suspensions (200 mg/mL) of crystalline antibody in PEG/ethanol mixtures were obtained which were injected subcutaneously into BALB/c mice (0.1 mL) where the antibody crystals dissolved within 12 h [208].

Thus a transfer of the strategy of *in-situ* protein precipitation within lipid based implants from the IFN $\alpha$ /PEG system [24, 29] to a IgG<sub>1</sub>/PEG system might be promising.

In order to proof the applicability of tsc-extruded lipid based implants for the controlled sustained delivery of a therapeutic antibody we performed antibody solubility studies and *in-vitro* release tests of an IgG<sub>1</sub> antibody from tsc-extruded lipid implants.

## **2. Materials and methods**

### **2.1. Materials**

MabB is a monoclonal IgG<sub>1</sub> antibody. It is formulated in 10.5 mM phosphate buffer pH 6.4 with a concentration of 17.0 mg/mL. It comprises 2 heavy and 2 light chains and has a molecular weight of about 150 kDa. Hydroxypropy- $\beta$ -cyclodextrin (HP- $\beta$ -CD) was a gift of Wacker Chemie AG (Burghausen, Germany). Carboxymethylcellulose 90,000 D.S 0.7 and Kollidon<sup>®</sup> 25 were purchase from Sigma-Aldrich (Steinheim, Germany), dextran 35,000 was from Biomedicals Lab (Aurora, Ohio, USA) and PEG 6000 was donated from Clariant (Wiesbaden, Germany). All salts were of analytical grade and purchased from Merck (Darmstadt, Germany).

### **2.2. Quantification of mabB**

Antibody quantification was performed UV-metrically (280 nm) after separation by SE-HPLC (Dionex Ultimate 3000, Dionex, Idstein, Germany). The flow rate was 0.5 mL/min and 100  $\mu$ L of each sample were injected onto two in-line Superose 12 (10/300 GL) size-exclusion columns (GE Healthcare, Uppsala, Sweden). The running buffer consisted of 200 mM potassium phosphate with 150 mM potassium chloride and was adjusted to pH 6.9 with 0.1 N solutions of potassium hydroxide and/or hydrochloric acid.

### **2.3. Precipitation and re-dissolution studies**

Preliminary solubility studies with mabB were performed with various excipients including carboxymethylcellulose 90,000 D.S 0.7, Kollidon<sup>®</sup> 25 (polyvinyl pyrrolidone), dextran 35,000, PEG 6000, sodium chloride, sodium sulfate and ammonium sulfate. Equal volumes of mabB (5 mg/mL) and highly concentrated solutions of the agents in PBS buffer pH 7.4 were admixed, shortly vortexed and incubated for 2 hours at 37 °C. Afterwards, samples were centrifuge (4K15, Sigma, Osterode, Germany), 20,000 RZB, 37 °C) for 10 minutes and visually assessed for protein precipitation (= formation of a pellet).

For re-dissolution studies, 50  $\mu$ L of mabB stock solution (10 mg/mL, pH 7.4) and 50  $\mu$ L of PEG 6000 stock solution (20% and 50% in PBS pH 7.4) or control (PBS buffer pH 7.4) were admixed and the protein was precipitated in samples containing PEG 6000. After incubation on a shaker (40 rpm) at 37 °C for 1, 2, 3, 6, 9, 14 and 20 days, the samples were diluted 15-fold with PBS pH 7.4 and assessed by SDS-PAGE and SE-HPLC. Total protein recovery and monomer content were determined UV-metrically (280 nm) after SE-HPLC separation.

#### **2.4. Antibody solubility studies in the presence of PEG 6000**

Solubility of mabB in the presence of various amounts of PEG was determined by admixing equal volumes of antibody solution (5 mg/mL or 10 mg/mL) with solutions of PEG 6000. Therefore, PEG solutions with concentrations ranging between 2% and 50% (w/v) were prepared by dissolution of PEG 6000 in PBS buffer pH 7.4.

In order to proof an influence of the pH on the precipitation capacity of PEG 6000, antibody solutions and PEG solutions were adjusted to pH 4.0, 6.0, 7.4, 9.0 and 11.0 with hydrochloric acid and sodium hydroxide prior to mixing.

After pipetting solutions were quickly vortexed (10 sec) and incubated at 37 °C on a horizontal shaker (40 rpm) for 2 hours. Afterwards, the solutions were centrifuged at 20,000 RZB for 10 minutes, the supernatant was drawn and diluted 4-fold and the antibody concentration was measured UV-metrically at 280 nm with the Fluostar Omega Platereader (BMG LABTECH GmbH, Offenburg, Germany). Linearity of UV measurements was established over a concentration range from 0.010 mg/mL to 1.0 mg/mL.

#### **2.5. Sodium dodecyl sulfate polyacrylamide gel electrophoresis (SDS-PAGE)**

Non-reducing denaturing SDS-PAGE was used to monitor the aggregation and fragmentation of the antibody after precipitation and re-dissolution. Analysis was performed using an XCell II Mini cell system (Novex, San Diego, CA, USA). Samples were diluted to a

final concentration of 0.05 mg/mL in a pH 6.8 Tris-buffer containing 2 % SDS and 2 % glycerine. The samples were denatured at 95 °C for 20 minutes and then 10 µL of the solutions were loaded to the gel wells.

Electrophoresis was performed using NuPAGE® Pre-Cast 7% Tris-Acetate gels 1 mm x 10 wells and NuPAGE® Tris-Acetate running buffer. Separation was accomplished with a constant current of 40 mA and running time was approximately 45 min.

Gels were stained with the SilverXPRESS® Silver Staining Kit (Invitrogen, Karlsruhe, Germany) or the Colloidal Blue Staining Kit (Invitrogen, Karlsruhe, Germany). To check the performance of the system a standard was analyzed on each gel. To determine the molecular weight of the detected bands a molecular weight standard was analyzed on each gel as well (Mark 12 Unstained Standard, Invitrogen, Karlsruhe, Germany).

## 2.6. Lyophilization of mabB

Lyophilization of mabB was performed according to the schema in Table 1 in a ε12G freeze-dryer (Christ, Osterode, Germany).

**Table 1: Lyophilization schema for mabB and PEG 6000**

step	temperature	time per step or heating/cooling rate	pressure
Cooling/freezing step	to - 45 °C	1.6 K/min	atmosphere pressure
	- 45 °C	90 min	atmosphere pressure
primary drying	to - 20 °C	0.1 K/min	to 10 <sup>-2</sup> mbar
	- 20 °C	35 hours	10 <sup>-2</sup> mbar
secondary drying	to + 20 °C	0.1 K/min	to 10 <sup>-3</sup> mbar
	+ 20 °C	20 hours	10 <sup>-3</sup> mbar
sealing of vials	The pressure chamber was filled with nitrogen to a pressure of 800 mbar and the vials were sealed with rubber stoppers.		

## 2.7. Lyophilization of PEG 6000

Lyophilization of PEG was performed according to the method of Ketan *et al.* [209]. In brief, PEG 6000 was dissolved in ultrapure water to give a final concentration of 10% (m/m) and aliquots of 1 mL were pipetted into 2R vials. Lyophilization was performed according to the cycle in Table 1 with a ε12G freeze-dryer (Christ, Osterode, Germany).

## 2.8. Coulometric Karl-Fischer headspace titration

The residual moisture of the samples was determined with a coulometric Karl Fischer titration using the Aqua 40.00 titrator (Analytik Jena AG, Halle, Germany) equipped with a headspace oven. Standard samples (Apura<sup>®</sup> water standard 1.0, Merck, Darmstadt, Germany) were analyzed to control the accuracy of the system. For measurements, samples were heated at 90 °C in the headspace oven and the evaporated water was transferred into the titration solution where the amount of water was determined. All samples were measured in triplicate.

## 2.9. Preparation of lipid implants by tsc-extrusion

Triglyceride based tsc-extrudates were prepared from a powder mixture comprising 56% D118, 24% H12, 10% lyophilized PEG 6000 and 10% lyophilized mabB (mabB:HP-β-CD 1:3) (Figure 9). The composition was chosen according to Schulze *et al.* [24, 29].

D118, and H12 were a gift from Sasol (Witten, Germany) and the chemical composition of the triglycerides as well as their melting ranges are depicted in Table 2. Lyophilized antibody and PEG powder cakes were ground in agate mortars before use. Equal masses of H12, lyophilized PEG 6000 and lyophilized mabB were weighed into an agate mortar and a uniform powder mixture was created. Afterwards, the rest of H12 and D118 were admixed in three single steps to ensure an even distribution of the components.

Tsc-extrusion was performed with a MiniLab<sup>®</sup> Micro Rheology Compounder (Thermo Haake GmbH Karlsruhe, Germany) as described by Schulze *et al.* [32]. In brief, the powder mixture

was fed into the barrel of the extruder and extrusion was performed with closed bypass channel at 41 °C through the extruder outlet die ( $\varnothing = 1.9$  mm, rotation speed: 40 rpm).

**Table 2: Triglyceride composition and melting ranges of H12 and D118.**

	Stearic acid	Palmitic acid	Myristic acid	Lauric acid	Melting range
D118	100%	-	-	-	70-72 °C
H12	-	71%	27%	2%	37-40 °C

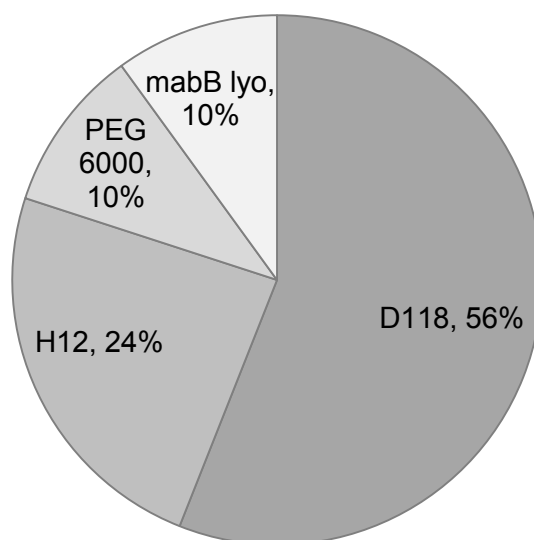


**Figure 9: Composition of mabB comprising lipid tsc-extrudates.**

### 2.10. Antibody release tests from tsc-extrudates

For antibody release tests, rod-shaped extrudates were cut at a length of approximately 2.0 cm and weighed on an analytical balance before and after *in-vitro* release. Extrudates (n = 5) were placed in 2.0 mL Eppendorf tubes and release tests were performed at 37 °C in a horizontal shaker (40 rpm) in 1.9 mL PBS buffer pH 7.4 and pH 4.0. At predetermined points of time samples were drawn by complete exchange of the incubation buffer. Protein content was analyzed after separation by SE-HPLC as described above (III.2.2).

### **2.11. Scanning electron microscopy**

After release, implants were washed three times with distilled water and vacuum dried to constant weight in a vacuum dryer (Memmert, Schwabach, Germany) at 25 °C and 11 mbar. Lipid implants were assessed with a scanning electron microscope 6500F (Jeol GmbH, Eching, Germany) without applying any coating procedure.

### 3. Results and discussion

#### 3.1. Preliminary precipitation studies

Precipitation studies with highly concentrated solutions of various precipitants and mabB (5 mg/mL) were performed to find a suitable precipitating agent. Results are displayed in Table 3. The antibody was rapidly precipitated after the addition of PEG 6000 and ammonium sulfate. This was not surprising as antibody precipitation with polyethylene glycol is well described in literature and established in downstream processing of pharmaceutical products [201, 210]. Ammonium sulfate precipitation of various proteins is also well described in literature and often used to purify proteins.

Carboxymethylcellulose (CMC), Kollidon® 25, dextran 35,000, sodium sulfate (NaSO<sub>4</sub>), and sodium chloride (NaCl) did not lead to a rapid precipitation of the antibody from solution and were thus not further investigated as pore-forming/precipitating agent.

**Table 3: MabB precipitation in isotonic PBS buffer pH 7.4**

Precipitant	Precipitant concentration [% - w/v]	Precipitation [yes/no]
CMC 90,000, D.S. 0.7	0.5	no
Kollidon® 25	15	no
Dextran 35,000	20	no
PEG 6000	25	YES
NaCl	15 (2.56 M)	no
NaSO <sub>4</sub>	8 (0.56 M)	no
(NH <sub>4</sub> ) <sub>2</sub> SO <sub>4</sub>	14 (1.04 M)	YES

#### 3.2. Antibody solubility studies in the presence of various amounts of PEG 6000

Solubility of mabB was found to decrease with increasing amounts of PEG 6000 (Figure 10). A minimum of 10% PEG 6000 (w/v) was necessary to completely precipitate the protein from solution. MabB solubility in the presence of PEG was also found to be dependent on the pH

of the incubation medium. At pH 4.0 no precipitation was observed in a 20% (w/v) PEG solution. However, between pH 6 to 11 antibody precipitation occurred (Figure 11).

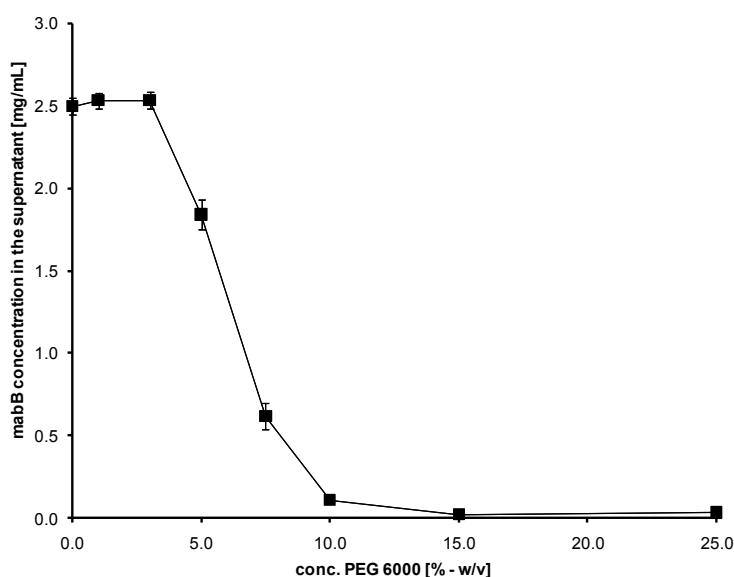


Figure 10: Solubility of mabB in the presence of increasing amounts of PEG 6000

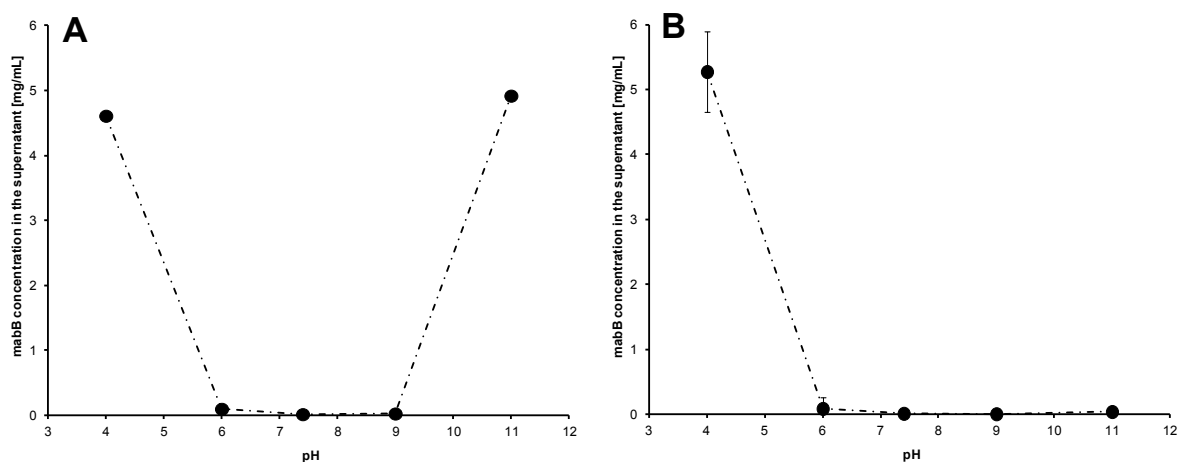
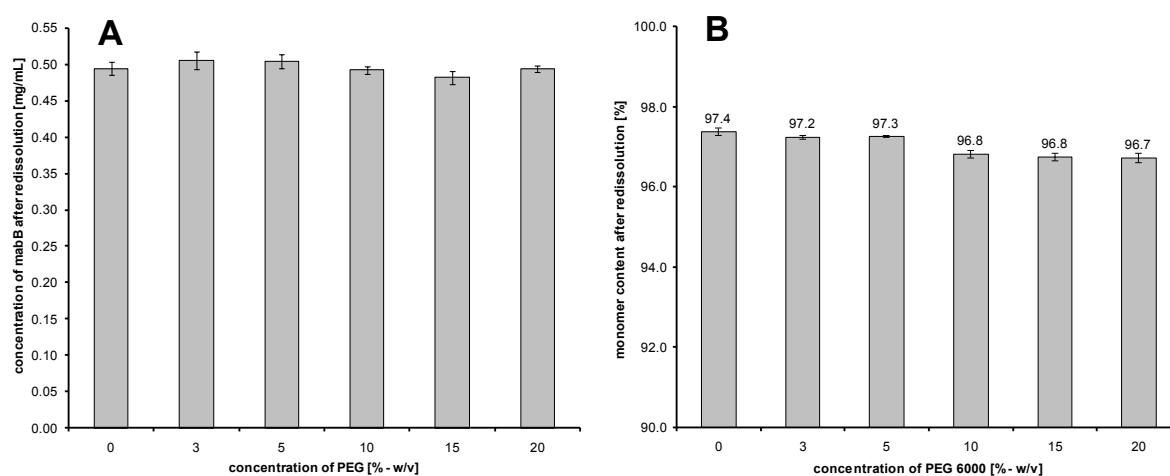


Figure 11: Influence of pH on the solubility of mabB (5 mg/mL) in solutions of (A) 10% PEG 6000 and (B) 20% PEG 6000 in PBS buffer.

Interestingly, a 10% solution of PEG did not lead to antibody precipitation at pH 11 but a 20% PEG solution precipitated the protein. Thus antibody precipitation is dependent on the pH and on PEG concentration and these two factors have synergistic effects. Antibody precipitation was found to be fully reversible after dilution (1:10) and 2 hours incubation in

PBS buffer pH 7.4 and only minor changes in monomer content were found compared to the stock solution (Figure 12).



**Figure 12: Recovery of mabB after precipitation with various amounts of PEG 6000 and re-dissolution by 10-fold dilution with PBS buffer pH 7.4. A: total recovery of mabB after re-dissolution, 100% = 0.5 mg/mL; B: monomer content of mabB after re-dissolution.**

### 3.3. MabB precipitation and re-dissolution after long-term incubation

MabB was precipitated from solution by mixing with PEG 6000 (pH 7.4 in PBS buffer) to give final concentrations of 5 mg/mL of protein and 10% or 25% of PEG 6000. Samples were incubated for up to 20 days at 37 °C and 40 rpm and subsequently re-dissolved by 1:10 dilution with PBS pH 7.4. Total protein recovery and monomer content after re-dissolution of precipitated mabB samples were analyzed by SE-HPLC and UV-detection. MabB was completely recovered after incubation from all samples and did not significantly differ between samples containing varying amounts of PEG and different incubation times (Figure 13). However, monomer recovery showed a decrease in monomer content with increasing incubation times and PEG content (Figure 14).

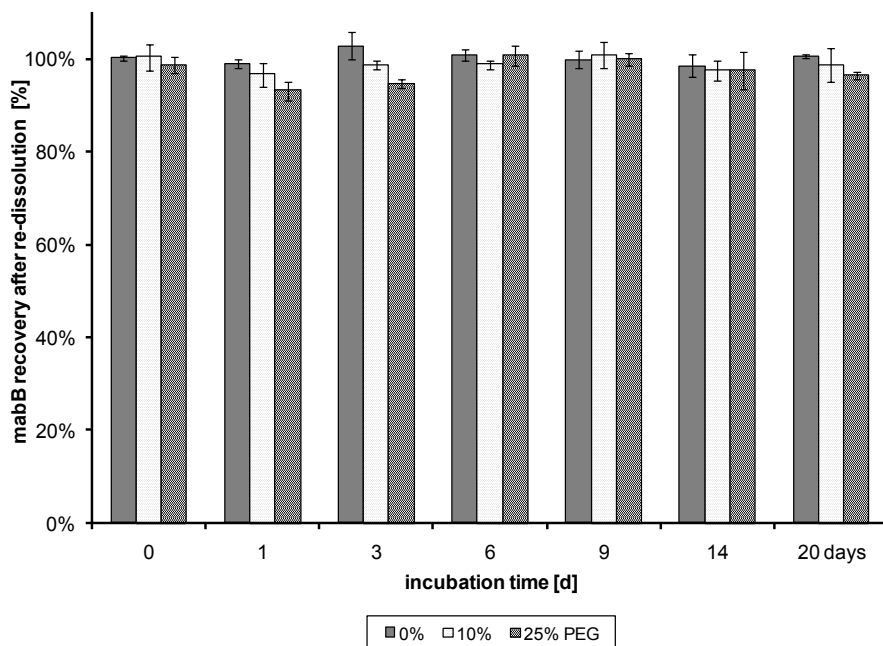


**Figure 13: Total recovery of mabB after precipitation with PEG 6000 and incubation at 37 °C. Samples were taken after 2 hours and after 1, 3, 6, 9, 14 and 20 days as displayed.**

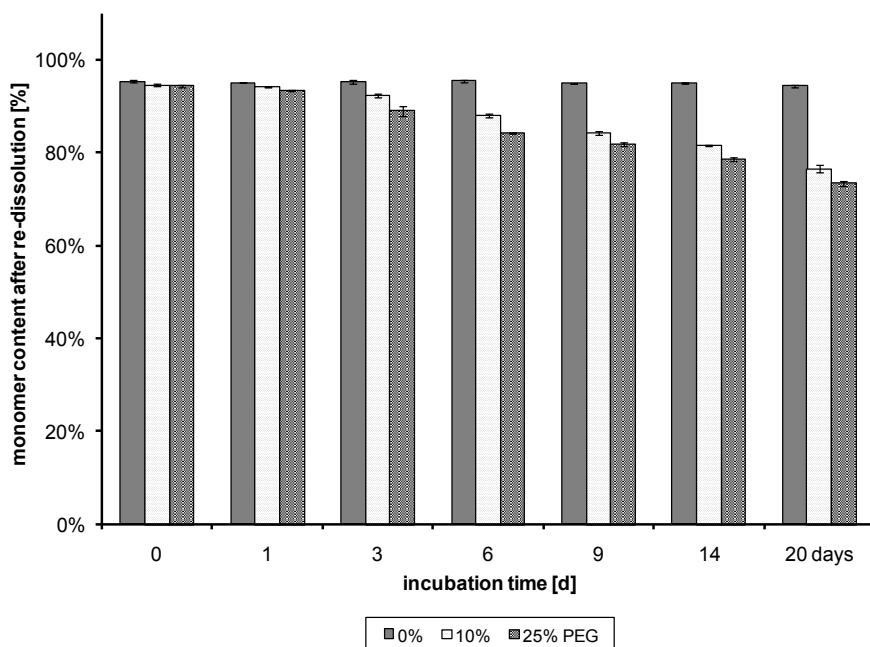


**Figure 14: Recovery of mabB monomer after precipitation with PEG 6000 and incubation at 37 °C. Samples were taken after 2 hours and after 1, 3, 6, 9, 14 and 20 days as displayed.**

### 3.3.1. Non-reducing SDS-PAGE of re-dissolved samples

Precipitation and re-dissolution of incubated samples after 2 hours incubation time did not show a difference between control samples (standard, 0% PEG) and re-dissolved samples (10%, 25% PEG – Figure 15) by SDS-PAGE.

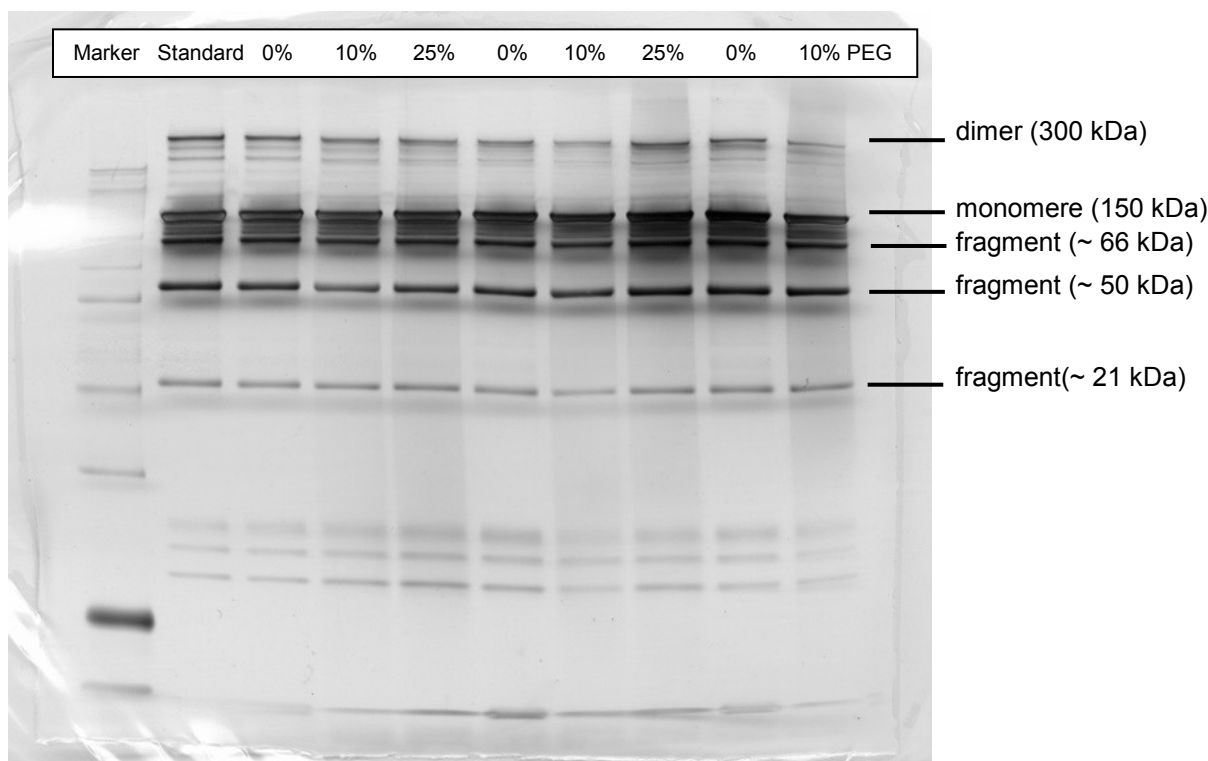


**Figure 15: SDS-PAGE of re-dissolved mabB: Samples were precipitated by PEG (10% or 25%) or treated with control buffer (PBS pH 7.4), incubated for 2 hours at 37 °C on a shaker (40 rpm) and re-dissolved by 15-fold dilution with PBS buffer pH 7.4.**

However, samples taken after 20 days of incubation showed increasing amounts of dimers, if incubated with higher amounts of PEG 6000 (10%, 25% PEG; Figure 16). Dimer formation might be a result of chemical reactions especially disulfide crosslinking, which is described in literature [211]. This aggregation pathway works via autooxidation of PEG by light and heat and leads to crosslinking of cystein residues. However, SDS-PAGE under reducing conditions was not performed with these samples and therefore no final answer regarding the origin of the increased dimer concentrations can be given.

The overall results were consistent with the findings after SE-HPLC analysis, where also increased amounts of dimers were detected.

Although a monomer loss of mabB was detected by SDS-PAGE and SE-HPLC, the system strongly resembled the IFN $\alpha$ /PEG systems described by Herrmann *et al.* [24, 29]. Therefore we decided to manufacture, mabB comprising tsc-extrudates and to investigate the release behavior of the antibody from these implants *in-vitro*. Total protein release was quantified by SE-HPLC analysis (280 nm), which allowed to detect and quantify the amount of aggregated mabB species.

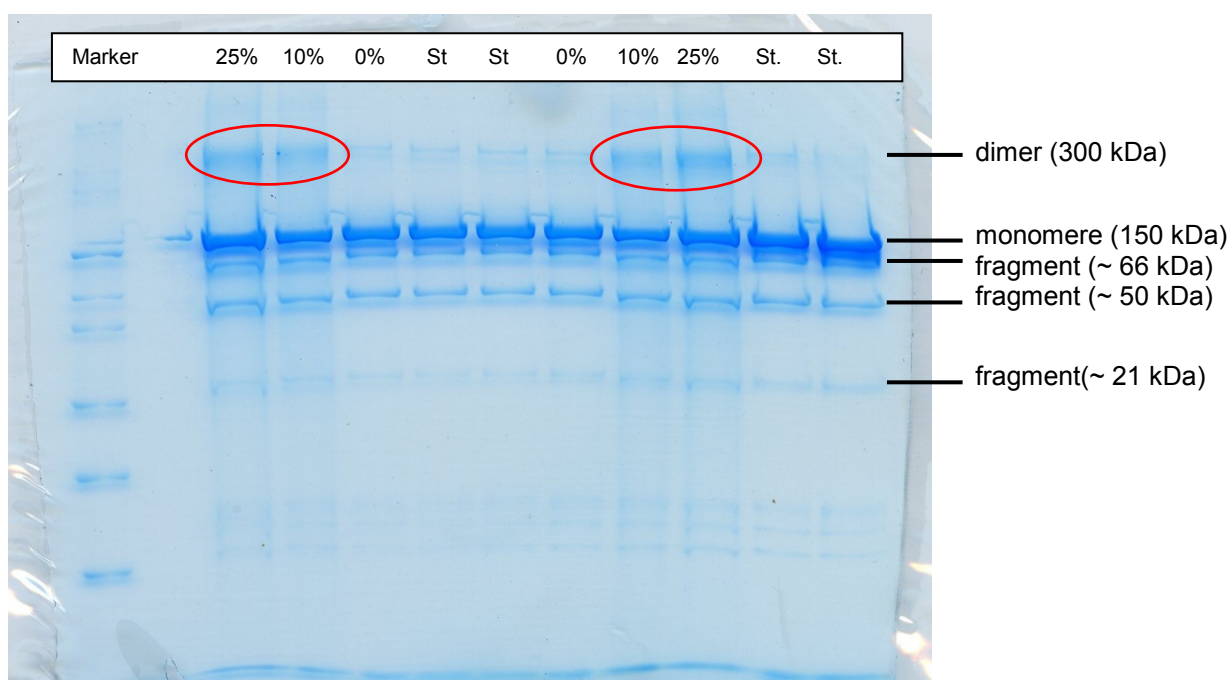


**Figure 16:** SDS-PAGE of re-dissolved mabB Samples were precipitated by PEG (10% or 25%) or treated with control buffer (PBS pH 7.4), incubated for 20 days at 37 °C on a shaker (40 rpm) and re-dissolved by 15-fold dilution with PBS buffer pH 7.4.

### 3.4. Production of lyophilized of mabB powder

For the production of mabB containing lipid implants, a dry powder of mabB was prepared by lyophilization of mabB solutions according to Table 1. In order to find a suitable formulation for antibody lyophilization, various batches were prepared with either Trehalose, HP- $\beta$ -CD or without any excipient as listed in Table 4.

Trehalose is widely described in literature as lyo- and cryoprotectant for protein drugs [212] and was used for the lyophilization of IFN $\alpha$  [28] or IgG<sub>1</sub> antibody [213]. HP- $\beta$ -CD was already used by Mohl *et al.* and Herrmann *et al.* for the preparation of triglyceride based implants and was shown to increase IFN $\alpha$  storage stability within the implants [24, 27, 28] compared to the application of sugars as matrix materials. Additionally HP- $\beta$ -CD stabilized protein drugs like EPO during the production of PLG microcapsules by a W/O emulsion technique during vortexing or ultrasonication [214] and Brewster *et al.* noted enhanced stability of somatotropin and IL-2 in the presence of HP- $\beta$ -CD [215]. Rassing *et al.* used HP- $\beta$ -CD as lyoprotectant for IgG antibodies and found increased protein stability and activity compared to samples which were freeze dried with sucrose or dextran [216].

After lyophilization of the antibody, total protein recovery and monomer content upon reconstitution were assessed by SE-HPLC and the water content of the lyophilisates was determined by Karl-Fischer titration.

**Table 4: Mixing ratios between antibody and excipients for mabB lyophilization.**

formulation	excipient	conc. excipient [mg/mL]	conc. mabB [mg/mL]
A	-	-	15
B	trehalose	45	15
C	HP- $\beta$ -CD	45	15
D	trehalose	15	15
E	HP- $\beta$ -CD	15	45
F	-	-	30

### 3.4.1. Total recovery of mabB after lyophilization

Total recovery of mabB after reconstitution in incubation buffer (isotonic PBS pH 7.4) did not show differences between formulations and incubation at 37 °C for up to 14 days did not result in a loss of protein (Figure 17). Assessment of monomer content after reconstitution showed a decrease of the monomer content in samples A + F which were lyophilized without

the addition of an excipient (Figure 18). This was accompanied with an increase in dimers and oligomers as detected by SE-HPLC (data not shown). No differences between trehalose and HP- $\beta$ -CD comprising formulations were detected and the antibody was stable in all formulations. The four formulations yielded about 95% of monomer and a total recovery of about 100%. In order to mimic the conditions during the release studies, samples were incubated at 37 °C for several days prior to analysis by SE-HPLC. Non-lyophilized mabB solution from bulk material was used as 'standard' and incubated at the same conditions. As can be seen in Figure 17 and Figure 18 no changes in monomer content and total protein content during the time of incubation (14 days) were observed. Thus, the protein was stable for at least up to 14 days in the incubation medium.

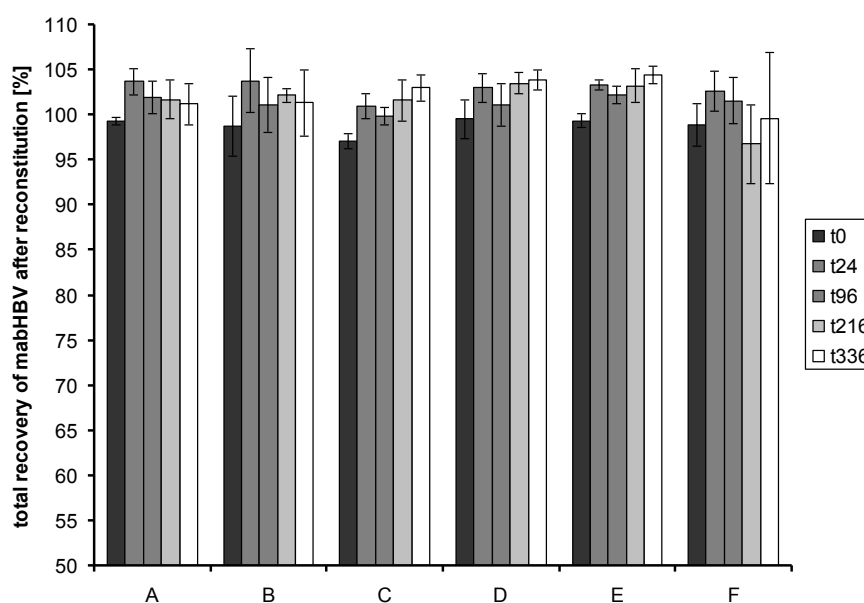


**Figure 17: Total recovery of mabB from lyophilized samples after reconstitution in PBS buffer. Samples were incubated upon reconstitution at 37 °C for 2 hours (t0), 24 hours (t24), 4 days (t96), 9 days (t216) and 14 days (t336). Formulations: A – 15 mg/mL mabB without excipient, B – 15 mg/mL mabB with 45 mg/mL trehalose, C – 15 mg/mL mabB with 45 mg/mL HP- $\beta$ -CD, D – 15 mg/mL mabB with 15 mg/mL trehalose, E – 15 mg/mL mabB with 15 mg/mL HP- $\beta$ -CD, F – 30 mg/mL mabB without excipient.**

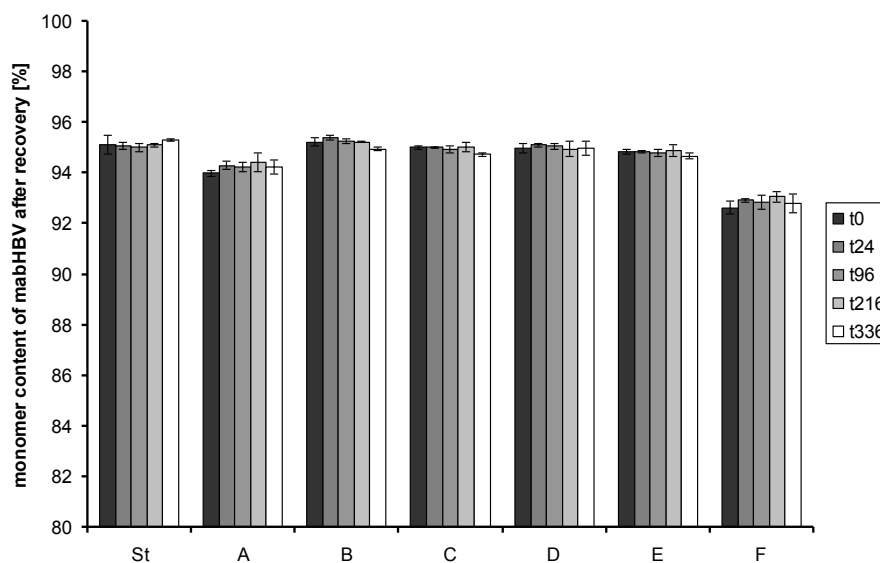


**Figure 18: Monomer content of mabB from lyophilized samples after reconstitution in PBS buffer. Samples were incubated upon reconstitution at 37 °C for 2 hours (t0), 24 hours (t24), 4 days (t96), 9 days (t216) and 14 days (t336). Formulations: St – standard, A, B, C, D, E and F – identical to Figure 17.**

### 3.4.2. Water content of lyophilized samples

It was shown, that water content differed strongly between formulations A-F. Samples which contained only the antibody but no excipient showed water content of 14.3% (m/m) and 5.6% (m/m) which is too high to guarantee protein stability during storage. Samples comprising 45 mg/mL and 15 mg/mL trehalose showed residual moistures of 5.6% and 2.4% and formulation E which consisted of 15 mg/mL HP- $\beta$ -CD showed a residual moisture content of 3.9%. An adequate water content of 1.5% (m/m) was obtained for formulation C which consisted of HP- $\beta$ -CD and the antibody in a ratio of 3:1 (45 mg/mL + 15 mg/mL). Although an optimization of the freeze-drying circle for the lowering of the residual moisture content would have been possible, it was decided to use formulation C for the preparation of tsc-extrudates for the following reasons.

Mohl [28] and Herrmann [29] also used HP- $\beta$ -CD in a ratio of 3:1 to formulated IFN $\alpha$  as a lyophilized powder and prepared triglyceride based implants thereof. Additionally, HP- $\beta$ -CD was shown to better preserve IFN $\alpha$  integrity in triglyceride implants compared to trehalose [28] and to stabilize proteins against denaturation at interfaces [217]. This last point might be

of crucial importance for the delivery of protein drugs from lipid implants as the lipid matrix exhibit big hydrophobic surface areas and thus a large hydrophobic solid-liquid interface. Therefore we decided to use HP- $\beta$ -CD as excipient for our mabB lyophilisate.

### **3.5. MabB release studies from tsc-extruded lipid implants**

Release studies were carried out according to III.2.10 at two different pHs (7.4 + 4.0). This was done, to prove the influence of *in-situ* antibody precipitation within the lipid implant on *in-vitro* release kinetics. It was already shown in chapter III.3.1, that PEG was able to precipitate the antibody at concentrations higher than 10% at pH 7.4 but not at pH 4.0, and thus, these pHs were used to control the rate of release.

#### **3.5.1. Weight assessment and SEM measurement of tsc-extrudates**

Tsc-extrudates were weighed before and after release tests on an analytical balance. Extrudates after release test were dried to constant weight prior to weighing as described in III.2.11. Weight assessment showed a decrease of implant weight of about 23% which was explained by dissolution and release of the water soluble parts of the implant matrix (PEG + HP- $\beta$ -CD + mabB) (Figure 19). As only 20% of the implants consisted of water-soluble PEG or mabB lyophilisate an additional weight loss of about 3% was detected after *in-vitro* incubation. This weight loss was explained by a partial breakdown of the lipid matrix during the long *in-vitro* release test.

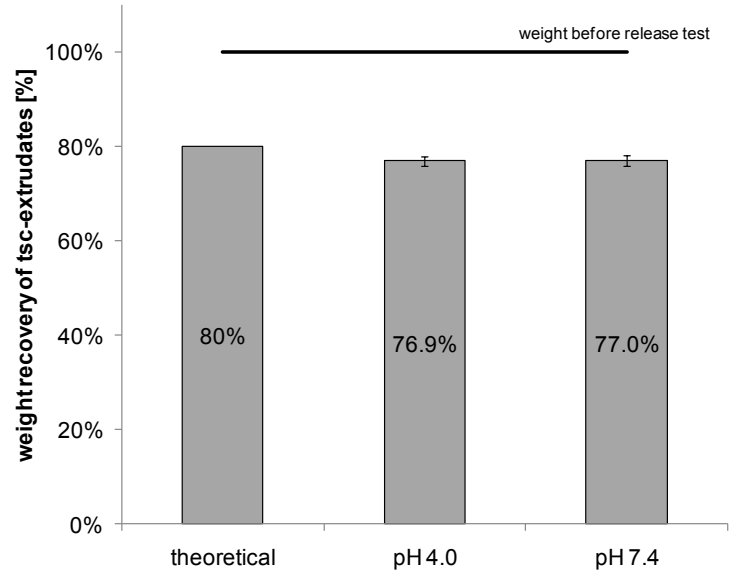


Figure 19: Remaining implant mass after *in-vitro* release tests at pH 4.0 and pH 7.4. Theoretical mass was calculated as total triglyceride mass (matrix).

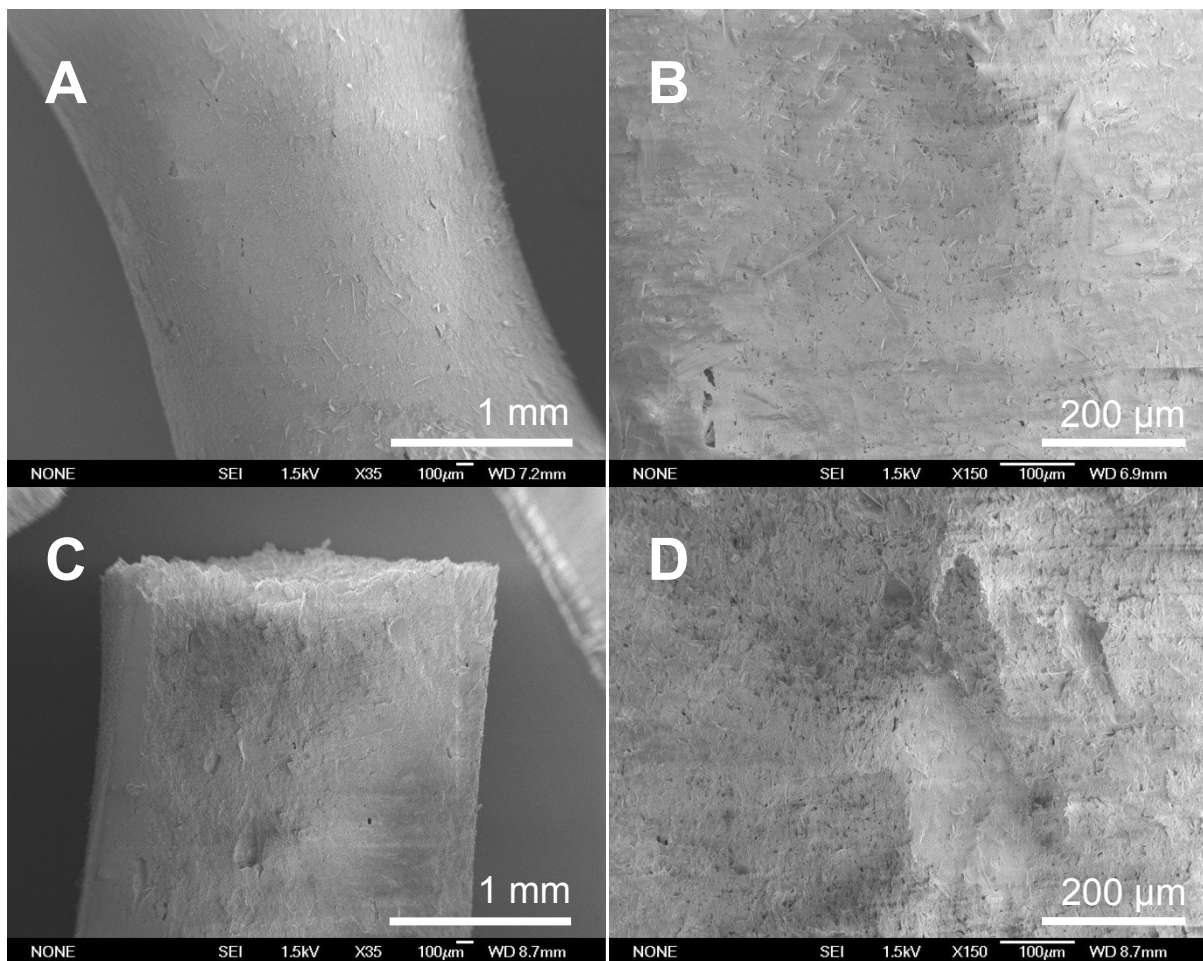


Figure 20: SEM measurement of lipid tsc-extrudates after *in-vitro* release test: A + B: surface of implants; C + D: longitudinal cross-sections of implants. Magnification: 35-fold (A + C) and 150-fold (B + D).

SEM measurements after release tests showed a highly porous implant matrix (Figure 20) with very small pores ranging in the lower  $\mu\text{m}$  size. The small pore size as well as the homogeneous distribution of the pores throughout the implant matrix was explained by the intensive mixing prior extrusion and during the extrusion process itself. Additionally, the lyophilized protein became a very fine powder after grinding and could be easily admixed to the lipid matrix material. Based on the SEM data and the assumption that the pores within the implants were created by dissolution of PEG and protein lyophilisate only, a particle size of the lyophilized product in the low  $\mu\text{m}$  range (1 - 20  $\mu\text{m}$ ) can be assumed. Homogenous drug distribution within implant matrices and small particle sizes have been successfully used by many authors [26, 177, 187] to achieve more sustained release profiles and are thus favorable for long-term release.

### 3.5.2. MabB release from lipid tsc-extrudates

Antibody release tests from tsc-extrudates were performed at pH 4.0 and pH 7.4. The pH of the incubation medium was found to have a significant effect on the precipitation capacity of PEG 6000 *in-vitro* as described in Figure 11. The antibody was easily precipitated at 'physiological' conditions (isotonic PBS buffer pH 7.4) but not if the PBS buffer was adjusted to pH 4.0.

MabB release from implants which were incubated at pH 4.0 was complete within 35 days (Figure 21 - A). The antibody was released in a sustained manner with very little initial burst release and a constant release phase between days 2 and 22. A total of 95% of the incorporated antibody mass was released.

Protein release from tsc-extrudates at pH 7.4 was more sustained and lasted over 150 days. After a small burst release of 7% during the first 14 hours, the antibody was released with zero-order kinetics over 149 days (Figure 21). A total of 95% of the incorporated protein was released and samples which were analyzed by SE-HPLC revealed that the released antibody fractions were mainly monomeric (93-95%) which was identical to antibody bulk material (Figure 22).

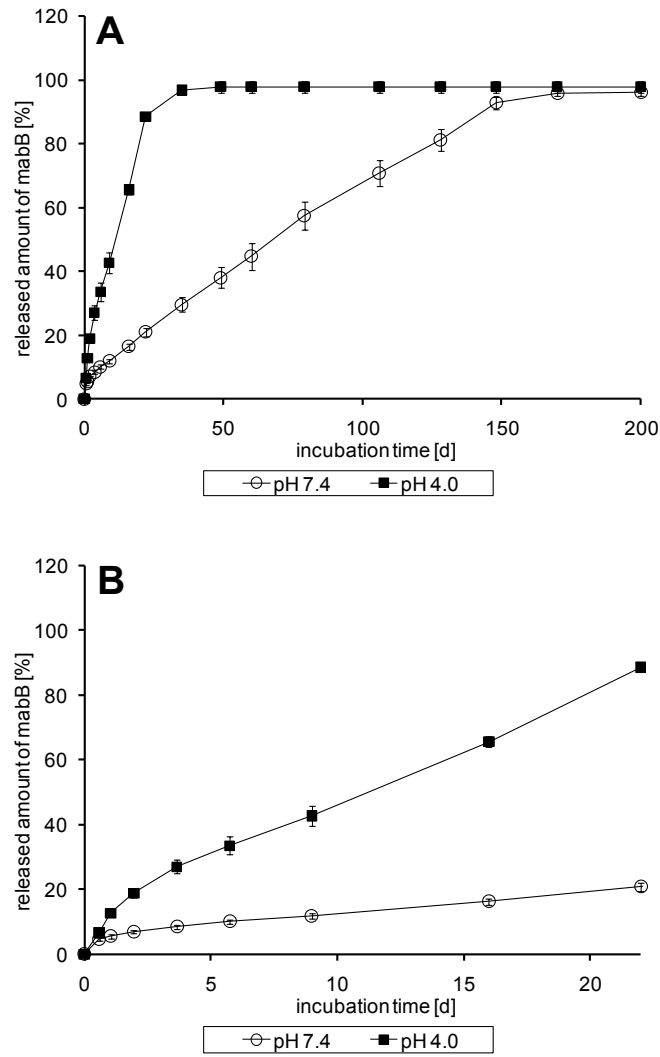


Figure 21: mabB release from tsc-extrudates at pH 7.4 (open circles) and pH 4.0 (closed squares) comprising PEG 6000 as pore forming agent. A – release curve till complete release was achieved. B – close-up of release curve till day 22.

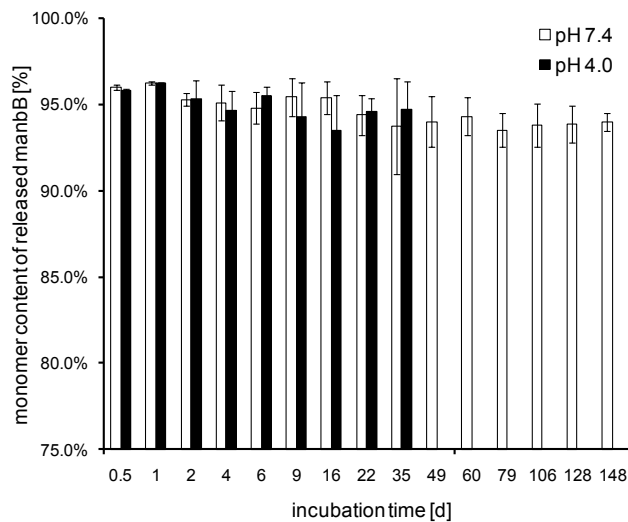


Figure 22: Monomer content of release mabB as percentage of total peak areas.

The linear release behavior was explained by an *in-situ* protein precipitation step at pH 7.4 which did not occur at pH 4.0. Upon contact with water, lyophilized PEG 6000 and mabB instantaneously dissolved and the protein was precipitated in a highly concentrated solution of PEG 6000. During release-tests PEG 6000 was diluted within the freshly formed implants pores and slowly washed out of the implant matrix. As a result, the PEG concentration within the implant pores decreased, mabB molecules re-dissolved and were finally released from the implant.

Thus in analogy to IFN $\alpha$  [24, 29] another proteinaceous drug can be released in a linear manner from lipid implants due to a precipitation and re-dissolution process. However, comparison between the IFN $\alpha$ /PEG system and the mabB/PEG system reveal certain differences.

- Release of mabB did not show a lag phase between burst release and the linear release phase which was observed in the IFN $\alpha$ /PEG system (Figure 23). This might be explained by the fact that a higher concentration of PEG is necessary to precipitate mabB (> 10%, Figure 10) than for the precipitation of IFN $\alpha$  (> 5%, [24]). Thus, a washing out of excessive PEG might take less time in the case of mabB re-dissolution.

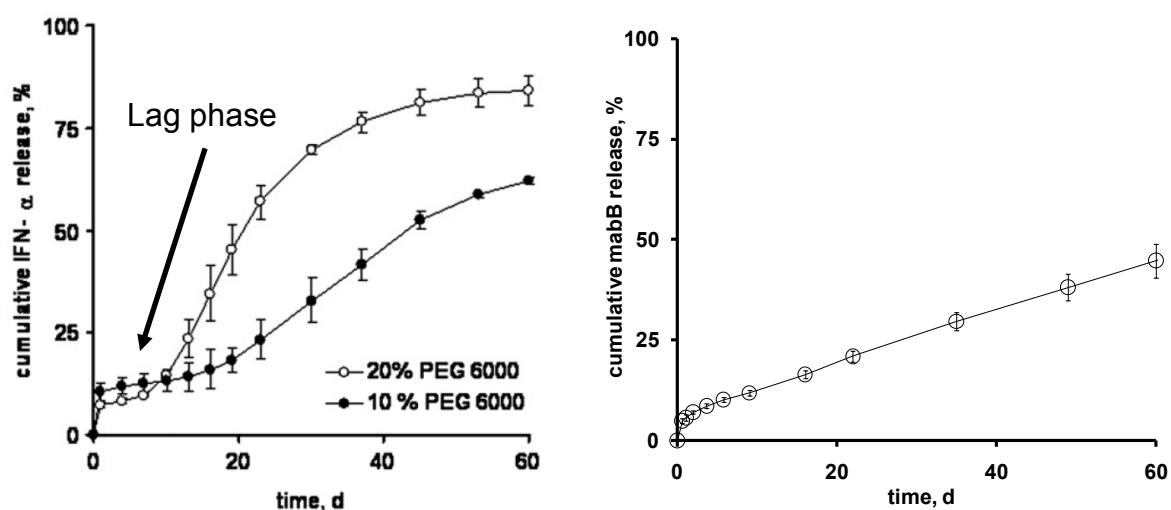


Figure 23: Left: Release of IFN $\alpha$  from tsc-extrudates comprising 20% (open circles) and 10% (closed circles) PEG 6000 and 10% lyophilized IFN $\alpha$ . Taken from [32]. Right: Release of mabB from tsc-extrudates comprising 10% PEG 6000 and 10% lyophilized mabB.

- *In-vitro* release lasted for 150 days in the case of mabB but only 60 days in the IFN $\alpha$ /PEG system [32]. Thus a more sustained release profile was observed for mabB compared to IFN $\alpha$ . This is explained by two factors. Firstly, mabB has a higher molecular weight than IFN $\alpha$  (150 kDa versus 19 kDa) and thus diffuses more slowly within the pores of the implant. However, such a change should not result in such a drastic increase of the time for drug release. Secondly, we used lyophilized PEG 6000 instead of PEG 6000 P (particle size: 60% > 200  $\mu$ m, Figure 38) for the preparation of the mabB comprising tsc-extrudates and this resulted in an implant structure with very small and finely distributed pores (Figure 20). As already described, smaller (drug) particle sizes and a finer distribution of drug (and pore-former) particles within the implant matrix result in a more sustained release profile from inert matrices [32, 177, 187].



#### **4. Conclusion**

A sustained release dosage form for the delivery of a monoclonal antibody over a period of 150 days was developed. The antibody was released mainly in its monomeric form throughout the incubation period and the linear release profile could clearly be attributed to a precipitation and re-dissolution step of the antibody.

No additional degradation products were detected by SE-HPLC assessment and the ratio between monomers and dimers was identical to antibody bulk solution. This high stability of the antibody might be explained by the presence of HP- $\beta$ -CD in the formulation which was shown to maintain protein stability in lipid matrices [27, 28].

Sustained release of the antibody was also observed at pH 4.0, where no precipitation and re-dissolution step was expected. Thus a major part of the sustained protein release can be clearly ascribed to the properties of the tsc-extrudate itself and makes them a very promising delivery platform to achieve long-term protein release.



## **IV. Influence of the manufacturing strategy on protein release kinetics from lipid based implants**

### ***1. Introduction***

The preparation of triglyceride based implants is usually performed by compression of lipid powders blends which were admixed with drug and excipients [25, 27, 33, 169, 218]. In 2007, Schulze et al. introduced a new preparation method for the manufacturing of triglyceride based lipid implant (tsc-extrusion [32]) which featured several advantages. The most important one, was a different release profile of IFN $\alpha$  from tsc-extrudates which was obviously more sustained compared to compressed implants. However, no direct comparison between tsc-extruded and compressed implants could be made as the matrix of tsc-extrudates consisted of a triglyceride mixture whereas compressed implants were prepared from pure tristearin. The triglyceride mixture of tsc-extrudates is necessary to allow extrusion of the solid powder blend by tsc-extrusion and consists of two (or more) different lipids which are described as 'low-melting' and 'high-melting' lipid further on. The high melting lipid stays solid throughout the extrusion experiment whereas the low-melting lipid is (partially) molten during the process, leading to a softening of the powder blend and allows extrusion of the mixture through the extruder outlet die.

In order to elucidate the differences between compressed and tsc-extruded implants and to verify a more sustained protein release from tsc-extrudates, we prepared triglyceride based lipid implants with equal matrix compositions by four different manufacturing processes and compared the release kinetics. Further on we characterized the different implants by scanning electron microscopy, differential scanning microscopy and X-ray diffraction measurements. Lysozyme was used as a model protein as it is well described in literature, very stable and does not precipitate in the presence of PEG which was used as pore-forming agent. Hereby the influence of protein precipitation on protein release from lipid implant was eliminated and the comparison between the different implants became easier.



## **2. Materials and methods**

### **2.1. Materials**

#### **2.1.1. Lysozyme**

Hen egg white lysozyme (synonym: Muraminidase, lysozyme c) was purchased from Sigma as lyophilized powder (Product Number: L 6876). Lysozyme is expressed in egg white of chicken and is one of the best described proteins in literature. It is a single chain protein of 129 amino acids and is cross linked by 4 disulfide bridges. Its secondary structure reveals 5  $\alpha$ -helixes and 3  $\beta$ -sheets. The protein shows enzymatic activity which hydrolyzes the peptidoglycan present in bacterial cell walls between N-acetyl-D-muraminic acid and N-acetyl-D-glucosamine residues. The molecular weight of the protein is 14.3 kDa and its IP is 11.4.

#### **2.1.2. Triglycerides**

Triglycerides D118 and H12 were donated from Sasol (Witten, Germany). D118 consists of glycerol tristearin and H12 is a mixed acid triglyceride consisting of palmitic, myristic and lauric acid (section III.2.9, Table 2).

#### **2.1.3. Buffer salts and chemical reagents**

PEG 6000 P was a gift from Clariant (Gensdorf, Germany). Di-sodium hydrogen phosphate dihydrate ( $\text{Na}_2\text{HPO}_4 \cdot 2\text{H}_2\text{O}$ ), sodium dihydrogenphosphate di-hydrate ( $\text{NaH}_2\text{PO}_4 \cdot 2\text{H}_2\text{O}$ ), potassium dihydrogen phosphate ( $\text{KH}_2\text{PO}_4$ ), sodium chloride and potassium chloride were purchased from Merck (Darmstadt, Germany). Sodium azide was purchased from Acros Organics (Geel, Belgium).

## 2.2. Methods

### 2.2.1. Lipid powder composition

The powder mixture for the preparation of triglyceride based implants was identical for all manufacturing processes and consisted of D118 (tristearate – 56%), H12 (mixed acid – 24%), PEG 6000 (17.5%) and chicken-egg white lysozyme (2.5%) (Figure 24). A single lipid blend was prepared for the manufacturing of all implants to guarantee identical matrix composition.

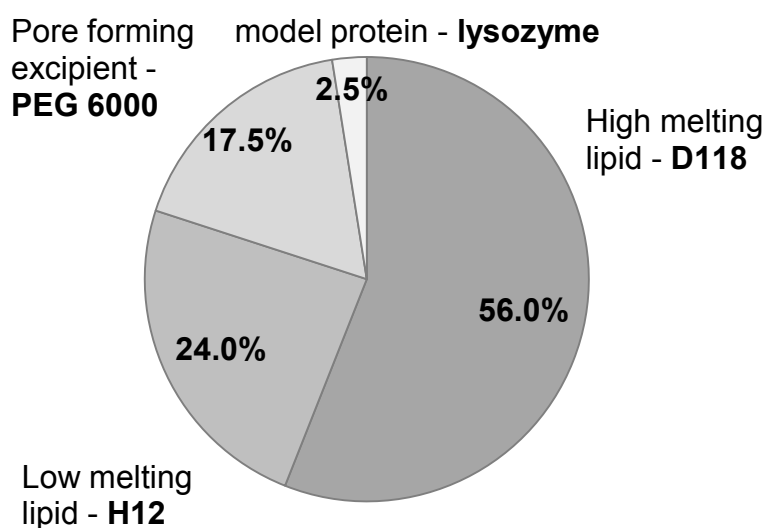


Figure 24: Composition of lipid powder blend used for the preparation of lipid implants by four different manufacturing processes.

### 2.2.2. Manufacturing strategies for lipid implants

#### 2.2.2.1. Compressed implants

Preparation of compressed implants was performed using a hydraulic press (Maassen, Eningen, Germany). Template diameter was 5.0 mm and a compression force of 0.6 t was applied for 45 sec. About 50 mg of lipid blend was weighed into the template prior to compression.

### 2.2.2.2. RAM extruded implants

RAM extrusion was performed using a purpose made extruder device. The lipid blend was directly extruded through the outlet dye (1.2 mm diameter) after application of sufficient pressure by a hydraulic press (Maassen, Eningen, Germany). RAM-extruded devices showed a diameter of 1.2 mm and an average length of 15 mm (Figure 25). Extrusion was performed at room temperature without the application of additional heat.

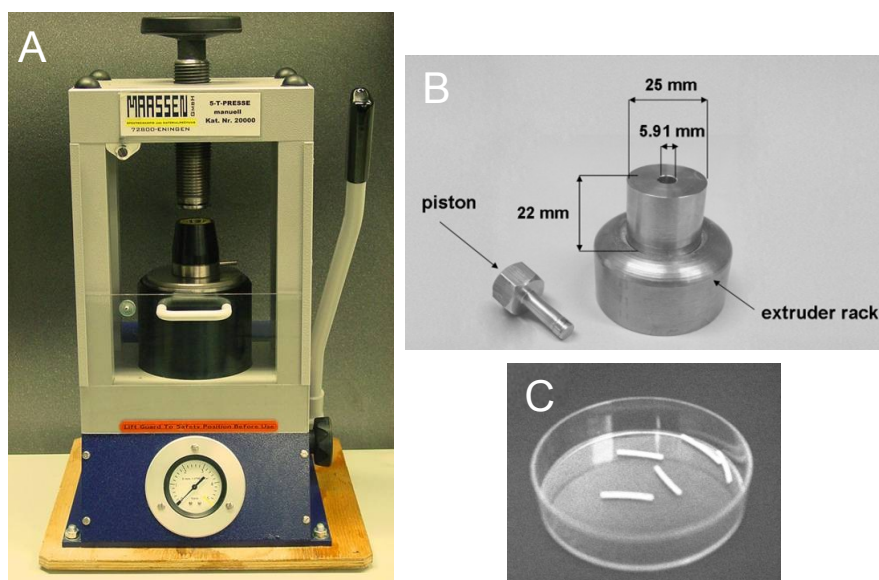


Figure 25: (A) Hydraulic press for the preparation of compressed implants, RAM extrudates and 'compressed tsc-extrudates'. (B) Purpose made RAM extruder devices with extruder rack and piston. (C) RAM extrudates. Pictures taken from [179].

### 2.2.2.3. Tsc-extruded implants

Tsc-extrusion was performed on a MiniLab<sup>®</sup> Micro Rheology Compounder (Thermo Haake GmbH, Karlsruhe, Germany, Figure 4). Twin-screw extrusion was performed at a temperature of 41 °C through the extruder outlet die (diameter 1.9 mm). The rotation speed of the extruder screws was set to 40 rpm and the bypass channel was closed to inhibit material circulation within the extruder.

#### **2.2.2.4. 'Compressed tsc-extrudates'**

'Compressed tsc-extrudates' were produced by grinding of tsc-extrudates in an agate mortar and subsequent compression with a hydraulic press (Maassen, Eningen, Germany) as described for compressed lipid implants. Sample diameter was 5.0 mm and sample weight about 50 mg. 'Compressed tsc-extrudates' feature the geometry of compressed implants but the matrix material was treated in analogy to tsc-extruded implants.

#### **2.2.3. Lysozyme release studies**

Rod shaped tsc-extrudates were cut into pieces of about 20 mm length, weighed on an analytical balance (BP 61 S, Sartorius AG, Göttingen, Germany) and placed in 2.0 mL microcentrifuge tubes (VWR, Darmstadt, Germany). Compressed implants, RAM-extruded implants and 'compressed tsc-extrudates' were weighed and placed in 2 mL microcentrifuge tubes. All samples (n = 3) were incubated in 1.8 mL isotonic PBS buffer pH 7.4 containing 0.05% sodium azide. Release studies were performed on a horizontal shaker at 37 °C (40 rpm, Certomat@IS, B. Braun Biotech International, Göttingen, Germany). On predetermined time points the incubation medium was completely removed and fresh buffer was filled into the tubes.

#### **2.2.4. Lysozyme concentration determination**

Samples were analyzed by SE-HPLC using a Superose column (Superose 12 10/300 GL; GE Healthcare, Uppsala, Sweden). The mobile phase consisted of 85.6 mmol sodium dihydrogenphosphate di-hydrate ( $\text{NaH}_2\text{PO}_4 \cdot 2\text{H}_2\text{O}$ ) and 103.6 mmol di-sodium hydrogenphosphate di-hydrate ( $\text{Na}_2\text{HPO}_4 \cdot 2\text{H}_2\text{O}$ ) which was adjusted to pH 6.8 by hydrochloric acid or sodium hydroxide. The flow rate was 0.62 mL/min and lysozyme was detected photometrically at 280 nm (Ultimate 3000, Variabel Wavelength Detector, Dionex Softron GmbH, Germering, Germany).

### 2.2.5. X-ray diffraction measurements

Wide angle X-ray diffraction measurements were performed on an X-ray diffractometer XRD 3000 TTT (Seifert, Ahrensberg, Germany). Radiation was generated by a copper anode (40 kV, 30 mA, wavelength 0.154178 nm). Experiments were conducted at  $0.05^\circ$  (2 theta) within a  $5^\circ$  -  $40^\circ$  range. Lipid implants were ground prior to the measurements in an agate mortar to prepare powders for analysis.

### 2.2.6. Differential scanning calorimetry (DSC)

Samples were ground and about 10 mg were exactly weighed into aluminum crucibles. Sealed crucibles were analyzed with DSC 204 Phoenix (Netzsch, Selb, Germany). Heating and cooling rates were set to 5 K/min within a  $-20^\circ\text{C}$  to  $100^\circ\text{C}$  temperature range.

### 2.2.7. Scanning electron microscopy (SEM) measurements

After the release tests, implants were vacuum-dried in a VO 200 vacuum chamber (Mettler, Schwabach, Germany) for 72 hours at  $25^\circ\text{C}$  to remove all adhering water. Scanning electron microscopy was carried out without coating with a 6500F (Jeol GmbH, Eching, Germany).

### 2.2.8. Helium pycnometry

The volume of lipid implants was determined by helium pycnometry (He-pycnometry) with an accuPyc 1330 (Micromeritics, Mönchengladbach, Germany). Therefore, dry lipid implants were placed in a 1 mL measuring cell to make a final volume of about 500  $\mu\text{L}$  (half cell volume) and measured after calibration of the instrument.



### **3. Results**

#### **3.1. Lysozyme release from lipid based implants**

Lysozyme release from the different lipid implants is depicted in Figure 26. RAM-extruded devices showed a very high burst release and 100% of the incorporated protein was released within the first 24 h. Compared to this immediate delivery, implant manufacturing by compression resulted in a sustained release of lysozyme which lasted for 14 days until complete protein release was achieved. Tsc-extruded lipid implants showed a more sustained release over a period of 42 days. Released leveled out at about 93% indicating incomplete protein release. Slowest release rates were achieved from 'compressed tsc-extrudates' (Figure 26). As implants were of different shape implant geometry and surface area were taken into account and a calculation of lysozyme release per surface area was performed. No difference between tsc-extruded implants and 'compressed tsc-extrudates' was found as protein release per implant surface area was identical for both formulations. Thus 'compressed tsc-extrudates' showed a more sustained lysozyme release only due to a smaller surface area compared to tsc-extrudates(Figure 27).

Based on this observation it can be concluded that different manufacturing protocols per se lead to different release kinetics. Importantly, from the comparison between 'compressed tsc-extrudates' and tsc-extrudates it can be reasoned, that twin-screw extrusion is superior to compression with respect to more sustained release. Hereby, the applied heat during tsc-extrusion might play a crucial role as RAM extrudates are produced without triglyceride melting and exhibit a much higher release rate than tsc-extrudates.

IV. - INFLUENCE OF THE MANUFACTURING STRATEGY ON PROTEIN RELEASE KINETICS

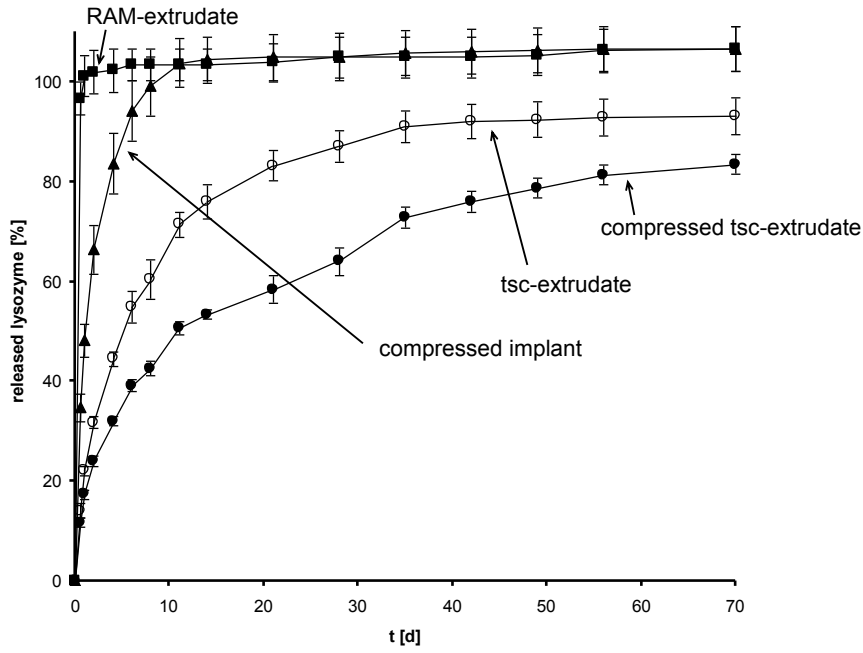


Figure 26: Lysozyme release from lipid implants which were prepared by four different manufacturing processes: compression, RAM extrusion, tsc-extrusion, and a combination of tsc-extrusion + compression ('compressed tsc-extrudates').

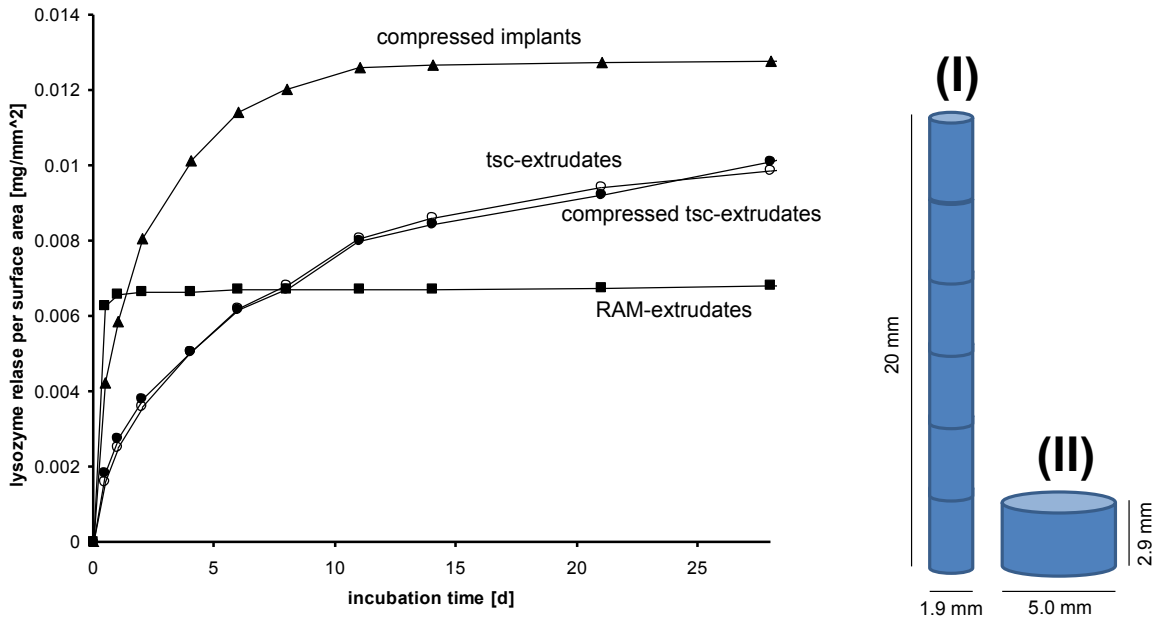


Figure 27: Cumulative lysozyme release per surface area [mg/mm<sup>2</sup>] from different lipid implant. (I) - dimensions of a tsc-extrudate. (II) - dimensions of a compressed implant.

### 3.2. Assessment of implant pore structure

SEM measurements were performed to examine the pore structure of the different implants as porosity is a main factor in controlling the rate of release from inert matrices [26, 187, 219, 220]. Obviously, RAM extrudates exhibited a very porous implant matrix even before release and thus rapid and complete lysozyme release can be explained easily. The surface of RAM-extrudates was rough and the implant was very fragile and easily broke apart during handling (Figure 28 A).

No pores were observed on the surface of compressed, tsc-extruded and 'compressed+tsc-extruded' implants (Figure 28 B, C, D). All formulations showed smooth surfaces and a compact structure with without pores prior to incubation. Thus the different release kinetics between compressed and extruded implants did not result from unequal surface porosity of the implants.

Implant porosity before incubation was calculated from true and apparent implant volume which was determined by He-pycnometry and a sliding rule, respectively. Porosities were calculated according to Equation 3 and showed higher values for RAM extrudates than for the other implants (Figure 29) which exhibited equal values. No difference in implant porosity or apparent implant density was detected between compressed devices and tsc-extrudates indicating similar matrix properties without void spaces.

**Equation 3**

$$\varepsilon = 1 - \frac{V_{\text{He-pycnometry}}}{V_{\text{slidingrule}}} [\%]$$

$\varepsilon$  = implant porosity [%]

$V_{\text{He-pycnometry}}$  = implant volume as determined by He-pycnometry

$V_{\text{slidingrule}}$  = implant volume as determined by sliding rule

Although the fast release from RAM extrudates can be easily explained by the high porosity of these implants, porosities cannot be taken into account for the explanation of the different release profiles of the other formulations. Therefore X-ray diffraction measurements and DSC measurements were performed to further assess the lipid implants.

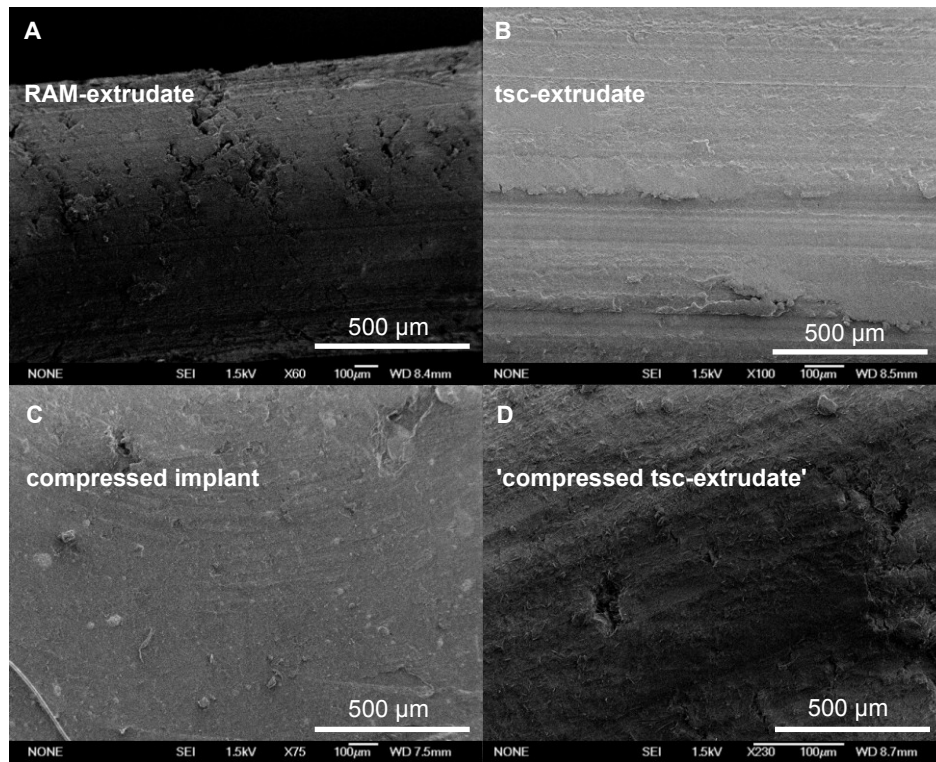


Figure 28: SEM pictures of the surfaces of RAM-extrudate, tsc-extrudate, compressed implant and 'compressed tsc-extrudate' before incubation.

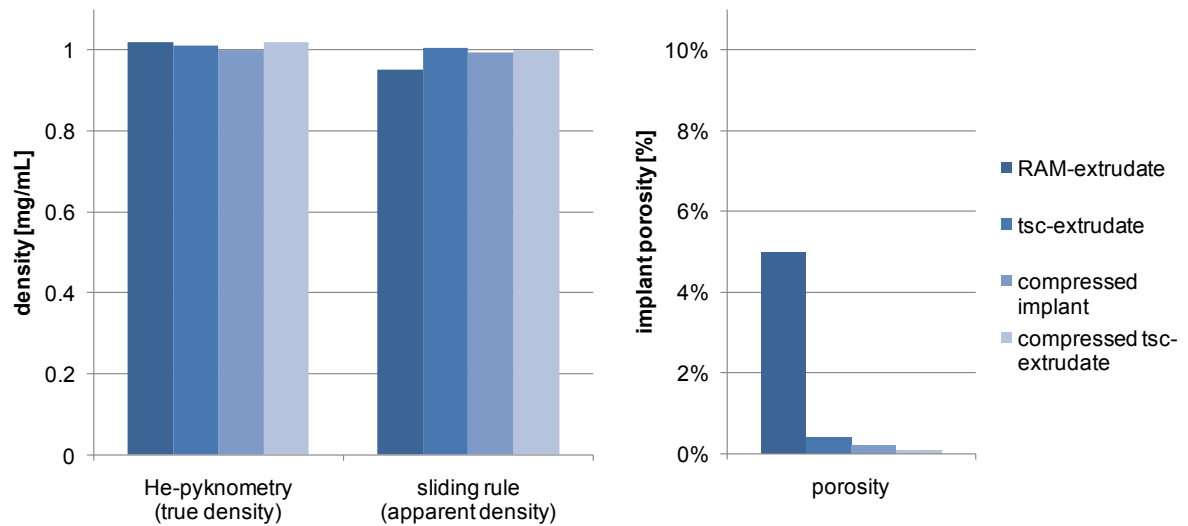


Figure 29: Assessment of apparent densities (left graph) and porosities (right graph) of triglyceride based implants.

### 3.3. X-ray diffraction measurements

Diffraction measurements were performed with triglyceride bulk materials, blends of bulk materials, ‘supercooled melts’ of bulk materials and with powders of ground implants (Table 5).

Diffraction pattern of D118 indicated the presence of  $\beta$ -modification with spacings at 0.465 nm, 0.391 nm and 0.375 nm (Figure 30 – I). Diffraction pattern of H12 indicated the presence of  $\beta'$ -modification and exhibited strong spacings at 0.430 nm and 0.389 nm (Figure 30 – II) [221].

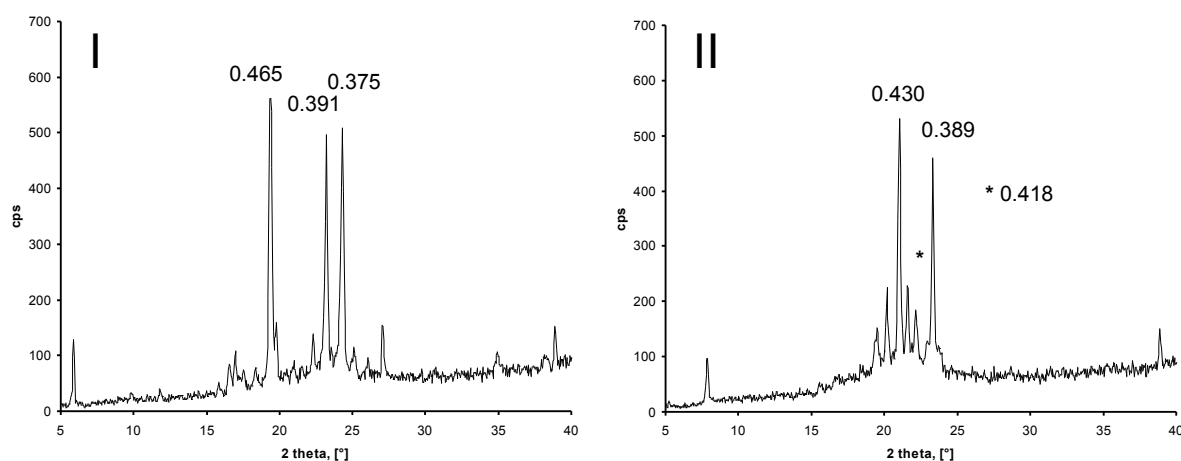
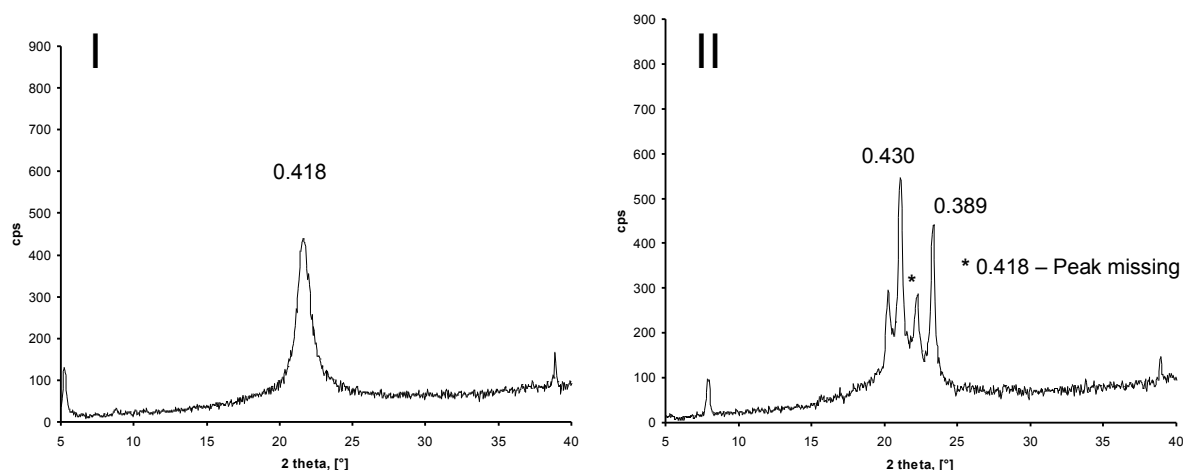


Figure 30: X-ray diffraction pattern: D118 (I) and H12 (II)

‘Supercooled melts’ of the bulk materials were prepared to create instable modifications of the triglyceride materials which could eventually be created during the melting step of the tsc-extrusion process. Preparation of ‘supercooled melts’ were performed by completely melting of bulk materials and rapid ‘supercooling’ of the lipid melts by liquid nitrogen. ‘Supercooling’ of D118 resulted in a drastically changed diffraction pattern with one broad spacing at 0.418 nm which indicated the metastable  $\alpha$ -modification (Figure 31 – I). Interestingly, after ‘supercooling’ of H12 spacings at 0.430 nm and 0.389 nm were still detectable, although an increase of metastable  $\alpha$ -modification was obvious from the diffraction spectrum (Figure 31 – II).

Of course, the lipid powder blend containing H12 (24%), D118 (56%) and PEG 6000 (20%) (Blend A) showed a combination of the diffraction pattern of all bulk materials (Table 5). The identical diffraction pattern was also found in RAM-extruded and compressed implants, indicating no changes in lipid crystallinity due to implant manufacturing (Table 5) by compression or RAM extrusion.



**Figure 31: X-ray diffraction pattern: 'supercooled melt' of D118 (I) and 'supercooled melt' of H12 (II)**

The weak H12 spacing at 0.418 nm which was detected in H12 bulk material, and Blend A was lost in tsc-extruded lipid implants. Nevertheless, tsc-extrudates still exhibited high crystallinity (Table 5, Figure 32) and an almost perfect overlay with Blend A (Figure 32 + Figure 33).

In order to mimic the extrusion process (H12 melting), Blend A was heated to 44 °C for 5 minutes and a so called Blend B was created. Diffraction pattern of Blend B also lacked the spacing at 0.418 nm what was in analogy to the diffraction pattern of tsc-extruded implants (Figure 32 and Figure 33). The loss of the spacing at 0.418 nm in tsc-extrudates was thus explained by melting of the low melting lipid (H12) during the tsc-extrusion process.

We concluded that tsc-extrusion led to a minor change (loss of spacing at 0.418 nm) in lipid phase properties due to the applied heat. However, crystallinity in tsc-extrudates was still high exhibiting a mixture of  $\beta$ - and  $\beta'$ -modification. No considerable amount of instable  $\alpha$ -modification was detected by X-ray diffraction measurements.

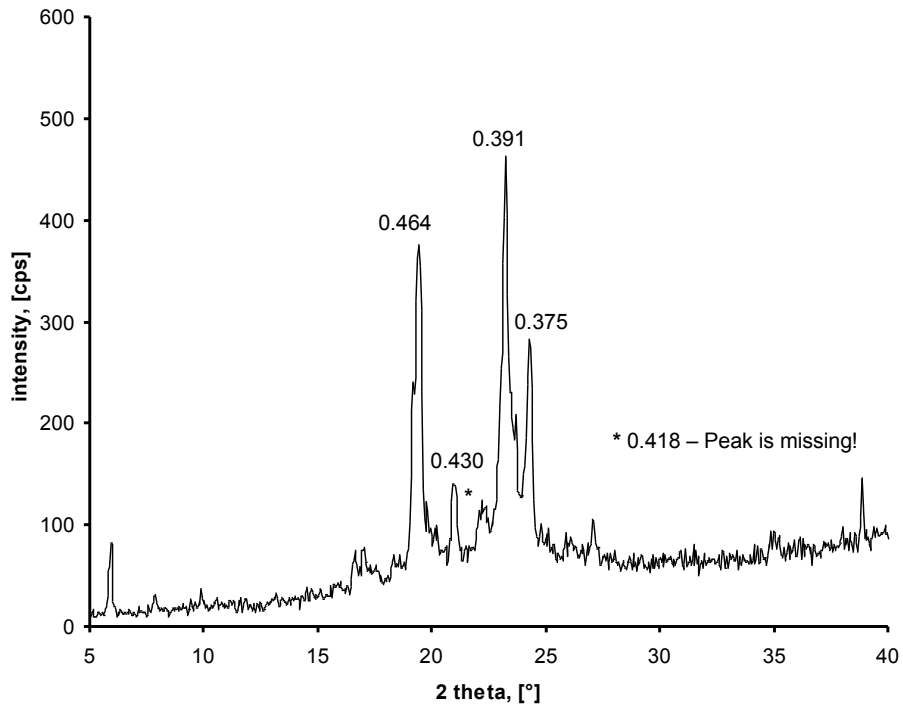


Figure 32: X-ray diffraction pattern of a tsc-extrudate

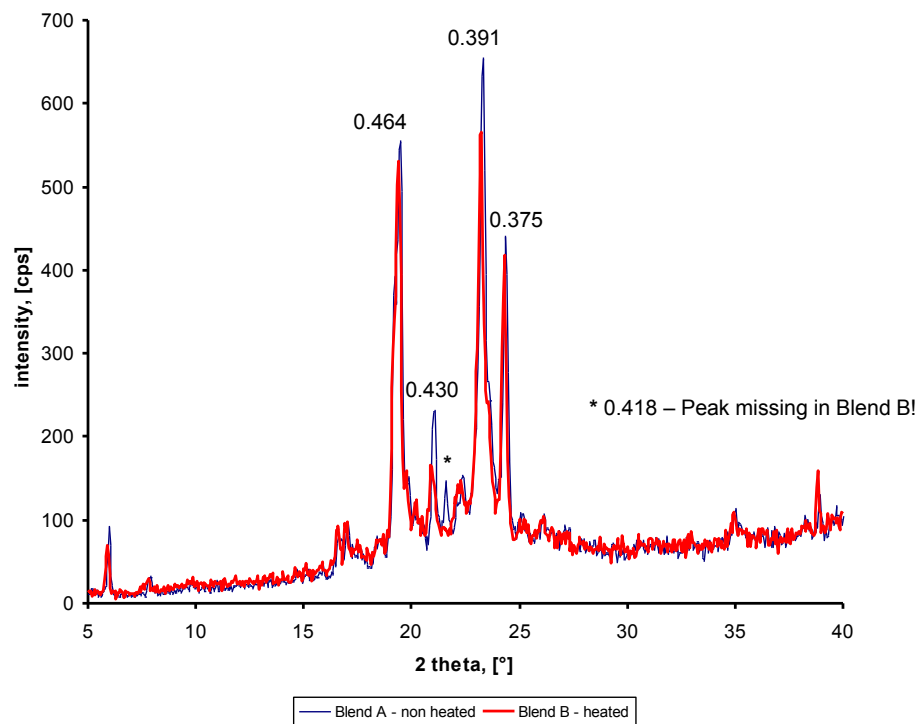


Figure 33: Overlay of X-ray diffraction pattern of blend A (D118 + H12 (70-30%)) (blue) and blend B(D118 + H12 heated to 40 °C) (red).

**Table 5: Diffraction pattern of bulk materials, lipid powder blends and lipid implants. Blend A and B consist of H12 (24%), D118 (56%) and PEG 6000 (20%).**

material	spacings [nm]					
H12 bulk	0.462	0.430	0.418		0.389	
D118 bulk	0.465			0.406	0.391	0.374
H12 'supercooled'	0.445	0.429		0.406	0.389	
D118 'supercooled'			0.418			
Blend A – non heated	0.462	0.430	0.418	0.404	0.389	0.374
Blend B – heated	0.462	0.430	X	0.404	0.389	0.374
tsc extrudate	0.465	0.430	X	0.406	0.391	0.374
RAM-extrudate	0.465	0.430	0.420	0.406	0.391	0.374
compressed implant	0.463	0.430	0.419	0.405	0.391	0.375

### 3.4. DSC-measurements

DSC measurements with ground lipid implants showed melting point depression for both D118 and H12 compared to the pure bulk materials (Table 6). D118 melting endotherm was lowered from 74.5 °C to 70.4 °C for all implants. H12 melting endotherm decreased from 40.2 °C to 37.5 °C in RAM-extruded and compressed implants and to 35.5 °C in tsc-extrudates or 'compressed tsc-extrudates'. Interestingly, Blends A (non heated) and B (heated) performed similarly to implants prepared by RAM-extrusion/compression or tsc-extrusion (Figure 34 and Table 6).

A explanation for the lower melting point of H12 after tsc-extrusion is an interaction between H12 and D118 during tsc-extrusion (temp.: 41 °C) where the low melting lipid H12 melts or at least partially melts generating a eutectic with D118.

**Table 6: Melting peaks of bulk material and lipid implants (1<sup>st</sup> heating scan)**

samples	melting endotherms		
H12 bulk ( $\beta'$ -modification)	40.2 °C		
PEG 6000	62.3 °C		
D118 ( $\beta$ -modification)	74.5 °C		
RAM-extrudate	37.5 °C	60 °C	70.4 °C
compressed implant	37.5 °C	60 °C	70.4 °C
tsc-extrudate	35.5 °C	60 °C	70.4 °C
compressed tsc-extrudate	35.5 °C	60 °C	70.4 °C
Blend A – non heated	38.1 °C	58.6 °C	70.4 °C
Blend B – heated	34.6 °C	61.7 °C	70.4 °C

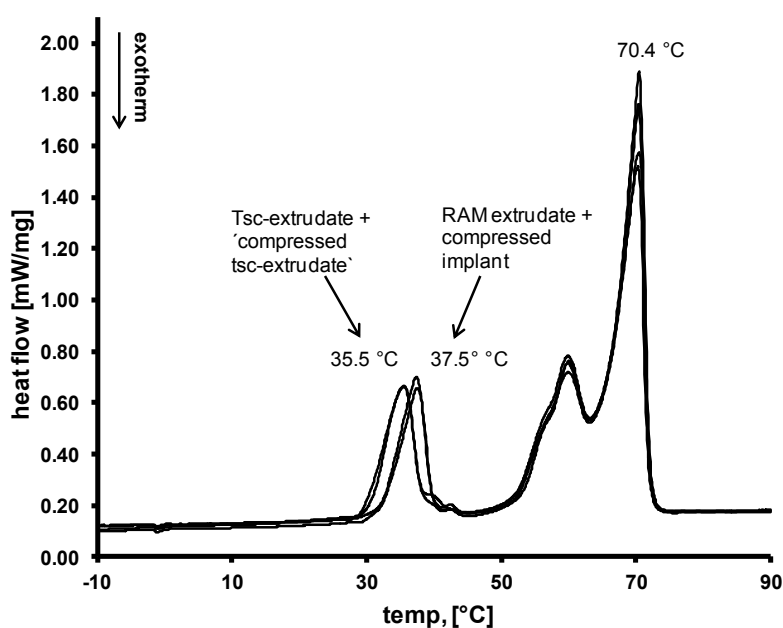


**Figure 34: DSC thermogram of lipid implants prepared by RAM-extrusion, compression and tsc-extrusion. First melting endotherm (35.5-37.5 °C) represents H12 melting, second endotherm (~ 60 °C) PEG 6000 melting and third endotherm (70.4 °C) D118 melting.**

Lipid powder mixtures with different ratios between H12 and D118 (0%-100% with 10% increments) were prepared and DSC measurements were carried out (Figure 35) to investigate on the lipid phase behavior of this triglyceride mixture. 1<sup>st</sup> heating scans showed melting point depression of D118 from 74.6 °C (pure D118) to 58.8 °C (10% D118). No

significant change in melting behavior of H12 could be detected in the 1<sup>st</sup> heating scan, although a slight depression of the maximum of the melting endotherm from 39.7 °C to 37.7 °C was observed (Figure 35). However, onset of H12 melting was identical in all triglyceride mixtures. Importantly, a 30/70 mixture of H12 and D118, which is identical to the lipid ratio used for implant preparation, exhibited the same melting points for H12 and D118 as in RAM extruded and compressed implants. This indicates that the melting point depression observed in these devices did not result from the manufacturing process.

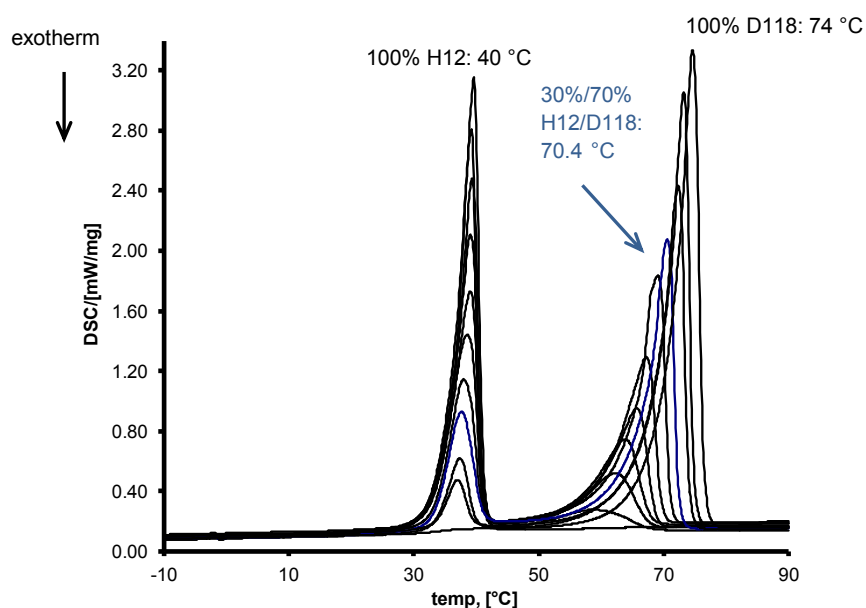


**Figure 35:** DSC-measurements of a lipid powder blend containing H12 and D118 bulk material: 1<sup>st</sup> heating scan. Lipids were step wisely mixed in ratios from 0-100% using 10% increments. Melting endotherm: 37 °C = H12 melting; 70 °C = D118 melting.

The 2<sup>nd</sup> heating scans of lipid powder mixtures showed a distinct melting point depression of H12 from 37.0 °C (pure H12) to 28.3 °C (10/90 - H12/D118 ) (Figure 36). The melting point depression of H12 in tsc-extrudates can be ascribed to the melting of H12 during tsc-extrusion.

The extrusion process was mimicked to confirm the assumption that the applied heat leads to a melting point depression of H12 in tsc-extrudates. Therefore a lipid powder mixture (Blend A) was placed inside the extruder barrel and heated to 44 °C for 5 min but not extrusion was performed (Blend B - heated). DSC melting peaks of Blend B were in good

agreement to the melting peaks obtained from tsc-extrudates. Thus, we concluded that the applied heat in the tsc-extrusion process leads to the changed melting profile of tsc-extruded implants (Figure 37).

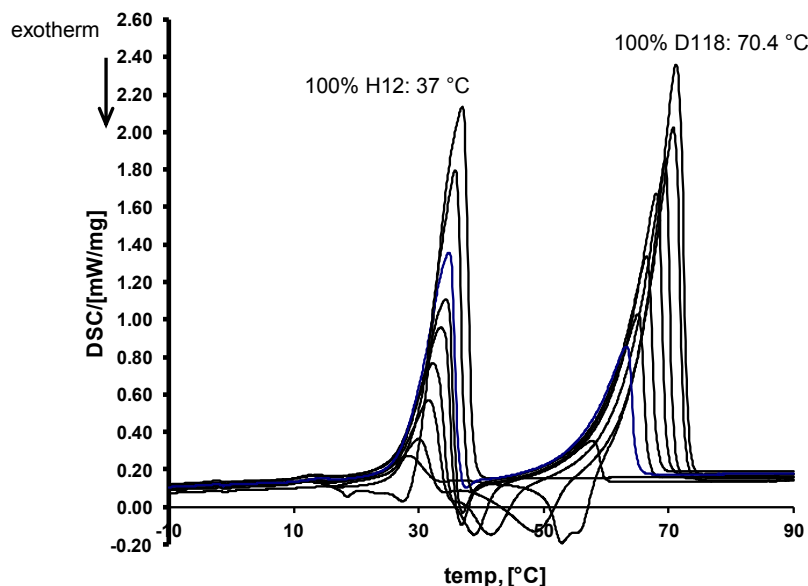


**Figure 36: DSC-measurements of a lipid powder blend containing H12 and D118 bulk material: 2<sup>nd</sup> heating scan. Lipids were step wisely mixed in ratios from 0-100% using 10% increments. Melting endotherm: 30 °C = H12 melting; 70 °C = D118 melting.**

The 2<sup>nd</sup> heating scans of H12-D118 mixtures showed additional exothermic melting events indicating instable lipid modifications after complete melting of the lipid mixture (Figure 36). This is especially important, as the formation of instable modifications might lead to polymorphic transformation during long term storage and thus altering of release kinetics. Importantly no exothermic peaks were detected in tsc-extruded implants (Figure 34). From that, we concluded that no instable lipid modification is formed during tsc-extrusion. This is in good agreement with X-ray diffraction measurements, where also no instable  $\alpha$ -modification was detected in tsc-extrudates.

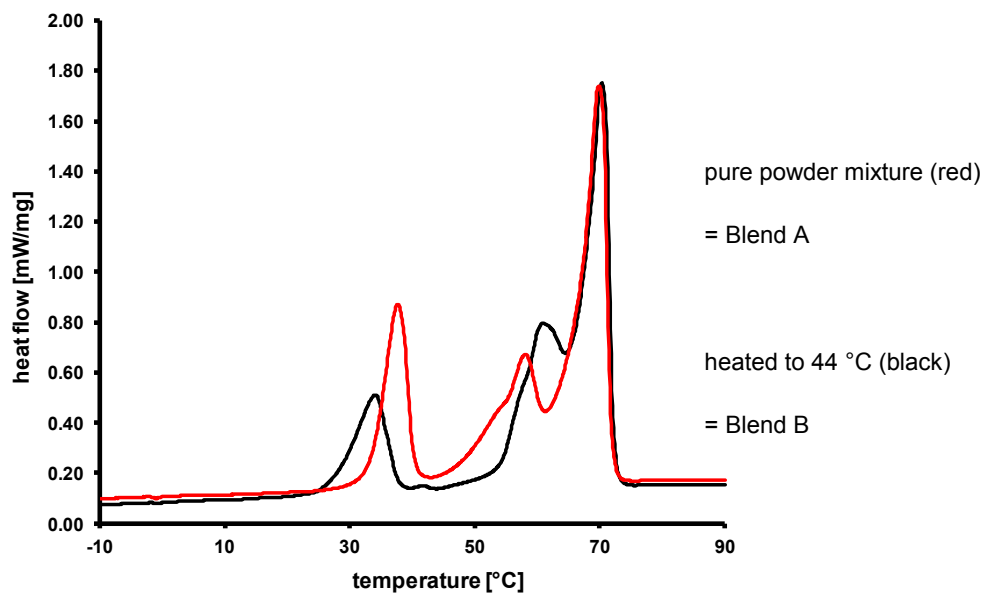


Figure 37: DSC thermogram of two powder mixtures containing 24% H12, 56% D118 and 20% PEG 6000. Red line indicates untreated lipid powder mixture (Blend A), black line indicates the same mixture heated to 44 °C for 5 min (Blend B). Melting endotherms: 34.6 °C + 38.1 °C = H12 melting; 60 °C = PEG melting; 70.4 °C = D118 melting.

#### **4. Summary**

RAM-extrudates showed high initial burst release and complete lysozyme liberation within 24 h. This release behavior was explained by the high porosity of RAM extruded devices as detected by SEM measurements. Compressed implants show sustained lysozyme release with continuous lysozyme delivery over 14 days. Tsc-extrudates and compressed tsc-extrudates showed even more sustained lysozyme release compared to compressed implants.

SEM pictures did not reveal a significant difference between compressed and tsc-extruded implants as both exhibit a smooth surfaces and a dense implant core.

X-ray diffraction measurements as well as DSC measurement indicate minor changes in lipid crystallinity after twin-screw extrusion, which were not detected in RAM-extruded or compressed implants. Presumably these differences in the lipid phase properties derive from partial melting of the implant matrix during the manufacturing process and contribute to the more sustained lysozyme release from tsc-extrudates compared to compressed implants. Presumably, melting of matrix material led to a better coating or sealing of protein particles during the preparation process than simple compression. Although implant density was identical for compressed and tsc-extruded implants, melting might contribute to a 'denser' core by sealing of tiny channels and thus led to reduced water penetration velocity into the device.

Most importantly, DSC and X-ray diffraction measurements showed the absence of instable lipid modifications after the extrusion process. This is of uppermost importance regarding long-term storage stability of the implant devices. The observed melting point depression simply derived from the formation of an eutectic by mixing of two triglycerides but not from modification changes. During tsc-extrusion, both triglycerides were thoroughly mixed and partially dissolve in each other, forming a stable triglyceride phase.

Thus it was shown that tsc-extrusion per se led to a more sustained protein release and this effect was attributed to the melting of the low-melting lipid during the manufacturing process.



## **V. Mechanistic studies on the release of lysozyme from twin-screw extruded lipid implants (I) – influence of pore-former and lipid composition**

### **1. Introduction**

In chapter 0 we showed that tsc-extrusion per se leads to a sustained release of proteins from triglyceride based implants and in chapter III we stated, that the release of an antibody or IFN $\alpha$  [24] can be modified by protein precipitation which allows an even more sustained release of the drug. However, no general work was performed so far, how release from tsc-extrudates can be controlled. Kaewvichit *et al.* [187] found that protein release from compressed lipid implants was influenced by factors like e.g. drug particle size and drug loading. We decided to modify the currently used matrix composition with respect to triglyceride composition and properties of pore-forming agent and thereby try to modify protein release from tsc-extrudates.

#### **1.1. Material**

Hen egg white lysozyme was purchased from Sigma (Product Number: L 6876). Various grades of PEG were donated from Clariant, Wiesbaden, Germany. For our studies we used PEG 3350 P, PEG 4000 P/PF/PS, PEG 6000 P/PF/PS, PEG 8000 P, PEG 12000 P and PEG 20000 P (P = powder, PF = powder fine, PS = powder spray-dried). Salts were of analytical grade and purchased from Merck (Darmstadt, Germany). Sodium azide was purchased from Acros Organics (Geel, Belgium). Triglycerides were a gift from Sasol (Witten, Germany).

#### **1.2. Methods**

Methods used within these studies include the preparation of tsc-extrudates, *in-vitro* release test of lysozyme from tsc-extrudates, lysozyme quantification and SEM measurements and were already described in chapter IV.2.2.



## **2. Results of the influence of the pore-forming agent on lysozyme release**

According to the studies of Siegel [17, 222], Kaewwichit [187], Mohl [27], and Herrmann [29] a sufficient amount of water soluble ingredient (drug and/or pore-former) is necessary to allow complete drug release from inert matrices like triglyceride based implants. Upon hydration, the water soluble parts of the inert implant dissolve and create an interconnected pore network through which the active can be released.

PEG was used by various groups [24, 179, 223-226] as pore former because it acts as a stabilizer and emulsifying agent and was shown to prevent aggregation and inactivation of proteins upon encapsulation in bioerodible polyester microspheres or stabilize BSA which was encapsulated in PLA-PEG microsphere blends [225, 227]. Additionally, PEG does not precipitate lysozyme (model protein in the study) nor does it have any adverse effects on lysozyme stability or integrity [228, 229]. We investigated the influence of PEG particle size, PEG viscosity and PEG dissolution velocity on lysozyme release from tsc-extrudates.

### **2.1. Influence of PEG 4000 particle size on lysozyme release**

The particle size of the pore former is described to have a major influence on drug release profiles from inert matrices. The larger the particle size the more likely will the particles touch the implant surface and the faster the drugs should be released [25, 177, 187]. A minimum concentration of hydrophilic component which can dissolve in water is however required to allow complete drug release from inert triglyceride based matrices [27, 28, 189]. By decreasing the porogen particle size, a finer distribution of the porogen within the implant is possible and the surface area of the porogen increases. Thus a greater ratio of the incorporated protein drug is in direct contact with this hydrophilic component and thus a complete drug release is more easily established. However, by decreasing the particle size of hydrophilic components the interconnected network which has to be formed from these particles will also become finer and due to this a more sustained protein release can be achieved. This was already shown by Könnings *et al.* for the release of brain-derived

neurotrophic factor (BDNF) [177] from compressed implants. However, if particles are too fine it is not possible to build an interconnected network, because the particles are separated within the matrix which again leads to an incomplete drug release.

In order to elucidate the effect of the size of the pore-forming agent on our system PEG 4000 and PEG 6000 with various particles sizes were used as pore formers and extruded into lipid matrices. For all formulations 20% of pore former and 2.5% of lysozyme as model protein was used. The high concentration of pore forming agent was chosen in accordance to Mohl [223] und Herrmann [179]. They found that total protein release from inert compressed D118 matrices was only possible at concentrations of more than 20% hydrophilic components. The triglyceride matrix of tsc-extrudates consisted of H12 and D118 in a ratio of 30/70 (m/m). Extrusion was performed at 40 rpm and 42 °C and *in-vitro* release tests were carried out. We used three batches of PEG 4000 and PEG 6000 powders with different particle sizes and determined the particle size by sieving. The size distributions for the 3 powders (‘powder’ = P, ‘powder fine’ = PF and ‘powder fine < 45µm’ = PF < 45 µm) are displayed in Figure 38. ‘Powder’ and ‘powder fine’ were used a purchased from the supplier and ‘powder fine < 45µm’ was prepared by sieving of ‘powder fine’.

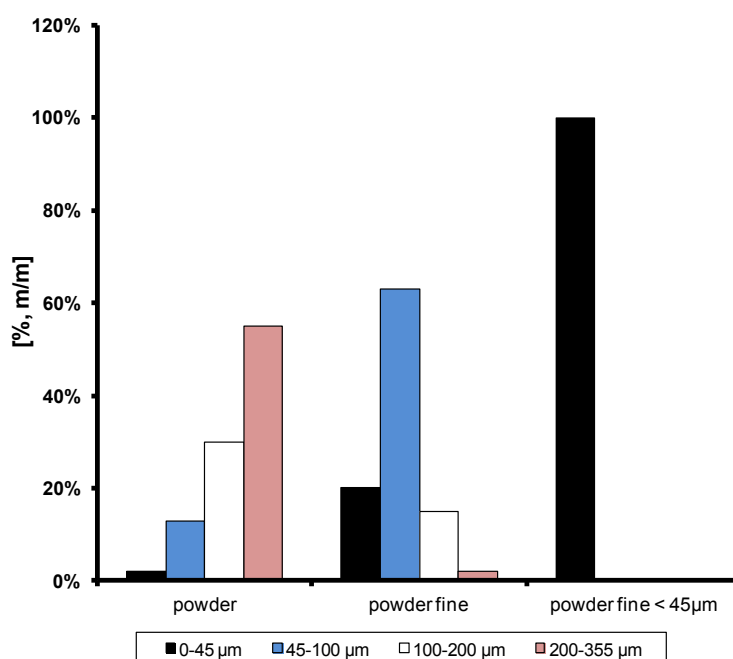


**Figure 38: Particle size distribution of various powders of PEG 4000/6000: P (powder), PF (powder fine) and PF < 45 µm (sieved fraction)**

Protein releases kinetics did not differ between the formulations containing different particle sizes (Figure 39 + Figure 40). Lysozyme was completely released within 27 days from all six formulations and showed similar release behavior independent of the PEG particle size or PEG variety (4000 versus 6000) used. This was explained by the small implant diameter compared to compressed implants and by the high concentrations of the pore-forming agent. Nevertheless, release lasted for up to 15 days. As lower concentrations of pore-forming agent eventually lead to incomplete drug release, we found that adjustment of porogen particle size was not helpful to control the rate of protein release.

In chapter I.1 we explained slow antibody release from tsc-extrudates with the small particle size of lyophilized PEG 6000. However no direct comparison between the lysozyme and antibody release is possible, as antibody precipitation in the presence of PEG changes the conditions for release drastically.

No change between lysozyme release from implants comprising PEG 4000 or PEG 6000 was observed in this study. The effect of different PEG qualities on protein release from tsc-extrudates will be discussed in the next chapter.

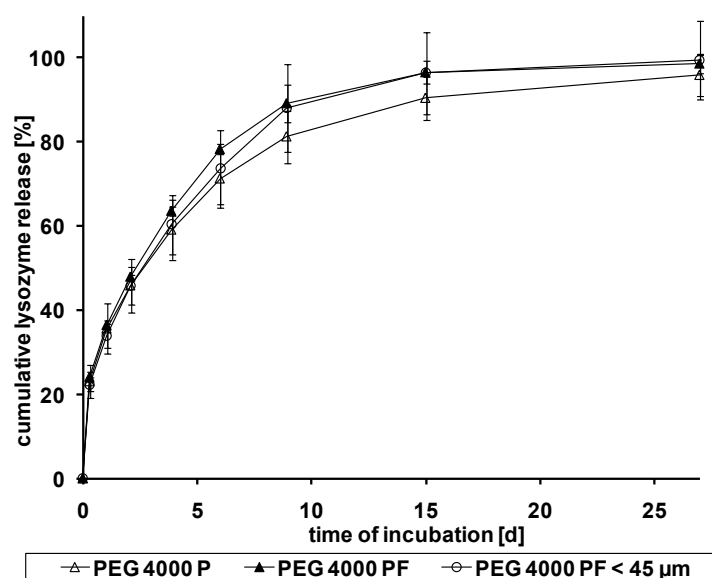


Figure 39: Lysozyme release from tsc-extrudates comprising 20% PEG 4000 of different particle sizes.

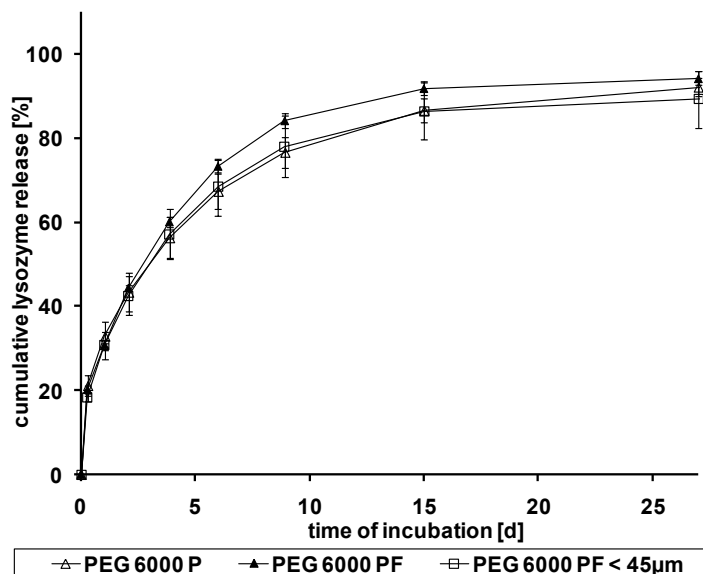


Figure 40: Lysozyme release from tsc-extrudates comprising 20% PEG 6000 of different particle sizes.

## 2.2. Influence of viscosity within the implant pores

As lysozyme release from tsc-extrudates was found to be diffusion controlled, factors like temperature and viscosity of the release medium within the implant pores play a crucial role for the release kinetics. According to the Boltzmann equation the diffusion coefficient strongly depends on temperature ( $T$ ), hydrodynamic radius ( $r_H$ ) of the molecule and dynamic viscosity ( $\eta$ ) of the solvent. Especially the viscosity of the fluid within the implant pores is of uppermost importance as it hinders water entry into and diffusion of protein molecules out of the implant. To investigate the influence of viscosity within the implant pores, we prepared implants containing various PEGs ranging from PEG 3350 to PEG 20000. With increasing molecular weight and increasing PEG concentration, the viscosities of PEG solutions increase. Figure 41 depicts the viscosities of the varieties of PEG which were used for our study in a 50% aqueous solution at 20 °C. The maximal solubility for each PEG quality lies between 52% (PEG 20000) and 56% (m/m) (PEG 3350). A distinct difference between the PEG qualities can be observed with PEG 20000 being 30 times more viscous than PEG 3350. As all other crucial factors like the incubation temperature, PEG particle size (and thus pore size within the matrix) and the composition of the lipid matrix (H12-D118 – 30/70 (m/m)) were equal, a

difference in the lysozyme release profile would clearly result from a change of the viscosity within the implant pores. For all PEG species dissolution time did not differ significantly, if 45% (m/m) solutions were prepared and ranged between 8 - 9 hours for complete PEG dissolution.

No differences in lysozyme release rates between tsc-extrudates comprising different qualities of PEG were observed (Figure 42). Protein release rate was independent of the molecular weight of the applied PEG variety. Within 27 days lysozyme was completely released from all tsc-extrudates.

Thus, viscosity of the aqueous PEG solution within the lipid implant pores has no major influence on the lysozyme release rate at 37 °C. Within the setup of the study the influence of viscosity on lysozyme release can be neglected and does not allow for an adjustment of the rate of release.

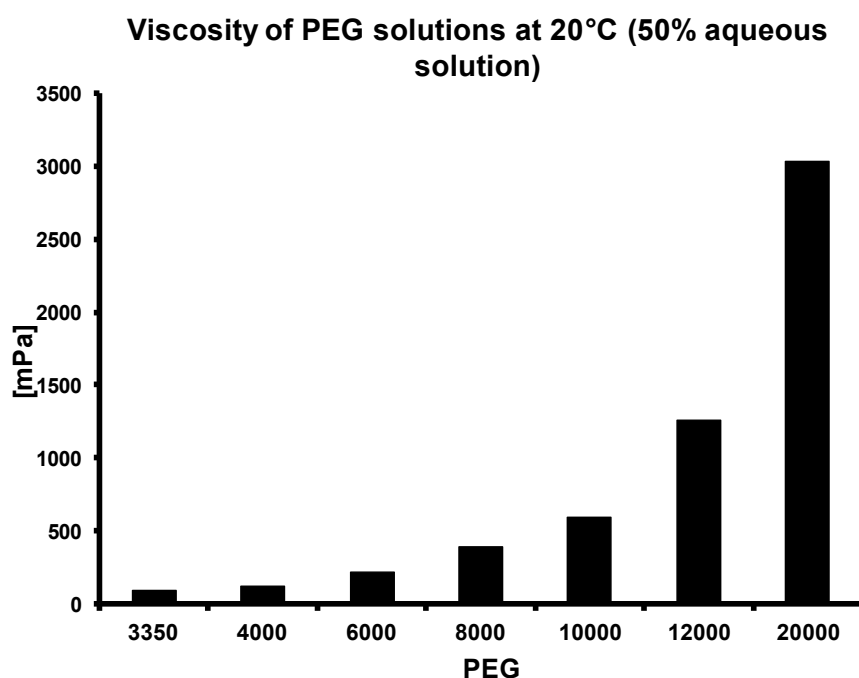
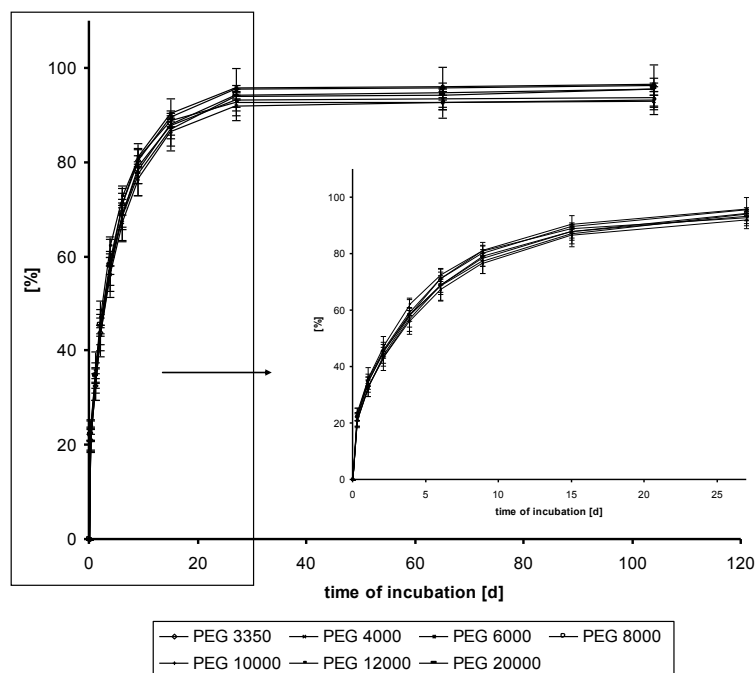


Figure 41:Viscosities of 50% aqueous solutions of PEGs which were used for the production of tsc-extrudates. (Data taken from certificate of analysis from supplier (Clariant, Wiesbaden, Germany).)



**Figure 42: Lysozyme release from tsc-extruded lipid implants comprising different qualities of PEG ranging between PEG 3350 and PEG 20000.**

### 2.3. Influence of the dissolution rate of PEG

In order to elucidate the influence of the dissolution rate of PEG on the lysozyme release kinetics from tsc-extrudates, we used fast dissolving lyophilized PEG 6000 as pore forming agent and compared the rate of release to PEG powder ( $< 45 \mu\text{m}$ ). The lyophilized powder was ground in a mortar, sieved and the particle fraction between  $0\text{-}45 \mu\text{m}$  was used to prepare tsc-extrudates.

Dissolution rates of powdered PEG and lyophilized PEG were measured by dissolving 50 mg of each variety in 50  $\mu\text{L}$  and 250  $\mu\text{L}$  PBS buffer (resulting in concentrations of 50.0% (m/m) and 20.0% (m/m) PEG). For both concentrations, lyophilized PEG dissolved instantaneously ( $< 1 \text{ min}$ ) and the dissolution of PEG  $< 45 \mu\text{m}$  was clearly sustained for up to 7 hours for the 50% solution (m/m) (Figure 43).

However, dissolution rates of PEG 6000 were found to exhibit only a minimal influence on the release kinetics. During the first 2 days of *in-vitro* release, no difference between lysozyme release from tsc-extrudates containing lyophilized PEG and the powdered form of

PEG was found. After 9 days, protein release from tsc-extrudates containing the lyophilized PEG was slightly faster and complete release was achieved earlier compared to crystalline PEG (Figure 44). In conclusion, no major influence of the dissolution rate of the pore-forming agent on protein release kinetics was found.

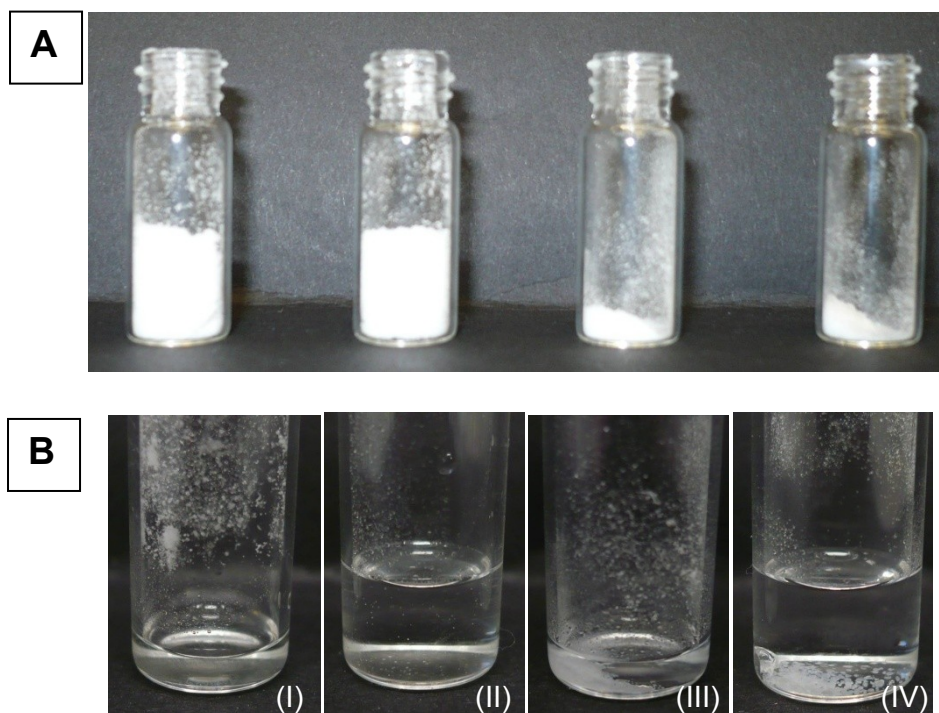


Figure 43: Dissolution rate of lyophilized PEG 6000 (2 vials on the left) and powdered PEG (2 vials on the right). A: before addition of PBS buffer pH 7.4. B: 60 seconds after addition of 50 µL (I + III) or 250 µL (II + IV) PBS buffer pH 7.4

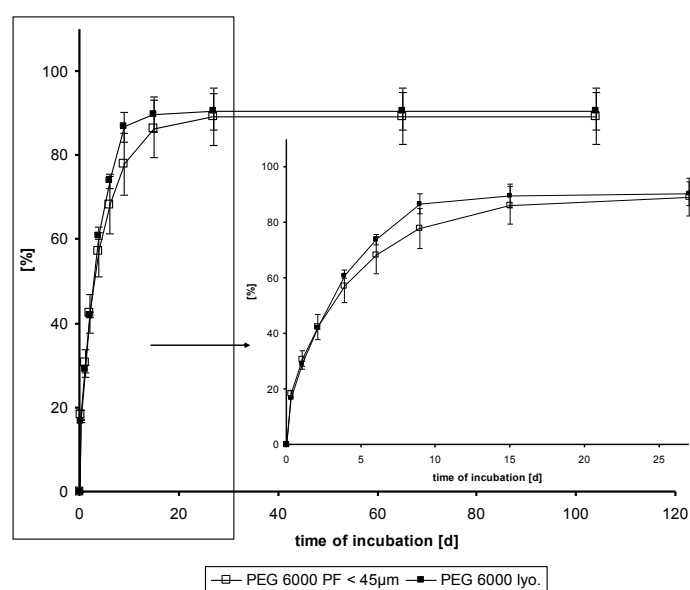


Figure 44: Lysozyme release from tsc-extrudates containing PEG 6000 PF < 45 µm (open squares) or lyophilized PEG 6000 (PEG lyo – black circles).

Changes in PEG particle size, PEG viscosity and PEG dissolution velocity did not significantly affect the rate of lysozyme release from tsc-extrudates. We therefore decided to further investigate the lipid matrix properties and try to adjust the rates of release by changes in triglyceride matrix composition.

### 3. Influence of lipid matrix composition

#### 3.1. Influence of the ratio between low and high melting lipid

As described above, tsc-extrudates comprise a lipid matrix consisting of a high melting and a low melting lipid. To study the influence of ratio between low and high melting lipid on protein release, tsc-extrudates comprising lysozyme, PEG 6000 P (pore-forming agent), D118 as high melting lipid and H12 as low melting lipid were prepared as displayed in Table 7. The ratio of D118 to H12 was varied from 80-20% to 60-40%, as tsc-extrusion could be performed best within these limits. If higher rates of H12 were used no or only little material flow could be established because the lipid mixture became too soft within the extruder barrel. At lower ratios of H12, the torque within the extruder barrel increased and abrasion in the material led to blackening of the tsc-extrudates. Additionally material flow was very low at this conditions.

Tsc-extrudates were prepared according to Table 7, subsequently cut into pieces and *in-vitro* release tests at pH 7.4 and 37 °C were performed.

**Table 7: Compositions and extrusion temperatures of tsc-extrudates.**

low melting lipid – H12 [%]	high melting lipid – D118 [%]	ratio D118:H12	PEG 6000 [%]	lysozyme [%]	extrusion temperature
16%	64%	80-20	17.5%	2.5%	41 °C
24%	56%	70-30	17.5%	2.5%	41 °C
32%	48%	60-40	17.5%	2.5%	41 °C

Interestingly, no influence of the amount of low melting point lipid was found at the first glance. Release from 80%-20% and 70%-30% D118-H122 implants were completely identical and 60%-40% D118-H12 was only slightly faster in the beginning of the experiment.

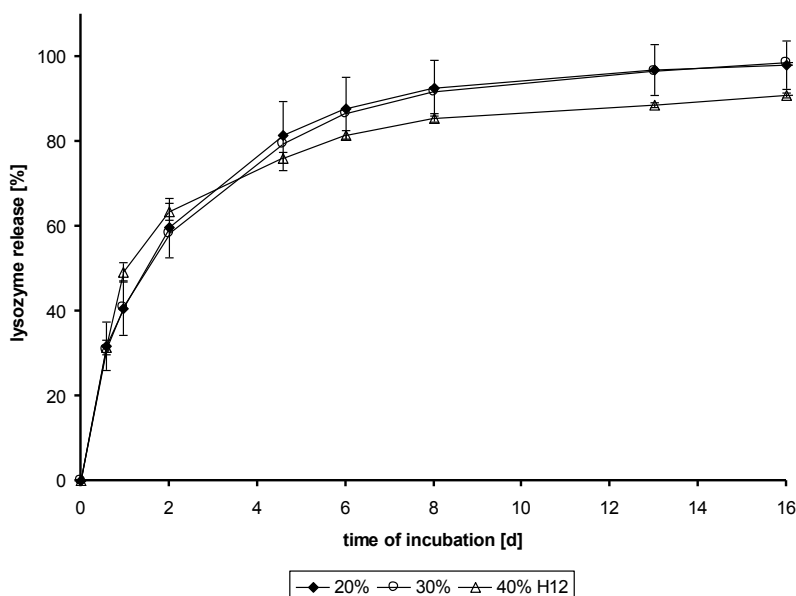


**Figure 45: Lysozyme release from tsc-extrudates: influence of the ratio between low melting point and high melting point lipid.**

In general, our findings suggest that protein release is quite independent of the matrix composition between ratios of 80-20% to 70-30% (D118-H12) if a concentration of 20% of hydrophilic components was used. For higher amounts of H12 a slight change in the release profile was observed. *In-vitro* release from tsc-extruded implants showed to be quite robust concerning the composition of the lipid matrix. Grinding of tsc-extrudates and extraction of lysozyme showed that lysozyme was completely released from all implants. As a consequence, the 60-40% (D118-H12) implants did not show incomplete release but only a loading of 90% of the theoretical value. Thus lysozyme release from these implants was faster and leveled earlier than release from the other devices. A reason for the lower loading might lie in an incorrect weighing step or the extrusion step which was more complicated due to the high H12 content of these implants.

However, protein release is clearly dominated by the highly porous implant structure which is created upon PEG dissolution and release.

### 3.2. Influence of the high melting lipid

In order to study the influence of the type of high melting lipid on lysozyme release, implants comprising D120, D118 and D116 were prepared according to Table 8 and *in-vitro* release tests were performed in isotonic PBS pH 7.4 at 37 °C.

As can clearly be seen in Figure 46 perfect overlays of the release profiles of the three different formulations were obtained. Thus no influence of the type of high-melting lipid was observed in this study.

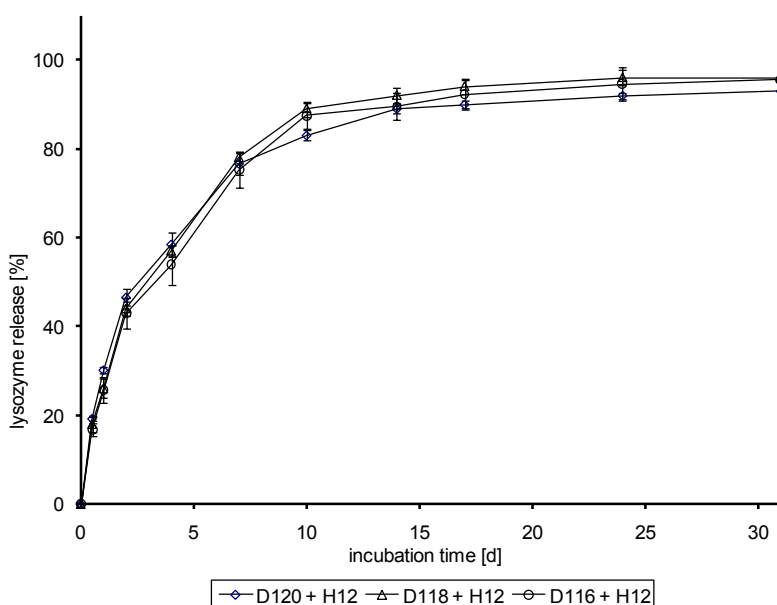


**Figure 46: Lysozyme release form tsc-extrudates consisting of H12 and various high-melting lipids (D120: glycerol triarachin, D118: glycerol tristearin, D116: glycerol tripalmitin)**

**Table 8: Compositions and extrusion temperatures of tsc-extrudates containing various high melting lipids.**

type of high melting point lipid	high melting point lipid [%]	low melting point lipid H12 [%]	PEG 6000 [%]	lysozyme [%]	extrusion temperature [°C]
D120	56%	24%	17.5%	2.5%	42 °C
D118	56%	24%	17.5%	2.5%	42 °C
D116	56%	24%	17.5%	2.5%	42 °C

### 3.3. Influence of the type of low-melting lipid

Lipid tsc-extrudates with various low melting lipids were prepared according to Table 9. Low melting lipids differed in their chemical composition (mono-acid: D112 (glycerol trilaurin) + D114 (glycerol trimyristin); mixed-acid: E85 + H12 (lauric, myristic and palmitic acid)) and their melting ranges (

Table 10).

Extrusion was easily possible for H12, E85 and D112 lipid powders but not for D114 (trimyristate). No lipid tsc-extrudate could be obtained by simply loading the extruder but pressure was applied to the material feeding to enable extrusion.

**Table 9: Compositions and extrusion temperatures of tsc-extrudates containing various low melting point lipids**

type of low melting point lipid	low melting point lipid [%]	high melting point lipid – D118 [%]	PEG 6000 [%]	lysozyme [%]	extrusion temperature [°C]
H12	24%	56%	17.5%	2.5%	42 °C
E85	24%	56%	17.5%	2.5%	45 °C
D112	24%	56%	17.5%	2.5%	50 °C
D114 <sup>*)</sup>	24%	56%	17.5%	2.5%	56 °C <sup>*)</sup>

<sup>\*)</sup> extrusion could hardly be performed

**Table 10: Endothermic DSC melting maximums and melting ranges of triglycerides as raw materials and within tsc-extruded lipid devices.**

	melting peak of lipid powder [°C]	melting ranges/peaks within tsc-extrudate [°C]
H12	37.9 °C	29 °C – 39 °C; peak: 35.1 °C
E85	45.8 °C	28 °C – 44 °C; peak: 42.8 °C
D112	45.0 °C	34 °C – 46 °C; peak: 41.1 °C
D114	58.6 °C	50 °C – XX °C <sup>*)</sup> ; peak: 55.7 °C

<sup>\*)</sup> end of D114 melting peak in tsc-extrudates could not be determined due to overlap with D118 melting peak

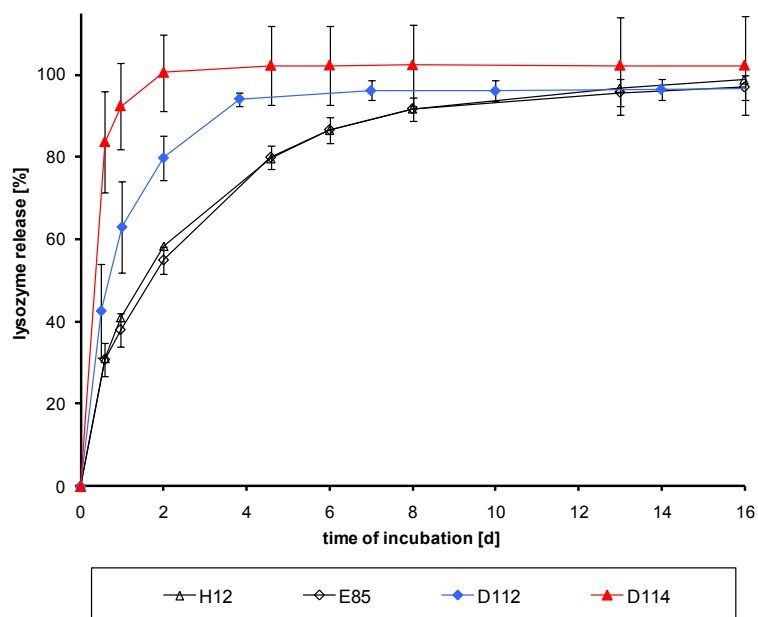


**Figure 47: Influence of the type of low melting point lipid on lysozyme release rate.**

As can clearly be seen from Figure 47, significant differences in the release rates between tsc-extrudates were found. Tsc-extrudates containing the mixed acid triglycerides H12 and E85 resemble each other and show identical release behaviors. However the use of the triglycerides D112 and D114 led to a faster release of lysozyme. This was explained by differences in the manufacturing process (temperatures).

It was already state above that extrusion of the mixture comprising D114 was hardly possible. Finally, extrusion could only be performed at 56 °C by applying pressure onto the material feed and thus forcing the lipid matrix through the extruder out let die in a sort of RAM extrusion. Extrusion of D112 could be established easily, however, extrusion temperature had to be set to 49 °C. As can be observed from Figure 48 melting of PEG 6000 starts at 46-48 °C and exhibits an endothermic melting peak at 62.2 °C. In consequence a melting of PEG 6000 can be expected for D114 containing extrudates during the production process and partial melting of PEG 6000 is expected in D112 comprising extrudates. To study the influence of a simultaneous melting of lipid and PEG, both substances were mixed and heated together to 60 °C. A phase separation was observed between both substances which was not surprising as triglycerides are hydrophobic per definition and PEGs are more

hydrophilic substances. A staining of PEG with methylene blue and of H12 with sudan red helped to visualize the phase separation (Figure 49).

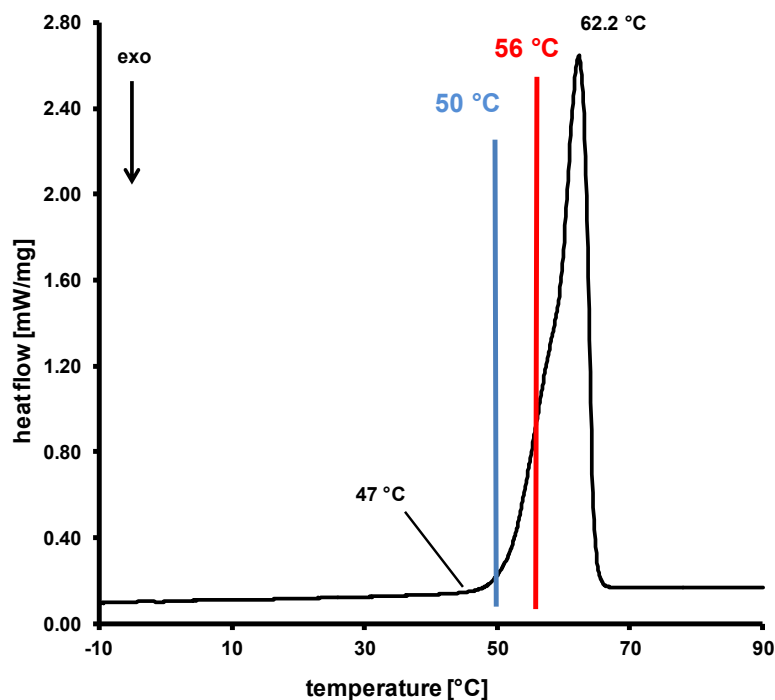


Figure 48: DSC thermogram of PEG 6000. Onset of melting: 47 °C; maximum of endothermic melting peak: 62.2 °C. Extrusion temperatures for D114 (56 °C - red) and D112 (50 °C - blue) comprising extrudates.

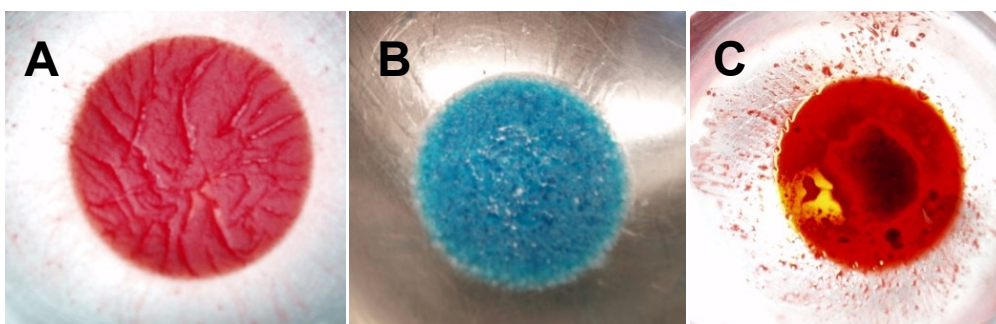
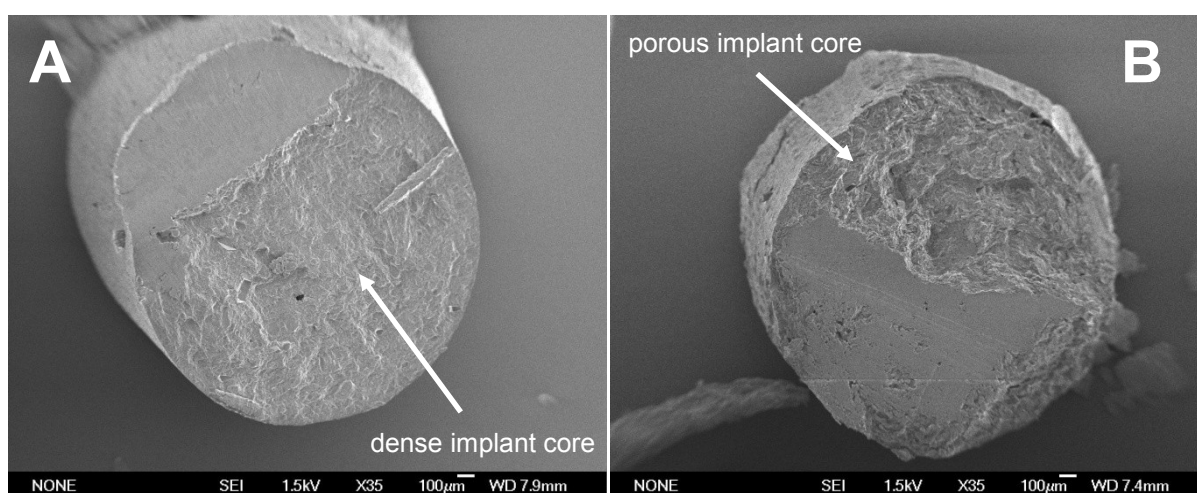


Figure 49: Simultaneous melting of lipid (H12 – stained with sudan red (A)) and PEG 6000 (stained with methylene blue (B)) results in phase separation between both phases (C).

It is very likely that the matrix structure of implants containing D114 and D112 differ strongly from the other extrudates as a melting of PEG and thus a phase separation step is involved

in the production. This phase separation would explain why lysozyme release from D114 containing implants is complete within two days and implants comprising D112 show accelerated release rates compared to the other tsc-extrudates. As the preparation temperature for D112 comprising implants was lower than for D114 comprising implants, PEG melting is expected to be less pronounced and thus the phase separation less developed. SEM measurement of D114 implants before release indicate that the matrix of these implants differs in core structure to e.g. H12 implants (Figure 50).



**Figure 50: SEM micrographs of cross sections of tsc-extrudates. (A) D118-H12 extrudate + 20% PEG + 2.5% lysozyme; (B): D118-D114 extrudate + 20% PEG + 2.5% lysozyme**



#### **4. Summary and outlook**

Lysozyme release studies from tsc-extrudates showed that tsc-extrudates were quite robust with respect to lysozyme release kinetics. Changes in the size of the pore-forming agent, increasing viscosities of the dissolving porogen or rapid dissolution of the porogen did not significantly affect release properties. However, high amounts of pore-forming agents were used in all experiments to ensure total protein release, which resulted in highly porous implant matrixes during the release studies and in consequence enhanced up release kinetics..

A change in the type of high melting lipid did not affect the release kinetics, which was not surprising due to the fact that the high melting lipid was not directly molten or affected during neither production nor release.

On the contrary, a change in the type of low melting lipid from H12 to D112 or D114 resulted in faster protein release. This was explained by the manufacturing process of these implants from lipid-PEG mixtures during which a phase separation process happens between molten PEG and molten low melting lipid. Tsc-extrudates with the low-melting lipids H12 and E85 exhibited identical and sustained lysozyme release rates.

Melting (or partial melting) of the implants during manufacturing and release turned out to be of major importance to completely understand the system. Melting was shown to lead to subtle changes in implant structure after manufacturing (chapter 0) and resulted in phase separation between PEG and the low-melting lipids D112 or D114. Additionally, DSC measurements showed that implant melting can be expected during release tests at 37 °C. Therefore we decided to further investigate the influence of partial implant melting on protein release kinetics as described in chapter 0.



## **VI. Mechanistic studies on the release of lysozyme from twin-screw extruded lipid implants (II) – influence of implant melting**

### **1. Introduction**

During the production of tsc-extrudates, the (partial) melting process of the low-melting lipid was found to be of major importance for the explanation of the long-term release of proteins from these implants. Melting (and tsc-extrusion) was found (I) to allow extrusion at gentle temperatures, (II) to increase implant density and to seal tiny pores, (III) to fuse the different triglyceride powder components and (IV) to lead to a very homogeneous distribution of the protein within the implants. DSC measurements of tsc-extrudates revealed that a phase of molten triglyceride must also be present during *in-vitro* release tests and might affect protein release rates. Therefore we conducted lysozyme release studies from different tsc-extrudates at various temperature. Additionally, we changed the amount of pore-forming agent in order to identify a 'percolation threshold' for the newly developed triglyceride based implant system and to study the mechanism of protein release.



## 2. Materials and methods

### 2.1. Materials

The monoacid lipid triglyceride glycerol-tristearin (Dynasan 118, micronized) as well as the mixed-acid lipid triglycerides H12 and E85 were kindly provided by Sasol GmbH (Witten, Germany). Mixed-acid lipid triglycerides Gelucire 33/01, Gelucire 39/01 and Gelucire 43/01 were a gift from Gattefossé (Saint Priest, France). The composition of the triglycerides is summarized in Table 11. Polyethylene glycol 4000 PF (PEG 4000) and 6000 P (PEG 6000) were donated from Clariant (Gendorf, Germany). Chicken egg white lysozyme (L 6876) was purchase from Sigma-Aldrich as lyophilized powder. All salts used were of analytical grade and purchased from Merck (Darmstadt, Germany).

**Table 11: Composition of lipid triglycerides**

Triglyceride type	D118	H12	E85	Gelucire 33/01	Gelucire 39/01	Gelucire 43/01
C8 fatty acid, %		-	-	9	2	2
C10 fatty acid, %		-	-	7	3	2
C12 fatty acid, %		71	27	48	43	33
C14 fatty acid, %		27	71	17	14	11
C16 fatty acid, %		2	2	8	10	15
C18 fatty acid, %	100	-	-	9	27	37

### 2.2. Preparation of lipid twin-screw extrudates (tsc-extrudates)

Lipid twin-screw extrudates were prepared as described by Schulze *et al.* [32] with a Haake MiniLab<sup>®</sup> Micro Rheology Compounder (Thermo Haake GmbH, Karlsruhe, Germany). In brief, a lipid powder blend comprising D118 as high melting lipid and H12, E85, Gelucire 33/01, Gelucire 39/01 or Gelucire 43/01 as low melting lipid was mixed with varying amounts of PEG (0-40%) and 2.5% of lysozyme as model protein. Extrusion temperature was set slightly above the melting maximum of the low melting lipid (Table 12) and extrusion of rod-

shaped implants was performed through a 1.9 mm outlet die in steady-state mode with closed bypass. The compositions of the lipid tsc-extrudates are summarized in Table 13.

**Table 12: Melting temperatures of triglyceride bulk materials**

Triglyceride type	onset of melting as determined by DSC, °C	melting maximum as determined by DSC, °C
H12	29 °C	39 °C
E85	20 °C	41 °C
Gelucire 33/01	8 °C	27 °C
Gelucire 39/01	15 °C	39 °C
Gelucire 43/01	21 °C	43 °C

**Table 13: Composition of lipid tsc-extrudates**

No.	low melting lipid	high melting lipid	pore forming agent	model protein
1	H12 – 22.5%	D118 – 52.5%	PEG 6000 – 22.5%	
2	E85 – 22.5%	D118 – 52.5%	PEG 6000 – 22.5%	
3	Gelucire 33/01 – 22.5%	D118 – 52.5%	PEG 6000 – 22.5%	
4	Gelucire 39/01 – 22.5%	D118 – 52.5%	PEG 6000 – 22.5%	
5	Gelucire 43/01 – 22.5%	D118 – 52.5%	PEG 6000 – 22.5%	
6	H12 – 29.25%	D118 – 68.25%	PEG 4000 – 0%	lysozyme 2.5%
7	H12 – 27.75%	D118 - 64.75%	PEG 4000 – 5%	
8	H12 – 26.25%	D118 – 61.25%	PEG 4000 – 10%	
9	H12 – 24.75%	D118 – 57.75%	PEG 4000 – 15%	
10	H12 – 23.25%	D118 – 54.25%	PEG 4000 – 20%	
11	H12 – 17.25%	D118 – 40.25%	PEG 4000 – 40%	

### **2.3. Differential scanning calorimetry (DSC)**

Twin-screw extrudates were ground in an agate mortar and approximately 10 mg were analyzed in sealed Al-crucibles. Measurements were performed with DSC 204 Phoenix (Netzsch, Selb, Germany) with heating and cooling rates of 10 K/min in a temperature range from 5 °C to 90 °C.

### **2.4. Wide-angle X-ray scattering (WAXS)**

Wide-angle X-ray scattering (WAXS) was performed by an X-ray Diffraktometer XRD 3000 TT (Seifert, Ahrensberg, Germany), equipped with a copper anode (40 kV, 30 mA wavelength 0.154178 nm). Experiments were conducted at 0.05° (2 theta) within a 5° - 40° range.

### **2.5. *In-vitro* release tests**

Lipid implants were cut into pieces of approximately 2.5 cm length, placed into 2.0 mL safe lock reaction tubes (Eppendorf AG, Hamburg, Germany) and incubated in 1.9 mL 0.01 M isotonic phosphate buffered saline (PBS) pH 7.4 containing 0.05% NaN<sub>3</sub> as preservative. Release tests at various temperatures were performed with implants consisting of D118, H12, PEG 6000 (22.5%) and lysozyme (2.5%) (Table 13). The tubes were placed in water baths at 20 °C, 25 °C, 33 °C, 35 °C, 37 °C and 40 °C (Julabo SW-20C, Julabo Labortechnik GmbH, Bad Seelbach, Germany) and temperature controls showed, that the temperature was constant within a range of +/- 0.3 K during the experiment. All other release experiments were performed in water baths at 37 °C. Samples were drawn by complete exchange of the incubation medium and centrifuged with a Sigma 4K15 centrifuge (Sigma, Osterode am Harz, Germany). The supernatant was assessed UV-photometrically at 280 nm with a FluoStar Omega plate reader (BMG Labtech GmbH, Offenburg, Germany).

## **2.6. Protein extraction from lipid implants**

Implants were ground in an agate mortar, incubated with PBS pH 7.4 and heated to 60 °C for 5 min in a Thermomixer Comfort (Eppendorf, Germany) at 40 rpm. Afterwards, the samples were cooled down, centrifuged and the protein concentration in the aqueous phase was determined by UV measurements at 280 nm with a FluoStar Omega plate reader (BMG Labtech GmbH, Offenburg, Germany). Protein extraction from freshly prepared implants showed a recovery of  $98.2\% \pm 1.3\%$  ( $n = 6$ ).

## **2.7. Assessment of implant weight and weight loss**

After the protein release studies tsc-extrudates were dried to constant weight in a vacuum dryer (Mettler, Schwabach, Germany) at 20 °C and 50 mbar and weighed on an analytical balance ( $d = 0.1$  mg, Sartorius BP 61S, Sartorius, Göttingen, Germany). Implant weight loss (WL) was calculated from the implant mass before ( $m_{\text{before}}$ ) and after incubation ( $m_{\text{after}}$ ). Theoretical implant weight loss (theoWL) was calculated from theoretical amounts of water soluble components per implant (PEG 4000 and lysozyme).

## **2.8. Scanning electron microscopy (SEM)**

After *in-vitro* release implants scanning electron microscopy was performed with a 6500F (Jeol GmbH, Eching, Germany) without further processing or a coating step.

### **3. Results**

#### **3.1. Preparation of lipid twin-screw extrudates.**

Preparation of lipid tsc-extrudates was possible for all formulations. To allow preparation of smooth lipid extrudates the extrusion temperatures were set slightly above the melting temperature of the low melting lipid, which resulted in a softening of the lipid mass within the twin-screw extruder. If the extrusion temperature was set too high, no material flow could be established, because no torque was built up in the extruder barrel.

#### **3.2. Lysozyme release at various temperatures**

During *in-vitro* release tests with tsc-extrudates consisting of H12, D118, PEG 6000 (22.5%) and lysozyme (Table 13 – formulation 1) at various temperatures all implants stayed solid and kept their shape. A major impact of temperature on lysozyme release was detected (Figure 51). With increasing incubation temperature lysozyme was released faster from the tsc-extrudates. Complete lysozyme release was achieved for incubation temperatures between 33 °C and 40 °C within 20 days and the release kinetics resembled each other. However, at 20 °C or 25 °C the release rates were much lower and release lasted for up to 200 days (data not shown), finally liberating only 80% of the incorporated protein. The borderline between fast (33 °C – 40 °C) and sustained (20 °C – 25 °C) lysozyme release was found at 29 °C where the lysozyme release rate was significantly higher than at 20/25 °C however lower than at 33/40 °C. Additionally, the protein was not completely released at 29 °C but approximately 15% remained trapped in the matrix. From all samples the remaining lysozyme mass was quantified after extraction from the matrix and the missing protein (15-20%) could be recovered.

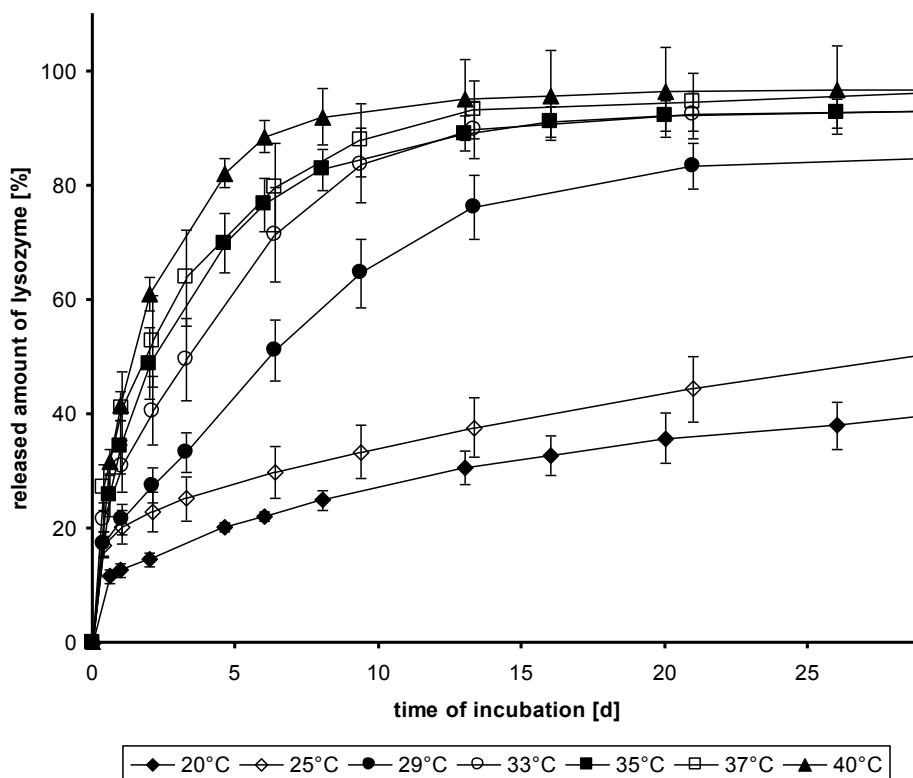


Figure 51: Lysozyme release from lipid tsc-extrudates at various temperatures. Extrudates consisted of 52.5% D118, 22.5% H12, 22.5% PEG 6000 and 2.5% lysozyme (Table 13 – formulation 1).

### 3.3. Lysozyme release from lipid implants comprising various low melting lipids

Implants prepared according to Table 13 (formulation 1-5) did not show any difference in protein release at 37 °C. All implants released 100% of the incorporated lysozyme mass within 16 days (Figure 52). However, when the release tests were performed at 20 °C significant differences between the formulations were found. Extrudates comprising D118 and Gelucire 33/01 or Gelucire 39/01 released the protein much faster than D118/H12 containing implants (Figure 53).

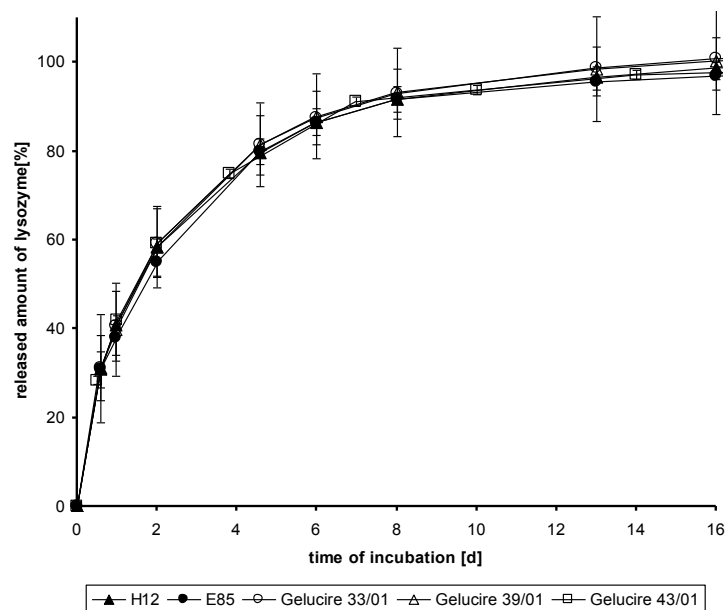


Figure 52: Lysozyme release from lipid extrudates comprising D118, PEG 6000 (22.5%) and different low melting lipids at 37 °C.

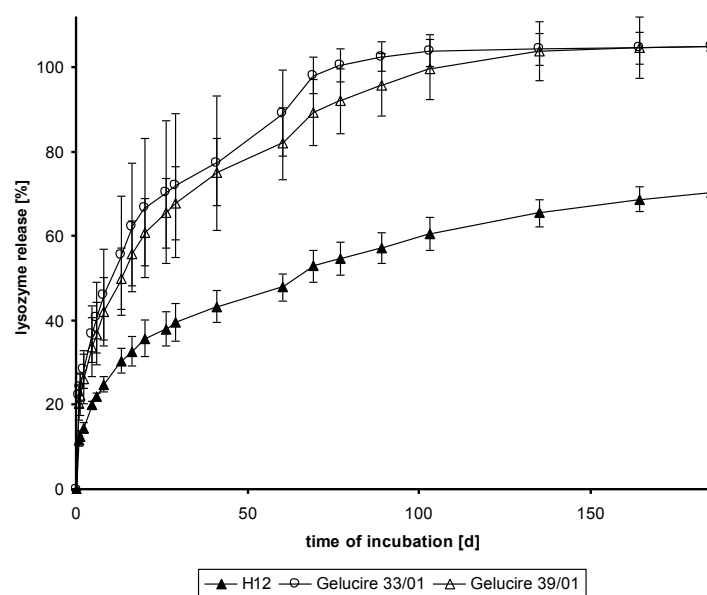
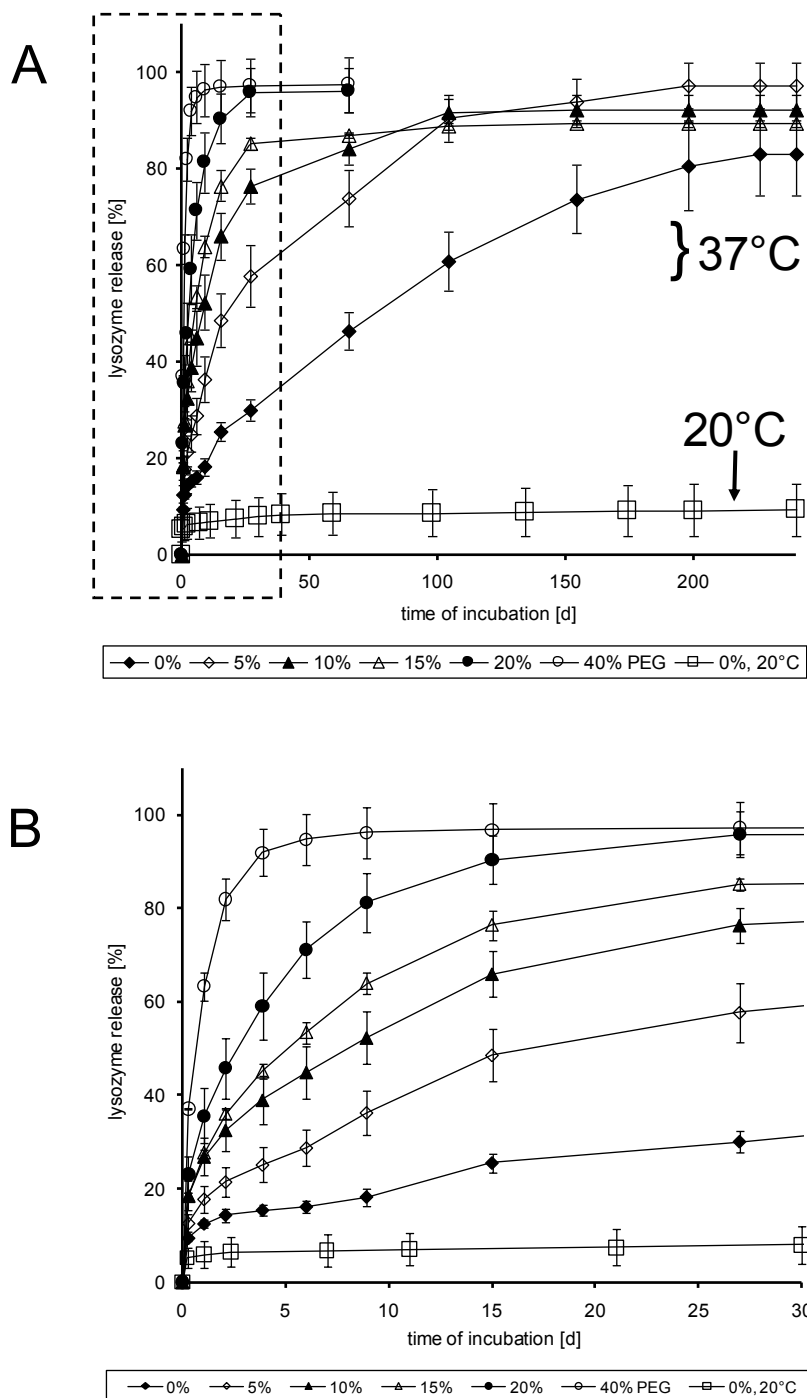


Figure 53: Lysozyme release from lipid extrudates comprising D118, PEG 6000 (22.5%) and different low melting lipids at 20 °C.

### 3.4. Lysozyme release with various amounts of pore forming agent

With increasing amounts of pore forming agent (PEG 4000) lysozyme was released faster from the implants at 37 °C (Figure 54). For samples comprising more than 15% of pore forming agent complete lysozyme release was achieved within 25 days of incubation.

Interestingly samples comprising only 5-15% PEG also released more than 90% of the embedded protein and even the samples which consisted of triglyceride, no PEG and 2.5% lysozyme, released 83% of lysozyme within 240 days. A reduction of the incubation temperature to 20 °C resulted in incomplete drug release from samples comprising no PEG 4000 and about 90% of the protein remained trapped in the triglyceride matrix.



**Figure 54: Lysozyme release from lipid extrudates comprising D118, H12 and various amounts of PEG 4000 at 20 °C (□) and 37 °C. (B) is a close-up of (A) depicting the first 30 days of release.**

### 3.5. Scanning electron microscopy of tsc-extrudates after *in-vitro* release

Scanning electron microscopy (SEM) images of H12-tsc-extrudates with 0%, 5% or 10% PEG showed a dense implant core after 240 days of incubation (Figure 55 – E, F, G). However, the sample surfaces were rough and broken (Figure 55 – A, B, C). Samples comprising 20% PEG showed a porous implant core (Figure 55 – H) and well defined pores embedded into a smooth implant surface after only 60 days of incubation and a ‘mantel zone’ surrounded the implant core. This mantel tended to break from the implant during *in-vitro* release and could easily be scrapped off the implant after incubation.

### 3.6. Result of DSC measurements

DSC measurements of tsc-extrudates directly after preparation did not indicate unstable modifications which could be attributed to the preparation process (Figure 56). All samples showed melting endotherms at 70 °C and 60 °C which derived from D118 and PEG 6000 melting respectively. Melting temperatures of high and low melting lipids showed a slight depression after extrusion compared to bulk materials (e.g. D118: 74 °C – 70 °C; H12: 39 °C – 35 °C). This can be explained by the formation of an ‘eutectic system’ or a ‘monotectic partial solid solution’ during the manufacturing process at which the low melting lipid was molten and re-crystallized in the presence of the high melting lipid [230].

The mantel layer of long-term incubated implants (240 days) showed a depletion of H12 and only minimal amounts of the low melting lipid could be detected whereas the peak for the D118 melting endotherm was very prominent (Figure 56).

After *in-vitro* release a distinct influence of the incubation temperature on the melting behavior of H12 in tsc-extrudates could be detected. At temperatures of 33 °C, 35 °C and 37 °C different ratios of H12 within the implants were molten during the release tests which resulted in altered DSC thermograms of tsc-extrudates after the release-test (Figure 57).

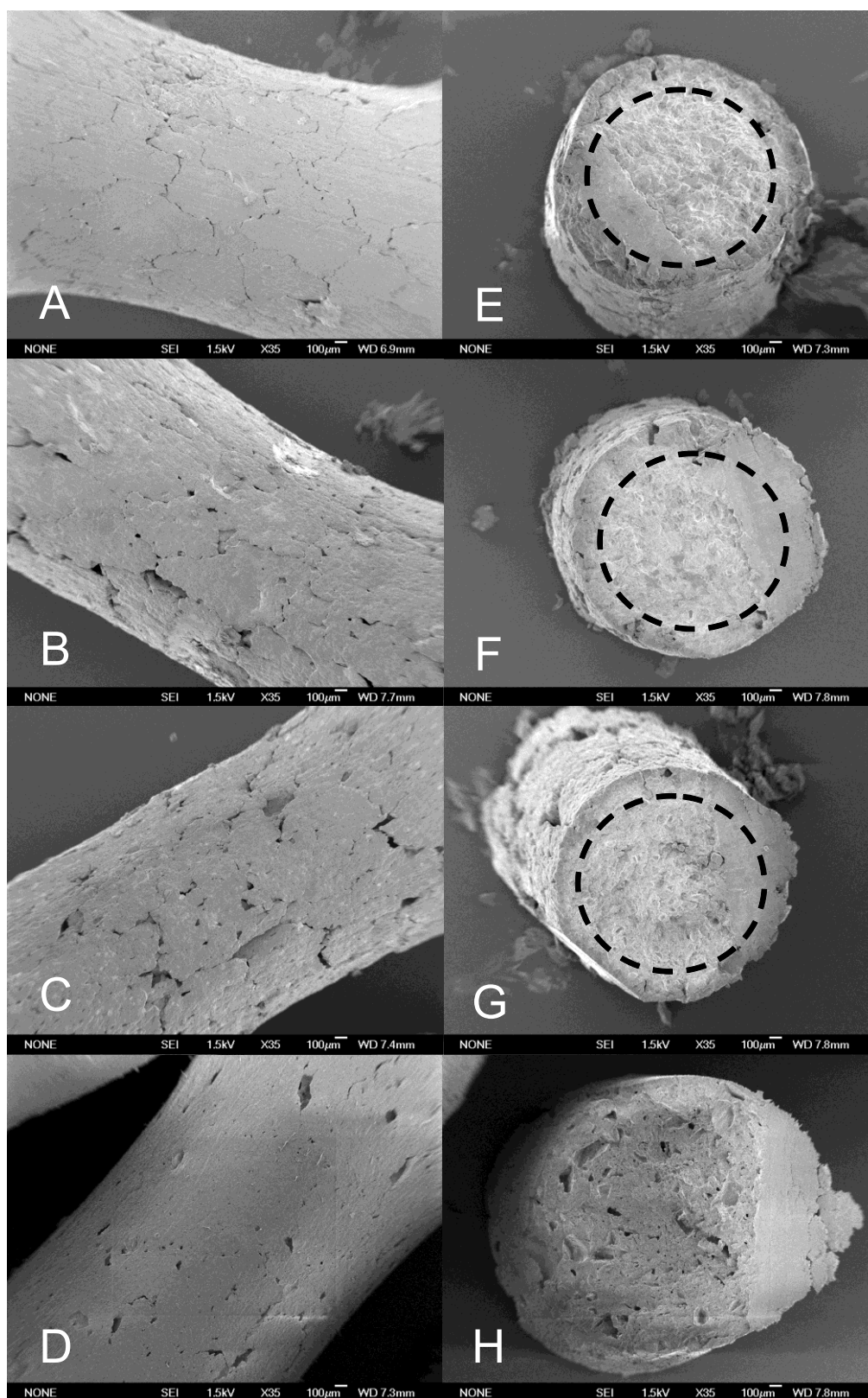


**Figure 55: SEM micrographs of surfaces and cross-sections of lipid extrudates after incubation. Samples A+E: 0% PEG – 250 days of incubation, B+F: 5% PEG – 250 days of incubation; C+G: 10% PEG – 250 days of incubation, D+H: 20% PEG – 60 days of incubation. Dotted line (E-G): borderline between fragile mantel layer and dense implant core.**

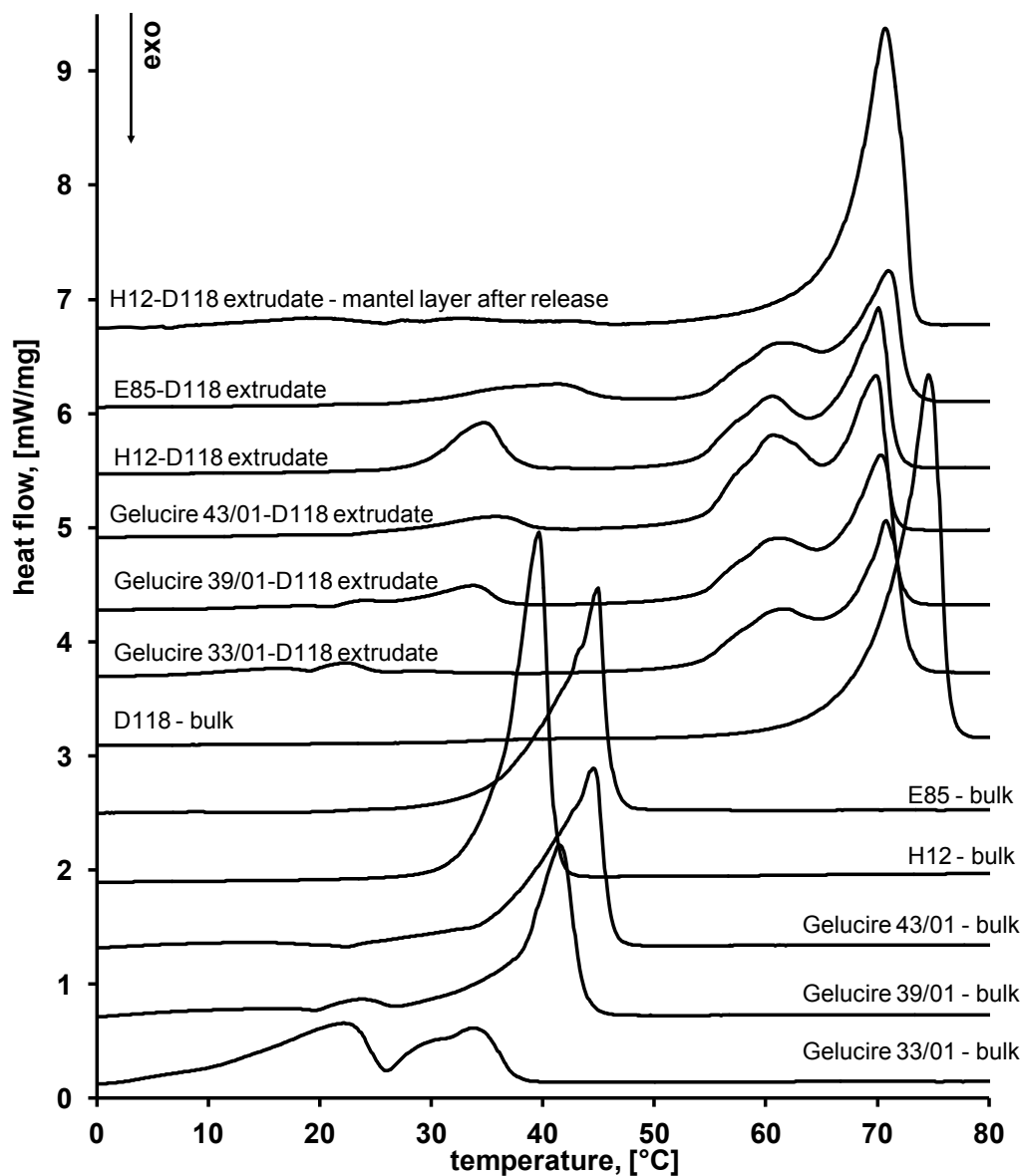


Figure 56: DSC thermograms from bottom to top: bulk materials (Gelucire 33/01, Gelucire 39/01, Gelucire 43/01, H12, E85 and D118); extrudates before incubation consisted of D118, PEG 6000 and different low-melting lipids (Gelucire 33/01, Gelucire 39/01, Gelucire 43/01, H12 and E85); mantel layer of extrudates (D118/H12) after 240 days of incubation.

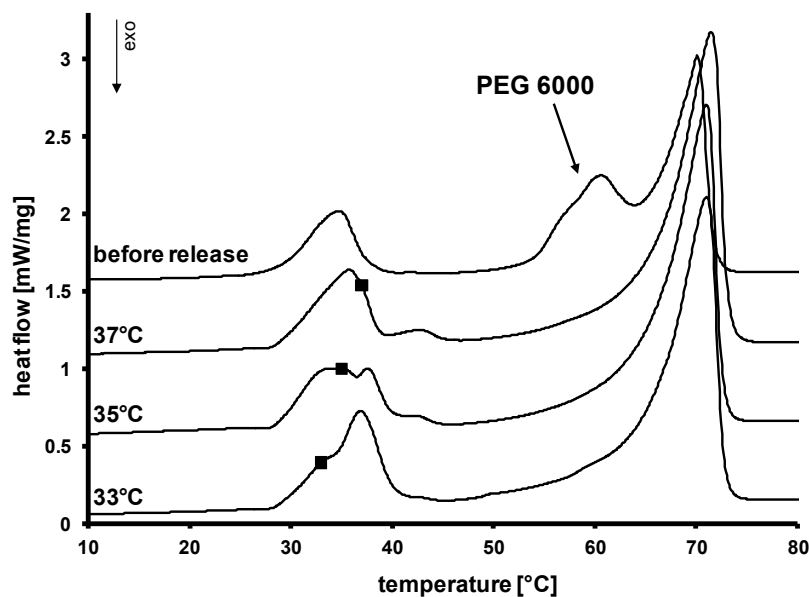


Figure 57: DSC thermograms of D118/H12/PEG 6000 extrudates from top to bottom: before release (60 °C - PEG melting, disappears upon incubation), after incubation/release at 37 °C, 35 °C and 33 °C. Squares (■) indicate the incubation temperatures during the release tests.

### 3.7. Results of X-ray measurements

X-ray measurements after preparation of tsc-extrudates indicated the presence of  $\beta$ - and  $\beta'$ -modifications of the lipids (Figure 58). Reflections occurred at  $2\theta=19.45^\circ$   $d=0.46$  nm,  $2\theta=23.30^\circ$   $d=0.39$  nm,  $2\theta=24.35^\circ$   $d=0.37$  nm and reflections of lower intensities occurred at  $2\theta=21.0^\circ$   $d=0.42$  nm and  $2\theta=22.40^\circ$   $d=0.41$  nm. The strong diffraction lines at 0.46 nm, 0.39 nm and 0.37 nm indicated  $\beta$ -modification of the lipid extrudates whereas the weaker diffractions lines at 0.42 nm and 0.41 nm derived from minor amounts of  $\beta'$ -modifications [221, 230]. Pure D118 and pure H12 exhibited  $\beta$ - and  $\beta'$ -modifications respectively [32].

After *in-vitro* release, a more distinct reflection pattern was observed from all samples (Figure 59). The diffraction lines were sharper and narrower; however, the position of the diffraction lines did not alter. In addition, the  $\beta'$ -spacing at 0.41 nm was found to be more prominent in these samples than before the *in-vitro* release test. These findings indicate an increase in crystallinity of the remaining implant rods after the release test.

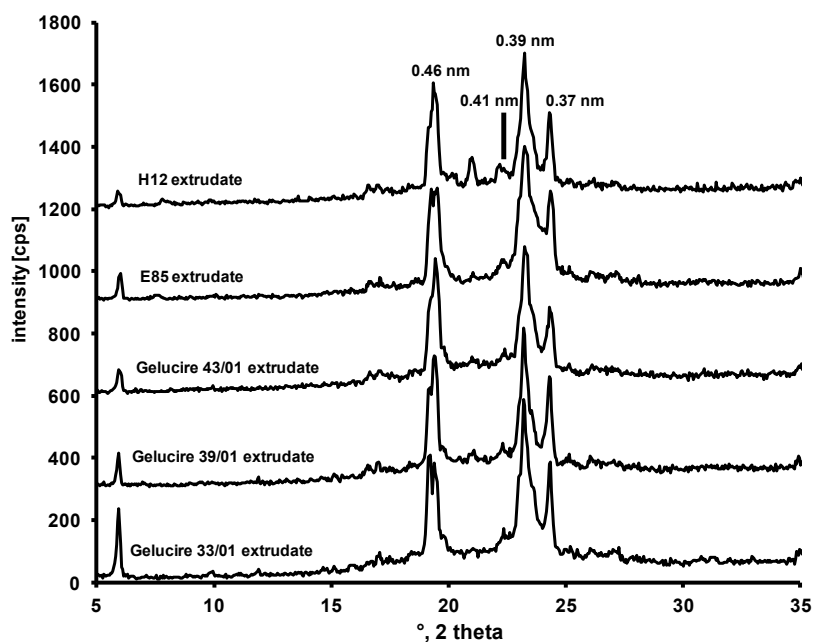


Figure 58: Diffraction pattern of tsc-extrudates directly after preparation. From top to bottom: extrudates comprising D118/H12, D118/E85, D118/Gelucire 43/01, D118/Gelucire 39/01 and D118/Gelucire 33/01.

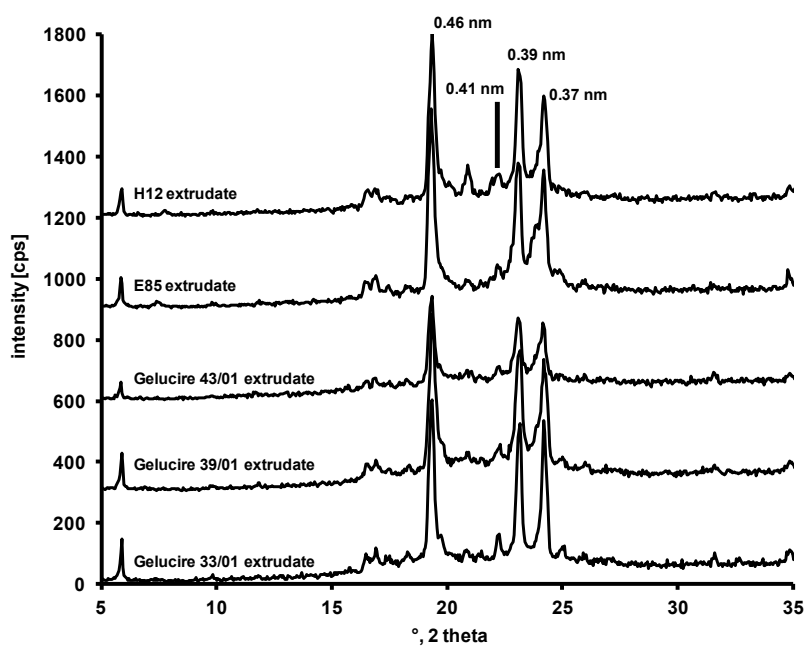


Figure 59: X-ray diffraction measurements of tsc-extrudates after *in-vitro* release. From top to bottom: extrudates comprising D118/H12, D118/E85, D118/Gelucire 43/01, D118/Gelucire 39/01 and D118/Gelucire 33/01.

### 3.8. Assessment of implant weight

Implant weight loss (WL) after incubation was compared with a theoretical weight loss (theoWL) as calculated from the total water soluble load. Weight losses in long-term incubated samples (240 days, 37 °C – grey bars. 0-15% PEG) were higher than the theoWLs. Incubation at 20 °C did not result in a mass loss of the tsc-extrudates (Figure 60).

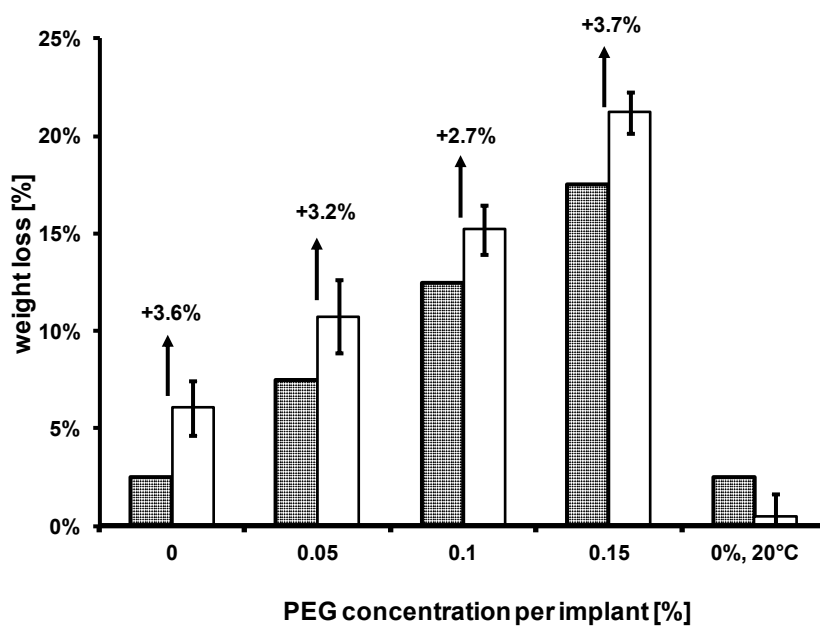


Figure 60: Checked bars: theoretical weight loss (theoWL); grey bars: weight loss (WL) after 240 days of incubation at 37 °C (0-15% PEG) and 20 °C (0% PEG); white bar: weight loss after 240 days of incubation (0% PEG) at 20 °C.

## 4. Discussion

### 4.1. Lysozyme release at various temperatures

Partial melting of the implant matrix during *in-vitro* release was expected at 37 °C and was confirmed by DSC measurements (Figure 56 + Figure 57) This partial implant melting was a consequence of the application of a 'low-melting' lipid during the preparation process (Table 12).

Lysozyme release tests from H12/D118 implants (Table 13: formulation 1-5) showed accelerated protein release with increasing incubation temperature. This was – in general – not surprising as faster dissolution times and higher diffusion coefficients of both PEG 6000 and lysozyme correlate with increasing temperatures. A closer look at the data, however, showed a highly accelerated release, when the temperature was increased from 25 °C to 29 °C. At temperatures at and above 29 °C nearly complete lysozyme release from the implants could be established whereas 20% of the protein mass remained trapped within the implant at 20 °C and 25 °C after 240 days of incubation (data not shown). At 29 °C an intermediate or borderline release profile was detected between slow/incomplete releasing implants at 20/25 °C and fast/complete releasing implants at 33/40 °C. Interestingly, 29 °C was determined to be the onset of melting of H12 within tsc-extrudates (Figure 56). Thus, at 20/25 °C and without melting of the low melting lipid 15-20% of lysozyme were trapped within the lipid matrix and could not be released into the buffer medium. At 29 °C, the matrix started to soften leading to accelerated release profiles and a higher amount of totally released protein. At 33/40 °C increasing fractions of the low-melting lipid were molten which allowed complete drug release (Figure 57). The release was found to be very robust towards changes in incubation temperature if the temperature was set at or above the melting range of the low melting lipid. However, the high amount of water-soluble excipient (22.5% PEG 6000) led to the rapid formation of highly porous implants and allowed fast protein release from the matrix. Thus only a minimal influence of partial implant melting on the release kinetics was detected if the incubation temperature was set at or above the melting endotherm of the low-melting lipid.

## **4.2. Lysozyme release from implants comprising various low melting lipids**

Release tests with implants comprising different low melting lipids (Gelucire 33/01, Gelucire 39/01, Gelucire 43/01, E85, H12 - Table 13) were performed at 20 °C and at 37 °C, to further investigate the influence of melting on the release kinetics. The lipids show different onsets of melting as bulk materials and within the tsc-extruded implants. It turned out that all implants released the model protein with similar release kinetics at 37 °C (Figure 54) which was well above the onset of melting for all implants. Complete drug release was achieved for all formulations which can be explained by a sufficient amount of pore-forming agent (22.5%) as well as by the partial melting of the implants. The system was very robust towards an exchange of the low-melting lipid at an incubation temperature of 37 °C.

On the contrary, at 20 °C the physical state of implants differed from each other. Onsets for melting as measured by DSC started below the incubation temperature (20 °C) for extrudates comprising Gelucire 33/01 and Gelucire 39/01 but not for D118/H12 extrudates (distinct onset: 29 °C, Figure 56). *In-vitro* release tests showed that lysozyme release from tsc-extrudates containing H12 was more sustained (> 200 days) and incomplete (78%) compared to implants containing Gelucire 33/01 or Gelucire 39/01 (Figure 55). These findings correlated well with the results from the temperature dependent release study and showed again, that melting enabled faster and more importantly total drug release.

## **4.3. Lysozyme release from implants comprising various amounts of pore forming agent**

During the first experiments lysozyme release was influenced by the high porosity of the matrix and the protein was probably released through an interconnected pore-network. Various authors have described a minimum amount of water soluble compounds also known as 'percolation threshold' [26, 222, 231] or 'critical porosity value' [219] to be necessary for complete drug release from insoluble hydrophobic matrices. This percolation threshold depends on the size, shape, loading and physical properties of the implant or dosing form.

Percolation thresholds ranging between 5% and 40% have been described in literature for various applications. Herrmann *et al.* [29] found a minimum of 20% of hydrophilic components necessary to allow total release of recombinant human interferon  $\alpha 2a$  release from compressed tristearin based implants. Bonny and Leuenberger identified porosities of 30% as sufficient for total drug release according to the percolation theory from tablets comprising hydrogenated castor oil [219]. Könning *et al.* found that total lysozyme release from compressed implant was possible for lysozyme loads of only 5%, however, the implants were only 2 mm in diameter and 2.2 mm in height [26].

In order to determine a percolation threshold for tsc-extrudates (diameter: 2 mm length: 2.5 cm) the amount of the pore former (PEG 4000 PF) was varied between 0% and 40% (w/w).

Lysozyme release tests at 37 °C showed that increasing amounts of PEG 4000 PF led to accelerated protein release which can be explained by a more rapid formation of an interconnected pore-network throughout the implant (Figure 54).

Interestingly, lysozyme was also almost completely released from implants comprising no or only low amounts of PEG (10%, 5% or 0%). Lipid implants released a total 90% of the incorporated protein mass if only 2.5% of the implant matrix consisted of hydrophilic components (lysozyme + 0% PEG). Total release was achieved by the addition of only 5% PEG to give a total of 7.5% hydrophilic components.

All implants showed burst release within the first 12 hours of incubation liberating 5-10% of the incorporated protein mass which was probably in close proximity to the implant surface. After burst release implants comprising high amounts of PEG (40%-15%) showed "normal", diffusion controlled release profiles until all lysozyme was released.

On the contrary, diffusion controlled release was observed from implants with less pore former only during the first days of incubation. Afterwards, a linear release phase appeared which lasted for several weeks (Figure 54). Implants comprising no PEG showed a burst release of 10% followed by a quasi-linear release phase up to day 150. When release tests were performed at 20 °C, identical implants (0% PEG) only showed a burst release of about

10% and directly leveled into a plateau phase without further release of lysozyme. Thus, at 20 °C and without partial implant melting, 90% of the protein remained trapped in the matrix. However, at 37 °C partial implant melting facilitates total drug release and led to a sustained release profile lasting for weeks. In 2009 Schulze *et al.* described a different method to achieve sustained release of rhIFN $\alpha$ 2a from tsc-extrudates. They used a protein precipitating agent and accomplished linear protein release for up to 60 days [32]. However, no such protein precipitating agent is necessary to achieve sustained protein release from tsc-extrudates at low-loadings. In addition, no pore-forming agent is necessary to facilitate nearly complete drug release. Thus the determination of a 'percolation threshold' is not possible as partial implant melting allows protein release from the matrix at 37 °C but not at 20 °C although the implant composition is identical. Moreover, lysozyme release from tsc-extrudates follows a novel release mechanism which is based on the melting of the low melting lipid during release and does not necessarily need a percolation threshold to allow complete protein release. By application of a pore-forming agent a biphasic release can be achieved after the initial burst release. In the beginning dissolution and diffusion of PEG and protein control the release kinetics and after liberation of the pore-forming agent a melting associated release takes over. At PEG concentrations above 10%, no melting associated linear release phase could be detected in the release profile any more.

The influence of melting on the lipid implant composition was also investigated by monitoring the weight loss of long-term incubated implants (240 days). A higher weight loss than expected from theoretical calculations was detected (assuming no chemical degradation of lipids *in-vitro*). Samples (0% PEG, 2.5% lysozyme) which were incubated at 20 °C for 240 days (Figure 60) even showed less weight loss than expected, which was explained by incomplete protein drug release. It is very likely, that 'non-molten' low-melting lipid sealed lysozyme particles from contact with release medium and thereby inhibited release of the protein from the dense implant matrix. Thus an erosion of the triglyceride matrix was only detected after *in-vitro* incubation in PBS buffer for 240 days at an incubation temperature of 37 °C. Interestingly, Schwab *et al.* showed that the lipid composition of tsc-extrudates

improved lipase induced degradability *in-vitro* compared to compressed implants of pure D118. They found that tsc-extrudates were well degradable by an lipase-assay [33] and ascribed it to the implant composition. Especially, the presence of the low-melting lipid rendered the implant better degradable due to (I) faster cleavage of fatty acids with shorter chain-length and (II) partial melting of the implant during incubation. From our data, we conclude, that partial melting of the implants might lead to better degradation of tsc-extrudates *in-vitro* and *in-vivo* and to allow protein release *in-vitro*.

SEM measurements of long term incubated samples also showed erosion processes and more fragile implant structures of long-term incubated samples at 37 °C compared to samples which were incubated for 60 days only (Figure 55) or at 20 °C (data not shown). The formation of a 'mantel layer' around the implants was observed (Figure 55- E, F, G) and this fragile zone easily broke off and consisted mainly of D118 as confirmed by DSC measurements (Figure 56). Interestingly, it took a rather long time until a change in the matrix composition occurred and the formation of the mantel layer could be detected. We conclude that the depletion of H12 from this mantel layer rendered this zone more fragile and led to an increase in porosity of the implants. Implant porosity and thus the ability of water to intrude into the matrix was determined to be one of the most important factors for the release of drug substance [26, 170, 232] No change between the ratios of D118 and H12 was detected in the implant 'core', which might explain the incomplete drug release (80%) from samples without PEG 4000. Samples which were incubated for 60 days only showed a porous implant structure which only derived from the dissolution and liberation of PEG and lysozyme (Figure 55 - H). However, after 240 days of incubation no such pores could be observed anymore in implants comprising 5% or 10% PEG (Figure 55 - F, G) which was explained by merging and rearrangement of lipid material due to melting.

#### **4.4. X-ray diffraction measurements**

X-ray diffraction measurements showed an increase in  $\beta$ - and  $\beta'$ -modification and higher crystallinity after *in-vitro* release. This can be explained by two complementary factors. First,

a tempering of the lipid during *in-vitro* release at 37 °C might have resulted in a reordering of the lipid chain structure thus an increase in the overall crystallinity of the implant. Similar effects were already described before to alter the drug release rates from lipid matrix systems [233-235]. Additionally, a loss of low-melting lipid as detected by DSC measurement from the mantle zone might have resulted in an increase of D118 concentration and thus a higher fraction of lipids with  $\beta$ -modification. Loss of H12 resulted in a more fragile and porous implant structure (Figure 55) which again resulted in accelerated protein release.

## 5. Conclusion

The influence of lipid melting on the *in-vitro* release of lysozyme from twin-screw extruded triglyceride based implants was examined. It was found that partial melting of the matrix facilitated total protein release from the implant and led to erosion of the lipid matrix *in-vitro*. Higher incubation temperatures resulted in accelerated lysozyme release. However, the release kinetic was quite robust if the incubation temperature was above the melting range of the low melting lipid. Additionally, the release kinetic was found to be independent of the type of low-melting lipid when partial melting occurred. As minor temperature variability is a common incidence *in-vivo*, these findings are important regarding the *in-vivo* applicability of tsc-extrudates.

The protein was released from the implant even without addition of a pore-forming agent, indicating a 'new' melting-induced release mechanism. Hereby, the triglyceride based implants softens - but does not instantaneously degrade – and allows long term protein release. If protein release was performed without partial implant melting, a 'non-release' of the protein (despite 5-10% burst release) was observed.

DSC measurements indicated a depletion of H12 from the triglyceride matrix during long term incubation, and X-ray measurements showed an increase in the crystallinity of the triglycerides. Both findings were ascribed to the partial melting and tempering of the implant during incubation. The melting of the low melting lipid facilitated a nearly complete and linear release of lysozyme over more than 150 days.

A mass loss of the matrix material after *in-vitro* long-term incubation was detected. This finding can be explained by depletion of molten H12 from the matrix which in consequence rendered the implant more fragile and prone to degradation and erosion.

We concluded that partial melting of the implant facilitated complete drug release, allowed a linear release profile and will induce a better degradability of this system. We suggest that by choice of a suitable implant composition long-term protein drug release from tsc-extrudates with subsequent biodegradation of the triglyceride matrix material is feasible *in-vivo*.



## VII. *In-vivo* biodegradability of lipid twin-screw extruded implants in rabbits

### 1. Introduction

A major obstacle in the development of a sustained release device is the choice of a suitable matrix material and an appropriate processing method. Usually, materials which are used for the manufacturing of implant matrices are processed at elevated temperatures (e.g. melt extrusion) and/or by the use of organic solvents [17, 236]. Both factors have a negative impact on protein stability during processing as they can lead to protein unfolding, denaturation and aggregation. Additionally, the matrix material should be biodegradable to avoid a surgical intervention for the removal of the implant after total/complete drug release. However, the commonly used biodegradable polymers poly-lactic acid (PLA) or poly-lactic-co-glycolic acid (PLGA) are often not applicable. During matrix degradation lactic and glycolic acid is produced which in consequence leads to an increase in osmotic pressure and a pH drop within the matrix which may result in protein acylation, deamidation or aggregation [69, 71, 237].

In order to overcome these limitations lipidic substances have been under investigation as implant matrix materials for protein drugs [18]. Lipids are natural substances and were shown to be biocompatible in various studies [31, 174, 177, 238]. For example, compressed tristearate implants (D118) were well biocompatible *in-vivo* over a period of 28 days in rabbits [31] and compressed tripalmitate implants (D116) over a period of 60 days in mice [23]. Additionally these substances (e.g. triglycerides, fatty acids) are inexpensive, easy to handle and have been shown to maintain the stability of proteins drugs during storage and release [18, 28, 32]. Different lipidic substances have been used for the preparation of sustained release dosage forms for protein drugs and multiple manufacturing methods have been proposed [18, 159, 177, 239, 240]. The preparation of solid implants is usually performed by compression of e.g. cholesterol [19, 23, 240], free fatty acids [19, 171] or triglycerides [25, 27, 31, 172] and is the most commonly used method. However, neither compressed triglyceride based implants nor cholesterol based implants showed any sign of erosion after

*in-vitro* and *in-vivo* release studies in species such as rabbit, mice, and sheep, which renders the systems unfavorable [23, 27, 31, 240]. Additionally, the use of free fatty acids and phospholipids has been shown to induce inflammatory reactions in mice and these are thus not first class substances [23] for the preparation of solid implants.

Recently, Schulze *et al.* described a new manufacturing technique for triglyceride-based protein loaded implants: tsc-extrusion (see I.3.1.8). This method features the advantage of a steady-state production process at moderate temperatures which secures the stability of the protein drug during manufacturing.

Schwab *et al.* compared the degradability of compressed and tsc-extruded lipid implants with an *in-vitro* lipase assay and found that tsc-extrudates were better degradable [33]. The matrices of compressed implants were not affected by incubation in lipase solutions, however a breakdown of the matrices of tsc-extrudates was observed. This was explained by (I) the composition of the lipid matrix as well as by (II) the structure of lipid tsc-extrudates resulting from the extrusion process. The mixture of high and low melting lipid and the production process seem to render the implants biodegradable. Thus *twin-screw extruded* lipid implants are a very promising option as parenteral depot formulation as biodegradability is of great importance for patient's compliance. Degradation products of triglycerides (glycerol and fatty acids) are natural substances thus no inflammatory reactions are expected at the site of implant erosion *in-vivo*.

However, to proof the degradability of lipid tsc-extrudates an *in-vivo* study is necessary, as *in-vivo* conditions can hardly be simulated *in-vitro*.

## **2. Materials and Methods**

### **2.1. Materials**

Lipids D118 (glycerol tristearin), H12 (triglyceride consisting of lauric, myristic and palmitic acid, melting point: 37 °C) and E85 (triglyceride consisting of lauric, myristic palmitic acid, melting point: 42 °C) were kindly donated by Sasol (Witten, Germany). PEG 6000 was a gift from Clariant, Wiesbaden, Germany.

### **2.2. Preparation of lipid implants**

Triglyceride based implants were prepared by twin-screw extrusion of mixtures of high melting lipid D118, a low melting lipid (H12 or E85) and a pore-forming agent (PEG 6000) according to Figure 61. Four formulations (A-D) were prepared which differed in the amount of pore forming agent (20%, 0% and 40% PEG 6000 – formulations A, B, C) and the type of low melting lipid (E85 instead of H12 – formulation D). Preparation of rod shaped implants was performed as described previously. Extrusion was performed using a Haake MiniLab<sup>®</sup> Micro Rheology Compounder with closed bypass channel and a rotation speed of 40 rpm (Thermo Haake GmbH, Karlsruhe, Germany). The resulting implants had a diameter of 1.9 mm and were cut to a length of 17 mm resulting in an implant mass of approximately 55 mg. Lipid implant rods were sterilized by gamma-irradiation (total dose: 30.5 kGy, Gamma Service Produktbestrahlung GmbH, Radeberg, Germany) before *in-vivo* application.

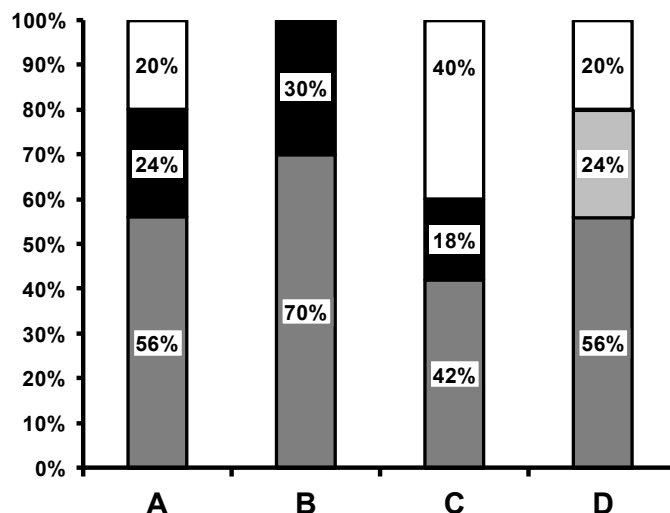


**Figure 61: Composition of triglyceride based tsc-extrudates. D118 = dark grey bars (formulation A-D), H12 = black bars (formulations A-C), E85 = light grey bar (formulation D) and PEG 6000 = white bars (formulation A, C, D).**

Prior to extrusion, the near fluorescent carbocyanine dye 1,1'-dioctadecyl-3,3,3',3'-tetramethylindotricarbocyanine iodide (DiR) (excitation: 750 nm; emission: 782 nm) (Invitrogen, Karlsruhe, Germany) was dissolved in methylen chloride (2 mg/mL), and dissolved in melts of H12 and E85 to obtain final concentrations of  $10^{-7}$  mol/mg. DSC measurements after recooling and tempering of the triglycerides for 1 day at 43 °C (H12) and 47 °C (E85) did not show the formation of unstable modifications or a melting point depression. X-ray measurements showed identical crystalline structure of H12 before and after mixing with DiR.

The fluorescent dye was used to allow location of the implants *in-vivo* and to follow the progress of biodegradation. DiR is a nontoxic lipophilic fluorescent dye with an excitation maximum of 750 nm and an emission maximum of 782 nm in the near infrared (NIR) region. Within this region, the auto-fluorescence of tissue is minimal and thus an accurate location of the implants should possible by use of the IVIS Lumina System and the Li-Cor gel scanner after explantation. DiR has been used in a variety of cell based *in-vitro* and as well *in-vivo* studies and was shown to be safe. For example, DiR was nontoxic and did not affect cell viability or cell functions in macrophages [241] and allowed the non-invasive *in-vivo* tracking

of e.g. inflammatory cells [241], low-density lipoprotein nanoparticles [242] and hematopoietic cells [243].

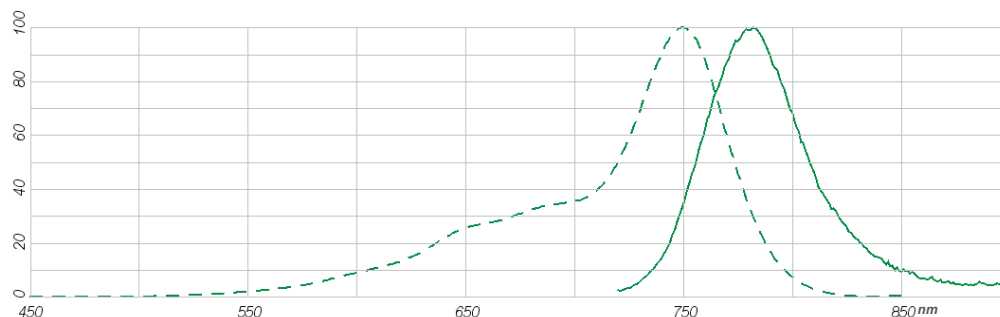


**Figure 62: Excitation and emission spectra of DiR.**

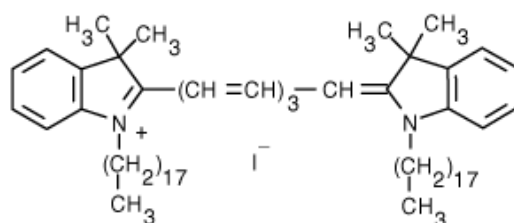


**Figure 63: Molecular structure of DiR (1,1'-dioctadecyl-3,3,3',3'-tetramethylindotricarbocyanine iodide, DiOC<sub>18</sub>(7))**

### 2.3. Preliminary testing

Detection of tsc-extrudates (marked with DiR) in tissue was tested in an *in-vitro* experiment prior to application in rabbits. Therefore tsc-extrudates were incubated in PBS buffer pH 7.4 at 37 °C for 4 weeks and subsequently placed underneath the hypodermis of a pig's ear (Figure 64). Additionally, fresh tsc-extrudates were also inserted into the pig's ear and the feasibility to detect these extrudates was tested with a Li-Cor Odyssey gel scanner (Bioscience GmbH, Bad Homburg) and the IVIS Lumina system (Caliper Life Science, Hopkinton, USA). A pig's ear was chosen for the experiment because it is denser and harder than rabbit tissue and thus forms a litmus test for our detection system.

## **2.4. Differential scanning calorimetry (DSC)**

Twin-screw extrudates were ground in an agate mortar and approximately 10 mg per sample was analyzed in sealed Al-crucibles. Measurements were performed with DSC 204 Phoenix (Netzsch, Selb, Germany) with heating and cooling rates of 10 K/min in a temperature range from 5 °C to 90 °C. The area under the curve (AUC) of melting endotherms was used to calculate the ratios of low melting and high melting triglycerides.

## **2.5. Scanning electron microscopy (SEM)**

Lipid implants were assessed with a scanning electron microscope 6500F (Jeol GmbH, Eching, Germany) without applying any coating procedure.

## **2.6. Selection of test animals**

Rabbits were selected as test animals because they show a lipidic hypodermis with fat tissue which is similar to the human one. For an *in-vivo* rhIFN $\alpha$  release study, Schwab *et al.* also used rabbits for the implantation of compressed lipid implants [31]. In addition to that, smaller animals like rats or mice do not develop a fat tissue and are quite muscular and active animals which would not allow our implants system to rest silent at the site of implantation. Therefore rabbits were chosen as test animals.

## **2.7. Animal treatment and *in-vivo* degradation study**

Rabbits were housed in pairs in standard cages, fed *ad libitum* with hay and commercial rabbit food. The tsc-extrudates were injected subcutaneously by a microchip applicator (Backhome BioTec®, Virbac, Bad Oldesloe, Germany) at t = 0 month, t = 3 months and t = 5 months. 6 months after the first application, animals were euthanized by intravenous administration of 0.4 mL xylazine (Xylazin, Serumwerk Bernburg, Germany) and 0.6 mL ketamine (Ursotamin, Serumwerk Bernburg, Germany), followed by 1.0 mL T61® (Intervet,

Unterschleissheim, Germany), thus resulting in incubation times of the implants of 1, 3 and 6 months (Table 14).

Control formulation A was implanted into each animal in order to increase statistical power ( $n = 9$ ) and to gain an internal standard throughout all animals. All other formulations were implanted in triplicate ( $n = 3$ ) for each point of time.

All experiments were approved by the responsible regulatory body (Regierung von Oberbayern, Aktenzeichen 55.2-1-54-2531-153-09).

**Table 14: Schedule for the implantation of tsc-extrudates into rabbits. Formulations A, B, C and D as described in Figure 61.**

animal no. / time	$t_0$	$t_{3 \text{ month}}$	$t_{5 \text{ month}}$	$t_{6 \text{ month}}$
1	A + B	A + B	A + B	end of study
2	A + B	A + B	A + B	end of study
3	A + B	A + B	A + B	end of study
4	A + C	A + C	A + C	end of study
5	A + C	A + C	A + C	end of study
6	A + C	A + C	A + C	end of study
7	A + D	A + D	A + D	end of study
8	A + D	A + D	A + D	end of study
9	A + D	A + D	A + D	end of study

## **2.8. Recovery of implants and assessment of implant weights after *in-vivo* study**

Six months after implantation the animals were sacrificed, tissue samples were excised and placed on an infrared scanner (Li-Cor Odyssey, Bioscience GmbH, Bad Homburg) and each sample was scanned at 700 nm and 800 nm. After removal of the implants from the samples, the remaining tissue was scanned again to ensure complete recovery of the tsc-extrudates.

The remaining implant material was washed three times with distilled water and vacuum dried to constant weight in a vacuum dryer (Mettler, Schwabach, Germany) at 25 °C and

11 mbar. Afterwards the implants were weighed on an analytical balance ( $d = 0.001\text{mg}$ ) and the recovery was calculated as a percentage of the initial implant mass.

### **2.9. *In-vitro* degradation study**

Freshly prepared implants were weighed, placed into 2.0 mL safe lock reaction tubes (Eppendorf AG, Hamburg, Germany) and incubated in 1.9 mL 0.01 M isotonic phosphate buffered saline (PBS) pH 7.4 containing 0.05%  $\text{NaN}_3$  as preservative. The samples (formulation A:  $n = 27$ ; formulations B, C and D:  $n = 9$ ) were placed in a water bath at  $39\text{ }^\circ\text{C}$  to mimic the body temperature in rabbits (Julabo SW-20C, Julabo Labortechnik GmbH, Bad Seelbach, Germany). After 1 day, 1 week and 2 weeks the buffer medium was completely exchanged to remove the dissolved PEG 6000 from the samples. After 1 month, 3 months and 6 months samples were drawn (formulation A:  $n = 9$ ; formulations B, C and D:  $n = 3$ ), treated as described for the *in-vivo* samples and the recovery was calculated as a percentage of the initial implant mass.

### 3. Results and discussion

#### 3.1. Preliminary studies

##### 3.1.1. Detection of fluorescent dyes within tissue

As DiR is a lipophilic dye it remained within the lipid tsc-extrudate over the period of *in-vitro* incubation (4 weeks, 37 °C). By use of the IVIS Lumina System and the gel scanner, the fresh implants as well as the incubated implants could be detected after insertion in the hypodermis of the pig's ear. In all cases the tsc-extrudate was clearly visible. However, the non-incubated implants showed stronger fluorescence than the incubated samples which means that the fluorescent dye was washed out to a small extent over time. Nevertheless, we were able to detect the implant by two different detection systems (Figure 65) within a real tissue.

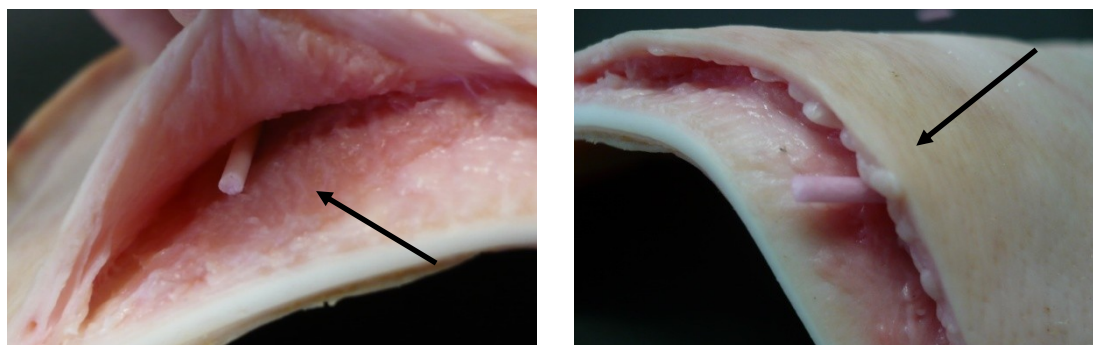
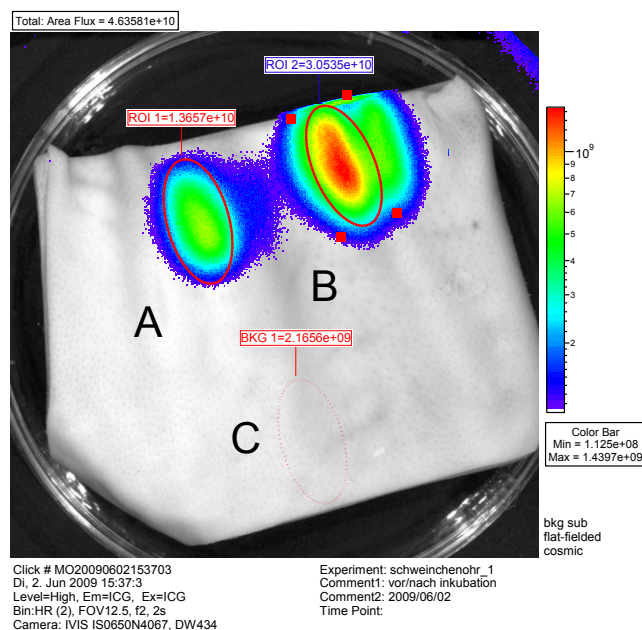
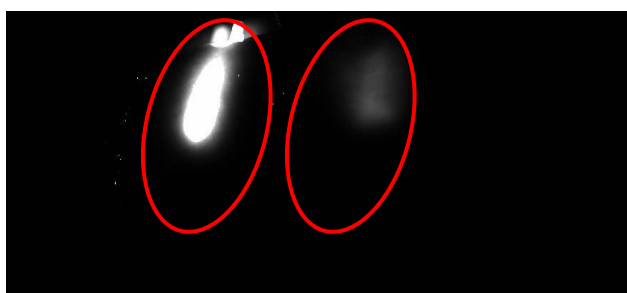


Figure 64: Fluorescently labeled tsc-extrudate are inserted under the hypodermis of a pig's ear.



**Figure 65:** Detection of fluorescently marked lipid implants inserted under the hypodermis of a pig's ear by the IVIS Lumina System. A: Implant after 4 weeks of incubation in PBS buffer at 37 °C; B: fresh implant; C: control area.



**Figure 66:** Image of tsc-extrudates which were inserted under the hypodermis of a pig's ear by Li-Cor gel scan (800 nm). Left side: freshly prepared implant. Right side: Implant after 4 weeks of incubation in PBS at 37 °C (still visible).

### 3.2. Animal treatment and recovery of implants

After euthanasia, rabbit hair was clipped on both sides of the abdomen, and implants were localized by digital palpation. Lipid implants were excised and adhering tissue was removed after localization of the implant fragments within the tissue with a Li-Cor gel scanner (Figure 68). Due to the fluorescent marker dye DiR the implants were easily located and completely excised from the surrounding tissue. The IVIS Lumina scanner, which was tested as a

backup system, was not used, because the remaining implant rods were easily detected after long-term incubation with the LiCor gel scanner and handling was easier with this system.

All implants were encapsulated by a fibrous capsule (Figure 67) which could be easily removed. Besides the fibrous capsule no further foreign body reactions were observed during the *in-vivo* study. Fibrous encapsulation is described in literature as the end-step healing process to biomaterials and was observed for various other materials including lipids, collagen and PLGA [23, 244-246].

During the *in-vivo* degradation study, one animal had to be euthanized after 4 months due to a fractured spinal column. However, the exitus was not related to the degradation study but happened by accident. Extrudates which were implanted in this animal for 1 month and 4 months (formulations A and B) were included into the 1 month and 3 months groups for analysis respectively.

### **3.1. *In-vitro* degradation study of lipid implants**

Weight assessment of implants of formulation A (n = 9) after the *in-vitro* degradation study showed remaining implant masses of 80% ( $\pm 2\%$ ), 79% ( $\pm 2\%$ ) and 77% ( $\pm 1\%$ ) after 1, 3 and 6 months respectively (Table 1). This was not surprising as 20% of the implant formulation consisted of water soluble PEG 6000 which was quickly released from the implant. Thus, we obtained recoveries of 100% ( $\pm 3\%$ ), 100% ( $\pm 3\%$ ) and 96% ( $\pm 2\%$ ) of triglyceride material after 1, 3 and 6 months respectively and only minimal matrix degradation was detected in a lipase free *in-vitro* model. Implants of formulations B, C and D (n = 3) showed mass losses which also derived from PEG 6000 dissolution (Table 1). However, after 6 months of incubation weight assessment of formulations A-C showed a minimal degradation (3%) of the triglyceride matrix material which was in contrast to implants of formulation D which remained constant throughout the experiment (Table 15).

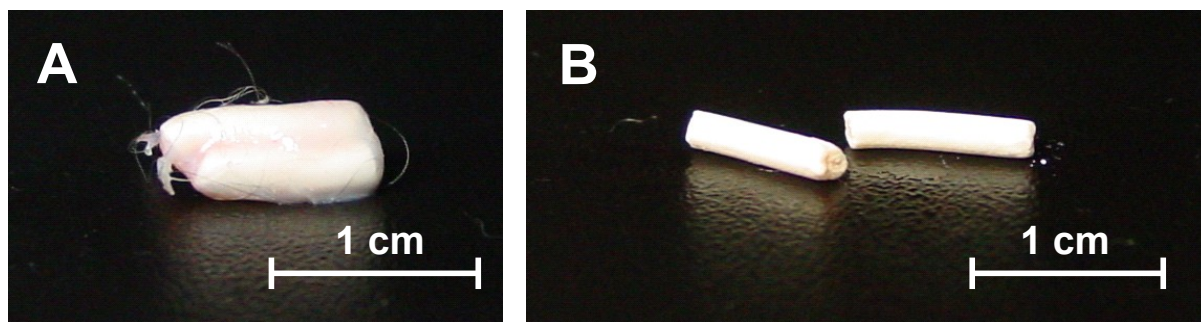


Figure 67: (A) Lipid implant surrounded by fibrous capsule and attached tissue. (B) Lipid implant after removal of tissue and the fibrous capsule.

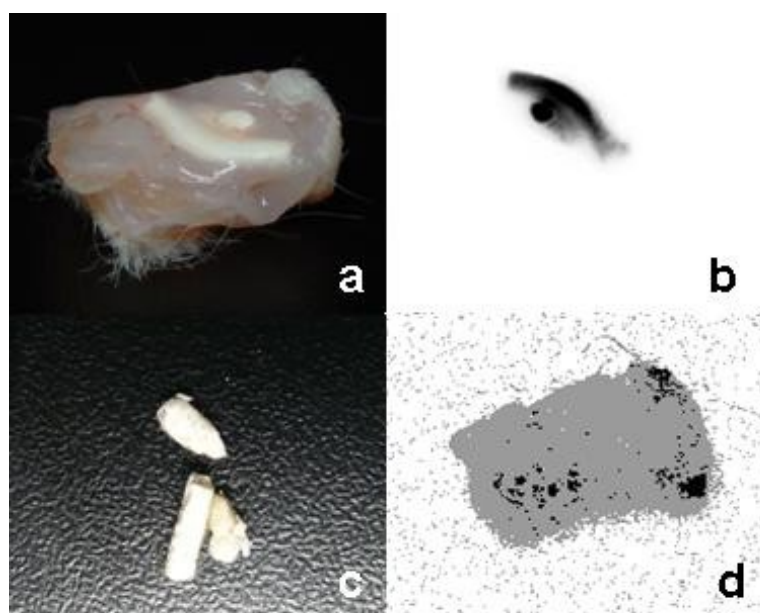


Figure 68: (a) – lipid implant embedded in rabbit tissue directly after excision, (b) – 800 nm scan of rabbit tissue before removal of the implant, (c) – implant after complete removal from rabbit tissue, (d) – 800 nm scan of the tissue after removal of the implant (grey staining derives from auto-fluorescence of the tissue).

DSC measurements of tsc-extrudates revealed endotherms for H12 melting at 36 °C and for D118 melting at 72 °C after incubation (Figure 69). The melting endotherms of D118 and H12 in tsc-extrudates were more distinct after incubation compared to samples before incubation and the endotherm of H12 split into two maxima (36 °C and 42 °C, formulations A-C). Formulation D (E85 instead of H12) also exhibited a split melting endotherm for the low melting lipid E85 after long-term incubation (Figure 69). This changed melting profile derived from a tempering step during long-term incubation at 39 °C. The PEG melting endotherm

(60 °C), which was observed as a prominent endothermic event in samples prior to the degradation study disappeared as the polymer was released from the implant during incubation (Figure 69).

Assessment of the triglyceride composition of all implants was carried out by comparison of the AUCs of the melting endotherms, since the AUCs of the melting endotherms correlate directly with the amount of triglyceride [221]. The analysis of the samples revealed a slight decrease of the mass of H12 (formulation A-C) after *in-vitro* incubation but no decrease of E85 (formulation D) (Table 15). H12 melts below and E85 melts above the incubation temperature. Thus the loss of triglyceride material from H12 containing implant derived from H12 melting during incubation and implants of formulation D were better preserved due to the higher melting point of E85 compared to H12.

For formulations A-C SEM measurements after 1 month of incubation revealed smooth implant surfaces with well defined pores which formed upon release of PEG 6000 (Figure 72 – lower part). The implant surfaces changed during incubation for 3 months (data not shown) and 6 months (Figure 72 – lower part) and the implants became more fissured and jagged with increasing incubation time. Additionally, implants became more fragile after long term *in-vitro* incubation. However, they all could still be recovered as intact rods.

Implants of formulation D were better preserved during the incubation period compared to formulation A which was explained by the different melting profiles of H12 and E85.

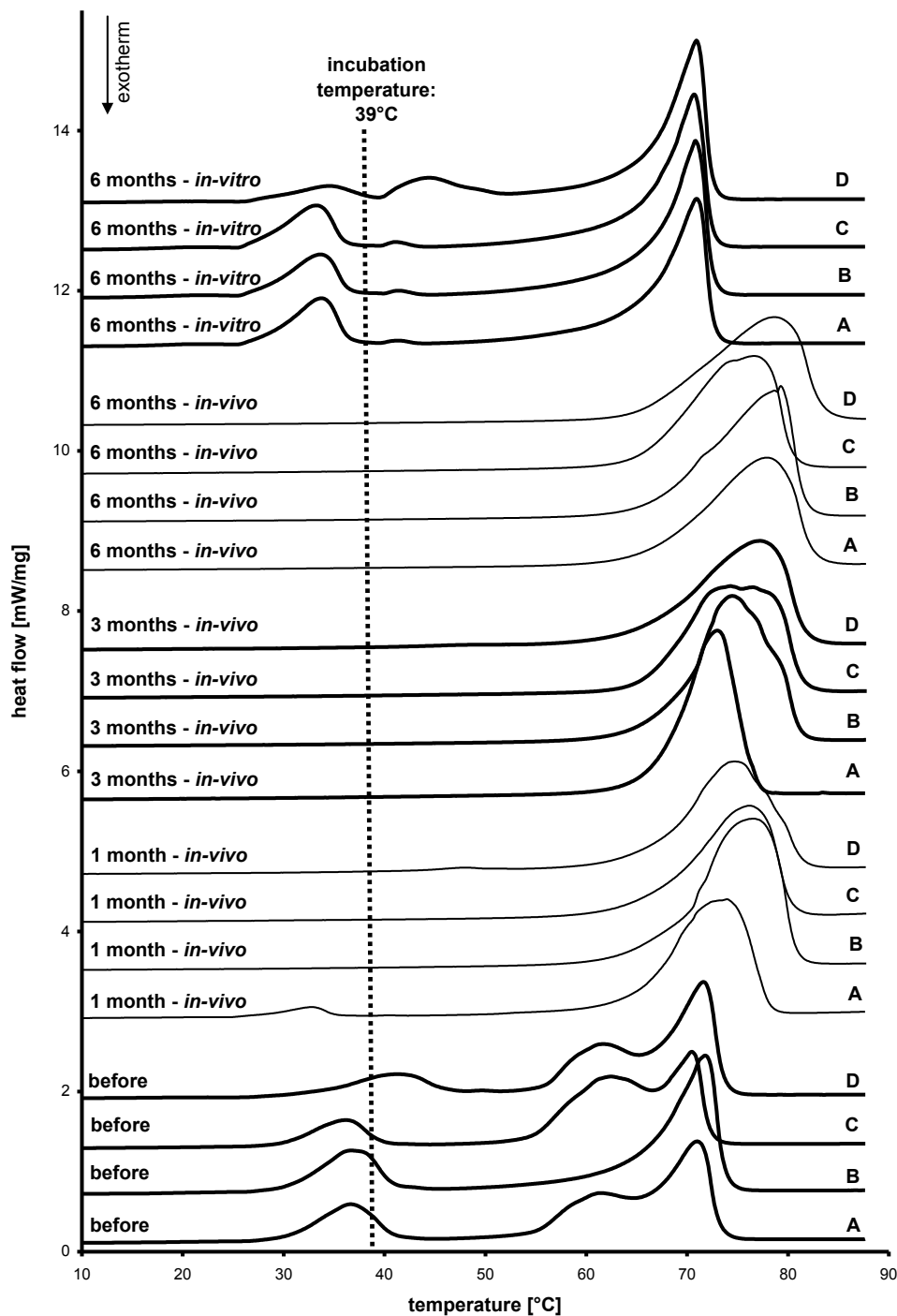


Figure 69: DSC thermograms of tsc-extrudates. From bottom to top: before the degradation study, after 1 month *in-vivo* degradation, after 3 month *in-vivo* degradation, after 6 month *in-vivo* degradation and after 6 month *in-vitro* degradation study (39 °C). A, B, C and D depict formulation A (D118/H12 + 20% PEG 6000), formulation B (D118/H12 + 0% PEG 6000), formulation C (D118/H12 + 40% PEG 6000) and formulation D (D118/E85 + 20% PEG 6000). Melting endotherms: D118 = 70-78 °C, PEG 6000 = 57-65 °C, E85 = 37-45 °C, H12 = 32-40 °C.

**Table 15: Results of weight assessments and DSC measurements of lipid tsc-extrudates after *in-vitro* incubation; \* starting point: 100%; \*\* theoretical value (weighed in amount of H12), determination not feasible due to the presence of PEG 6000.**

formulation	incubation time	total recovery [%]	recovery of triglycerides [%]	AUCs of H12/E85 [%]
A (D118/H12, 20% PEG)	before incubation	100%*	100%*	24% **
	1 month	80% ± 2%	100% ± 3%	23.9% ± 1.2%
	3 months	79% ± 2%	100% ± 3%	24.6% ± 0.7%
	6 months	77% ± 1%	96% ± 2%	21.0% ± 0.7%
B (D118/H12, 0% PEG)	before incubation	100%	100%	25.3% ± 0.4%
	1 month	100% ± 0%	100% ± 0%	24.7% ± 0.5%
	3 months	100% ± 0%	100% ± 0%	24.0% ± 0.5%
	6 months	98% ± 0%	98% ± 0%	21.2% ± 0.7%
C (D118/H12, 40% PEG)	before incubation	100%*	100%*	24% **
	1 month	60% ± 1%	100% ± 2%	26.3% ± 0.5%
	3 months	60% ± 1%	100% ± 2%	24.2% ± 0.5%
	6 months	58% ± 1%	96% ± 2%	21.0% ± 0.6%
D (D118/E85, 20% PEG)	before incubation	100%*	100%*	24% **
	1 month	79% ± 1%	98% ± 2%	25.6% ± 0.5%
	3 months	79% ± 1%	98% ± 1%	26.4% ± 0.6%
	6 months	79% ± 1%	98% ± 2%	24.0% ± 0.5%

### 3.2. *In-vivo* degradation of formulation A

After the *in-vivo* degradation study the total recoveries of the explanted lipid tsc-extrudates of formulation A decreased to 62% (± 11%), 44% (± 11%) and 19% (± 14%) after 1, 3 and 6 months respectively (Figure 70). DSC data showed the total absence of PEG within eight of nine samples after 1 month of incubation which is in accordance with the *in-vitro* data where a total depletion was detected after 1 month (Figure 71). Thus the remaining implant masses

consisted only of triglycerides, and recoveries of 77% ( $\pm 14\%$ ), 55% ( $\pm 14\%$ ) and 25% ( $\pm 17\%$ ) of the lipidic material after 1, 3 and 6 months (Figure 70) were obtained.

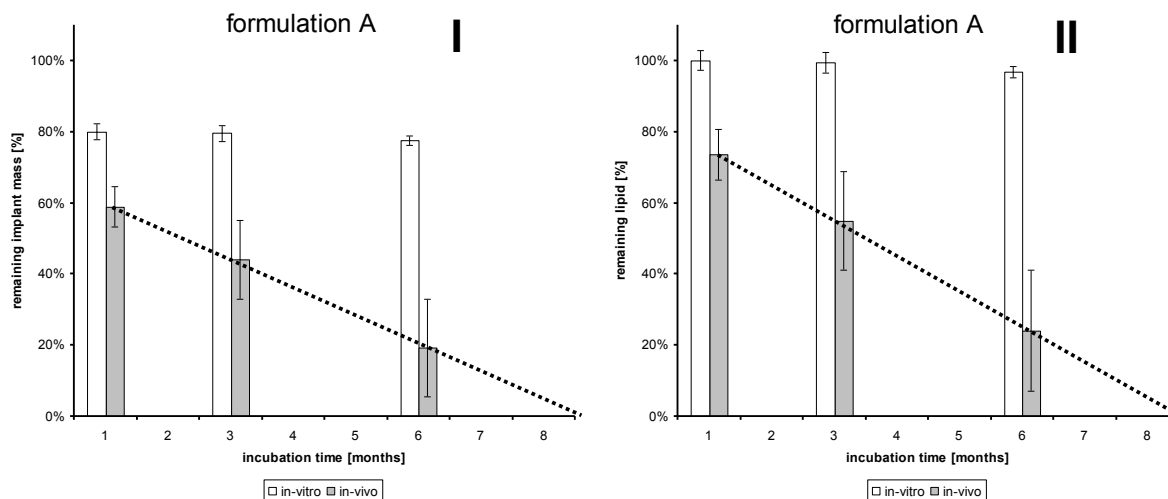


**Figure 70: Comparison between remaining masses after *in-vitro* (white bars) and *in-vivo* (grey bars) degradation studies of tsc-extrudates of formulation A. I: Remaining implant mass after 1, 3 and 6 months (n = 9; except *in-vivo* (6 months): n = 8). II: Remaining triglyceride matrix material after 1, 3 and 6 months (n = 9; except *in-vivo* (6 months): n = 8). Dotted line = extrapolation of the assumed slope of the *in-vivo* degradation.**

The results for different incubation times (1 month versus 3 months, 1 month versus 6 months and 3 months versus 6 months) showed statistically significant differences ( $P < 0.01$ ). An approximated linear extrapolation of the degradation rate indicated that all implants will be totally degraded within 8-9 months (Figure 70 – I, II). The comparison between *in-vivo* and *in-vitro* incubation data showed that *in-vivo* degradation was significantly faster compared to *in-vitro* degradation ( $P < 0.001$ ).

Visual inspection of the remaining implant rods showed fragmentation and deformation of the implants with increasing incubation time. SEM micrographs and visual inspection of the remaining implants revealed a porous and rod-shaped structure after 1 month of *in-vivo* incubation. This structure was lost after 3 months (data not shown) and 6 months (Figure 72) and only dense implant fragments could be recovered from animal tissue. This is in contrast

to the *in-vitro* incubation data where the rod-shaped form of the implant and the porous implant structure were conserved during 6 months of incubation (Figure 72).

DSC data after 3 and 6 months of incubation showed a total depletion of PEG from the implant matrices whereas small amounts PEG could still be found within the implants after an incubation time of only 1 month (Figure 71). Deviations between remaining implant masses can be explained by different ratios of released H12 during *in-vivo* incubation (Table 16).

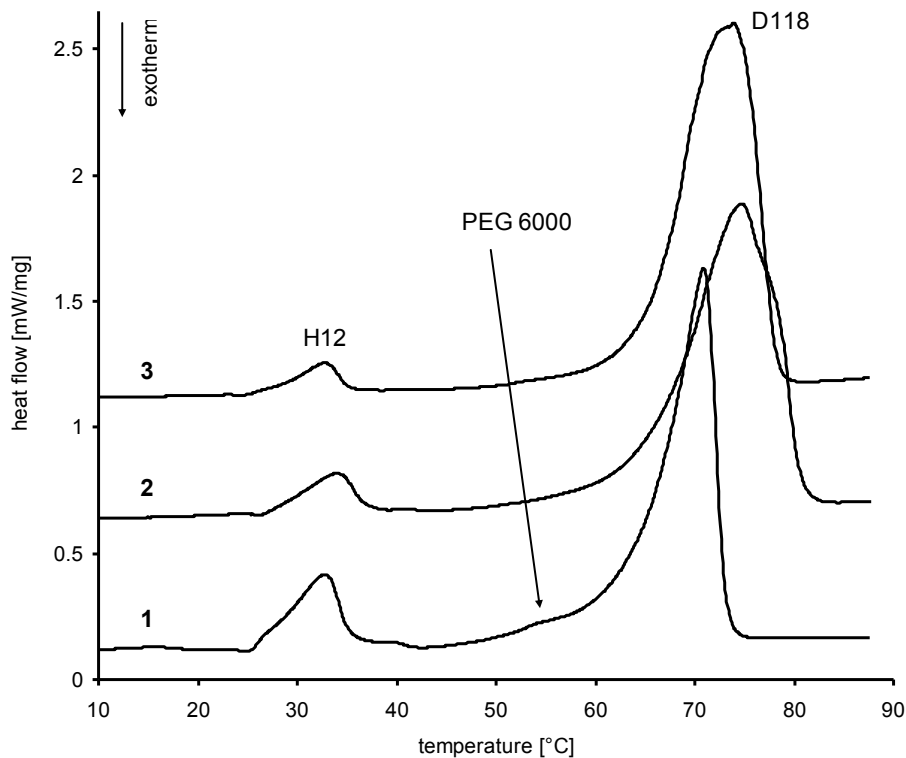


**Figure 71: DSC thermograms of three tsc-extruded lipid implants (formulation A) after *in-vivo* incubation for 1 month. In sample 1 residues of PEG 6000 are observable. Melting endotherms: H12 = 35 °C, PEG 6000 = 55 °C and D118 = 72 °C.**

**Table 16: Results of DSC measurements of tsc-extrudates after 1 month *in-vivo* implantation in rabbits. Displayed are the area under the curve (AUC) of the low melting lipid (H12) and high melting lipid (D118) as percentage of the total AUC. \*) sample contained residues of PEG 6000**

formulation	sample number	remaining implant mass	remaining lipid material	AUC of H12 [%]	AUC of D118 [%]
A	1	82%	100% *)	12.6%	87.4% *)
	2	59%	74%	7.2%	92.8%
	3	51%	64%	4.3%	95.7%

We conclude that the initial 20% of the weight loss during *in-vivo* degradation was mainly related to PEG dissolution and release. Subsequently, H12 was depleted from the implant and after 3 and 6 months only marginal amounts of H12 were present in the implants.

H12 depletion from the implant matrix was explained by two factors: (A) simple transportation phenomena of molten H12 at body temperature (39 °C) or (B) fast cleavage of the low melting triglycerides by lipases which are omnipresent in the body fluids.

Schwab *et al.* [33] have already shown that the application of lipases induced faster *in-vitro* degradation of tsc-extrudates than of compressed implants. This was found to be a consequence of the manufacturing process and the presence of the low melting triglycerides which were more prone to the lipolytic activity of lipases. The triglyceride material of tsc-extrudates had been rapidly degraded *in-vitro* and the implants completely lost their shape after a few days of incubation, resulting in fine particles in the range of 40-90 µm. In contrast to tsc-extruded implants, only small amounts of triglyceride had been cleaved from compressed implants consisting of pure D118 and these implants had kept their shape throughout the experiment [33]. In our experiment, however, the implant erosion of tsc-extrudates took months instead of days and this was explained by lower lipase concentrations in the body fluids compared to the concentrations applied for the *in-vitro* studies of Schwab *et al.* [33].

DSC measurement after *in-vivo* implantation showed a depletion of H12 from the implants which can result in a fragmentation of the matrix and the formation of fine D118 particles,

comparable to the resulting particles found by Schwab *et al.* [33]. The low melting lipid is thought to act as 'glue' during manufacturing which fixes the fine D118 particles together during preparation. After depletion of the 'glue' these small particles can easily erode from the matrix and are of course more prone to degradation than compact D118 implants. For examples they can be washed away by body fluids, undergo degradation by lipases or are eliminated by phagocytosis.

Thus the fragmentation and the matrix breakdown of lipid tsc-extrudates were explained mainly by the depletion of H12 from the triglyceride matrix. But H12 did not only 'glue' D118 particles together, it also worked as softening agent during manufacturing which enabled extrusion of the solid powder formulation and led to the creation of a dense implant matrix. Consequently, melting of H12 during the *in-vivo* study within the solid triglyceride implant at body temperature also led to a softening of the extrudates *in-vivo* which became formable again. SEM measurements after the *in-vivo* study showed that the void spaces and the porous implant structure which were created upon PEG dissolution were lost due to deformation of the implants. This phenomenon was not observed to the same extent after *in-vitro* studies where no mechanical stress was applied to the implants (Figure 72).

In our study we observed an erosion of 23% of the lipidic matrix components after only 1 months of incubation and after 6 months an average erosion of 75% was detected. One implant even eroded to 95%. This was in strong contrast to the *in-vivo* degradation data of compressed implants of pure D118 which did not showed any sign of erosion after 4 weeks of subcutaneous implantation in rabbits [31]. Thus tsc-extrudates showed excellent biodegradability in rabbits and this can be explained by the implant composition and the characteristics of tsc-extrudates.

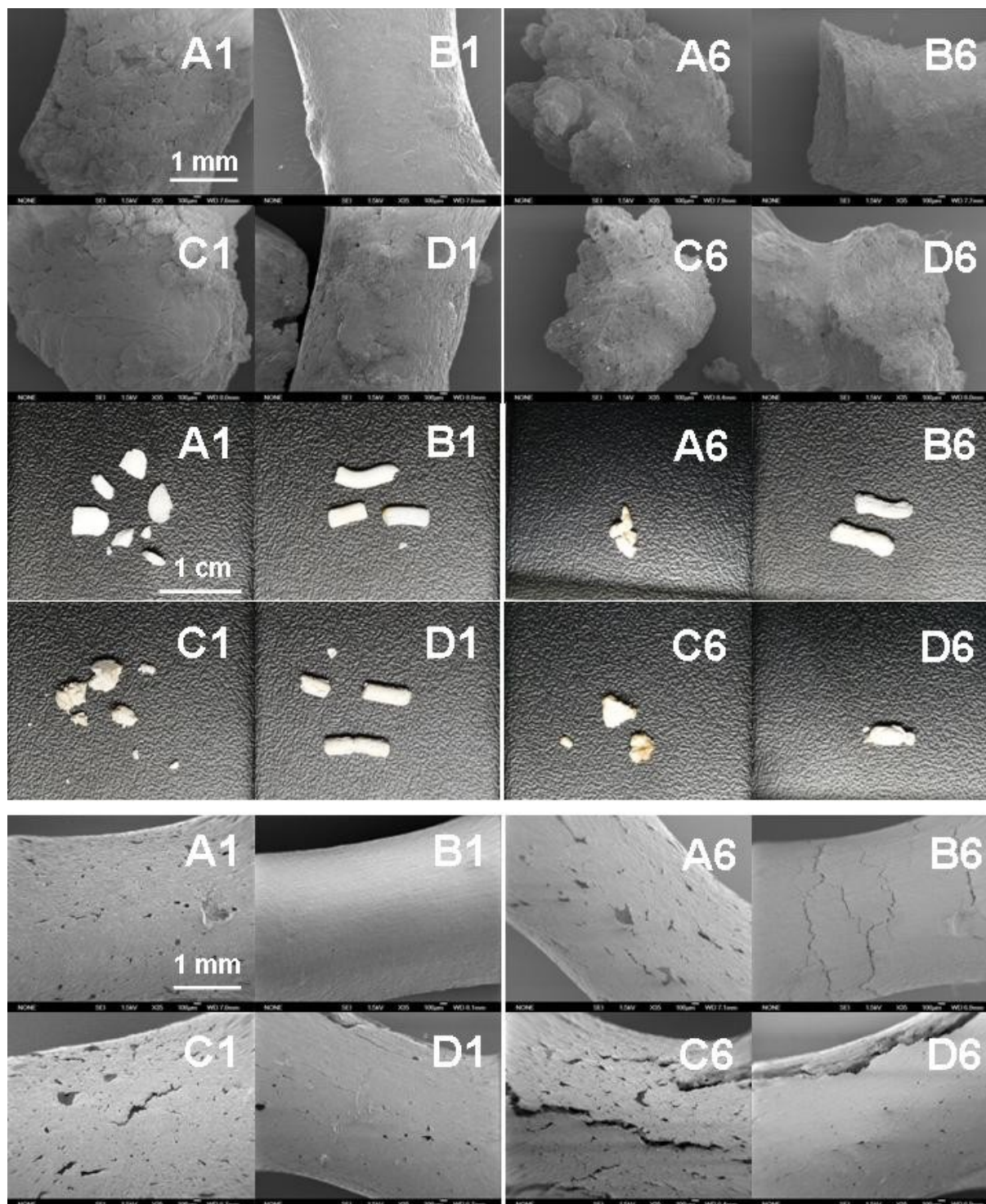


Figure 72: SEM measurements and digital photographs of implants after degradation studies. Upper part – SEM micrographs after *in-vivo* incubation of formulations A-D for 1 and 6 months (A1-D6); middle part – digital photographs after *in-vivo* incubation of formulations A-D for 1 and 6 months (A1-D6); bottom part – SEM micrographs after *in-vitro* incubation of formulations A-D for 1 and 6 months (A1-D6).

### 3.3. Influence of the amount of pore-former on the degradability of lipid tsc-extrudates

To study an influence of the amount of pore forming agent on the *in-vivo* degradation of tsc-extrudates, the ratios between H12 and D118 were kept constant but the amount of pore forming agent PEG 6000 was varied between 0% (formulation B) and 40% (formulation C).

Implants of formulation B showed a time dependent biodegradation with recoveries of 81% ( $\pm 11\%$ ,  $n = 3$ ), 69% ( $\pm 2\%$ ,  $n = 3$ ) and 48% ( $\pm 5\%$ ,  $n = 2$ ) of the implant mass (Figure 73). Implants consisting of formulation C ( $n = 3$ ) eroded faster and recoveries of 44% ( $\pm 5\%$ ), 31% ( $\pm 6\%$ ) and 21% ( $\pm 7\%$ ) were measured (Figure 73). This higher degradation rate was not surprising as 40% of the implants of formulation C consisted of water soluble PEG 6000 whereas formulation B did not comprise PEG 6000. A calculation of the recovery of the lipidic material of formulation C resulted in 74% ( $\pm 9\%$ ), 52% ( $\pm 11\%$ ) and 35% ( $\pm 12\%$ ) recovery after 1, 3 and 6 months compared to 77% ( $\pm 14\%$ ), 55% ( $\pm 14\%$ ) and 25% ( $\pm 17\%$ ) for formulation A respectively. DSC data showed an identical depletion of H12 from all formulations independent of the implantation period (Figure 69). Comparison between formulations A, B and C showed no statistical significant difference in the degradation of the triglyceride matrix material (Figure 74). However, mass recoveries from formulation B (0% PEG 6000) were higher compared to formulations A and C and visual assessment as well as SEM measurements indicated that implants of formulation B were better preserved than the more porous and fragile implants of formulations A and C (Figure 72). We conclude that increasing amounts of pore former led to an enhanced *in-vivo* degradability of triglyceride matrices due to higher matrix porosities after release of the pore former.

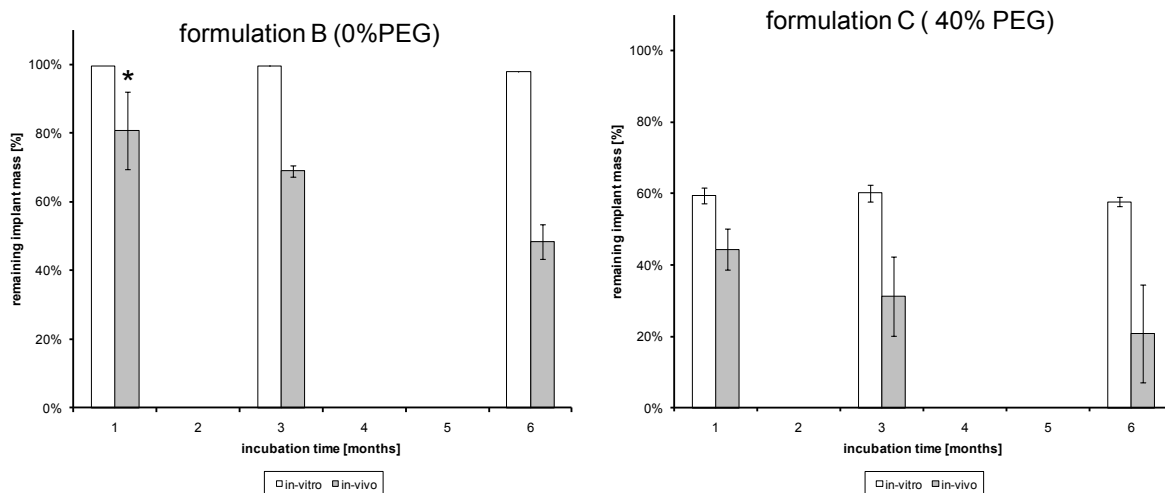


Figure 73: Comparison between *in-vitro* (white bars) and *in-vivo* (grey bars) degradation data of tsc-extrudates of formulations B and C. Left: Remaining implant mass of formulation B after 1, 3 and 6 months. Right: Remaining implant mass of formulation C after 1, 3 and 6 months (*n* = 3 except for formulation B, 6 months, *in-vivo*: \* *n* = 2)

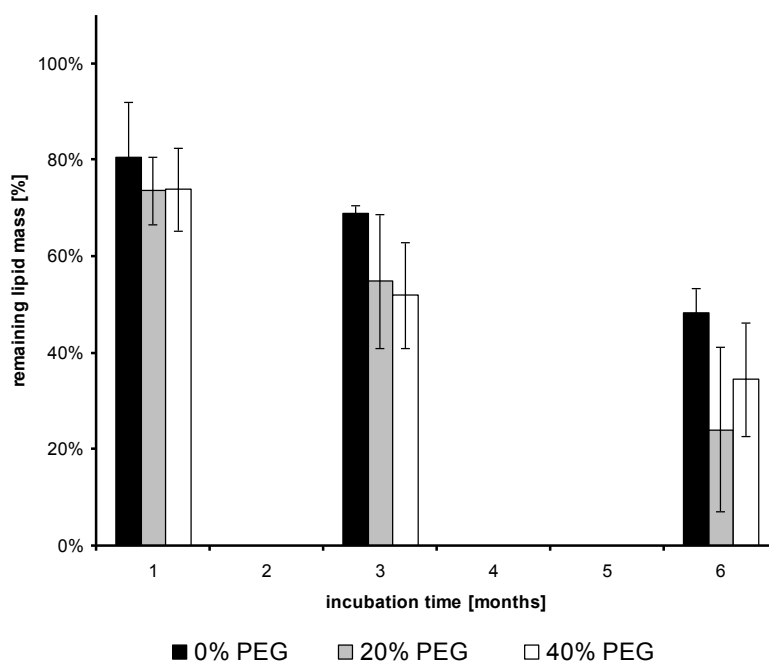


Figure 74: Remaining triglyceride matrix material after *in-vivo* degradation study in rabbits for 1, 3 and 6 months: black bars = D118/H12 implants containing 0% PEG (formulation B), grey bars = D118/H12 implants containing 20% PEG (formulation A) and white bars = D118/H12 implants containing 40% PEG (formulation C).

### 3.4. Influence of the type of low-melting lipid

In formulation D the triglyceride H12 was replaced by the triglyceride E85 because this formulation was shown to be less degradable in an *in-vitro* degradation study where lipases were used to cleave the lipid material [33].

The biodegradation study in rabbits showed that 62% ( $\pm 9\%$ ), 55% ( $\pm 5\%$ ) and 29% ( $\pm 9\%$ ) of the total implant mass was recovered from implants of formulation D which was equal to 78% ( $\pm 12\%$ ), 69% ( $\pm 6\%$ ) and 37 ( $\pm 14\%$ ) of triglyceride material after 1, 3 and 6 months of incubation, respectively. The degradability of the lipid implants was dependent on incubation time and differences between the mass losses after 1 month and 6 months and after 3 months and 6 months of incubation were statistically significant ( $P < 0.01$ ).

Visual inspections and SEM measurements indicated that implants of formulation D better preserved their shape and form compared to implants of formulation A (Figure 72). Additionally, higher mass recoveries were measured from implants of formulation D compared to standard formulation A (Figure 75). However, the differences in recovery between formulations A and D were not statistically significant. DSC measurements of formulation D showed only marginal amount of E85 within the lipid matrix after 1 month of *in-vivo* incubation and almost total depletion of the low-melting lipid from the implant after 3 and 6 month of *in-vivo* incubation which was similar to the standard formulation A (Figure 69). Thus no significant difference between formulation A and D was detectable although a tendency (mass loss and SEM micrographs) indicated that implants comprising D118/E85 degraded to a smaller extent than implant consisting of D118/H12. Our findings of the *in-vivo* study correlate well with the *in-vitro* data and the data from the *in-vitro* lipase assay were the D118/E85 extrudates were also less degradable. Thus we conclude that by choosing a suitable low melting lipid (melting temperature, cleavage rate) the *in-vivo* degradation rate of tsc-extrudates can be prolonged or shortened. However, the rate of biodegradation is quite robust regarding small variations in lipid compositions which would allow for a reliable long-term biodegradation in patients.

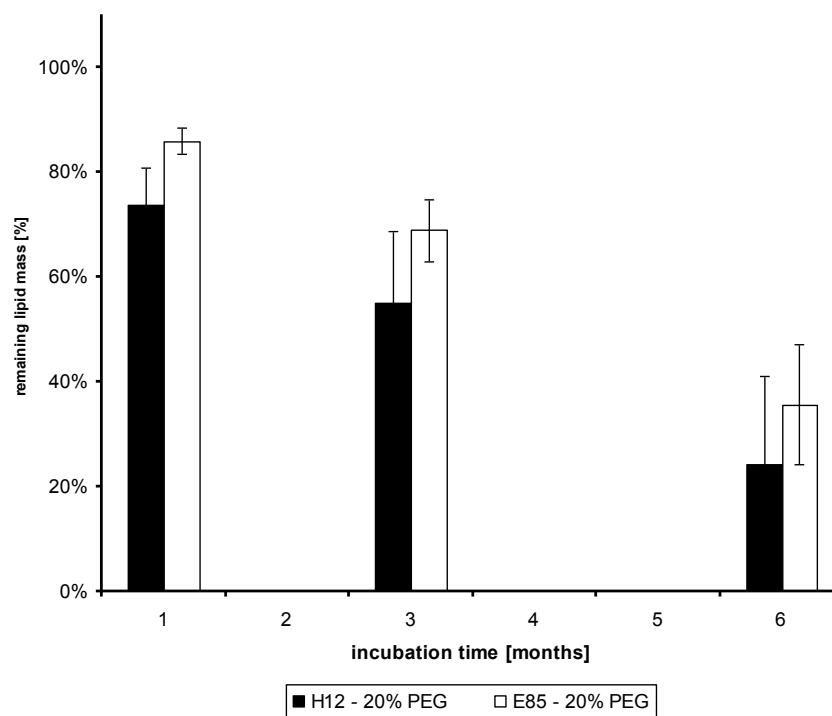


**Figure 75: Remaining masses of triglyceride matrix material of tsc-extrudates after *in-vivo* degradation study in rabbits for 1, 3 and 6 months: black bars = D118/H12 implants containing 20% PEG 6000 (n = 9, formulation A), white bars = D118/E85 implants containing 20% PEG (n = 3, formulation D).**

#### **4. Conclusion**

Tsc-extrudates showed excellent *in-vivo* biodegradability in rabbits. The implants degraded continuously over a time period of 6 months and only 25% of the lipid matrix material was recovered. In contrast to *in-vitro* degradation (= incubation in lipase free buffer) a significant mass loss and a breakdown of the porous implant matrix structure was detected. The degradation rate allows a linear extrapolation indicating total implant degradation within 9 months. DSC measurements and comparison between *in-vitro* and *in-vivo* data indicated that in the beginning of implant erosion the water soluble amount of the implant (PEG 6000) was dissolved and released. Afterwards the low melting lipid was degraded *in-vivo* or was simply cleared from the implant as a melt and the remaining implant matrix broke to pieces and eroded over time.

Increasing amounts of pore-forming agent resulted in faster degradation rates of the total implant mass. However, this effect was mainly dominated by the dissolution of PEG 6000. Data indicate a better degradability of tsc-extrudates with increasing amounts of pore-forming agent. However due to the limited sample numbers in this orientation study the differences between the formulations were not statistically significant. Application of a different low melting lipid (E85) with a higher melting point resulted in a higher recovery of the implant mass and a better preservation of the implant structure. We conclude that the degradation rate can be controlled by variation of the triglyceride components and the amount of hydrophilic excipients.

In order to achieve appropriate biodegradation rates of tsc-extrudates the choice of the low melting lipid as well as the amount of incorporated hydrophilic components is of importance. For the preparation of biodegradable tsc-extrudates the use of low melting lipids with melting endotherms below the body temperature is recommended. Total degradation of implants of a typical size of 2 cm length and 1.9 mm diameter can be expected after 9 months.



## VIII. Lipase induced *in-vitro* degradation study with tsc-extrudates

### 1. Introduction

For a long time one of the major drawbacks of triglyceride based implant systems was their low 'bio'-degradability *in-vivo*. Although lipids *per se* are natural substances, the concentration of lipases in the subcutaneous tissue is too low to allow rapid degradation of compressed implant [31, 33]. Tsc-extrudates show partial implant melting during *in-vitro* and *in-vivo* incubation and were therefore shown to be degradable over a period of several months (see chapter 0). However, often shorter periods for drug release are desired (2 weeks to 3 months) and therefore it seems to be a very promising attempt to control or even tailor the rate of implant degradation. As it was shown by Schwab *et al.* lipases can be used to enhance the rate of implant degradation [33]. Therefore we tried to incorporate lipases into tsc-extrudates and analyze the rate of implant degradation. In further studies we investigated whether faster implant degradation can be used for controlled protein release.



## **2. Materials and methods**

### **2.1. Materials**

#### **2.1.1. Lipase**

Lipase from *Rhizopus oryzae* (> 30 U/mg) was purchase from Sigma-Aldrich (Germany). It consists of a light brown powder and its activity optimum is at pH 7.2 but the enzyme is highly active between pH 6.4 and 7.5. Therefore degradation studies were performed in isotonic PBS pH 7.4.

#### **2.1.2. Triglycerides**

D118, H12 and E85 were donated from Sasol (Witten, Germany) and their composition is described in VI.2.1 (Table 11).

### **2.2. Methods**

#### **2.2.1. Preparation of tsc-extrudates**

**Tsc-extrudates were prepared as described above (III.2.9). Lipid powder blends (Table 17 +**

Table 18) comprising D118 as high melting lipid and either H12 or E85 as low melting lipid were prepared and mixed with various amounts of lipase or lipase + lysozyme. Mixing was performed in a mortar which was lined with the low-melting lipid to seal the mortar's porous surface. Lipase and/or lysozyme were added to the mortar and mixed with the same volume of H12. Afterwards H12 was added to double the volume again and in continuative steps the extrusion-mixture was built up by addition of H12 and D118.

Extrusion of rod-shaped implants was performed through a 1.9 mm outlet die in steady-state mode with closed bypass.

The resulting rod-shape (light brownish) implants (Figure 76) were cut at length (~ 3.0 cm), accurately weighed and used for degradation and release studies.

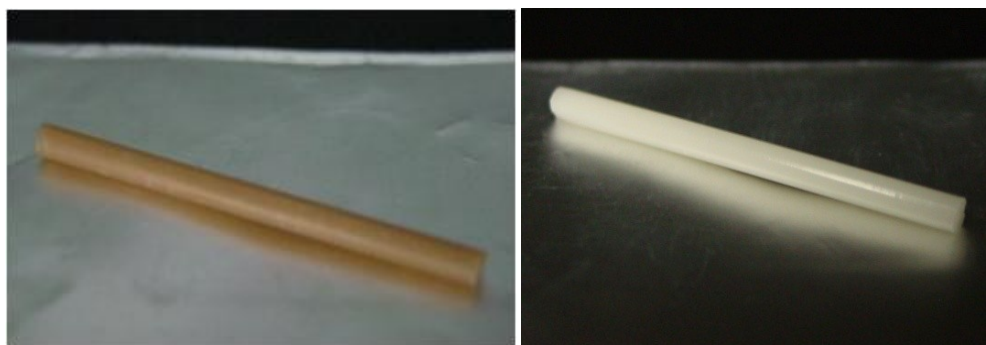


Figure 76: Twin-screw extrudates directly after preparation (~ 3 cm length). A: implant comprises 10% lipase (formulation 4, Table 17), B: implant comprises 0.1% lipase (formulation 2, Table 17).

Table 17: Composition of tsc-extrudates for degradation studies

No.	D118 high melting lipid	H12 low melting lipid	ratio between D118:H12	lipase
1	80.0%	20.0% H12	80:20	0%
2	79.9%	20.0% H12	80:20	0.1%
3	79.2%	19.8% H12	80:20	1.0%
4	72%	18% H12	80:20	10.0%

Table 18: Composition of tsc-extrudates for lysozyme release studies

No.	D118 high melting lipid	H12 low melting lipid	ratio between D118:H12	lysozyme	lipase
11	68.3%	29.2%	70:30	2.5%	-
12	66.5%	28.5%	70:30	5.0%	-
13	63.0%	27.0%	70:30	10.0%	-
14	68.2%	29.2%	70:30	2.5%	0.1%
15	68.0%	29.2%	70:30	2.5%	0.3%
16	67.9%	29.1%	70:30	2.5%	0.5%
17	67.8%	29.0%	70:30	2.5%	0.7%
18	67.6%	28.9%	70:30	2.5%	1.0%
19	66.2%	28.3%	70:30	5.0%	0.5%
20	62.7%	26.8%	70:30	10.0%	0.5%

### 2.2.2. Degradation study

For tsc-extrudate degradation studies a similar setup was chosen as it was used by Schwab *et al.* [33]. In brief, implants were incubated in 1.9 mL isotonic PBS pH 7.4 in low bind protein tubes (2 mL, Eppendorf AG, Hamburg) at 37 °C in a water-bath. At predetermined points of time the incubation medium was completely exchanged and free fatty acids were extracted from the incubation medium according to a method proposed by Schwab *et al.* and Dole *et al.* [33, 247]. In brief, 1 mL of sample solution was admixed with 2.5 mL of extraction medium (propan-2-ol : heptan : phosphoric acid (2 M) 40 : 10 : 1 (v/v)), vortexed for 15 sec and placed in a ultrasonic bath (Sonorex Super RK 510, Bandelin Electronic GmbH & Co KG, Berlin, Germany) for 2 min. Afterwards the samples were vortexed again (15 sec) and incubated at room temperature for 10 minutes. After addition of 1 mL heptan and 1.5 mL water the samples were vortexed (15 sec) and ultrasonicated (2 min) again und finally centrifuged at 1000 g at 4 °C for 10 min. 1 mL of the organic phase which separated on top of the sample was transferred to a HPLC vial (VWR, Germany) and dried in a stream of dry nitrogen (in-house supply line). Standard solutions of lauric, myristic, palmitic and stearic acid were prepared in dichloromethanol (0.2 mg/mL) and treated like sample material in order to prepare calibration curves

### 2.2.3. Assessment of free fatty acids

Free fatty acids were quantified by RP-HPLC after derivatization according to Schwab *et al.* [33] and Wood *et al.* [248]. Dried samples (free from heptan) were dissolved in acetone (1 mL) and admixed with 70 µL of phenacyl bromide solution (10 mg/mL in acetone) and 70 µL of triethylamine solution (10 mg/mL in acetone). The vials were sealed and incubated for 20 min at 70 °C in a drying oven (Mettler, Schwabach, Germany). After cooling to room temperature 112 µL of a solution of acetic acid in acetone (2 mg/mL) was added to react with the excess of derivatization reagents and incubated for additional 10 minutes at 70 °C. Samples were again dried under a stream of dry nitrogen and reconstituted in 1 mL methanol for RP-HPLC analysis

### 2.2.4. Quantification of free fatty acids by RP-HPLC

Reconstituted samples were analyzed by RP-HPLC and peak areas were used to quantify the amount of free fatty acids. Calibration curves were prepared from 5-200 µg/mL of each fatty acid and showed linear correlation between peak area and fatty acid concentration (Figure 78). RP-HPLC settings are described below:

HPLC:	Dionex Ultimate 3000 (Dionex Softron GmbH, Germany)
Pre-column:	LiChroCART®250-4, Merck Darmstadt
RP-column:	LiChrosper®100 RP-18 (5 µm), Merck Darmstadt
Mobile phase:	methanol : acetonitrile : water (80 : 10 : 10)
Flowrate:	2 mL/min, isocratic
Run time:	30 min
Detection:	254 nm (Ultimate 3000, Variable Wavelength Detector, Dionex Softron)
Injection volume:	100 µL

Baseline separation for free fatty acids was achieved (see Figure 77).

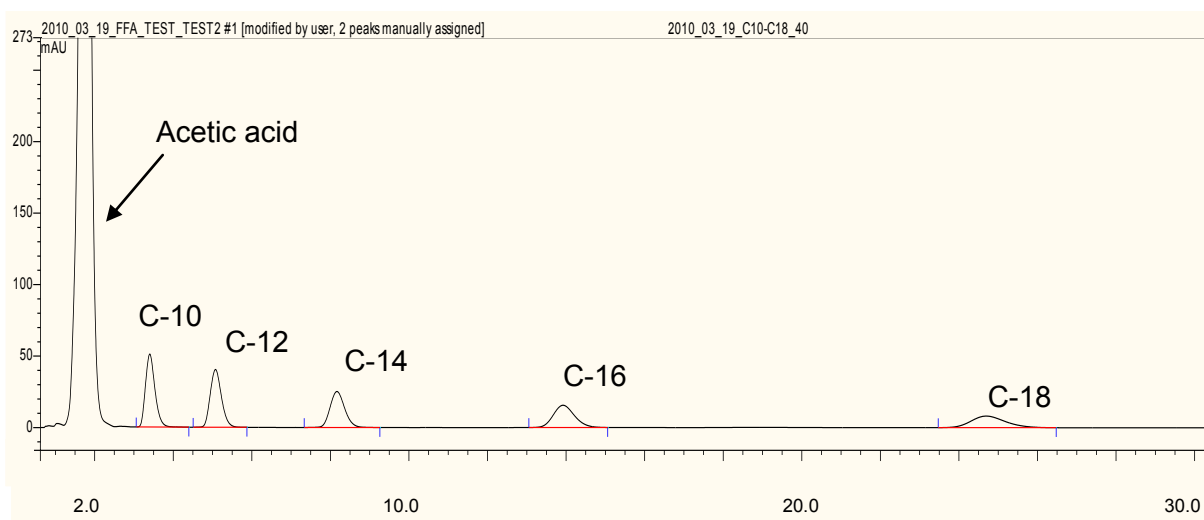


**Figure 77: RP-HPLC chromatogram of 5 fatty acids (capric (C-10), lauric (C-12), myristic (C-14), palmitic (C-16) and stearic acid (C-18)) after derivatization according to 2.2.3. Fatty acid concentration was 40 µg/mL of each acid. Fatty acids were baseline separated.**

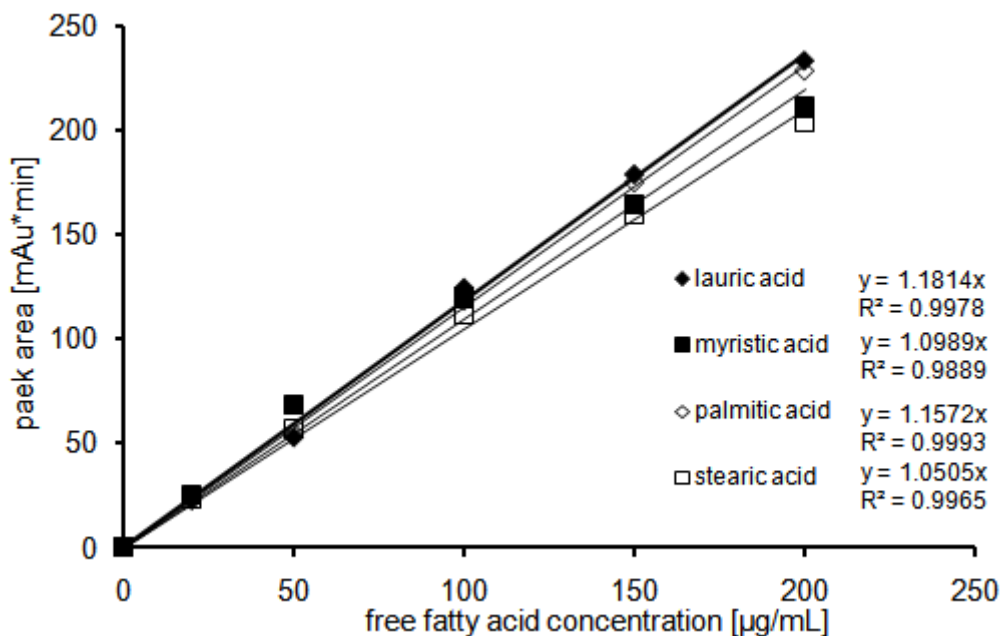


Figure 78: Calibration curves for free fatty acid determination.

### 2.2.5. Quantification of lysozyme and lipase release from tsc-extrudates

Implants comprising lysozyme and lipase were incubated in protein low bind Eppendorf tubes with 1.9 mL isotonic PBS pH 7.4 (+ 0.05% sodium azide) at 37 °C and placed in water baths. At predetermined points of time, samples were drawn by complete exchange of the incubation medium and samples were analyzed by SE-HPLC as described below:

HPLC: Dionex Ultimate 3000 (Dionex Softron GmbH, Germany)  
 SEC-column: Superose 12, 10/300 GL (GE Healthcare, Uppsala, Sweden)  
 Mobile phase: 0.2 M potassium phosphate + 0.15 M potassium chloride, adjusted to pH 6.8  
 Flowrate: 0.65 mL/min  
 Run time: 33 min  
 Detection: 215 nm (Ultimate 3000, Variable Wavelength Detector, Dionex Softron)  
 Injection volume: 100 µL

Lysozyme (25 min) and lipase (20 min) were baseline separated and quantification was possible in a range from 0.01 mg/mL to 1 mg/mL. Separation and quantification of lysozyme and lipase was possible from solutions containing both proteins (Figure 79).

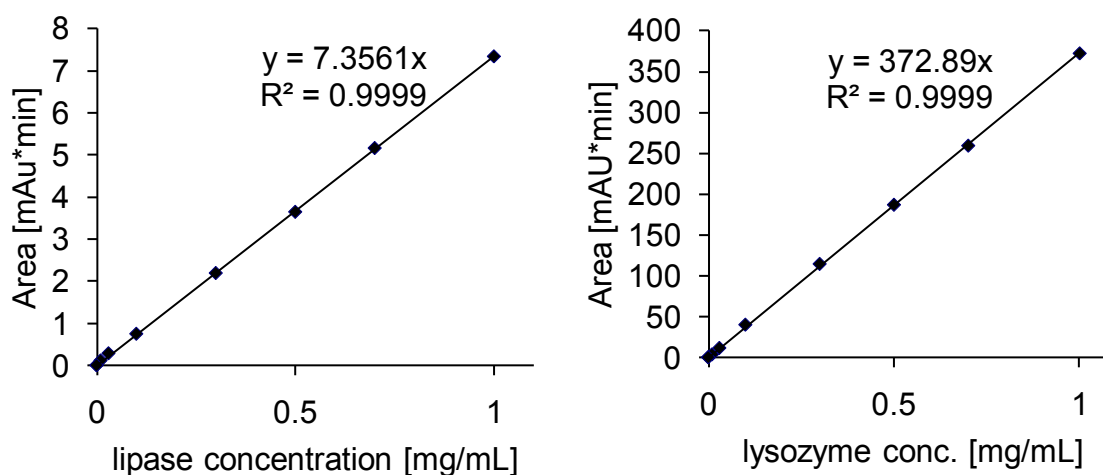


Figure 79: Calibration curves for lipase and lysozyme after SE-HPLC separation and UV detection at 215 nm. Calibration curves were generated from mixed solutions of lysozyme and lipase as well as from solution of pure lysozyme or lipase and yielded identical results.

#### 2.2.6. SEM measurements

SEM measurements were performed with a 6500F (Jeol GmbH, Eching, Germany). Samples were dried in a vacuum chamber (VO 200, Mammert, Schwabach, Germany) at 25 °C and 20 mbar for 6 days and analyzed without coating.

### 3. Results

#### 3.1. Implant degradation after embedding of lipase

After embedding of various amounts of lipase (0.1% - 10.0%, formulations Table 17) and incubation of implants in PBS pH 7.4, implants degraded to a different extent depending on the applied amount of the enzyme. Visual observations showed that the embedding of 10% lipase resulted in a rapid degradation and total matrix breakdown of the implant within 24 hours. The usage of less lipase (1.0% and 0.1%) did not result in a breakdown of the matrix within 14 days of observation (Table 19 + Figure 80).

Table 19: Visual assessment of degradation rate of lipase containing lipid tsc-extrudates

no.	type of low melting lipid	amount of lipase	degradation
1	H12	0%	no degradation
2	H12	0.1%	no matrix breakdown, lipid particles cleaved from matrix
3	H12	1.0%	no complete matrix breakdown, lipid particles cleaved from matrix
4	H12	10.0%	total matrix breakdown within 1 day

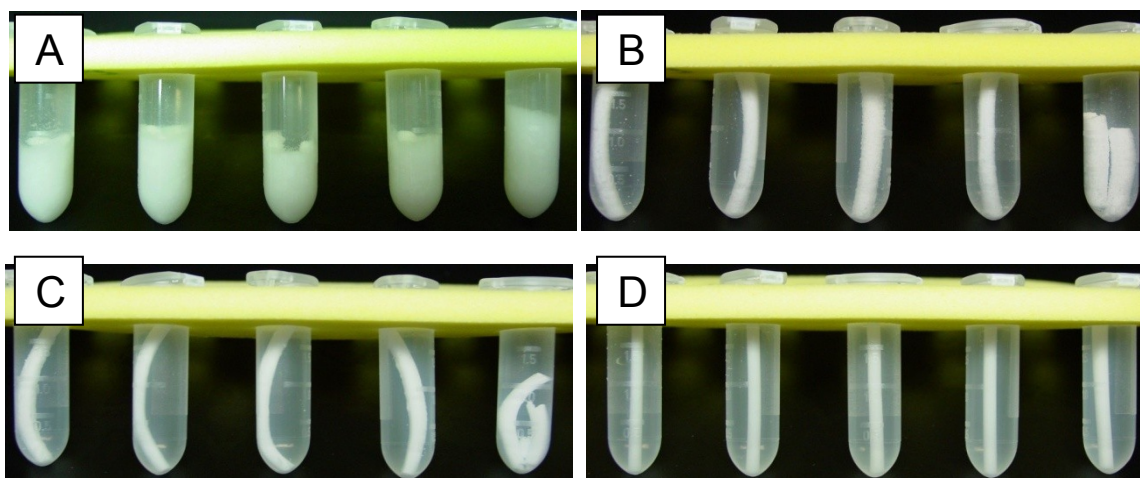
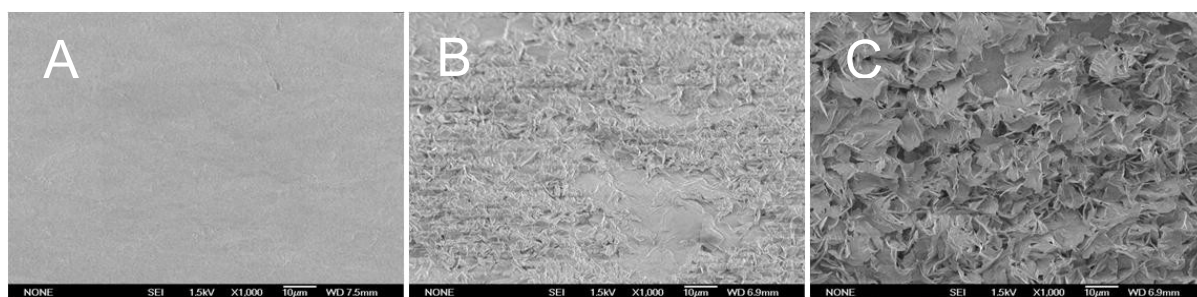
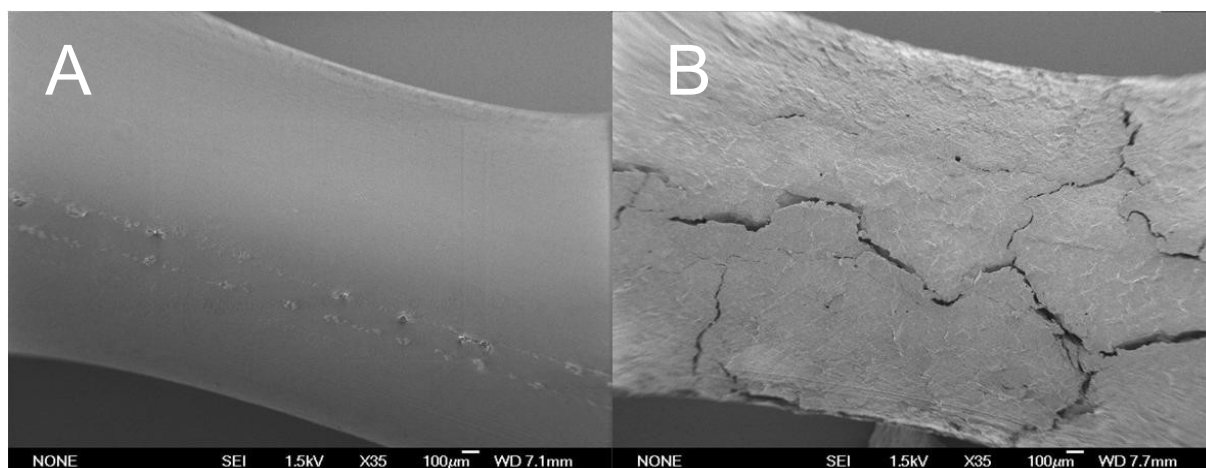


Figure 80: Lipid tsc-extrudates after incubation in PBS pH 7.4. A: 10% lipase (1 day), B: 1.0% lipase (1 day), C: 1.0% lipase (14 days), D: no lipase (14 days).

SEM measurements of samples which were incubated for 24 h showed increasing roughness of the implant surface if increasing amounts of lipase were used (Figure 81). Samples which comprised 10% lipase were assessed by SEM measurements after 1 hour of incubation only and showed a broken implant surface compared to the control formulation (no lipase) (Figure 82). Thus lipase lead to matrix breakdown and changed the implant surface although it was embedded into the matrix of the implant. It is highly likely, that lipase was release from the implant during incubation and affected the implant not only from the matrix core but also at the surface.



**Figure 81: SEM measurements with 1000-fold magnification of surfaces of lipid tsc-extrudates comprising no lipase (A), 0.1% lipase (B) and 1.0% lipase (C) after 24 hours of incubation in PBS pH 7.4**



**Figure 82: SEM measurements with 35-fold magnification of lipid tsc-extrudates comprising no lipase (A) and 10% lipase (B) after 1 hour incubation in PBS pH 7.4.**

Quantification of free fatty acid release was not performed for samples comprising 10% lipase as total matrix breakdown was achieved within 24 hours. Free fatty acid release from samples comprising 0%, 0.1% and 1.0% lipase is depicted in Figure 83.

For control implants with 0% lipase a release 0.4% free fatty acid was detected after seven days of incubation. At every point of time, the released amount of free fatty acids from implants without lipase accounted for approximately 0.08% of the total implant mass and it was mainly lauric acid which was detected after derivatization. This marginal 'release' of free fatty acid can be explained by two factors. Firstly free fatty acids might still be present within the triglyceride bulk material and can be slowly released into the incubation medium like any other molecule. Secondly, partial implant melting might result in a very fine dispersion or even solution of triglyceride material in incubation buffer. Due to the extraction procedure the fatty acids might thus be accessible for the derivatization reaction. Lauric acid was the main component which was detected by RP-HPLC and this acid derives from the low melting H12 but not from D118 (stearic acid).

Calculation of the amount of free fatty acids showed erosion of 2.2% of implant matrix material after approximately two days if 0.1% lipase was used and 2.5% of implant matrix material if 1.0% lipase was used. These values are in the same region as reported by Schwab *et al.* [33] who found about 4% free fatty acids after incubation in lipase solution for 30 days based on the initial mass of the implant matrix material. However, in contrast to Schwab *et al.* we detected a high degradation rate at the beginning of the experiment and slow implant degradation or no degradation of the implant towards the end of the experiment. Schwab *et al.* replenished the incubation medium with fresh lipase buffer after sampling and did not completely exchanged the incubation buffer like we did. Thus our approach resulted in a depletion of lipase from the implants and from the incubation medium.

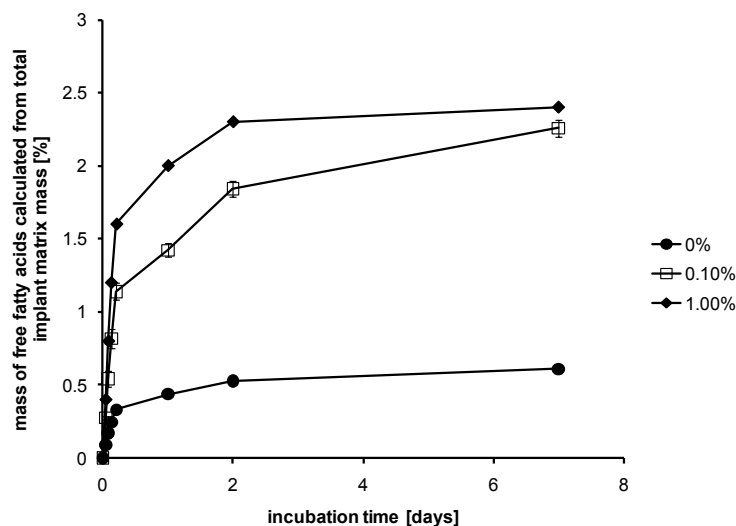


**Figure 83: Degradation of lipid tsc-extrudates. Calculation based on the mass of free fatty acids in the incubation buffer**

### 3.2. Simultaneous release of lipase and lysozyme from lipid tsc-extrudates

In order to investigate the effect of embedding of lipase into triglyceride matrices on the lysozyme release kinetics from tsc-extrudates, implants comprising lysozyme and lipase were prepared according to

Table 18 and release of both proteins was quantified simultaneously by SE-HPLC assessment.

Preliminary studies were performed to ensure that incubation of mixtures of lipase and lysozyme did not cause problems regarding protein stability. Therefore lysozyme and lipase were dissolved in PBS pH 7.4, mixed to give final concentrations of 0.01 mg/mL to 1.0 mg/mL and incubated at 37 °C for seven days. Total recovery of lipase and lysozyme was achieved for all mixing ratios and no increase in aggregated species was detected by SE-HPLC detection.

Within tsc-extrudates the maximum loading of lipase was 1.0%, as higher loadings (10%) resulted in immediate breakdown of the implant matrix (within 24 h) as observed in former experiments.

Release studies showed immediate release of lipase from all tsc-extrudates independent of the amount of lipase applied (Figure 84 + Figure 86). Interestingly, total release of lipase was achieved for all formulations although only relatively small amounts of the enzyme were embedded into the implant matrices which - from theory - would be insufficient to allow complete and rapid protein release. We conclude that lipase frees itself by implant matrix degradation upon incubation in PBS at 37 °C and rapidly cuts its way through the matrix by cleavage of matrix material. This rapid release of lipase also explains the high initial 'release' of free fatty acids from triglyceride matrices. Subsequently no free fatty acids are generated at longer incubation times due to depletion of lipase from the incubation medium by exchange of the incubation buffer (Figure 83).

Release of lysozyme was strongly influence by the presence of lipase. As can be seen in Figure 85 and Figure 87 the application of lipase resulted in a 'non-release' of lysozyme from tsc-extrudates. 'Normal' release rates were obtained if only 2.5%, 5.0% or 10% lysozyme but no lipase were used to prepare tsc-extrudates. The embedding of only 2.5% lysozyme resulted in a slow but measurable release and higher release rates were obtained for higher loadings (Figure 85). The application of only 0.5% lipase to the implant matrix completely changed the release rate and a non-release of lysozyme was observed even if at high lysozyme loadings (10%) (Figure 85). This was completely contrary to our expectations as we expected faster lysozyme release in the presence of lipases due to higher implant porosity and faster implant matrix breakdown. After a burst release of approximately 1% lysozyme no liberating of further lysozyme was detected although lipase had already been completely released after 24 h. Figure 87 shows lysozyme release from implants comprising 2.5% lysozyme and increasing amounts of lipase. The application of only 0.1% lipase led to a decrease of lysozyme release and even the burst release was reduced from 14% to 3%. Application of higher lipase concentrations led to 'non-release' of lysozyme with only 1% burst release.

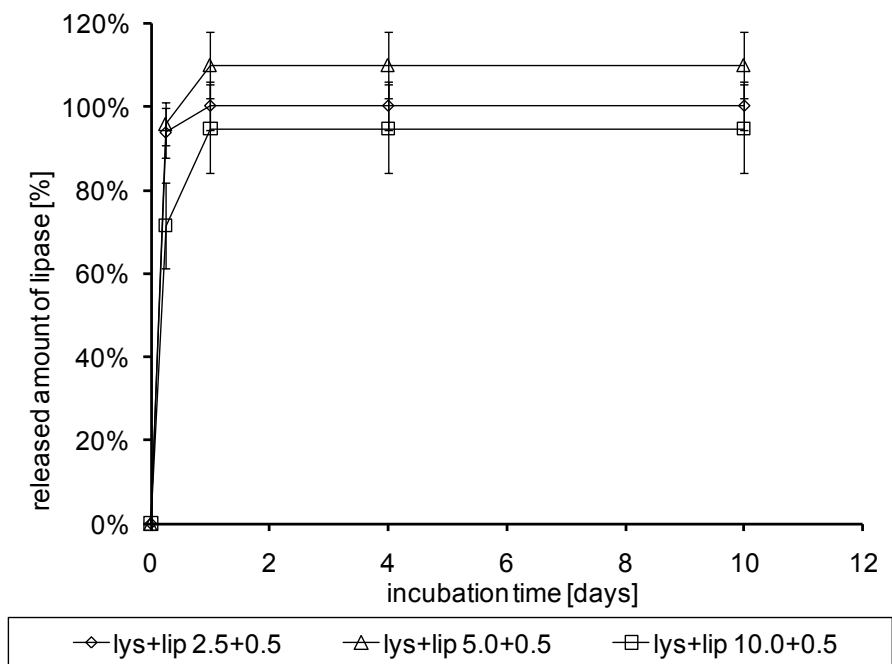


Figure 84: Release of lipase from tsc-extrudates comprising 0.5% lipase (m/m) and 2.5, 5.0 and 10.0% lysozyme respectively.

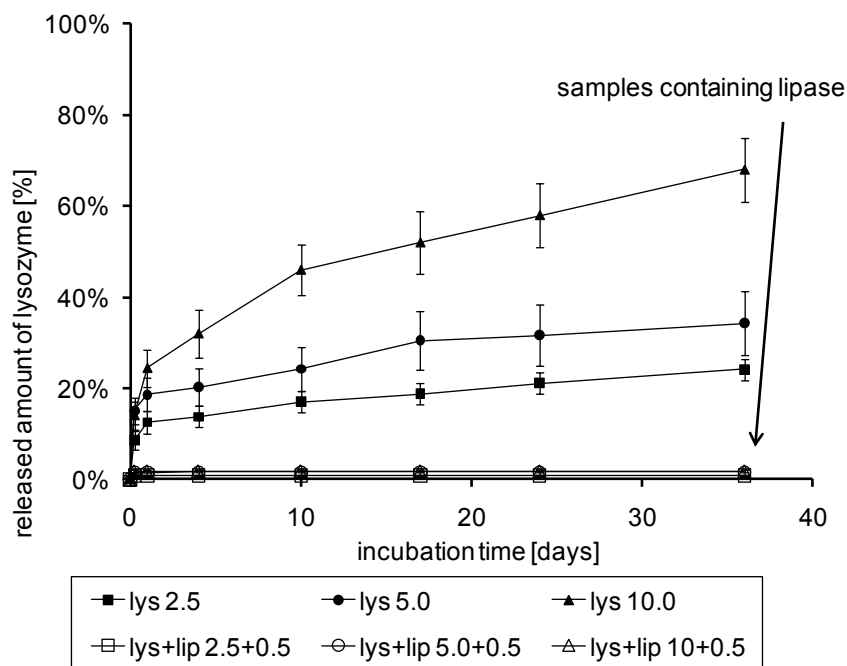


Figure 85: Release of lysozyme from tsc-extrudates comprising no lipase (closed symbols) or 0.5% lipase (m/m) (open symbol) and 2.5, 5.0 and 10.0% lysozyme respectively.

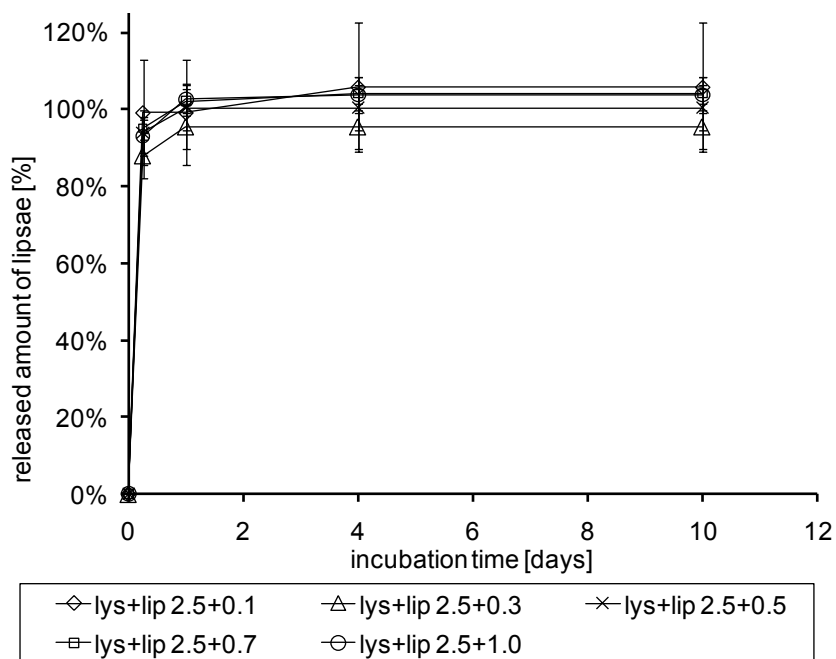


Figure 86: Release of lipase from tsc-extrudates comprising 2.5% lysozyme and 0.1%, 0.3%, 0.5%, 0.7% or 1.0% lipase (m/m).

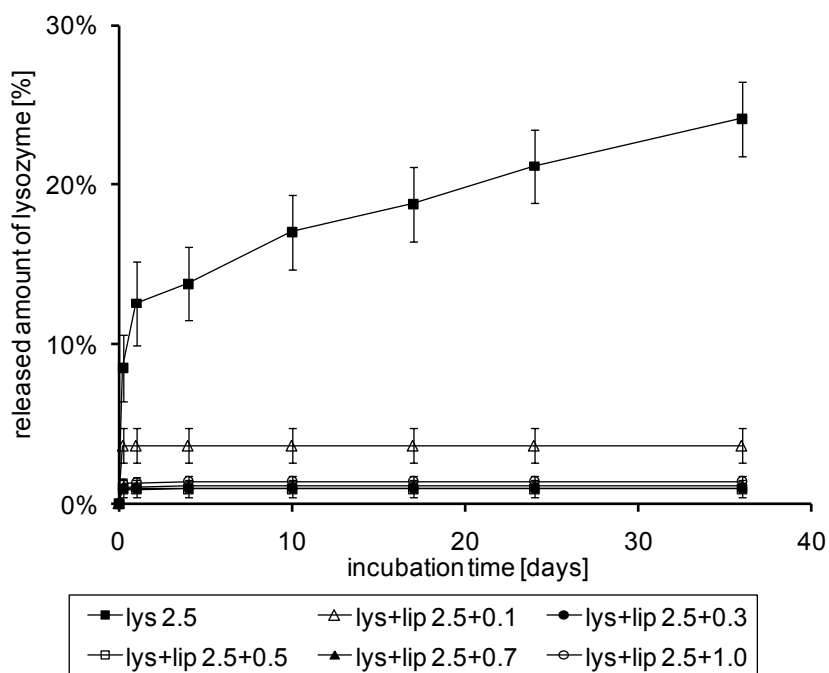


Figure 87: Release of lysozyme from tsc-extrudates comprising 2.5% lysozyme and 0%, 0.1%, 0.3%, 0.5%, 0.7% or 1.0% lipase (m/m).

After incubation for 17, 24 and 38 days a gel-like substance was detected on top of the release medium. We concluded that this substance might be aggregated lysozyme. However, no direct proof was shown besides the fact, that a non-release of lysozyme was detected and the substance looked like acid denaturated lysozyme (100 mg/mL lysozyme + acetic acid). Preliminary experiments have already shown that lysozyme stability was not affected by the presence of lipase in PBS. However, lipases cleave triglycerides into free fatty acids and di-glycerides besides mono-glycerides and glycerol. Thus lipase within tsc-extrudates creates free fatty acids and glycerides which can increase the osmotic pressure and can act as surface active substances within the implant matrix.

Figure 83 shows the amount of degraded matrix material upon incubation of tsc-extrudates comprising 1.0% lipase. As free fatty acids were mainly lauric acid a rough calculation of the lauric acid concentration in the release medium can be made. Hereby a concentration of 0.94 mg/mL lauric acid (0.0047 M) was calculated (Equation 4).

**Equation 4**

$$conc_{lauric} = \frac{m_{implant} \cdot f_{degraded}}{V_{buffer}} (mg / mL)$$

$conc_{lauric}$  = concentration of lauric acid in incubation buffer

$m_{implant}$  = mass of tsc-extrudate before incubation – 90 mg

$f_{degraded}$  = relative mass of free fatty acids calculated from total implant mass [%] – 2.0%

$V_{buffer}$  = volume of incubation buffer PBS – 1.9 mL

Within the implant matrix the concentration of this free fatty acid may be even much higher. Interestingly, the stability of IFN $\alpha$  and G-CSF has been shown to be dramatically negatively affected in matrices of stearic acid [223].

In general, four main effects may result from triglyceride cleavage within lipid tsc-extrudates. First, free fatty acids can lead to an acidification within the implant matrix similarly to the effect which was observed during PLGA erosion. Although free fatty acids are less acidic ( $pK_a \sim 5-6$ ) than acetic acid ( $pK_a \sim 4.8$ ) and glycolic acid ( $pK_a \sim 3.8$ ) a high concentration of acidic substances is generated in a short period of time. [69, 78]. Second, the osmotic

pressure within the implant can increase and this can cause protein aggregation [69]. Third, triglyceride cleavage by lipase activity generates mono- and di-glycerides which can act as glue, leading to pore-closure within tsc-extrudates. Although SEM pictures indicate that tsc-extrudates became more porous upon lipase incubation, no investigations on the microscale were conducted so far to clarify this. Fourth, the generation of surface active substances like mono- and di-glycerides as well as free fatty acids and their deprotonated forms can result in decreased protein stability. The last factor seems to be the most critical one as high osmotic pressure can be assumed to be present in the implant core anyway and a pH drop from 7.4 to 5 should not result in a massive loss of lysozyme which is a very stable protein with respect to pH. Surface active substances on the contrary can ease protein unfolding and thereby destabilize the protein and promote aggregation.



#### **4. Conclusion**

The embedding of lipase into tsc-extrudates led to accelerated matrix degradation and release of free fatty acids. Although lipase did not directly degrade the model protein lysozyme, co-embedding of lipase and lysozyme into tsc-extrudates led to a non-release of lysozyme. Various factors might account for this non-release, however, no final conclusion could be drawn from the data so far. Further investigations should focus on the effect of triglyceride cleavage on protein stability and the implant (micro-)structure.

It is yet unclear to which extent the observe effect may influence the applicability of triglyceride based implant systems *in-vivo*. Tsc-extrudate erosion *in-vivo* has been proven (chapter 0) and it is highly likely that lipases (besides implant melting) have an influence on the degradation of the implants. However, low lipase concentrations in the human body, as well as a surface erosion of the implants *in-vivo* render it highly unlikely that matrix erosion might lead to protein degradation within the implant. However, concerns during long-term release might arise and thus further investigations about protein stability in triglyceride implants during *in-vivo* release need to be carried out.

From our data, the embedding of lipases into triglyceride formulations to increase the degradation rate of implants should however be avoided as *in-vitro* experiment clearly showed the detrimental effect of this approach. However, if lipases get in contact with the implant from the outer medium (e.g. *in-vivo*), lipase activity even might positively affect the release kinetics by reduction of the burst effect due to pore-closure.



## **IX. Single molecule fluorescence microscopy studies and release pathways of protein drug molecules from triglyceride based implants**

### **1. Introduction**

The general mechanisms of sustained protein release from inert matrices were already extensively reviewed [17, 222, 249]. Various factors including drug/compound particle sizes, drug load, implant geometry and preparation technique have been identified to influence protein release kinetics [187]. Furthermore it was found that macromolecular drug release from such devices was much more sustained than mathematical models predicted even if varying porosity values of the devices and smaller diffusion coefficients of the incorporated drugs were taken into account [222]. Multiple factors were identified to account for the sustained release: concentration dependent diffusion, random pore topology, sealing effects and a constricted pore geometry [17, 249]. Based on the groundbreaking work of Langer *et al.* [16, 17, 222, 249] it is common sense that the 'constricted pore-geometry' leads to a so-called 'random walk' of the protein within the inert implant matrix and is the major contributor to the sustained release behavior. Hereby, the protein diffuses upon hydration within water-filled pores inside the implant and is trapped within each pore until it finds its way out through a narrow connecting channel [222]. Due to this retention within individual pores, the release becomes sustained and very slow release rates can be achieved. However, this 'random-walk' could never be visualized or proven by any other technique than mathematical modeling [30].

Today, new techniques are available which allow the tracking of single molecules, e.g. within mesoporous matrices by wide-field fluorescence microscopy [250]. This technique was successfully used to elucidate the three-dimensional structure of nano-channels in mesostructured silica by tracking of individual dye molecules [251]. We used this technique to track individual fluorescent labeled recombinant human IFN $\alpha$  protein molecules within lipid tsc-extrudates and determined the diffusion coefficients of these molecules. Hereby we were able to elucidate the major contributors to the sustained release mechanism from tsc-

extrudates and to visualize the 'random walk' of single IFN $\alpha$  molecules in micro-pores of the triglyceride based device.

## **2. Materials and methods**

### **2.1. Materials**

Triglycerides (H12, Dynasan D118) were a gift from Sasol (Witten, Germany). PEG 6000 was donated from Clariant (Wiesbaden, Germany). Hydroxypropyl- $\beta$ -cyclodextrin (HP- $\beta$ -CD) was provided from Wacker (Burghausen, Germany). For dye labeling ATTO647N NHS-ester was purchased from ATTO-TEC (Siegen, Germany). The  $\mu$ -Stick 8-well microscopy slides and hydrophobic uncoated 0.2 mm  $\mu$ -Slide Luer® ibiTreat microscopy slides were purchased from IBIDI (Martinsried, Germany). Buffer salts were of analytical grade and bought from Merck (Darmstadt, Germany).

IFN $\alpha$  was a gift from Roche Diagnostics, Penzberg, Germany. It is formulated in 25 mM acetate buffer of pH 5.0 containing 120 mM sodium chloride. The protein concentration was 1.53 mg/mL. IFN $\alpha$  contains 165 amino acids (AA) with 4 cysteines and 2 disulfide linkages (AA 1-AA 98 and AA 29-AA 138) and has a molecular weight of 19.225 kDa. In contrast to native IFN $\alpha$ 2a it is not glycosylated and contains an extra N-terminal methionine. The secondary structure consists of a total of 6  $\alpha$ -helices (65% alpha helical) which arrange in the typical tertiary structure [252, 253]. The isoelectric point (IP) of the protein is between pH 6.0 and pH 7.0 [254].

### **2.2. Fluorescence labeling of IFN $\alpha$**

30  $\mu$ l of an IFN $\alpha$  solution (1.56 mg/mL, MW = 19.2 kDa,  $n = 2.44 \cdot 10^{-9}$  mol) were mixed with 70  $\mu$ l of a PBS solution of pH 8.0. Then approximately 0.1 mg of ATTO647N NHS-ester ( $M = 843$  g/mol,  $n = 1.18 \cdot 10^{-7}$  mol) were added. The mixture was heated at 30 °C for 1.5 h and vortexed shortly every 10 minutes. Excess unlabeled dye was removed afterwards from the fluorescent labeled proteins (fluo-IFN $\alpha$ ) by centrifugation at 2000 rcf for 1 min in a Micro Bio-Spin 6 Chromatography Column (Bio-Rad Laboratories) where the free dye was bound to the column, but the labeled protein remained in solution.

### 2.3. Protein analysis

IFN $\alpha$  was quantified by SE-HPLC in analogy to the method described by Mohl *et al.* (Dionex Ultimate 3000, flow rate: 0.5 mL/min, UV: 215 nm + 280 nm, Tosoh TSKgel 3000SWXL) [27]. Samples were additionally assessed by a fluorescence detector (excitation 644 nm; emission 669 nm) after separation by SE-HPLC.

### 2.4. Preparation of IFN $\alpha$ lyophilisates

IFN $\alpha$  was lyophilized as described by Herrmann and Mohl [24, 223]. In brief IFN $\alpha$  stock solution was concentrated to 20 mg/mL with Vivaspin 20 tubes (MWCO 5,000 – VS 2011) and admixed with a solution containing 240 mg/mL HP- $\beta$ -CD giving a final concentration of 16 mg/mL IFN $\alpha$  and 48 mg/mL HP- $\beta$ -CD (1:3 (m/m)). The solution was spiked with a dilution of freshly labeled fluo-IFN $\alpha$  and was adjusted to pH 4.2 (with acetic acid). After freeze-drying of 1 mL aliquots in 2R glass vials with an  $\epsilon$ 12G apparatus (Christ, Osterode, Germany) samples containing 64 mg of lyophilized cake were obtained. Freeze drying was performed using the following program (Table 20). The resulting cake comprised 10<sup>-9</sup> (m/m) fluo-IFN calculated from total solid mass.

### 2.1. Preparation of lipid twin-screw extrudates and protein-lipid dispersions for wide-field fluorescence spectroscopy

Lipid tsc-extrudates were prepared as described by Schulze *et al.* [32] with a Haake MiniLab<sup>®</sup> Micro Rheology Compounder (Thermo Haake GmbH, Karlsruhe, Germany). In brief, a lipid powder blend comprising D118 as high melting lipid and H12 as low melting lipid was mixed with 10% of lyophilized PEG 6000 and 10% of lyophilized IFN $\alpha$  (1:3 with HP- $\beta$ -CD [32]). Extrusion of rod-shaped implants was performed through a 1.9 mm outlet die in steady-state mode with closed bypass. Rod shaped implants were forged into a flatter cylinder by the application of pressure on the warm and formable implant after tsc-extrusion. The flat cylinder was placed into a  $\mu$ -Stick 8-well microscopy slide (ibidi GmbH, Martinsried,

Germany) and incubated in PBS pH 4.0 for wide-field fluorescence microscopy (Figure 88, left). Additionally lyophilized IFN $\alpha$  was mixed with pure H12 in a ratio of 1:10 (m/m) and heated in a beaker until the lipid became creamy. The melt was casted into  $\mu$ -Stick 8-well microscopy slides (Figure 88, right). The protein-lipid dispersion was also analyzed by wide-field fluorescence microscopy.

**Table 20: Lyophilization program for IFN $\alpha$**

	temp. [°C]	time or temperature rise	pressure [mbar]
<b>cooling step</b>	to -45 °C	1.6 °C/min	atmospheric pressure
	-45 °C	90 min	atmospheric pressure
<b>primary drying</b>	to -20 °C	0.1 °C/min	to 10 <sup>-2</sup> [mbar]
	-20 °C	30 hours	10 <sup>-2</sup> [mbar]
<b>secondary drying</b>	to +20 °C	0.1 °C/min	to 10 <sup>-3</sup> [mbar]
	+20 °C	15 hours	10 <sup>-3</sup> [mbar]
<b>sealing of vials</b>	The pressure chamber was filled with nitrogen to a pressure of 800mbar and the vials were sealed with rubber stoppers.		

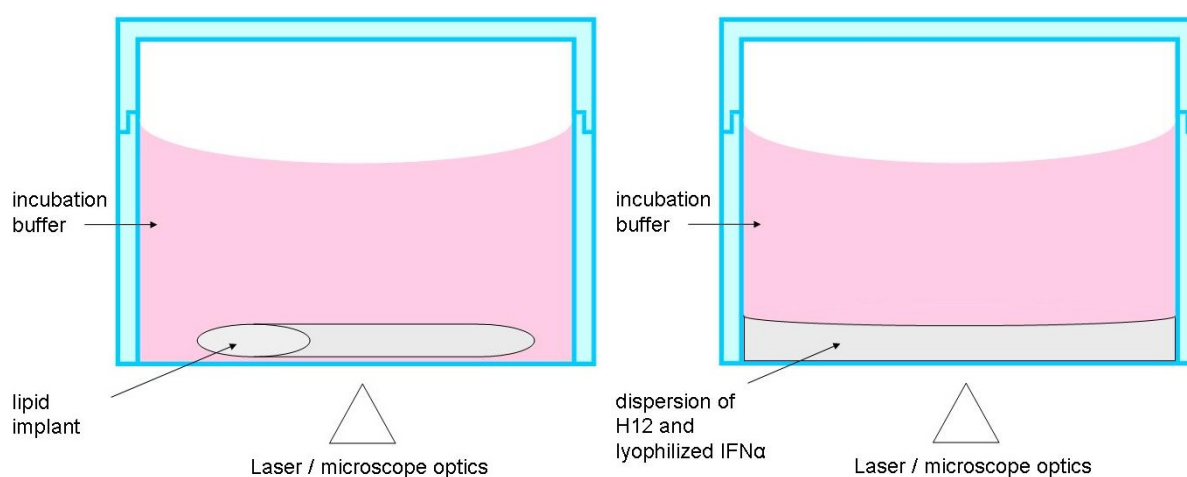


**Figure 88: Experimental setup for wide-field fluorescence spectroscopy studies of tsc-extrudates (left) and protein-lipid dispersions (right).**

## **2.2. Preparation of PEG samples for fluorescence microscopy**

PEG 6000 was dissolved in PBS pH 4.0 to give final concentrations of 30%, 40% and 53% (w/w). 15 mL of these solutions were spiked with 15  $\mu$ L of a solution of IFN $\alpha$  (conc. 1.56 mg/mL) which comprised  $1.0 \times 10^{-9}$  mg/mL of fluo-IFN $\alpha$ . Thus the theoretical concentration of fluo-IFN $\alpha$  was  $1.0 \times 10^{-12}$  mg/mL in the PEG solutions. The solution was injected into a 0.2 mm  $\mu$ -Slide Luer® ibiTreat (ibidi GmbH, Martinsried, Germany) and single fluorescence wide-field fluorescence microscopy was performed.

## **2.3. Scanning electron microscopy (SEM)**

SEM was performed with a 6500F (Jeol GmbH, Eching, Germany). Samples were dried in a vacuum chamber (VO 200, Mammert, Schwabach, Germany) at 25 °C and 20 mbar for 6 days and analyzed without coating.

## **2.4. Wide-field fluorescence microscopy**

Fluorescence images were acquired with a wide-field setup, using a Nikon Eclipse TE200 epifluorescence microscope and an oil-immersion objective with high numerical aperture (Nikon Plan Apo 100x/1.40 N.A. Oil). The Atto647N dye molecules were excited at 633 nm with a Coherent He-Ne gas laser (75 mW max. at 632.8 nm) with an intensity of 0.1-0.7 kW cm<sup>-2</sup>. The fluorescence was detected with an Andor iXion DV897 back-illuminated EM-CCD camera in frame transfer mode (512 px x 512 px). Incident laser light was blocked by a dichroic mirror (640 nm cutoff, AHF) and a band-pass filter (730/140, AHF) [251].

## **2.5. Tracking of the proteins, visualization of the random walk and calculation of diffusion coefficients**

Single particle tracking (SPT) was employed to obtain the trajectories of individual protein molecules by fitting frame by frame theoretical diffraction patterns to the spots (described in

detail by Kirschstein *et al.* [251]). With this method the positions of the fluorophores can be obtained with an accuracy of down to 10 nm.

The diffusion coefficients for each individual trajectory can be extracted from the linear part of the mean square displacement (MSD) plots according to the Einstein-Smoluchowski relation (Equation 5), assuming an isotropic Brownian diffusion in all three dimensions while only using the two-dimensional projection of the recorded images.

Equation 5 
$$MSD = 4 \cdot Dt$$

*MSD* = mean square displacement [ $nm^2$ ]

*D* = diffusion coefficient [ $nm/s$ ]

*t* = time [ $s$ ]

## 2.6. Protein release studies

Tsc-extrudates were cut into rod-shaped implants with 2.5 cm length and incubated in protein low-bind tubes (Eppendorf AG, Hamburg, Germany). For release studies from protein-lipid dispersions, the triglyceride H12 was molten at 40 °C and admixed with 10% of IFN $\alpha$  lyophilisate. Afterwards the dispersion was cast into protein low-bind Eppendorf tubes.

Protein release studies were performed in 1.9 mL isotonic PBS buffer pH 4.0 (+ 0.05% sodium acid) to avoid protein precipitation in the presence of PEG 6000 [29]. At predetermined time points the incubation buffer was completely exchanged and the samples were assessed for protein content by SE-HPLC as described above. Tsc-extrudates were incubated at 37 °C in a water bath without agitation. Protein release from lipid-protein dispersions was assessed at 20 °C, 29 °C, 33 °C and 37 °C.



### **3. Results and discussion**

#### **3.1. Scanning electron microscopy**

Scanning electron microscopy of tsc-extrudates before release tests showed a smooth and compact surface and a compact matrix with no porous structure in the core (Figure 89 A). After the release test (27 days) the matrix of the implant changed and pores and channels became visible which ranged between 1-100  $\mu\text{m}$  (Figure 89 B). The creation of large pores and an interconnected pore network was explained by dissolution and release of lyophilized PEG and protein powder from the matrix. Various authors described the formation of such a pore network to be the major driving force for total drug release from inert matrices [17, 27, 222] and the formation of pores and channels within tsc-extrudates was already described in previous chapters (IV.3.2, VI.3.5, 3.1).

#### **3.2. Quantification of fluo-IFN $\alpha$**

Determination of total protein concentration after fluorescence labeling by SE-HPLC (UV detection 215 nm + 280 nm) showed a decrease of the protein concentration from 1.6 mg/mL to 1.0 mg/mL which can be attributed to the labeling process and the subsequent protein purification step. Calculation was based on total peak area of fluorescently labeled IFN $\alpha$  monomer compared to non-labeled protein of known concentration. The UV chromatograms and the fluorescence chromatogram did not show the presence of dimers or soluble oligomers after the labeling process and thus all labeled protein was ascertained to be monomeric. The slight shift between the retention times of the UV and the fluorescence signal results from the in-line connection of the fluorescence detector after the UV detector (Figure 90).

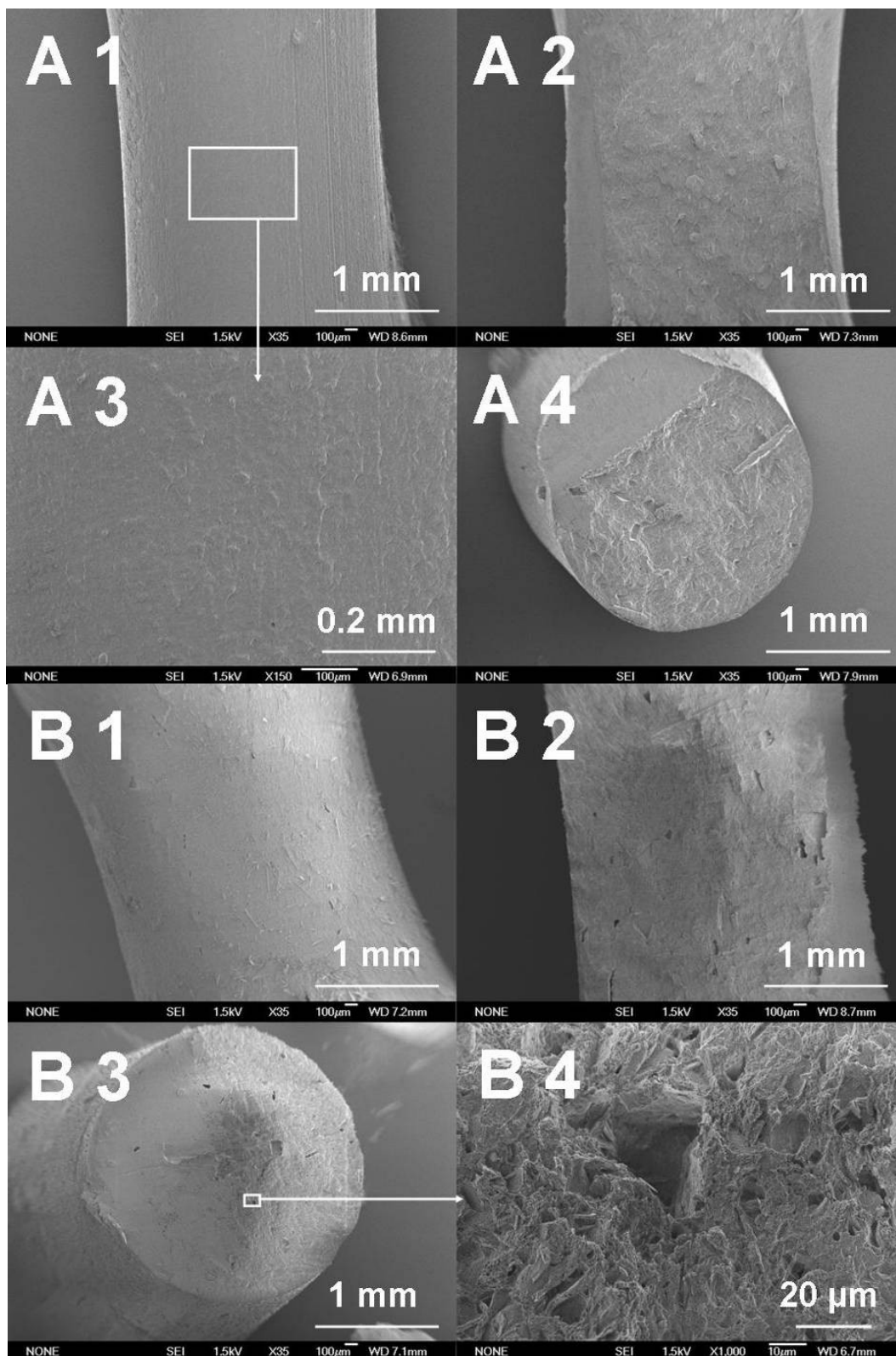
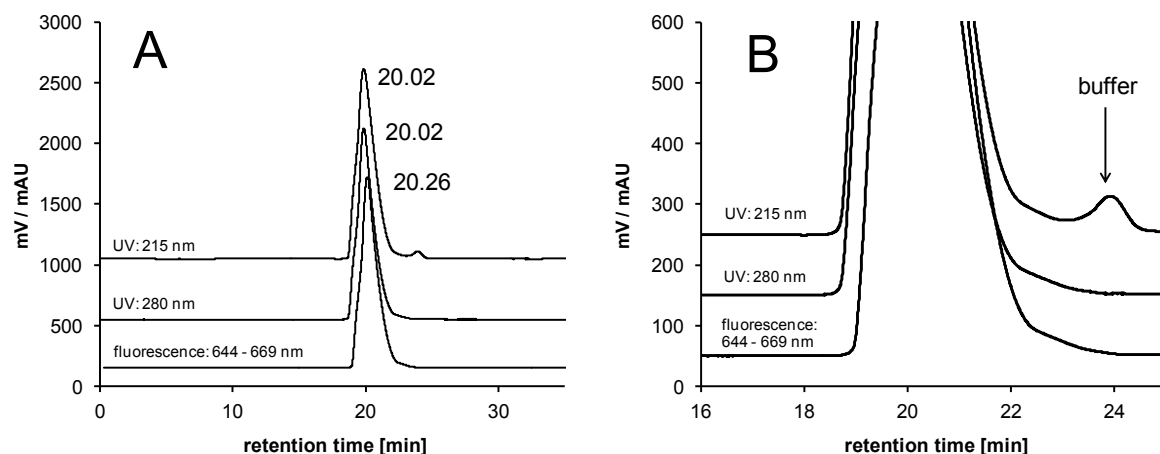


Figure 89: Scanning electron microscopy images of tsc-extrudates before (A) and after (B) *in-vitro* release tests. A 1 + B 1: Implant surface; A 2 + B 2: longitudinal cross-section; A 3: close-up of implant surface; A 4 + B 3: upright cross section; B 4: close-up of upright cross section



**Figure 90: (A) SEC chromatograms with UV (215 nm + 280 nm) and fluorescence (excitation 644 nm, emission 669 nm) detection of Atto647N dye labeled IFN $\alpha$  (fluo-IFN $\alpha$ ). (B) zoom-in of chromatogram (A)**

### 3.3. IFN $\alpha$ release studies from tsc-extrudates

The protein was released from tsc-extrudates at pH 4.0 and 37 °C in a diffusion controlled way over a period of 27 days liberating up to 96% of the incorporated protein mass. Incubation pH was set to 4.0 to prevent IFN $\alpha$  precipitation in the presence of PEG 6000 as reported by Schulze *et al.* [24, 29]. They studied IFN $\alpha$  release in the presence of PEG at two pHs (4.0 + 7.4) and showed, that PEG can be used to achieve a triphasic IFN $\alpha$  release profile from tsc-extrudates at pH 7.4 which was induced by a protein precipitation step. However, a change to pH 4.0 revealed 'normal' diffusion controlled IFN $\alpha$  release, which was also observed in our study. A linear relation between the square-root of time ( $t^{1/2}$ ) and the released amount of IFN $\alpha$  could be established (Figure 91) which is typical for a diffusion controlled release from inert matrixes according to Higuchi's square root of time kinetics [40].

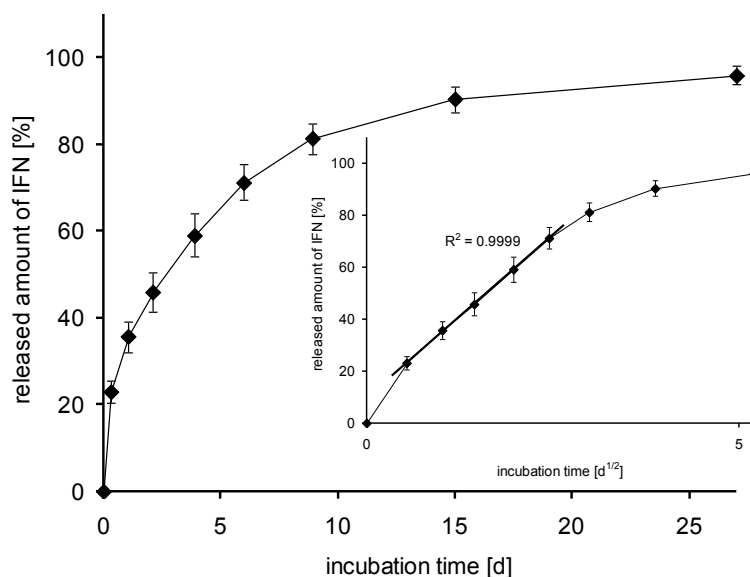


**Figure 91: IFN $\alpha$  release from tsc-extrudates (n = 6) at 37 °C in PBS buffer pH 4.0. A linear correlation between the square root of time and the released amount of protein is shown in the insert.**

### 3.4. IFN $\alpha$ release from protein-lipid dispersions

In order to mimic the behavior of IFN $\alpha$  within the H12 phase of tsc-extrudates, release experiments from H12-protein dispersion were performed. Release kinetics of IFN $\alpha$  from such dispersions were strongly dependent on incubation temperature. At 20 °C and 29 °C an initial burst release of about 4% was detected and afterwards a linear release phase started which lasted to day 14 and leveled into a plateau phase liberating a maximum of only 25% IFN $\alpha$ . DSC thermograms showed that the triglyceride was solid at these temperatures and thus only a small fraction of the protein was released whereas the main fraction remained trapped in the triglyceride matrix. At 33 °C, the release kinetics accelerated and 91% of the protein were released within 14 days. Only a part of the lipid was molten at 33 °C and the lipid-protein dispersion became 'waxy' but stayed at the bottom of the Eppendorf tube during the release test. Immediate and complete release of IFN $\alpha$  (99% within 1 day) was achieved if the incubation temperature was increased to 37 °C (Figure 92). Hereby the lipid was completely molten separated on top of the aqueous phase. Thus a strong influence of the physical properties of the lipid on the release behavior of IFN $\alpha$  was found which was identical

to our observations regarding long-term lysozyme release from tsc-extrudates without pore-forming agent (chapter VI.4.3).

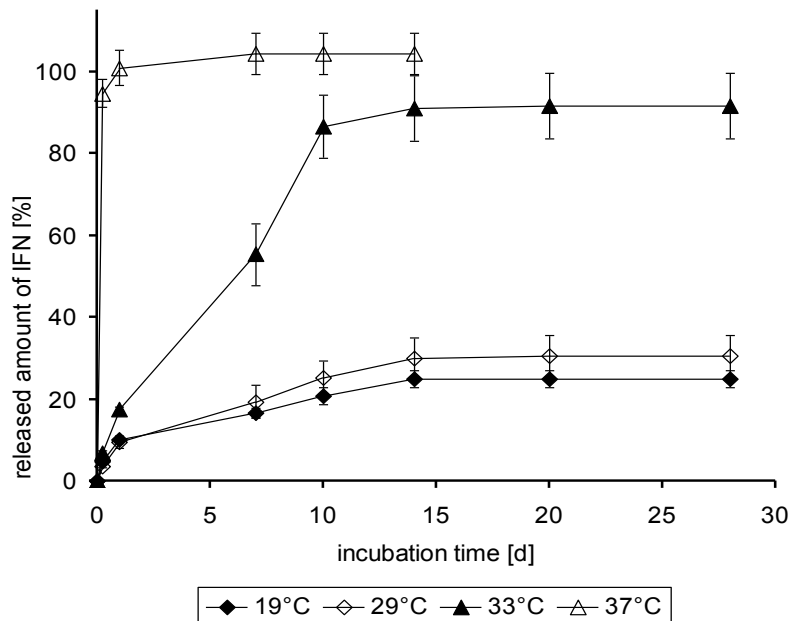
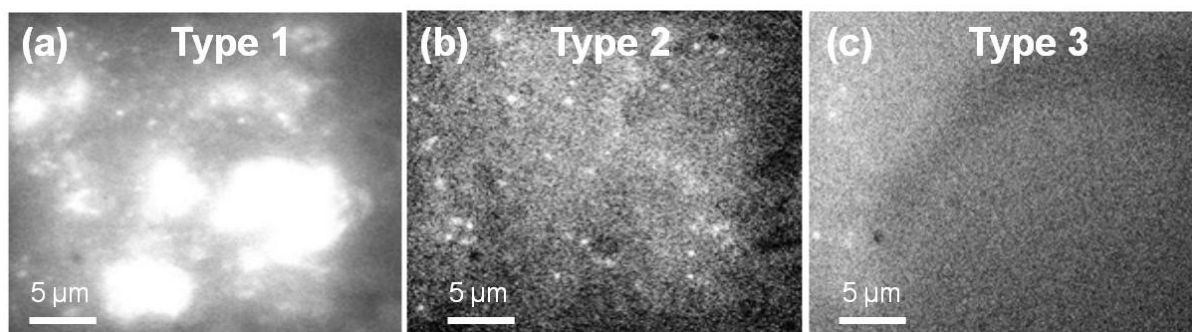


Figure 92: IFN $\alpha$  release from lipid-protein dispersions at different temperatures (19 °C, 29 °C, 33 °C, 37 °C).

### 3.5. Wide-field fluorescence microscopy of tsc-extrudates

Fluorescence microscopy of lipid tsc-extrudates at room temperature and before incubation in PBS buffer revealed a heterogeneous structure of the implant matrix. Large areas with strong fluorescence signals were detected, which had dimensions of about 1-100  $\mu\text{m}$  in diameter and were attributed to fluorescently marked protein particles (Figure 93a), as they correlated well in size and shape with the previously shown SEM images (Figure 89). Surprisingly, all other areas were not completely dark as it was expected for an inert matrix system. Instead, fluorescence signals of immobile single protein molecules were detected indicating finely distributed protein all over the implant (Figure 93b).



**Figure 93: Fluorescence microscopy images of tsc-extrudates. a) Dye-labeled protein particle reservoirs. b) Finely distributed single protein molecules. c) 'Empty pore' = area without fluorescent molecules which is created upon incubation in release medium.**

Upon incubation in PBS buffer (37 °C, pH 4.0) the situation within the implant changed and areas with strong fluorescence vanished over time (within days). In return, 'black areas' (10-100 μm) were detected with the microscope, which had the same size as the former protein particles and were identified as void spaces or 'pores' (Fig. 6c). Within these 'pores' in most cases more no fluorescent molecules could be detected which was surprising as not all of the protein was yet released from the implant (Figure 91). This finding was explained by the high velocity of the diffusing fluo-IFN $\alpha$  molecules above the resolution of the microscope and the low penetration depth of the microscope (100 μm). Thus it is possible that larger protein reservoirs were still present within the core of the implant without being visualized but still enabling IFN $\alpha$  release. Despite these limitations, we were able to track some fluo-IFN $\alpha$  molecules inside the cavities in the outer section of the implant. The mean square displacement (MSD) of the molecular movement was linear (Figure 94) and thus the movement of the proteins inside these pores was clearly diffusion controlled with an apparent mean diffusion coefficient of  $\langle D \rangle = 8.5 \pm 2.5 \times 10^{-6}$  [nm<sup>2</sup>/s].

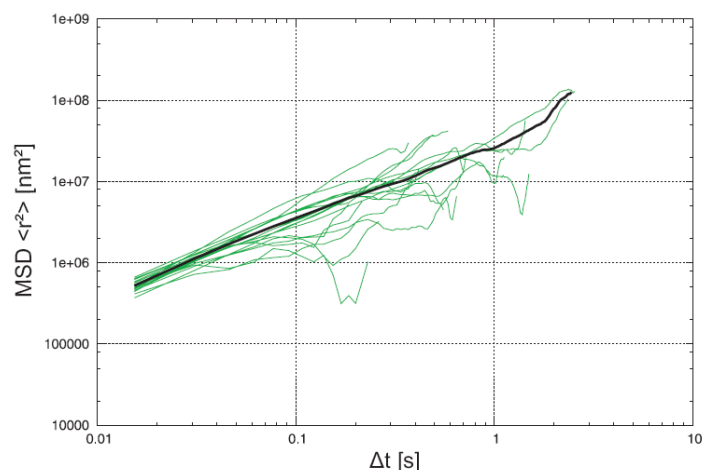


**Figure 94: Mean square displacements (MSDs) of single IFN $\alpha$  molecules (green) diffusing in a pore of a tsc-extrudate. The black line shows the mean value all single tracking experiments.**

Fluo-IFN $\alpha$  molecules which were finely dispersed in the matrix also started to move upon incubation. These molecules wandered more slowly than the ones found in the ‘pores’ and the mean diffusion coefficient was determined to be  $\langle D \rangle = 1.6 \pm 0.9 \times 10^6$  [nm<sup>2</sup>/s], which was about 10-fold lower than for proteins in the ‘pores’. The motion of this second species of fluo-IFN $\alpha$  was also only controlled by diffusion and no directed flow was found as the MSD was linearly correlated to time (Figure 95). Thus diffusion was found to be the main driving force for protein release from tsc-extrudates. However, we could clearly distinguish between two populations of diffusing proteins.

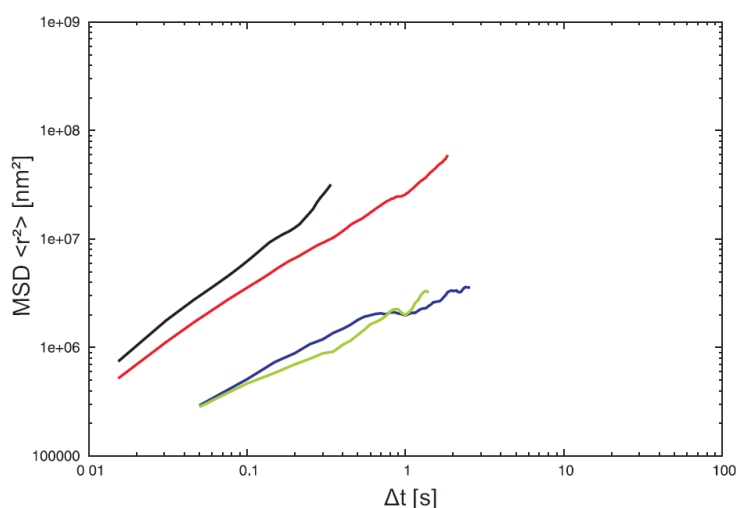


**Figure 95: MSDs of ‘fast’ (red) and ‘slow’ (blue) IFN $\alpha$  molecules diffusing in tsc-extrudates and respective molecules in PEG solution (black) or dispersions with H12 (green). The linear correlation indicates normal diffusion of the molecules. All MSDs are displayed as mean values from individual tracking experiments.**

### 3.6. Diffusion pathways of fluo-IFN $\alpha$ molecules in tsc-extrudates

So far we were able to distinguish between two different populations of fluo-IFN $\alpha$  molecules inside the implant regarding to their diffusion coefficients. We assumed that the two populations might reside in different phases of the host matrix. Theoretically, one would expect all protein to be present in the water-soluble parts of the implant, the 'pores', which are filled with solid PEG 6000 and lyophilized protein powder after preparation and later contain an aqueous solution/suspension of these compounds upon incubation in buffer. The second population of fluo-IFN $\alpha$  molecules however was thought to diffuse within the matrix of the implant in phases of molten H12. In order to proof our theory, we investigated the diffusion of IFN $\alpha$  molecules in solutions of PEG 6000 in isotonic PBS (pH 4.0, 37 °C), and also the diffusion of IFN $\alpha$  in molten H12 for comparison with the two populations found in the implant after incubation.

As already described before, highly fluorescent areas were identified in the implants before incubation in buffer and were ascribed to lyophilized protein particles. Upon incubation in buffer, protein and PEG particles dissolved and these highly fluorescent areas vanished. Only a few molecules were detected within the newly formed 'void' pores. The fact that so few molecules were found was explained by the fast diffusion of the molecules in diluted solutions of PEG. In our control experiments, a minimum concentration of 53% (w/v) PEG was necessary to allow the visualization of diffusing fluo-IFN $\alpha$  molecules. If the concentration of PEG was lower, the diffusion coefficient of the protein was too high to allow the detection and tracking of fluo-IFN $\alpha$ . Within a 53% PEG solution we tracked individual fluo-IFN $\alpha$  molecules and calculated the mean diffusion coefficient to be  $\langle D \rangle = 14.1 \pm 6.5 \times 10^6$  [nm<sup>2</sup>/s] which was in good correlation to the 'fast' fluo-IFN $\alpha$  population in the implant pores ( $\langle D \rangle = 8.5 \pm 2.5 \times 10^6$  [nm<sup>2</sup>/s]). For comparison, Herrmann *et al.* measured the diffusion coefficient of IFN $\alpha$  molecules in solutions of PBS by a modified open-end capillary technique proposed by Anderson and Saddington [29, 255]. They calculated a diffusion coefficient of IFN $\alpha$  in PBS of  $1.8 \times 10^8$  [nm<sup>2</sup>/s] which is about 17-times faster than the molecules which were detected by wide-field fluorescence spectroscopy. According to the data from Schulze *et al.* and our

control measurement with 30% and 40% PEG 6000 (in which we were not able to detect diffusing fluo-IFN $\alpha$  molecules) we concluded that IFN $\alpha$  might have been still present in the 'black areas' of our tsc-extrudate, however we were not able to detect it as the velocity of the IFN $\alpha$  molecules was too high upon rapid dissolution of PEG within the release buffer. Release data from tsc-extrudates strengthened this conclusion as release was going on for 27 days and protein must still have been present in the pores of the implants while the measurement were performed.

The second population of molecules was attributed to diffusion of IFN $\alpha$  in the molten triglyceride phase (H12) of the implant. DSC thermograms of tsc-extruded implants indicated that the low-melting lipid H12 was mostly molten at the incubation temperature of 37 °C within the implant while the other compounds (PEG 6000 and D118) were still solid or dissolved in PBS buffer (Figure 96). As already shown in release experiments, IFN $\alpha$  was rapidly released from molten protein-lipid dispersions (37 °C) and from softened lipid at 33 °C. Single-molecule tracking experiments with the lipid-protein dispersion showed that the dispersions were very heterogeneous at room temperature and large areas with strong fluorescence could be detected besides finely dispersed single protein molecules. Thus the system resembled well the situation in a tsc-extrudate before incubation. Diffusion of the finely dispersed protein molecules was observable in the lipid dispersion at 37 °C and tracking of the single molecules allowed to calculate a mean diffusion coefficient of  $\langle D \rangle = 0.9 \pm 0.4 \times 10^6$  [nm<sup>2</sup>/s] ( $\langle D \rangle_{(\text{implant})} = 1.6 \pm 0.9 \times 10^6$  [nm<sup>2</sup>/s]).

A comparison of the mean diffusion coefficients of fluoIFN $\alpha$  in either the 53% PEG solution or the lipid-protein dispersion with the diffusion coefficients of the two populations of proteins in the implant showed a striking match (Figure 97, Figure 95, Table 21). A plot of the cumulative probability ( $P(D \leq D_0)$ ) against the diffusion coefficient ( $D$ ) – which depicts the probability of  $D$  to be smaller than  $D_0$  within the chosen setup – showed a very good correlation between the 'fast' population and fluoIFN $\alpha$  in 53% PEG solution and between 'slow' population and fluoIFN $\alpha$  molecules diffusing in molten H12. 60% of proteins diffusing in 53% PEG solution had the same diffusion velocity as 'fast' molecules which were detected

within the implant and 90% of IFN $\alpha$  molecules in molten H12 diffused with the same velocity as the 'slow' population. Additionally, no overlap between the two populations was detected (Figure 97) strengthening the assumption that the populations were indeed independent from each other. We suppose, that the higher diffusion coefficient of IFN $\alpha$  in 53% PEG resulted higher concentrated PEG solution in the implant pores at a moment when the water front just reached this area. When dilution in the pores by more water took place, single molecules diffused too fast, and we could not detect them anymore. This also explains why only so few of the fast diffusing molecules could be tracked within the system.

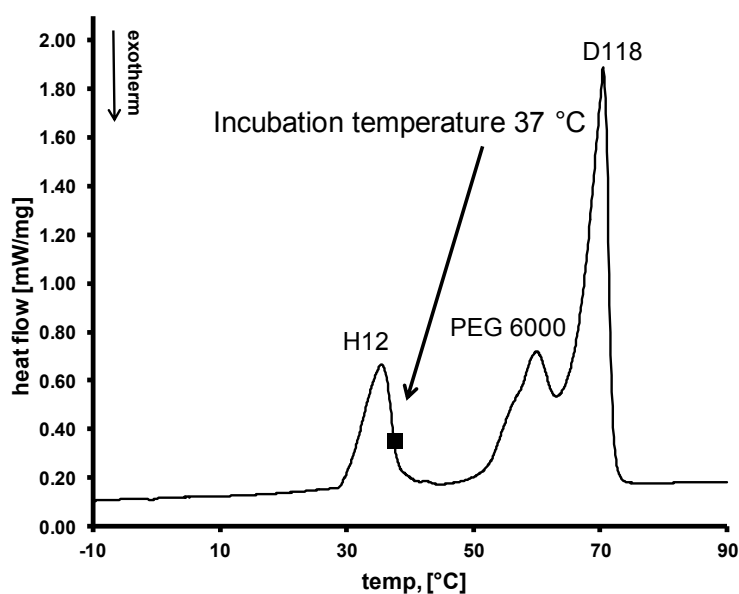


**Figure 96: DSC thermogram of a tsc-extrudate comprising the triglycerides H12, D118 and the water-soluble excipient PEG 6000.**

The diffusion of the 10-fold 'slower' protein population in the host matrix closely resembles the diffusion of IFN $\alpha$  in the protein-lipid dispersion (Figure 97, Figure 95, Table 21). This proved that IFN $\alpha$  proteins can indeed diffuse within H12 melts and explains the existence of the slow diffusing protein population in the tsc-extrudate. Diffusion of IFN $\alpha$  molecules in partially molten triglycerides also explains the IFN $\alpha$  release profiles from protein lipid dispersions. It also explains lysozyme release profiles from tsc-extrudates where total protein release was only achieved if parts of the implants were incubated above the onset of melting of the low-melting lipid (chapter 0). Thus a novel release mechanism is described here via a

non-aqueous diffusion pathway. Sustained protein release from a tsc-extruded implant system is possible by partial implant melting from a phase of molten triglycerides.

**Table 21: Diffusion coefficients of fluoIFN $\alpha$  molecules as calculated from wide-field microscopy measurements in different environments: tsc-extrudates (fast and slow species), 53% PEG solution and molten H12.**

	$\langle D \rangle$ [nm <sup>2</sup> /s]
tsc-extrudate – fast species	$8.5 \pm 2.5 \times 10^6$
53% PEG solution	$14.1 \pm 6.5 \times 10^6$
tsc-extrudate – slow species	$1.6 \pm 0.9 \times 10^6$
H12 melt at 37 °C	$0.9 \pm 0.4 \times 10^6$

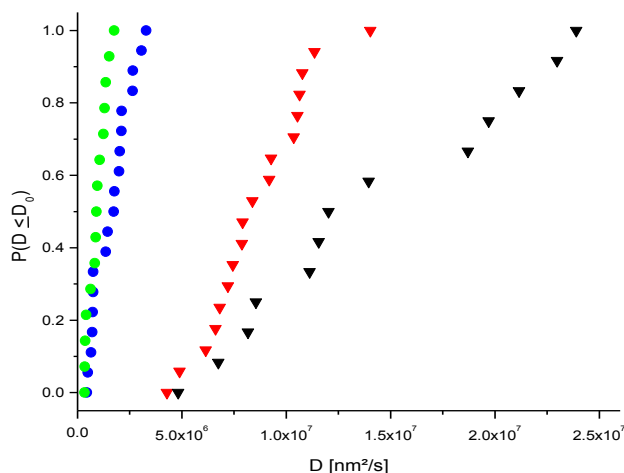


**Figure 97: Cumulative probability  $P(D \leq D_0)$  of the diffusion coefficient of fluoIFN $\alpha$  measured in control experiments to be smaller than the highest measured value found in tsc-extrudates. Blue dots: Slow diffusing protein species in tsc-extrudates. Green dots: IFN $\alpha$  molecules in molten H12. Red triangles: Fast diffusion IFN $\alpha$  proteins in pores of tsc-extrudates. Black triangles: Protein molecules diffusing in 53% PEG solution in PBS.**

### 3.7. Random walk of IFN $\alpha$ molecules

At 37 °C two different populations of diffusing proteins were detected within tsc-extrudates and were attributed to diffusion in PEG-buffer solutions and molten H12. Assessment of MSDs clearly showed a linear correlation to  $\Delta t$  which indicates free diffusion of the molecules (Figure 95) and no directed flow or 'random walk' between neighboring pores could be

visualized. This was explained by the large 3-dimensional pore-cavities ranging up to 100  $\mu\text{m}$  and the high diffusion velocities of the protein molecules. Thus the boundaries of the cavities were too far stretched to visualize a 'random walk' and only free diffusion within these pores was detected. Additionally, only a few molecules could be visualized within the implant pores, and this made it impossible to follow a molecule long enough to visualize it while it 'randomly' diffused through a connecting channel between two neighboring pores.

However, during incubation at 23 °C (below the melting temperature of H12) fast diffusing molecules were detected which wandered within micropores (0.5 x 0.5  $\mu\text{m}$ ) of the implants. As the diffusion coefficients were faster than those in H12 melts and no molten H12 was present at 23 °C the signals were attributed to protein diffusion in highly concentrated PEG-buffer-solutions. The micropores were probably created upon cooling of the lipid matrix after the manufacturing process and ranged in the nanometer and low micrometer size. Upon incubation at 37 °C no such structures were detectable anymore which was explained by a sealing of these microcavities by partial implant melting. Molecules which were detected within these microstructures showed a defined movement and free diffusion was limited by the boundaries of the micropores (Figure 98). In agreement with the random walk theory, the protein molecules were trapped within microcavities until they randomly found their way out and diffused into the next cavity. Thus the observation of the random walk on a micro-scale was feasible with the chosen setup; however not within large implant pores in the range of 100  $\mu\text{m}$ .

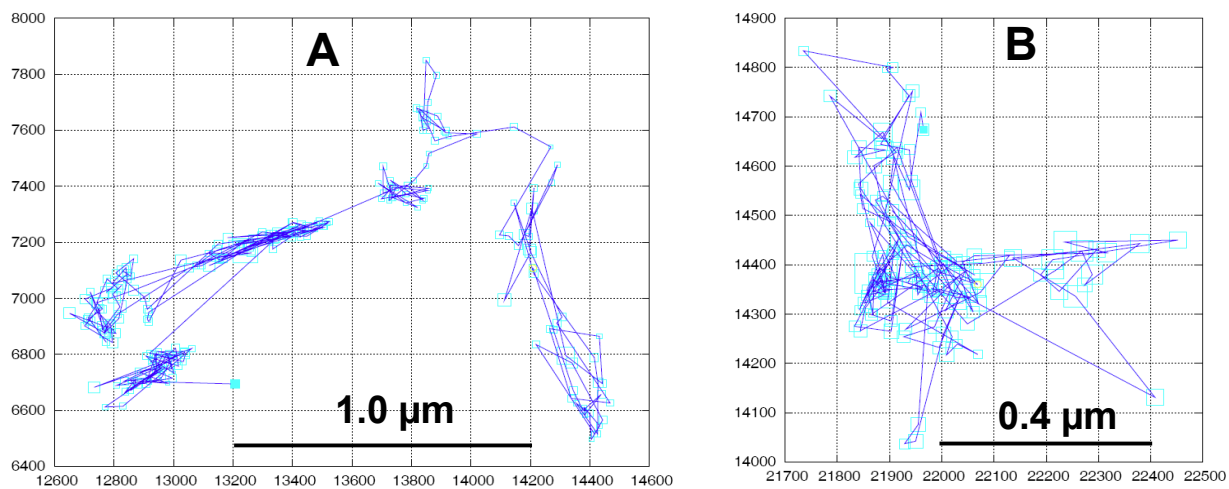


**Figure 98: Trajectories of single IFN $\alpha$  molecules diffusing in micropores within lipid tsc-extrudates with boxerrorbars.**



#### **4. Conclusion**

Various authors investigated protein release rates from inert matrices and found it being controlled by a plethora of factors including wettability of the implant [170], water entry velocity [26], particle sizes of the compounds [17, 177, 187], drug solubility [24, 29], and drug loading [17, 27, 249]. In order to achieve more sustained release profiles the use of smaller protein drug particles and a more homogeneous drug distribution within the implant matrix has been successfully used by various authors [17, 26, 177, 188, 249]. Our lipid tsc-extrudates show a sustained protein release profile which can be explained by the dense implant matrix which prevents rapid water access to the implant core (chapter 0) and a very fine and homogeneous distribution of the protein particles [179]. Additionally, partial implant melting during production (chapter 0) and release (chapter 0) have been identified to strongly influence release kinetics. Besides all mentioned factors, protein diffusion velocity within the implant system is the most important factor controlling the rate of release [26] and therefore it is reasonable to calculate an apparent drug diffusion coefficient [24, 30] to allow mathematical modeling of drug release kinetics. This apparent diffusion coefficient takes into account drug solubility, the tortuosity of implant matrix, the constricted pore-geometry between neighboring pores and of course the absolute diffusion coefficient which can be influenced by temperature and viscosity [249].

We prepared slowly releasing triglyceride based implants by tsc-extrusion and embedded fluorescent labeled IFN $\alpha$  into the matrix. Tracking of individual IFN $\alpha$  molecules within tsc-extrudates by single-molecule wide-field fluorescence microscopy allowed for the first time to measure the absolute diffusion coefficient of IFN $\alpha$  in different phases of the implants and allowed a more accurate description of the processes involved in protein release from triglyceride based matrices.

Two populations of diffusing protein molecules were detected within the implants. The first population was found to diffuse within PEG and buffer filled pores which were created upon incubation. This finding was in good agreement with theoretical considerations which explain protein release from lipid implants through an interconnected pore-network which was

created upon dissolution of hydrophilic excipients and the drug itself. Surprisingly, a second population was found to diffuse in a phase of molten lipid. We explained this by the partial melting of the implant matrix during release and concluded that implant melting during preparation led to a molecular distribution of IFN $\alpha$  in the implant matrix. Upon incubation at 37 °C the implant matrix was not completely 'inert' but acted as protein reservoir. This finding was also in good agreement to previously reported results of incomplete protein release from tsc-extrudates at incubation temperatures below the melting range of the low melting component (chapter 0). Thus, tsc-extrusion created a 'protein reservoir' in the lipid matrix which was slowly depleted by protein diffusion in the triglyceride phase and this non-aqueous diffusion explained the very slow release kinetics from tsc-extrudates at incubation temperature above the melting point of the low-melting lipid.

According to our results in chapter VI the portion of the protein which was embedded in the low melting part of the matrix accounted for approximately 20% of the total protein load. This value derived from the observation that after *in-vitro* release studies of lysozyme at 20/25 °C from highly porous implant (20% porogen) about 20% of the total protein loading had remained trapped in the matrix and had not been released.

No 'random-walk' of fluo-IFN $\alpha$  between neighboring pores was observed which was explained by the rather large three-dimensional pore-cavities and the high diffusion coefficients of the proteins. Responsible for the large pores was the particle size distribution of PEG and protein lyophilisate mechanically mixed into the lipid during extrusion. The 'random walk' between neighboring pores could only be shown in very small cavities of the implants at 20 °C which are sealed upon incubation at elevated temperatures. Although the random-walk was not directly visualized, the measurement of the *real* diffusion coefficient within pores of lipid tsc-extrudates strengthened the random-walk theory as the measured values were identical with theoretical assumptions used for modeling approaches. A mathematical modeling of the release conditions in tsc-extrudates might help to calculate the apparent diffusion coefficient from tsc-extrudates and clarify the contributions of diffusions in PEG/buffer and lipid to the sustained protein release.

## X. Final Summary

Triglyceride based lipid implants which were prepared by tsc-extrusion (tsc-extrudates) were investigated for their characteristics regarding protein release and biodegradation. Tsc-extrudates consist of a low melting and a high melting lipid, a dry protein powder formulation (drug) and a pore-forming/precipitating agent. The mixture of low melting and high melting lipids facilitates extrusion at moderate temperature without affecting protein integrity and the porogen/precipitant is used to control the rate of protein release.

We were able to establish a linear and sustained release of a monoclonal IgG<sub>1</sub> antibody (mabB) from tsc-extrudates by utilizing a precipitation and re-dissolution mechanism (chapter III). PEG was used as porogen/precipitating agent and allowed complete release of mabB from tsc-extrudates. We were able to achieve a sustained release of the antibody over a period of 150 days with very little burst. Furthermore we could proof the influence of the protein precipitation step on the antibody release rate by changing the pH of the incubation medium from 7.4 to 4.0 and thereby preventing *in-situ* precipitation of mabB. Indeed, release rates at pH 4.0 were much faster than at 7.4. Interestingly, mabB was released from tsc-extrudates mainly in its monomeric form, which was ascribed to the application of HP- $\beta$ -CD which was used as cryo-/lyo-protectant and stabilizes the protein within the triglyceride material like it was already shown for IFN $\alpha$  [28].

In chapter IV we compared 4 different methods for the preparation of triglyceride based implants (RAM extrusion, tsc-extrusion, compression and compression of tsc-extruded material) and showed that tsc-extrusion led to a more sustained lysozyme release than compression or RAM extrusion. The production of 'compressed tsc-extrudates' by grinding and subsequent compression of tsc-extrudates resulted in a more sustained protein release profile than simple compression but exhibited a similar release rate than tsc-extrusion. We got a clear indication that partial melting of the triglyceride matrix materials during the manufacturing process plays a major role in controlling release kinetics from tsc-extrudates. Minor changes in triglyceride crystallinity and melting behavior were detected in tsc-

extrudates by X-ray and DSC measurements. These changes derived from the melting process but were not negatively impacting implant stability.

Further investigations to control the rate of protein release from tsc-extrudates were carried out with lysozyme as model protein (chapter V). Various types of PEG were used to study the influence of viscosity (within implant pores) on protein release kinetics. Additionally, lyophilized PEG was compared with crystalline PEG and three different PEG particle sizes were used to prepare tsc-extrudates. It turned out, that the system was quite robust towards these factors and no major influence was detected. A change of the low-melting or high-melting lipid also had no effect on the release kinetics of lysozyme at 37 °C as long as the melting onset of the low-melting lipid was below the incubation temperature.

In chapter VI the influence of partial implant melting at 37 °C on the release kinetics was studied. Lysozyme was released from tsc-extrudates (comprising 20% porogen) at various temperatures ranging from 20 °C to 40 °C. Increasing incubation temperature resulted in accelerated protein release and a borderline between fast + complete release and slow + incomplete release was detected at an incubation temperature of 29 °C. This temperature was also identified to be the onset of melting of the low-melting lipid which led to the conclusion that lipid melting accelerated protein release. A reduction of the amount of pore forming agent PEG from 20% to 0% resulted in slower release rate and altered release profiles. Even without pore-forming agent (and only 2.5% of lysozyme), the protein was almost completely released at 37 °C over a period of 200 days. Implant rods did not change their macroscopic shape or disintegrated but remained 'intact' throughout the experiment. DSC and SEM studies as well as assessment of implant weight after long-term incubation revealed that the low-melting lipid (H12) was depleted from the implant and the implant rods became more porous and fragile. Additionally, minor changes in triglyceride crystallinity were detected (increase of  $\beta$ -modification) which might also derive from a depletion of H12 which exhibited  $\beta'$ -modification. A control experiment at 20 °C showed that only 10% of lysozyme was released under this conditions but the rest remained trapped in the solid implant matrix. In summary, it turned out that tsc-extrudates do not consist of an impermeable matrix but a

triglyceride composition which softened and partially melted during *in-vitro* release studies. Thus we detected a novel, melting associated release mechanism from 'solid' triglyceride based implants which explains complete and sustained protein release at incubation temperature above the melting point of the low-melting lipid from porogen free matrices.

Melting was identified to be a major driving force governing protein release and we found a depletion of the low-melting lipid (H12) from the implant matrix. In addition, an *in-vitro* lipase assay had already shown previously, that tsc-extrudates were more prone to lipase-induced degradation than e.g. compressed implants [33]. We assumed therefore that partial implant melting might also render tsc-extrudates more biodegradable.

In chapter 0 an *in-vivo* biodegradation study with rabbits ( $n = 9$ ) was performed over a period of 6 months by subcutaneous application of tsc-extrudates. Tsc-extrudates consisted of three ratios of PEG (0%, 20%, 40%), two different low-melting lipids (H12 or E85) and D118 as high melting lipid, and identical compositions were used in an *in-vitro* lipase-induced degradation study [33]. During *in-vivo* application, a time dependent erosion of tsc-extrudates (three timepoints: 1, 3 and 6 months) was observed and tsc-extrudates nearly completely eroded over the 6 months period (20% recovery of the triglyceride material from implants consisting of H12 + 20% PEG). Higher loadings of pore forming agent (PEG) resulted in a slightly increased mass loss and a change between low-melting lipids (E85 instead of H12) was found to slightly slow down the degradation rate. This was explained by a higher melting maximum of E85 (41 °C) than of H12 (37 °C) and thus E85-implant did not melt (and erode) to the same extent as H12-implants. Additionally, studies with lipase showed, that the enzyme preferentially cleaved lauric acid from triglycerides and this fatty acid is dominant in H12 (71%) but not in E85 (27%). Partial implant melting and triglyceride cleavage by lipases led to *in-vivo* implant erosion.

In chapter 0 the application of lipases as degradation enhancer for lipid tsc-extrudates was investigated. It turned out that the embedding of only 1% lipase (m/m) into tsc-extrudates led to a rapid breakdown of the implant matrix. Lipase was rapidly released from tsc-extrudates within 24 h even if low concentrations of only 0.1% (m/m) were embedded into the tsc-

extrudate matrix. The co-extrusion of lipase and lysozyme led to a non-release of lysozyme (model protein) from tsc-extrudates. As incubation of lipase together with lysozyme did not harm the protein, we concluded that the creation of free fatty acids, mono- and di-glycerides affected the release kinetics. Further work should focus on the influence of (bio-)degradation products on release kinetics and investigate the influence of drug diffusion and implant erosion on the overall release kinetics.

In chapter 0 single molecule tracking experiments were conducted to elucidate the sustained release of proteins from tsc-extrudates and to visualize the 'random-walk' of proteins between neighboring pores. It turned out that a visualization of the random-walk between neighboring pores was only possible at 20 °C and in the low  $\mu\text{m}$  range (0.5 – 2  $\mu\text{m}$ ). Due to the high diffusion coefficient of the fluorescently labeled proteins and the large three-dimensional structure of the implant pores (up to 100  $\mu\text{m}$ ), no long-term tracking of protein molecules was possible. Determination of the real diffusion coefficients of proteins in different phases of the implant was possible and two populations of proteins were detected. The first population diffused in PEG/water filled pores of the implant which was in accordance to theoretical expectations. The second population was much slower and diffused in a phase of molten lipid. Thus partial implant melting was confirmed to facilitate protein release and strongly contribute to the sustained release kinetics of tsc-extrudates.

In conclusion, melting processes are the key to understand the properties of twin-screw extrudates. Melting processes during extrusion allows the preparation of rod-shaped and easily applicable implants at gentle temperatures without major changes in lipid modification or deterioration of dry protein powders. The extrusion process leads to a very homogeneous distribution of drug particles within the implants and generates a triglyceride matrix which acts as a 'reservoir' by incorporation of single protein molecules. Upon incubation, partial implant melting allows long-term release of proteins from this 'reservoir' without affecting protein integrity and without the use of an additional pore-forming agent. This novel release mechanism is driven by non-aqueous diffusion of protein molecules in phases of molten

triglyceride within solid implants. Melting also facilitates biodegradation of tsc-extrudates *in-vivo* because it led to a depletion of the low-melting lipid from the implant matrix and increased the accessibility of tsc-extrudates for lipase induced degradation processes. Future work will therefore need to focus on the influence of melting-associated implant degradation (*in-vitro* and *in-vivo*) on protein release. The impact of diffusion and erosion processes on protein release from tsc-extrudates needs to be clarified in future work to allow tailoring of the release kinetics.







## REFERENCES

- [1] R.G. Werner, Economic aspects of commercial manufacture of biopharmaceuticals, *Journal of Biotechnology*, 113 (2004) 171-182.
- [2] G. Walsh, Biopharmaceutical benchmarks 2006, *Nat Biotech*, 24 (2006) 769-776.
- [3] W. Wang, Instability, stabilization, and formulation of liquid protein pharmaceuticals, *International Journal of Pharmaceutics*, 185 (1999) 129-188.
- [4] W. Wang, S. Singh, D.L. Zeng, K. King, S. Nema, Antibody structure, instability, and formulation, *Journal of Pharmaceutical Sciences*, 96 (2007) 1-26.
- [5] M.A.H. Capelle, R. Gurny, T. Arvinte, High throughput screening of protein formulation stability: Practical considerations, *European Journal of Pharmaceutics and Biopharmaceutics*, 65 (2007) 131-148.
- [6] A. Hawe, M. Sutter, W. Jiskoot, Extrinsic Fluorescent Dyes as Tools for Protein Characterization, *Pharmaceutical Research*, 25 (2008) 1487-1499.
- [7] S. Kiese, A. Pappenberg, W. Friess, H.-C. Mahler, Shaken, not stirred: Mechanical stress testing of an IgG1 antibody, *Journal of Pharmaceutical Sciences*, 97 (2008) 4347-4366.
- [8] L.T. Nguyen, J.M. Wiencek, L.E. Kirsch, Characterization methods for the physical stability of biopharmaceuticals, *PDA Journal of Pharmaceutical Science and Technology*, 57 (2003) 429-445.
- [9] J.L. Cleland, A. Daugherty, R. Mersny, Emerging protein delivery methods, *Current Opinion in Biotechnology*, 12 (2001) 212-219.
- [10] E.H. Moeller, L. Jorgensen, Alternative routes of administration for systemic delivery of protein pharmaceuticals, *Drug Discovery Today: Technologies*, 5 (2008) e89-e94.
- [11] M. van de Weert, L. Jorgensen, E. Horn Moeller, S. Frokjaer, Factors of importance for a successful delivery system for proteins, *Expert Opinion on Drug Delivery*, 2 (2005) 1029-1037.
- [12] S.E. Fineberg, T.T. Kawabata, A.S. Krasner, N.S. Fineberg, Insulin Antibodies with Pulmonary Delivery of Insulin, *Diabetes Technol. Ther.*, 9 (2007) S102-S110.
- [13] R. Langer, New methods of drug delivery, *Science*, 249 (1990) 1527-1533.
- [14] D.S. Pisal, M.P. Kosloski, S.V. Balu-Iyer, Delivery of therapeutic proteins, *Journal of Pharmaceutical Sciences*, 99 (2010) 2557-2575.
- [15] F. Ahmann, D. Citrin, H. deHaan, P. Guinan, V. Jordan, W. Kreis, M. Scott, D. Trump, Zoladex: a sustained-release, monthly luteinizing hormone-releasing hormone analogue for the treatment of advanced prostate cancer, *Journal of Clinical Oncology*, 5 (1987) 912-917.
- [16] R. Langer, J. Folkman, Polymers for the sustained release of proteins and other macromolecules, *Nature (London)*, 263 (1976) 797-800.
- [17] R.A. Siegel, J. Kost, R. Langer, Mechanistic studies of macromolecular drug release from macroporous polymers. I. Experiments and preliminary theory concerning completeness of drug release, *Journal of Controlled Release*, 8 (1989) 223-236.
- [18] F. Kreye, F. Siepmann, J. Siepmann, Lipid implants as drug delivery systems, *Expert Opinion on Drug Delivery*, 5 (2008) 291-307.
- [19] P.Y. Wang, Lipids as excipient in sustained release insulin implants, *International Journal of Pharmaceutics*, 54 (1989) 223-230.
- [20] J.S. Kent, Cholesterol matrix delivery system for sustained release of macromolecules, in, (Syntex (U.S.A.), Inc., USA). Application: US US, 1984, pp. 8 pp.
- [21] A. Maschke, Lucke, A., Vogelhuber, W., Fischbach, C., Apple, A., Blunk, T., Göpferich, A., Lipids: An alternative Material for Protein and Peptide Release, *ACS Symposium Series*, 879 (2004) 176-196.
- [22] A.K. Walduck, J.P. Opdebeeck, H.E. Benson, R. Prankerd, Biodegradable implants for the delivery of veterinary vaccines: design, manufacture and antibody responses in sheep, *Journal of Controlled Release*, 51 (1998) 269-280.
- [23] C. Guse, S. Koennings, A. Maschke, M. Hacker, C. Becker, S. Schreiner, T. Blunk, T. Spruss, A. Goepferich, Biocompatibility and erosion behavior of implants made of triglycerides and blends with cholesterol and phospholipids, *International Journal of Pharmaceutics*, 314 (2006) 153-160.
- [24] S. Herrmann, S. Mohl, F. Siepmann, J. Siepmann, G. Winter, New Insight into the Role of Polyethylene Glycol Acting as Protein Release Modifier in Lipidic Implants, *Pharmaceutical Research*, 24 (2007) 1527-1537.
- [25] S. Koennings, E. Garcion, N. Faisant, P. Menei, J.P. Benoit, A. Goepferich, In vitro investigation of lipid implants as a controlled release system for interleukin-18, *International Journal of Pharmaceutics*, 314 (2006) 145-152.
- [26] S. Koennings, J. Tessmar, T. Blunk, A. Göpferich, Confocal Microscopy for the Elucidation of Mass Transport Mechanisms Involved in Protein Release from Lipid-based Matrices, *Pharmaceutical Research*, 24 (2007) 1325-1335.

## REFERENCES

- [27] S. Mohl, G. Winter, Continuous release of rh-interferon [alpha]-2a from triglyceride matrices, *Journal of Controlled Release*, 97 (2004) 67-78.
- [28] S. Mohl, G. Winter, Continuous Release of rh-Interferon &agr;-2a from Triglyceride Implants: Storage Stability of the Dosage Forms, *Pharmaceutical Development and Technology*, 11 (2006) 103 - 110.
- [29] S. Herrmann, G. Winter, S. Mohl, F. Siepmann, J. Siepmann, Mechanisms controlling protein release from lipidic implants: Effects of PEG addition, *Journal of Controlled Release*, 118 (2007) 161-168.
- [30] F. Siepmann, S. Herrmann, G. Winter, J. Siepmann, A novel mathematical model quantifying drug release from lipid implants, *Journal of Controlled Release*, 128 (2008) 233-240.
- [31] M. Schwab, B. Kessler, E. Wolf, G. Jordan, S. Mohl, G. Winter, Correlation of in vivo and in vitro release data for rh-INF[alpha] lipid implants, *European Journal of Pharmaceutics and Biopharmaceutics*, 70 (2008) 690-694.
- [32] S. Schulze, G. Winter, Lipid extrudates as novel sustained release systems for pharmaceutical proteins, *Journal of Controlled Release*, 134 (2009) 177-185.
- [33] M. Schwab, G. Sax, S. Schulze, G. Winter, Studies on the lipase induced degradation of lipid based drug delivery systems, *Journal of Controlled Release*, 140 (2009) 27-33.
- [34] A. Zaffaroni, Systems for controlled drug delivery, *Medicinal Research Reviews*, 1 (1981) 373-386.
- [35] M.F. Saettone, L. Salminen, Ocular inserts for topical delivery, *Advanced Drug Delivery Reviews*, 16 (1995) 95-106.
- [36] S.W. Ha, E. Wintermantel, Kontrollierte therapeutische Systeme (Controlled drug delivery systems), in: E. Wintermantel, S.-W. Ha (Eds.) *Medizintechnik*, Springer Berlin Heidelberg, 2009, pp. 1297-1312.
- [37] H. Bari, A prolonged release parenteral drug delivery system - an overview, *Int. J. Pharm. Sci. Rev. Res.*, 3 (2010) 1-11.
- [38] R.S. Langer, N.A. Peppas, Present and future applications of biomaterials in controlled drug delivery systems, *Biomaterials*, 2 (1981) 201-214.
- [39] T. Higuchi, Mechanism of sustained-action medication. Theoretical analysis of rate of release of solid drugs dispersed in solid matrices, *Journal of Pharmaceutical Sciences*, 52 (1963) 1145-1149.
- [40] W.I. Higuchi, Diffusional models useful in biopharmaceutics. Drug release rate processes, *Journal of Pharmaceutical Sciences*, 56 (1967) 315-324.
- [41] W.R. Gombotz, D.K. Pettit, Biodegradable Polymers for Protein and Peptide Drug Delivery, *Bioconjugate Chemistry*, 6 (1995) 332-351.
- [42] R. Langer, N. Peppas, Chemical and Physical Structure of Polymers as Carriers for Controlled Release of Bioactive Agents: A Review, 23 (1983) 61 - 126.
- [43] V.R. Sinha, A. Trehan, Biodegradable microspheres for protein delivery, *Journal of Controlled Release*, 90 (2003) 261-280.
- [44] A. Sharma, U.S. Sharma, Liposomes in drug delivery: Progress and limitations, *International Journal of Pharmaceutics*, 154 (1997) 123-140.
- [45] K.-M. Jin, Y.-H. Kim, Injectable, thermo-reversible and complex coacervate combination gels for protein drug delivery, *Journal of Controlled Release*, 127 (2008) 249-256.
- [46] H. Kranz, R. Bodmeier, A novel in situ forming drug delivery system for controlled parenteral drug delivery, *International Journal of Pharmaceutics*, 332 (2007) 107-114.
- [47] R.M. Patel, Parenteral suspension: an overview, *Int. J. Curr. Pharm. Res.*, 2 (2010) 4-13.
- [48] A. Motulsky, M. Lafleur, A.-C. Couffin-Hoarau, D. Hoarau, F. Boury, J.-P. Benoit, J.-C. Leroux, Characterization and biocompatibility of organogels based on l-alanine for parenteral drug delivery implants, *Biomaterials*, 26 (2005) 6242-6253.
- [49] C.B. Packhaeuser, J. Schnieders, C.G. Oster, T. Kissel, In situ forming parenteral drug delivery systems: an overview, *European Journal of Pharmaceutics and Biopharmaceutics*, 58 (2004) 445-455.
- [50] D.B. Larsen, S. Joergensen, N.V. Olsen, S.H. Hansen, C. Larsen, In vivo release of bupivacaine from subcutaneously administered oily solution. Comparison with in vitro release, *Journal of Controlled Release*, 81 (2002) 145-154.
- [51] S.W. Larsen, J. Østergaard, H. Friberg-Johansen, M.N.B. Jessen, C. Larsen, In vitro assessment of drug release rates from oil depot formulations intended for intra-articular administration, *European Journal of Pharmaceutical Sciences*, 29 (2006) 348-354.
- [52] R.H. Müller, G.E. Hildebrand, Feste Lipidnanopartikel (SLN) Pharmazeutische Technologie: Moderne Arzneiformen, Lehrbuch für Studierende der Pharmazie, Nachschlagewerk für Apotheker in Offizin, Krankenhaus und Forschung, Wissenschaftliche Verlagsgesellschaft mbH, 70191 Stuttgart, (1997) 265-271.

- [53] R.H. Muller, K. Mader, S. Gohla, Solid lipid nanoparticles (SLN) for controlled drug delivery - a review of the state of the art, *European Journal of Pharmaceutics and Biopharmaceutics*, 50 (2000) 161-177.
- [54] R.H. Müller, D. Rühl, S.A. Runge, Biodegradation of solid lipid nanoparticles as a function of lipase incubation time, *International Journal of Pharmaceutics*, 144 (1996) 115-121.
- [55] K. Park, Editor, *Controlled Drug Delivery: Challenges and Strategies*, ACS, 1997.
- [56] Genentech, Genentech and Alkermes Announce Decision to Discontinue Commercialization of Nutropin Depot in, 2004.
- [57] L. Cleland Jeffrey, R. Langer, Formulation and Delivery of Proteins and Peptides, in: *Formulation and Delivery of Proteins and Peptides*, American Chemical Society, 1994, pp. 1-19.
- [58] M. Yang, S. Frokjaer, *Novel Formulation Approaches for Peptide and Protein Injectables*, John Wiley & Sons, Ltd, 2009.
- [59] S. Mao, D. Cun, Y. Kawashima, *Novel Non-Injectable Formulation Approaches of Peptides and Proteins*, John Wiley & Sons, Ltd, 2009.
- [60] C. Dai, B. Wang, H. Zhao, Microencapsulation peptide and protein drugs delivery system, *Colloids and Surfaces B: Biointerfaces*, 41 (2005) 117-120.
- [61] A. Göpferich, R. Gref, Y. Minamitake, L. Shieh, J. Alonso Maria, Y. Tabata, R. Langer, Drug Delivery from Bioerodible Polymers, in: *Formulation and Delivery of Proteins and Peptides*, American Chemical Society, 1994, pp. 242-277.
- [62] G. Zhu, S.P. Schwendeman, Stabilization of Proteins Encapsulated in Cylindrical Poly(lactide-co-glycolide) Implants: Mechanism of Stabilization by Basic Additives, *Pharmaceutical Research*, 17 (2000) 351-357.
- [63] C. Matschke, U. Isele, P. van Hoogevest, A. Fahr, Sustained-release injectables formed in situ and their potential use for veterinary products, *Journal of Controlled Release*, 85 (2002) 1-15.
- [64] M. van de Weert, W.E. Hennink, W. Jiskoot, Protein Instability in Poly(Lactic-co-Glycolic Acid) Microparticles, *Pharmaceutical Research*, 17 (2000) 1159-1167.
- [65] A. Sanchez, R.K. Gupta, M.J. Alonso, G.R. Siber, R. Langer, Pulsed controlled-release system for potential use in vaccine delivery, *Journal of Pharmaceutical Sciences*, 85 (1996) 547-552.
- [66] A. Ghassemi, M. van Steenberg, H. Talsma, C. van Nostrum, D. Crommelin, W. Hennink, Hydrophilic Polyester Microspheres: Effect of Molecular Weight and Copolymer Composition on Release of BSA, *Pharmaceutical Research*, 27 (2010) 2008-2017.
- [67] T. Arakawa, Y. Kita, J. Carpenter, Protein-Solvent Interactions in Pharmaceutical Formulations, *Pharmaceutical Research*, 8 (1991) 285-291.
- [68] H.-C. Mahler, F. Senner, K. Maeder, R. Mueller, Surface activity of a monoclonal antibody, *Journal of Pharmaceutical Sciences*, 98 (2009) 4525-4533.
- [69] A. Brunner, K. Mäder, A. Göpferich, pH and Osmotic Pressure Inside Biodegradable Microspheres During Erosion, *Pharmaceutical Research*, 16 (1999) 847-853.
- [70] L. Li, S.P. Schwendeman, Mapping neutral microclimate pH in PLGA microspheres, *Journal of Controlled Release*, 101 (2005) 163-173.
- [71] A. Lucke, A. Göpferich, Acylation of peptides by lactic acid solutions, *European Journal of Pharmaceutics and Biopharmaceutics*, 55 (2003) 27-33.
- [72] G. Crotts, T.G. Park, Protein delivery from poly(lactic-co-glycolic acid) biodegradable microspheres: Release kinetics and stability issues, *Journal of Microencapsulation*, 15 (1998) 699-713.
- [73] H. Sah, Stabilization of proteins against methylene chloride/water interface-induced denaturation and aggregation, *Journal of Controlled Release*, 58 (1999) 143-151.
- [74] L. Chen, R.N. Apte, S. Cohen, Characterization of PLGA microspheres for the controlled delivery of IL-1[alpha] for tumor immunotherapy, *Journal of Controlled Release*, 43 (1997) 261-272.
- [75] J.L. Cleland, A.J.S. Jones, Stable Formulations of Recombinant Human Growth Hormone and Interferon- $\gamma$  for Microencapsulation in Biodegradable Microspheres, *Pharmaceutical Research*, 13 (1996) 1464-1475.
- [76] K. Griebenow, A.M. Klibanov, On Protein Denaturation in Aqueous-Organic Mixtures but Not in Pure Organic Solvents, *Journal of the American Chemical Society*, 118 (1996) 11695-11700.
- [77] A. Taluja, Y.S. Youn, Y.H. Bae, Novel approaches in microparticulate PLGA delivery systems encapsulating proteins, *Journal of Materials Chemistry*, 17 (2007) 4002-4014.
- [78] G. Zhu, S.R. Mallery, S.P. Schwendeman, Stabilization of proteins encapsulated in injectable poly(lactide-co-glycolide), *Nat Biotech*, 18 (2000) 52-57.
- [79] P. Johansen, Y. Men, R. Audran, G. Corradin, H.P. Merkle, B. Gander, Improving Stability and Release Kinetics of Microencapsulated Tetanus Toxoid by Co-Encapsulation of Additives, *Pharmaceutical Research*, 15 (1998) 1103-1110.
- [80] J.T. García, M. Jesús Dorta, O. Munguía, M. Lladrés, J.B. Fariña, Biodegradable laminar implants for sustained release of recombinant human growth hormone, *Biomaterials*, 23 (2002) 4759-4764.

## REFERENCES

- [81] T.H. Kim, H. Lee, T.G. Park, Pegylated recombinant human epidermal growth factor (rhEGF) for sustained release from biodegradable PLGA microspheres, *Biomaterials*, 23 (2002) 2311-2317.
- [82] M. Diwan, T.G. Park, Stabilization of recombinant interferon-[alpha] by pegylation for encapsulation in PLGA microspheres, *International Journal of Pharmaceutics*, 252 (2003) 111-122.
- [83] K.F. Pistel, B. Bittner, H. Koll, G. Winter, T. Kissel, Biodegradable recombinant human erythropoietin loaded microspheres prepared from linear and star-branched block copolymers: Influence of encapsulation technique and polymer composition on particle characteristics, *Journal of Controlled Release*, 59 (1999) 309-325.
- [84] M. Morlock, T. Kissel, Y.X. Li, H. Koll, G. Winter, Erythropoietin loaded microspheres prepared from biodegradable LPLG-PEO-LPLG triblock copolymers: protein stabilization and in-vitro release properties, *Journal of Controlled Release*, 56 (1998) 105-115.
- [85] M. Morlock, H. Koll, G. Winter, T. Kissel, Microencapsulation of rh-erythropoietin, using biodegradable poly(d,l-lactide-co-glycolide): protein stability and the effects of stabilizing excipients, *European Journal of Pharmaceutics and Biopharmaceutics*, 43 (1997) 29-36.
- [86] J. Yang, J.L. Cleland, Factors affecting the in vitro release of recombinant human interferon- $\gamma$  (rhIFN- $\gamma$ ) from PLGA microspheres, *Journal of Pharmaceutical Sciences*, 86 (1997) 908-914.
- [87] J. Heller, Use of Poly(ortho esters) and Polyanhydrides in the Development of Peptide and Protein Delivery Systems, in: *Formulation and Delivery of Proteins and Peptides*, American Chemical Society, 1994, pp. 292-305.
- [88] K. Nagpal, S.K. Singh, D.N. Mishra, Chitosan Nanoparticles: A Promising System in Novel Drug Delivery, *Chemical & Pharmaceutical Bulletin*, 58 (2010) 1423-1430.
- [89] M. Amidi, E. Mastrobattista, W. Jiskoot, W.E. Hennink, Chitosan-based delivery systems for protein therapeutics and antigens, *Advanced Drug Delivery Reviews*, 62 (2010) 59-82.
- [90] R. Fernández-Urrusuno, P. Calvo, C. Remuñán-López, J.L. Vila-Jato, M. José Alonso, Enhancement of Nasal Absorption of Insulin Using Chitosan Nanoparticles, *Pharmaceutical Research*, 16 (1999) 1576-1581.
- [91] S. Dumitriu, E. Chornet, Inclusion and release of proteins from polysaccharide-based polyion complexes, *Advanced Drug Delivery Reviews*, 31 (1998) 223-246.
- [92] M.F. Shamji, P. Hwang, R.W. Bullock, S.B. Adams, D.L. Nettles, L.A. Setton, Release and activity of anti-TNF $\alpha$  therapeutics from injectable chitosan preparations for local drug delivery, *Journal of Biomedical Materials Research Part B: Applied Biomaterials*, 90B (2009) 319-326.
- [93] W. Friess, H. Uludag, S. Foskett, R. Biron, C. Sargeant, Characterization of absorbable collagen sponges as rhBMP-2 carriers, *International Journal of Pharmaceutics*, 187 (1999) 91-99.
- [94] W. Friess, Collagen - biomaterial for drug delivery, *European Journal of Pharmaceutics and Biopharmaceutics*, 45 (1998) 113-136.
- [95] M.G. Marks, C. Doillon, F.H. Silvert, Effects of fibroblasts and basic fibroblast growth factor on facilitation of dermal wound healing by type I collagen matrices, *Journal of Biomedical Materials Research*, 25 (1991) 683-696.
- [96] K. Fujioka, Y. Takada, S. Sato, T. Miyata, Novel delivery system for proteins using collagen as a carrier material: the minipellet, *Journal of Controlled Release*, 33 (1995) 307-315.
- [97] O.C.M. Chan, K.F. So, B.P. Chan, Fabrication of nano-fibrous collagen microspheres for protein delivery and effects of photochemical crosslinking on release kinetics, *Journal of Controlled Release*, 129 (2008) 135-143.
- [98] Y.M. Kolambkar, K.M. Dupont, J.D. Boerckel, N. Huebsch, D.J. Mooney, D.W. Hutmacher, R.E. Guldberg, An alginate-based hybrid system for growth factor delivery in the functional repair of large bone defects, *Biomaterials*, 32 (2011) 65-74.
- [99] M. Kimura, H. Mizushima, T. Igarashi, T. Matsuishi, Water-insoluble sustained-release compositions containing proteins or peptides, and manufacture thereof by precipitation method, in, (LTT Inst. Co., Ltd., Japan). Application: JP  
JP, 2003, pp. 9 pp.
- [100] W.M. Tian, C.L. Zhang, S.P. Hou, X. Yu, F.Z. Cui, Q.Y. Xu, S.L. Sheng, H. Cui, H.D. Li, Hyaluronic acid hydrogel as Nogo-66 receptor antibody delivery system for the repairing of injured rat brain: in vitro, *Journal of Controlled Release*, 102 (2005) 13-22.
- [101] A.R. Ahmed, A. Dashevsky, R. Bodmeier, Drug release from and sterilization of in situ cubic phase forming monoglyceride drug delivery systems, *European Journal of Pharmaceutics and Biopharmaceutics*, 75 (2010) 375-380.
- [102] K. Malik, I. Singh, M. Nagpal, S. Arora, Atrigel: A potential parenteral controlled drug delivery system, *Pharm. Sin.*, 1 (2010) 74-81.
- [103] G.M. Zentner, R. Rathi, C. Shih, J.C. McRea, M.-H. Seo, H. Oh, B.G. Rhee, J. Mestecky, Z. Moldoveanu, M. Morgan, S. Weitman, Biodegradable block copolymers for delivery of proteins and water-insoluble drugs, *Journal of Controlled Release*, 72 (2001) 203-215.

- [104] S. Singh, D.C. Webster, J. Singh, Thermosensitive polymers: Synthesis, characterization, and delivery of proteins, *International Journal of Pharmaceutics*, 341 (2007) 68-77.
- [105] F. Kang, J. Singh, In vitro release of insulin and biocompatibility of in situ forming gel systems, *International Journal of Pharmaceutics*, 304 (2005) 83-90.
- [106] E. Fahy, S. Subramaniam, H.A. Brown, C.K. Glass, A.H. Merrill, R.C. Murphy, C.R.H. Raetz, D.W. Russell, Y. Seyama, W. Shaw, T. Shimizu, F. Spener, G. van Meer, M.S. VanNieuwenhze, S.H. White, J.L. Witztum, E.A. Dennis, A comprehensive classification system for lipids, *Journal of Lipid Research*, 46 (2005) 839-862.
- [107] Swarbrick J., J.C. Boylan, Lipids in pharmaceutical dosage forms, in: *Encyclopedia of pharmaceutical technology*, Marcel Dekker Inc., 1992, pp. 417-476.
- [108] S. Chakraborty, D. Shukla, B. Mishra, S. Singh, Lipid - An emerging platform for oral delivery of drugs with poor bioavailability, *European Journal of Pharmaceutics and Biopharmaceutics*, 73 (2009) 1-15.
- [109] V. Jannin, J. Musakhanian, D. Marchaud, Approaches for the development of solid and semi-solid lipid-based formulations, *Advanced Drug Delivery Reviews*, 60 (2008) 734-746.
- [110] K.R.J. Anand U. Kyatanwar \*, Vilasrao J. Kadam., Self micro-emulsifying drug delivery system (SMEDDS) : Review, 2009.
- [111] C.W. Pouton, C.J.H. Porter, Formulation of lipid-based delivery systems for oral administration: Materials, methods and strategies, *Advanced Drug Delivery Reviews*, 60 (2008) 625-637.
- [112] M. Rawat, D. Singh, S. Saraf, S. Saraf, Lipid Carriers: A Versatile Delivery Vehicle for Proteins and Peptides, *YAKUGAKU ZASSHI*, 128 (2008) 269-280.
- [113] R. Bodmeier, J. Wang, H. Bhagwatwar, Process and formulation variables in the preparation of wax microparticles by a melt dispersion technique. I. Oil-in-water technique for water-insoluble drugs, *Journal of Microencapsulation*, 9 (1992) 89-98.
- [114] R. Bodmeier, J. Wang, H. Bhagwatwar, Process and formulation variables in the preparation of wax microparticles by a melt dispersion technique. II. W/O/W multiple emulsion technique for water-soluble drugs, *Journal of Microencapsulation*, 9 (1992) 99-107.
- [115] C. Thies, I. Ribeiro Dos Santos, J. Richard, V. VandeVelde, H. Rolland, J.P. Benoit, A supercritical fluid-based coating technology 1: Process considerations, *Journal of Microencapsulation*, 20 (2003) 87-96.
- [116] W. Steber, R. Fishbein, S.M. Cady, Compositions for parenteral administration of biologically active proteins and peptides, in, (American Cyanamid Co., USA). Application: EP  
EP, 1988, pp. 26 pp.
- [117] H. Reithmeier, J. Herrmann, A. Gopferich, Lipid microparticles as a parenteral controlled release device for peptides, *Journal of Controlled Release*, 73 (2001) 339-350.
- [118] H. Reithmeier, J. Herrmann, A. Göpferich, Development and characterization of lipid microparticles as a drug carrier for somatostatin, *International Journal of Pharmaceutics*, 218 (2001) 133-143.
- [119] M.D. Del Curto, D. Chicco, M. D'Antonio, V. Ciolli, H. Dannan, S. D'Urso, B. Neuteboom, S. Pompili, S. Schiesaro, P. Esposito, Lipid microparticles as sustained release system for a GnRH antagonist (Antide), *Journal of Controlled Release*, 89 (2003) 297-310.
- [120] R.I. Dos Santos, J. Richard, B. Pech, C. Thies, J.P. Benoit, Microencapsulation of protein particles within lipids using a novel supercritical fluid process, *International Journal of Pharmaceutics*, 242 (2002) 69-78.
- [121] I.R. Dos Santos, J. Richard, C. Thies, B. Pech, J.P. Benoit, A supercritical fluid-based coating technology. 3: Preparation and characterization of bovine serum albumin particles coated with lipids, *Journal of Microencapsulation*, 20 (2003) 110 - 128.
- [122] I.R. Dos Santos, C. Thies, J. Richard, D.L. Meurlay, V. Gajan, V. Vandevelde, J.P. Benoit, A supercritical fluid-based coating technology. 2: Solubility considerations, *Journal of Microencapsulation*, 20 (2003) 97 - 109.
- [123] A. Bot, D. Smith, S. Bot, L. Dellamary, T. Tarara, S. Harders, W. Phillips, J. Weers, C. Woods, Receptor-Mediated Targeting of Spray-Dried Lipid Particles Coformulated with Immunoglobulin and Loaded with a Prototype Vaccine, *Pharmaceutical Research*, 18 (2001) 971-979.
- [124] A.I. Bot, T.E. Tarara, D.J. Smith, S.R. Bot, C.M. Woods, J.G. Weers, Novel Lipid-Based Hollow-Porous Microparticles as a Platform for Immunoglobulin Delivery to the Respiratory Tract, *Pharmaceutical Research*, 17 (2000) 275-283.
- [125] A. Maschke, C. Becker, D. Eyrich, J. Kiermaier, T. Blunk, A. Gopferich, Development of a spray congealing process for the preparation of insulin-loaded lipid microparticles and characterization thereof, *European Journal of Pharmaceutics and Biopharmaceutics*, 65 (2007) 175-187.
- [126] A. Zaky, A. Elbakry, A. Ehmer, M. Breunig, A. Goepferich, The mechanism of protein release from triglyceride microspheres, *Journal of Controlled Release*, 147 (2010) 202-210.

## REFERENCES

- [127] J. Richard, F. Fais, H.G. Baldascini, Solid lipid microcapsules for sustained-release containing human growth hormone, in, (Merck Serono S.A., Switz.). Application: WO WO, 2010, pp. 60pp.
- [128] A. Domb, Liposheres for controlled delivery of substances, United States Patent 5,188,837, (1993).
- [129] A. Domb, Lipospheres for Controlled Delivery of Substances, in: Microencapsulation, Informa Healthcare, 2005, pp. 297-316.
- [130] S. Koennings, A. Goepferich, Lipospheres as delivery systems for peptides and proteins, *Lipospheres in Drug Targets and Delivery*, (2005) 67-86.
- [131] S.A. Wissing, O. Kayser, R.H. Müller, Solid lipid nanoparticles for parenteral drug delivery, *Advanced Drug Delivery Reviews*, 56 (2004) 1257-1272.
- [132] S. Martins, B. Sarmento, D.C. Ferraira, E.B. Souto, Lipid-based colloidal carriers for peptide and protein delivery - liposomes versus lipid nanoparticles, *International Journal of Nanomedicine*, 2 (2007) 595-607.
- [133] S. Li, B. Zhao, F. Wang, M. Wang, S. Xie, S. Wang, C. Han, L. Zhu, W. Zhou, Yak interferon-alpha loaded solid lipid nanoparticles for controlled release, *Research in Veterinary Science*, 88 (2010) 148-153.
- [134] R. Yang, R.-C. Gao, C.-F. Cai, H. Xu, F. Li, H.-B. He, X. Tang, Preparation of Gel-Core-Solid Lipid Nanoparticle: A Novel Way to Improve the Encapsulation of Protein and Peptide, *Chemical & Pharmaceutical Bulletin*, 58 (2010) 1195-1202.
- [135] R. Yang, R. Gao, F. Li, H. He, X. Tang, The influence of lipid characteristics on the formation, in vitro release, and in vivo absorption of protein-loaded SLN prepared by the double emulsion process, *Drug Development and Industrial Pharmacy*, 37 (2011) 139-148.
- [136] A.J. Almeida, S. Runge, R.H. Müller, Peptide-loaded solid lipid nanoparticles (SLN): Influence of production parameters, *International Journal of Pharmaceutics*, 149 (1997) 255-265.
- [137] M.A. Schubert, C.C. Muller-Goymann, Characterisation of surface-modified solid lipid nanoparticles (SLN): Influence of lecithin and nonionic emulsifier, *European Journal of Pharmaceutics and Biopharmaceutics*, 61 (2005) 77-86.
- [138] N. Pedersen, S. Hansen, A.V. Heydenreich, H.G. Kristensen, H.S. Poulsen, Solid lipid nanoparticles can effectively bind DNA, streptavidin and biotinylated ligands, *European Journal of Pharmaceutics and Biopharmaceutics*, 62 (2006) 155-162.
- [139] A.J. Almeida, E. Souto, Solid lipid nanoparticles as a drug delivery system for peptides and proteins, *Advanced Drug Delivery Reviews*, 59 (2007) 478-490.
- [140] A.D. Bangham, M.M. Standish, J.C. Watkins, Diffusion of univalent ions across the lamellae of swollen phospholipids, *Journal of molecular biology*, 13 (1965) 238-252, IN226-IN227.
- [141] V.P. Torchilin, Recent advances with liposomes as pharmaceutical carriers, *Nat Rev Drug Discov*, 4 (2005) 145-160.
- [142] J.W. Park, D.B. Kirpotin, K. Hong, R. Shalaby, Y. Shao, U.B. Nielsen, J.D. Marks, D. Papahadjopoulos, C.C. Benz, Tumor targeting using anti-her2 immunoliposomes, *Journal of Controlled Release*, 74 (2001) 95-113.
- [143] M. Woodle, G. Storm, M. Newman, J. Jekot, L. Collins, F. Martin, J.F. Szoka, Prolonged Systemic Delivery of Peptide Drugs by Long-Circulating Liposomes: Illustration with Vasopressin in the Brattleboro Rat, *Pharmaceutical Research*, 9 (1992) 260-265.
- [144] E. Kanaoka, K. Takahashi, T. Yoshikawa, H. Jizomoto, Y. Nishihara, K. Hirano, A novel and simple type of liposome carrier for recombinant interleukin-2, *Journal of Pharmacy and Pharmacology*, 53 (2001) 295-302.
- [145] G. Storm, F. Koppenhagen, A. Heeremans, M. Vingerhoeds, M.C. Woodle, D.J.A. Crommelin, Novel developments in liposomal delivery of peptides and proteins, *Journal of Controlled Release*, 36 (1995) 19-24.
- [146] A. Kim, M.-O. Yun, Y.-K. Oh, W.-S. Ahn, C.-K. Kim, Pharmacodynamics of insulin in polyethylene glycol-coated liposomes, *International Journal of Pharmaceutics*, 180 (1999) 75-81.
- [147] M.A. Kisel, L.N. Kulik, I.S. Tsybovsky, A.P. Vlasov, M.S. Vorob'yov, E.A. Kholodova, Z.V. Zabarovskaya, Liposomes with phosphatidylethanol as a carrier for oral delivery of insulin: studies in the rat, *International Journal of Pharmaceutics*, 216 (2001) 105-114.
- [148] H. Li, J.-H. Song, J.-S. Park, K. Han, Polyethylene glycol-coated liposomes for oral delivery of recombinant human epidermal growth factor, *International Journal of Pharmaceutics*, 258 (2003) 11-19.
- [149] N.S. Postma, D.J.A. Crommelin, W.M.C. Eling, J. Zuidema, Treatment with Liposome-Bound Recombinant Human Tumor Necrosis Factor- $\alpha$  Suppresses Parasitemia and Protects against Plasmodium berghei k173-Induced Experimental Cerebral Malaria in Mice, *Journal of Pharmacology and Experimental Therapeutics*, 288 (1999) 114-120.

- [150] S. Mantripragada, A lipid based depot (DepoFoam® technology) for sustained release drug delivery, *Progress in Lipid Research*, 41 (2002) 392-406.
- [151] J. Qiu, X.-h. Wei, F. Geng, R. Liu, J.-w. Zhang, Y.-h. Xu, Multivesicular liposome formulations for the sustained delivery of interferon [alpha]-2b, *Acta Pharmacol Sin*, 26 (2005) 1395-1401.
- [152] N.V. Katre, J. Asherman, H. Schaefer, M. Hora, Multivesicular liposome (DepoFoam) technology for the sustained delivery of insulin-like growth factor-I (IGF-I), *Journal of Pharmaceutical Sciences*, 87 (1998) 1341-1346.
- [153] M.V. Langston, M.P. Ramprasad, T.T. Kararli, G.R. Galluppi, N.V. Katre, Modulation of the sustained delivery of myelopoietin (Leridistim) encapsulated in multivesicular liposomes (DepoFoam), *Journal of Controlled Release*, 89 (2003) 87-99.
- [154] Q. Ye, J. Asherman, M. Stevenson, E. Brownson, N.V. Katre, DepoFoam(TM) technology: a vehicle for controlled delivery of protein and peptide drugs, *Journal of Controlled Release*, 64 (2000) 155-166.
- [155] C. Tardi, M. Brandl, R. Schubert, Erosion and controlled release properties of semisolid vesicular phospholipid dispersions, *Journal of Controlled Release*, 55 (1998) 261-270.
- [156] M. Brandl, Vesicular Phospholipid Gels: A Technology Platform, *Journal of Liposome Research*, 17 (2007) 15-26.
- [157] U. Massing, S. Cicko, V. Zirolì, Dual asymmetric centrifugation (DAC)--A new technique for liposome preparation, *Journal of Controlled Release*, 125 (2008) 16-24.
- [158] G. Winter, Vesicular phospholipid gels comprising proteinaceous substances, in: Winter, Gerhard (Penzberg, DE), United States, 2010.
- [159] W. Tian, S. Schulze, M. Brandl, G. Winter, Vesicular phospholipid gel-based depot formulations for pharmaceutical proteins: Development and in vitro evaluation, *Journal of Controlled Release*, 142 (2010) 319-325.
- [160] W. Tian, The Development of Sustained Release Formulation for Pharmaceutical Proteins based on Vesicular Phospholipid Gels, in: Department of Chemistry and Pharmacy, LMU Munich, Munich, 2010.
- [161] J.C. Shah, Y. Sadhale, D.M. Chilukuri, Cubic phase gels as drug delivery systems, *Advanced Drug Delivery Reviews*, 47 (2001) 229-250.
- [162] S.B. Leslie, S. Puvvada, B.R. Ratna, A.S. Rudolph, Encapsulation of hemoglobin in a bicontinuous cubic phase lipid, *Biochimica et Biophysica Acta (BBA) - Biomembranes*, 1285 (1996) 246-254.
- [163] B. Ericsson, K. Larsson, K. Fontell, A cubic protein-monoolein-water phase, *Biochimica et Biophysica Acta (BBA) - Biomembranes*, 729 (1983) 23-27.
- [164] Y. Sadhale, J.C. Shah, Stabilization of insulin against agitation-induced aggregation by the GMO cubic phase gel, *International Journal of Pharmaceutics*, 191 (1999) 51-64.
- [165] Y. Sadhale, J.C. Shah, Biological activity of insulin in GMO gels and the effect of agitation, *International Journal of Pharmaceutics*, 191 (1999) 65-74.
- [166] P.T. Spicer, K.L. Hayden, M.L. Lynch, A. Ofori-Boateng, J.L. Burns, Novel Process for Producing Cubic Liquid Crystalline Nanoparticles (Cubosomes), *Langmuir*, 17 (2001) 5748-5756.
- [167] S.B. Rizwan, D. Assmus, A. Boehnke, T. Hanley, B.J. Boyd, T. Rades, S. Hook, Preparation of phytantriol cubosomes by solvent precursor dilution for the delivery of protein vaccines, *European Journal of Pharmaceutics and Biopharmaceutics*, In Press, Corrected Proof.
- [168] S.B. Rizwan, T. Hanley, B.J. Boyd, T. Rades, S. Hook, Liquid crystalline systems of phytantriol and glyceryl monooleate containing a hydrophilic protein: Characterisation, swelling and release kinetics, *Journal of Pharmaceutical Sciences*, 98 (2009) 4191-4204.
- [169] B. Appel, A. Maschke, B. Weiser, H. Sarhan, C. Englert, P. Angele, T. Blunk, A. Gopferich, Lipidic implants for controlled release of bioactive insulin: Effects on cartilage engineered in vitro, *International Journal of Pharmaceutics*, 314 (2006) 170-178.
- [170] S. Koennings, A. Berie, J. Tessmar, T. Blunk, A. Gopferich, Influence of wettability and surface activity on release behavior of hydrophilic substances from lipid matrices, *Journal of Controlled Release*, 119 (2007) 173-181.
- [171] P.Y. Wang, Palmitic acid as an excipient in implants for sustained release of insulin, *Biomaterials*, 12 (1991) 57-62.
- [172] W. Vogelhuber, E. Magni, M. Mouro, Spru, szlig, T., C. Guse, A. Gazzaniga, ouml, A. pferich, Monolithic Triglyceride Matrices: A Controlled-Release System for Proteins, *Pharmaceutical Development and Technology*, 8 (2003) 71 - 79.
- [173] P.Y. Wang, Prolonged release of insulin by cholesterol-matrix implant, *Diabetes*, 36 (1987) 1068-1072.
- [174] M.Z.I. Khan, I.G. Tucker, J.P. Opdebeeck, Cholesterol and lecithin implants for sustained release of antigen: release and erosion in vitro, and antibody response in mice, *International Journal of Pharmaceutics*, 76 (1991) 161-170.

## REFERENCES

- [175] M.Z.I. Khan, I.G. Tucker, J.P. Opdebeeck, Evaluation of cholesterol-lecithin implants for sustained delivery of antigen: release in vivo and single-step immunisation of mice, *International Journal of Pharmaceutics*, 90 (1993) 255-262.
- [176] T. Morita, Y. Horikiri, H. Yamahara, T. Suzuki, H. Yoshino, Formation and Isolation of Spherical Fine Protein Microparticles Through Lyophilization of Protein-Poly(ethylene Glycol) Aqueous Mixture, *Pharmaceutical Research*, 17 (2000) 1367-1373.
- [177] S. Koennings, A. Sapin, T. Blunk, P. Menei, A. Goepferich, Towards controlled release of BDNF -- Manufacturing strategies for protein-loaded lipid implants and biocompatibility evaluation in the brain, *Journal of Controlled Release*, 119 (2007) 163-172.
- [178] G. Winter, S. Schulze, Extruded rod-shaped implants comprising high melting and low melting lipid components, for controlled release of biological substances to humans and animals, in, (Ludwig-Maximilians-Universitaet, Germany). Application: WO  
WO, 2009, pp. 92pp.
- [179] S. Herrmann, Lipidic Implants for Pharmaceutical Proteins: Mechanisms of Release and Development of Extruded Devices, in, 2007.
- [180] R. Langer, Polymeric delivery systems for controlled drug release, *Chemical Engineering Communications*, 6 (1980) 1 - 48.
- [181] P.L. Ritger, N.A. Peppas, A simple equation for description of solute release I. Fickian and non-fickian release from non-swellable devices in the form of slabs, spheres, cylinders or discs, *Journal of Controlled Release*, 5 (1987) 23-36.
- [182] F. Brandl, F. Kastner, R.M. Gschwind, T. Blunk, J. Teßmar, A. Göpferich, Hydrogel-based drug delivery systems: Comparison of drug diffusivity and release kinetics, *Journal of Controlled Release*, 142 (2010) 221-228.
- [183] J.R.S. Peery, CA, US), Dionne, Keith E. (Menlo Park, CA, US), Eckenhoff, James B. (Los Altos, CA, US), Eckenhoff, Legal Representative Bonnie J. (Los Altos, CA, US), Landrau, Felix A. (Punta Gorda, FL, US), Lautenbach, Scott D. (San Mateo, CA, US), Magruder, Judy A. (Mountain View, CA, US), Wright, Jeremy C. (Los Altos, CA, US), Sustained delivery of an active agent using an implantable system, in, Intarcia Therapeutics, Inc. (Hayward, CA, US), United States, 2010.
- [184] D.G. Kanjickal, S.T. Lopina, Modeling of drug release from polymeric delivery systems-a review, *Critical Reviews in Therapeutic Drug Carrier Systems*, 21 (2004) 345-386.
- [185] F.v. Burkensroda, L. Schedl, A. Göpferich, Why degradable polymers undergo surface erosion or bulk erosion, *Biomaterials*, 23 (2002) 4221-4231.
- [186] J. Siepmann, A. Göpferich, Mathematical modeling of bioerodible, polymeric drug delivery systems, *Advanced Drug Delivery Reviews*, 48 (2001) 229-247.
- [187] S. Kaewwichit, I.G. Tucker, The release of macromolecules from fatty acid matrixes: complete factorial study of factors affecting release, *Journal of Pharmacy and Pharmacology*, 46 (1994) 708-713.
- [188] C. Guse, S. Koennings, F. Kreye, F. Siepmann, A. Goepferich, J. Siepmann, Drug release from lipid-based implants: Elucidation of the underlying mass transport mechanisms, *International Journal of Pharmaceutics*, 314 (2006) 137-144.
- [189] S. Koennings, Lipid implants for controlled release of proteins, in, 2006, pp. No pp.
- [190] D.W. Grainger, Controlled-release and local delivery of therapeutic antibodies, *Expert Opinion on Biological Therapy*, 4 (2004) 1029-1044.
- [191] A.L. Daugherty, R.J. Mersny, Formulation and delivery issues for monoclonal antibody therapeutics, *Advanced Drug Delivery Reviews*, 58 (2006) 686-706.
- [192] K.A. Poelstra, N.A. Berekzi, A.M. Rediske, A.G. Felts, J.B. Slunt, D.W. Grainger, Prophylactic treatment of gram-positive and gram-negative abdominal implant infections using locally delivered polyclonal antibodies, *Journal of Biomedical Materials Research*, 60 (2002) 206-215.
- [193] A.G. Felts, G. Giridhar, D.W. Grainger, J.B. Slunt, Efficacy of locally delivered polyclonal immunoglobulin against *Pseudomonas aeruginosa* infection in a murine burn wound model, *Burns*, 25 (1999) 415-423.
- [194] A.G. Felts, D.W. Grainger, J.B. Slunt, Locally Delivered Antibodies Combined with Systemic Antibiotics Confer Synergistic Protection against Antibiotic-Resistant Burn Wound Infection, *The Journal of TRAUMA Injury, Infection, and Critical Care*, 49 (2000) 873-878.
- [195] M.R. Parkhurst, W.M. Saltzman, Controlled delivery of antibodies against leukocyte adhesion molecules from polymer matrices, *Journal of Controlled Release*, 42 (1996) 273-288.
- [196] B.H. Annex, M.G. Davies, G.J. Fulton, T.T.T. Huynh, K.M. Channon, M.D. Ezekowitz, P.-O. Hagen, Local Delivery of a Tissue Factor Antibody Reduces Early Leukocyte Infiltration but Fails to Limit Intimal Hyperplasia in Experimental Vein Grafts<sup>1</sup>, *Journal of Surgical Research*, 80 (1998) 164-170.

- [197] P. Homayoun, T. Mandal, D. Landry, H. Komiskey, Controlled release of anti-cocaine catalytic antibody from biodegradable polymer microspheres, *J. Pharm. Pharmacol.*, 55 (2003) 933-938.
- [198] C.-H. Wang, K. Sengothi, T. Lee, Controlled release of human immunoglobulin G. 1. Release kinetics studies, *Journal of Pharmaceutical Sciences*, 88 (1999) 215-220.
- [199] J.S. Andrew, E.J. Anglin, E.C. Wu, M.Y. Chen, L. Cheng, W.R. Freeman, M.J. Sailor, Sustained Release of a Monoclonal Antibody from Electrochemically Prepared Mesoporous Silicon Oxide, *Advanced Functional Materials*, 20 (2010) 4168-4174.
- [200] N. Guzewicz, A. Best, B. Perez-Ramirez, D.L. Kaplan, Lyophilized silk fibroin hydrogels for the sustained local delivery of therapeutic monoclonal antibodies, *Biomaterials*, 32 (2011) 2642-2650.
- [201] K.C. Ingham, P.D. Murray, [23] Precipitation of proteins with polyethylene glycol, in: *Methods in Enzymology*, Academic Press, 1990, pp. 301-306.
- [202] S. Matheus, W. Friess, D. Schwartz, H.-C. Mahler, Liquid high concentration IgG1 antibody formulations by precipitation, *J. Pharm. Sci.*, 98 (2009) 3043-3057.
- [203] M. Page, R. Thorpe, Purification of IgG by precipitation with polyethylene glycol, *Protein Protocols Handbook (2nd Edition)*, (2002) 991.
- [204] D.H. Atha, K.C. Ingham, Mechanism of precipitation of proteins by polyethylene glycols: analysis in terms of excluded volume, *Journal of Biological Chemistry*, 256 (1981) 12108-12117.
- [205] T. Arakawa, S.N. Timasheff, Mechanism of polyethylene glycol interaction with proteins, *Biochemistry*, 24 (1985) 6756-6762.
- [206] R. Bhat, S.N. Timasheff, Steric exclusion is the principal source of the preferential hydration of proteins in the presence of polyethylene glycols, *Protein Science*, 1 (1992) 1133-1143.
- [207] I.R.M. Juckes, Fractionation of proteins and viruses with polyethylene glycol, *Biochimica et Biophysica Acta (BBA) - Protein Structure*, 229 (1971) 535-546.
- [208] M.X. Yang, B. Shenoy, M. Distler, R. Patel, M. McGrath, S. Pechenov, A.L. Margolin, Crystalline monoclonal antibodies for subcutaneous delivery, *Proceedings of the National Academy of Sciences of the United States of America*, 100 (2003) 6934-6939.
- [209] A. Ketan, D. Rose-Marie, Z. Joseph, W. Barbara, Lyophilization of polyethylene glycol mixtures, *Journal of Pharmaceutical Sciences*, 93 (2004) 2244-2249.
- [210] A. Polson, G.M. Potgieter, J.F. Largier, G.E.F. Mears, F.J. Joubert, The fractionation of protein mixtures by linear polymers of high molecular weight, *Biochimica et Biophysica Acta (BBA) - General Subjects*, 82 (1964) 463-475.
- [211] X.M. Lam, J.Y. Yang, J.L. Cleland, Antioxidants for prevention of methionine oxidation in recombinant monoclonal antibody HER2, *Journal of Pharmaceutical Sciences*, 86 (1997) 1250-1255.
- [212] H.R. Costantio, M.J. Pikal, Editors, *Lyophilization of Biopharmaceuticals*. [In: *Biotechnol.: Pharm. Aspects*; 2004, 2], AAPS Press, 2004.
- [213] K. Schersch, O. Betz, P. Garidel, S. Muehlau, S. Bassarab, G. Winter, Systematic investigation of the effect of lyophilizate collapse on pharmaceutically relevant proteins I: Stability after freeze-drying, *Journal of Pharmaceutical Sciences*, 99 (2010) 2256-2278.
- [214] M. Morlock, H. Koll, G. Winter, T. Kissel, Microencapsulation of rh-erythropoietin, using biodegradable poly( $\epsilon$ -lactide-co-glycolide): protein stability and the effects of stabilizing excipients, *European Journal of Pharmaceutics and Biopharmaceutics*, 43 (1997) 29-36.
- [215] M.E. Brewster, M.S. Hora, J.W. Simpkins, N. Bodor, Use of 2-Hydroxypropyl- $\beta$ -cyclodextrin as a Solubilizing and Stabilizing Excipient for Protein Drugs, *Pharmaceutical Research*, 8 (1991) 792-795.
- [216] M. Ressing, W. Jiskoot, H. Talsma, C. van Ingen, E.C. Beuvery, D. Crommelin, The Influence of Sucrose, Dextran, and Hydroxypropyl- $\beta$ -cyclodextrin as Lyoprotectants for a Freeze-Dried Mouse IgG2a Monoclonal Antibody (MN12), *Pharmaceutical Research*, 9 (1992) 266-270.
- [217] T. Serno, J.F. Carpenter, T.W. Randolph, G. Winter, Inhibition of agitation-induced aggregation of an IgG-antibody by hydroxypropyl-beta-cyclodextrin, *Journal of Pharmaceutical Sciences*, 99 (2009) n/a.
- [218] W. Vogelhuber, E. Magni, A. Gazzaniga, A. Gopferich, Monolithic glyceryl trimyristate matrices for parenteral drug release applications, *European Journal of Pharmaceutics and Biopharmaceutics*, 55 (2003) 133-138.
- [219] J.D. Bonny, H. Leuenberger, Matrix type controlled release systems II. Percolation effects in non-swellable matrices, *Pharmaceutica Acta Helveticae*, 68 (1993) 25-33.
- [220] T. Pongjanyakul, N.J. Medlicott, I.G. Tucker, Melted glyceryl palmitostearate (GPS) pellets for protein delivery, *International Journal of Pharmaceutics*, 271 (2004) 53-62.
- [221] N. Garti, K. Sato, *Crystallization and Polymorphism of Fats and Fatty Acids*, Marcel Dekker Inc., (1988).
- [222] R.A. Siegel, R. Langer, Controlled Release of Polypeptides and Other Macromolecules, *Pharmaceutical Research*, 1 (1984) 2-10.
- [223] S. Mohl, The Development of a Sustained and Controlled Release Device for Pharmaceutical Proteins based on Lipid Implants, in, 2003, pp. No pp given.

## REFERENCES

- [224] M. Windbergs, C.J. Strachan, P. Kleinebudde, Tailor-made dissolution profiles by extruded matrices based on lipid polyethylene glycol mixtures, *Journal of Controlled Release*, 137 (2009) 211-216.
- [225] W. Jiang, S.P. Schwendeman, Stabilization and Controlled Release of Bovine Serum Albumin Encapsulated in Poly(D, L-lactide) and Poly(ethylene glycol) Microsphere Blends, *Pharmaceutical Research*, 18 (2001) 878-885.
- [226] Z. Ghalanbor, M. Körber, R. Bodmeier, Improved Lysozyme Stability and Release Properties of Poly(lactide-co-glycolide) Implants Prepared by Hot-Melt Extrusion, *Pharmaceutical Research*.
- [227] I.J. Castellanos, R. Crespo, K. Griebenow, Poly(ethylene glycol) as stabilizer and emulsifying agent: a novel stabilization approach preventing aggregation and inactivation of proteins upon encapsulation in bioerodible polyester microspheres, *Journal of Controlled Release*, 88 (2003) 135-145.
- [228] D. Malamud, J.W. Drysdale, Isoelectric points of proteins: A table, *Analytical Biochemistry*, 86 (1978) 620-647.
- [229] A. Malzert, F. Boury, D. Renard, P. Robert, L. Lavenant, J.P. Benoit, J.E. Proust, Spectroscopic studies on poly(ethylene glycol)-lysozyme interactions, *International Journal of Pharmaceutics*, 260 (2003) 175-186.
- [230] C. Himawan, V.M. Starov, A.G.F. Stapley, Thermodynamic and kinetic aspects of fat crystallization, *Advances in Colloid and Interface Science*, 122 (2006) 3-33.
- [231] R. Bawa, R. A. Siegel, B. Marasca, M. Karel, R. Langer, An explanation for the controlled release of macromolecules from polymers, *Journal of Controlled Release*, 1 (1985) 259-267.
- [232] F. Kreye, F. Siepmann, J. Siepmann, Drug release mechanisms of compressed lipid implants, *International Journal of Pharmaceutics*, In Press, Uncorrected Proof.
- [233] Y.W. Choy, N. Khan, K.H. Yuen, Significance of lipid matrix aging on in vitro release and in vivo bioavailability, *International Journal of Pharmaceutics*, 299 (2005) 55-64.
- [234] C. Reitz, P. Kleinebudde, Solid lipid extrusion of sustained release dosage forms, *European Journal of Pharmaceutics and Biopharmaceutics*, 67 (2007) 440-448.
- [235] A. San Vicente, R.M. Hernández, A.R. Gascón, M.B. Calvo, J.L. Pedraz, Effect of aging on the release of salbutamol sulfate from lipid matrices, *International Journal of Pharmaceutics*, 208 (2000) 13-21.
- [236] D. Bodmer, T. Kissel, E. Traechslin, Factors influencing the release of peptides and proteins from biodegradable parenteral depot systems, *Journal of Controlled Release*, 21 (1992) 129-137.
- [237] T. Estey, J. Kang, S.P. Schwendeman, J.F. Carpenter, BSA degradation under acidic conditions: A model for protein instability during release from PLGA delivery systems, *Journal of Pharmaceutical Sciences*, 95 (2006) 1626-1639.
- [238] S. Allababidi, J.C. Shah, Efficacy and Pharmacokinetics of Site-Specific Cefazolin Delivery Using Biodegradable Implants in the Prevention of Post-operative Wound Infections, *Pharmaceutical Research*, 15 (1998) 325-333.
- [239] Z.-h. Gao, W.R. Crowley, A.J. Shukla, J.R. Johnson, J.F. Reger, Controlled Release of Contraceptive Steroids from Biodegradable and Injectable Gel Formulations: *In Vivo* Evaluation, *Pharmaceutical Research*, 12 (1995) 864-868.
- [240] J.P. Opdebeeck, I.G. Tucker, A cholesterol implant used as a delivery system to immunize mice with bovine serum albumin, *Journal of Controlled Release*, 23 (1993) 271-279.
- [241] M. Eisenblatter, J. Ehrchen, G. Varga, C. Sunderkotter, W. Heindel, J. Roth, C. Bremer, A. Wall, In Vivo Optical Imaging of Cellular Inflammatory Response in Granuloma Formation Using Fluorescence-Labeled Macrophages, *J Nucl Med*, 50 (2009) 1676-1682.
- [242] K. Vyacheslav, S. Shoham, M. Victoria, L. Kfir, H. Sharon, L. Tsvee, B. Alexander, H. Alon, Use of lipophilic near-infrared dye in whole-body optical imaging of hematopoietic cell homing, *Journal of Biomedical Optics*, 11 (2006) 050507.
- [243] J. Chen, I.R. Corbin, H. Li, W. Cao, J.D. Glickson, G. Zheng, Ligand Conjugated Low-Density Lipoprotein Nanoparticles for Enhanced Optical Cancer Imaging in Vivo, *Journal of the American Chemical Society*, 129 (2007) 5798-5799.
- [244] J.M. Anderson, In vivo biocompatibility of implantable delivery systems and biomaterials, *Eur. J. Pharm. Biopharm.*, 40 (1994) 1-8.
- [245] I. Metzmacher, Enzymatic degradation and drug release behavior of dense collagen implants, in, 2005, pp. Thesis.
- [246] J. Hilborn, L.M. Bjursten, A new and evolving paradigm for biocompatibility, *Journal of Tissue Engineering and Regenerative Medicine*, 1 (2007) 110-119.
- [247] V.P. Dole, H. Meinertz, Microdetermination of Long-chain Fatty Acids in Plasma and Tissues, *Journal of Biological Chemistry*, 235 (1960) 2595-2599.

- [248] R. Wood, T. Lee, High-performance liquid chromatography of fatty acids: quantitative analysis of saturated, monoenoic, polyenoic and geometrical isomers, *Journal of Chromatography A*, 254 (1983) 237-246.
- [249] R.A. Siegel, R. Langer, Mechanistic studies of macromolecular drug release from macroporous polymers. II. Models for the slow kinetics of drug release, *Journal of Controlled Release*, 14 (1990) 153-167.
- [250] A. Zurner, J. Kirstein, M. Doblinger, C. Brauchle, T. Bein, Visualizing single-molecule diffusion in mesoporous materials, *Nature*, 450 (2007) 705-708.
- [251] J. Kirstein, B. Platschek, C. Jung, R. Brown, T. Bein, C. Brauchle, Exploration of nanostructured channel systems with single-molecule probes, *Nat Mater*, 6 (2007) 303-310.
- [252] T. Dingermann, R. Hansel, I. Zundorf, *Pharmaceutical Biology: Molecular Basis and Clinical Application*, Springer, 2002.
- [253] W. Klaus, B. Gsell, A.M. Labhardt, B. Wipf, H. Senn, The three-dimensional high resolution structure of human interferon  $\alpha$ -2a determined by heteronuclear NMR spectroscopy in solution, *J. Mol. Biol.*, 274 (1997) 661-675.
- [254] V. Kumar, V.K. Sharma, D.S. Kalonia, In situ precipitation and vacuum drying of interferon alpha-2a: Development of a single-step process for obtaining dry, stable protein formulation, *International Journal of Pharmaceutics*, 366 (2009) 88-98.
- [255] J.S. Anderson, K. Saddington, S 80. The use of radioactive isotopes in the study of the diffusion of ions in solution, *Journal of the Chemical Society (Resumed)*, (1949) S381-S386.